Papers Presented
at the

51st Annual Meeting of the Meteoritical Society
Fayetteville, Arkansas
July 18-22, 1988

Sponsored by

The University of Arkansas, Fayetteville
The Lunar and Planetary Institute, Houston

Co-sponsored by

The Barringer Crater Company
Fayetteville Promotions & Advertising Commission
World-Wide Travel, Fayetteville
The Fayetteville Hilton
Inn of the Ozarks, Eureka Springs
Arkansas Geological Commission
Arkansas State Tourism Board
Pergamon Press
Washington County Historical Society

ABSTRACTS AND PRELIMINARY PROGRAM FOR THE 51ST ANNUAL MEETING OF THE METEORITICAL SOCIETY

Fayetteville, Arkansas
July 18 - 22, 1988

Sponsored by

Lunar and Planetary Institute
University of Arkansas, Fayetteville

Co-sponsored by

The Barringer Crater Company
Fayetteville Promotions and Advertising Commission
World Wide Travel, Fayetteville
The Fayetteville Hilton
Inn of the Ozarks, Eureka Springs
Arkansas Geological Commission
Arkansas State Tourism Board
Pergamon Press
Washington County Historical Society

Compiled by

Lunar and Planetary Institute
3303 NASA Road One
Houston, Texas 77058-4399

LPI Contribution 665

Compiled in 1988

by

Lunar and Planetary Institute

PREFACE

This volume contains abstracts that have been accepted by the Program Committee for presentation at the 51st Annual Meeting of the Meteoritical Society.

The Program Committee consisted of Derek W. G. Sears (Chairman), Fouad Hasan, Charles Hohenberg, Bradley D. Keck, Gary E. Lofgren, Harry Y. McSween, Jr., Larry Taylor, and Pamela Jones (Secretary).

Logistics and administrative support were provided by Pamela Jones, LeBecca Turner, and Terry Gore (at the Lunar and Planetary Institute) and Hazel Sears and Deborah Stark (at the University of Arkansas). This abstract volume was prepared by the Publications Office staff at the Lunar and Planetary Institute.

The Organizing Committee for the meeting consisted of J. David Batchelor, John DeHart, Michael Howard, R. Kyle Guimon, Chris Hartmetz, Fouad Hasan, Lu Jie, Bradley D. Keck, Walter Manger, Nancy Rogers (Conference Coordinator), Hazel Sears, Derek W. G. Sears (Chairman), and Kenneth Steele.

The Lunar and Planetary Institute is operated by the Universities Space Research Association under contract No. NASW-4066 with the National Aeronautics and Space Administration.

PLENARY ADDRESSES

Your attention is drawn to the following special addresses which will be delivered during the meeting:

Leonard Address, Thursday, July 21, 1:30 - 2:00 p.m., Room 1
Enstatite Meteorites and Their Parent Bodies by Klaus Keil.

Barringer Address, Thursday, July 21, 2:00 - 2:30 p.m., Room 1
Circular Arguments: The Peaks and Troughs in the Crater Game by Michael Dence.

Presidential Address, Monday, July 18, 8:45 - 9:00 a.m., Room 1
Somewhere Over the Rainbow by Gerald Wasserburg.

Invited paper, Tuesday, July 19, 8:30 - 9:00 a.m., Room 1
Foreign OC-type Clasts in Meteoritic Breccias: What They Tell Us about the Abundance of OC-type Asteroids in the Main Belt by Paul Pellas.

Invited paper, Wednesday, July 20, 8:30 - 9:00 a.m., Room 1
The Plutonium-244 Story by Paul Kuroda.

Invited paper, Wednesday, July 20, 8:15 - 9:00 a.m., Arkansas Union Theatre
To Pergamon and Back: An Account of an Homeric Voyage with Observations on the Beliefs and Practices of Fellow Travellers and Natives by Denis Shaw

Invited Paper, Friday, July 22, 8:30 -9:00 p.m., Room 1
Interstellar Grains in Meteorites: Diamond and Silicon Carbide by Edward Anders.

STUDENT AWARDS

We gratefully acknowledge the contribution of The Barringer Crater Company which made the participation of these students possible:

Richard Ash (Open University, UK)
Cheryl Brigham (California Institute of Technology, USA)
Catherine Broadhurst (University of Arizona, USA)
C. Caillett (Universite Pierre et Marie Curie, France)
Thomas Graf (ETH-Zurich, Switzerland)
Alan Hildebrand (University of Arizona, USA)
Zhang Jing (Lehigh University, USA)
Jean Kozul (Rutgers University, USA)
Andrew Morse (Open University, UK)
Donald Musselwhite (University of Arizona, USA)
Jun Saito (University of Tokyo, Japan)
Thomas Stephan (Max-Planck-Institut fur Kernphysik, F. R. Germany)
Brigette Zanda (Institut d'Astrophysique de Paris, France)

PLAN OF SESSIONS

Day	Room		Morning	Afternoon
Mon.	1	Wasserburg	A. Carbon	C. Chondrules
	2		B. Howardites, eucrites, diogenites	D. Impact structures and materials
Tues.	1	Pellas	E. Regolith breccias and shock	G. Enstatite and carbonaceous chondrites
	2		F. Antarctic meteorites	H. Lunar petrology and lunar meteorites
Wed.	1	Kuroda	I. Nucleosynthesis and extinct isotopes	K. Ordinary chondrites
	2		J. Cosmic dust	L. Cosmogenic nuclides and Ar-Ar shock effects
			Evening: Campus Shaw	
Thurs.	1		M. Asteroids and planets	Keil and Dence
	2		N. K-T boundary	
Fri.	1	Anders	O. Calcium-aluminum-rich inclusions	
	2		P. Differentiated meteorites	

Morning sessions begin at 8:30 a.m.
Afternoon sessions begin at 1:30 p.m.
Evening session begins at 8:00 p.m. Shuttle buses leave the Fayetteville Hilton at 6:45 - 7:15 p.m. (Museum and reception, 7:00 - 8:00 p.m.)

MEETING CALENDAR

Friday, July 15	Briefings for the two-day field trips, 8:00 p.m., Fayetteville Hilton: for the Diamonds/Magnet Cove trip, meet in the Virgil Blossum Room; for the Ouchitas/Ozarks trip, meet in the Albert Pike Room.
Saturday, July 16	Two-day field trips. Bus leaves the Fayetteville Hilton at 7:30 p.m. and the dormitory at 7:35 a.m.
Sunday, July 17	Buffalo Float. Bus leaves the Fayetteville Hilton at 7:30 a.m. and the dormitory at 7:35 a.m.
	Mrs. Wasson's and Ozark Hike. Bus leaves the Fayetteville Hilton at 1:00 p.m. and the dormitory at 1:05 p.m.
	Council Meeting, 2:00 p.m., Albert Pike Room, Fayetteville Hilton.
	Welcome Reception by the Chancellor, Sequoyah Ballroom, Fayetteville Hilton, 7:00 - 9:00 p.m.
Monday, July 18	Opening Ceremony, Room 1, 8:30 - 8:45 a.m. The Chancellor will welcome delegates to the University and the President of the Society will open the meeting.
	Presidential Address, Room 1, 8:45 - 9:15 a.m., Gerald Wasserburg.
	9:45 - 11:30 a.m., Room 1: Carbon
	9:45 - 11:45 a.m., Room 2: Howardites, eucrites, diogenites
	Guest Trip to Tahlequah. Bus leaves the Fayetteville Hilton at 10:00 a.m. and the dormitory at 10:05 a.m.
	Nomenclature Committee Meeting, Albert Pike Room, Fayetteville Hilton, 12:00 - 1:30 p.m.
	1:30 - 5:15 p.m., Room 1: Chondrules
	1:30 - 4:30 p.m., Room 2: Impact structures and materials
	Ice Cream Social, Headquarters House, 7:00 - 9:00 p.m.
Tuesday, July 19	Plenary, Room 1, 8:30 - 9:00 a.m., Paul Pellas
	9:30 - 11:30 a.m., Room 1: Regolith breccias and shock
	9:30 - 12:00 p.m., Room 2: Antarctic meteorites
	Guest Trip to War Eagle Cavern and Mill. Bus leaves the Fayetteville Hilton at 10:00 a.m. and the dormitory at 10:05 a.m.
	1:30 - 4:15 p.m., Room 1: Enstatite and carbonaceous chondrites

	1:30 - 4:00 p.m., Room 2: Lunar petrology and lunar meteorites
	Picnic at the lake hosted by the Fayetteville Advertising and Promotions Commission. Buses leave the Fayetteville Hilton at 5:00 p.m. and 6:00 p.m.
Wednesday, July 20	Plenary, Room 1, 8:30 - 9:00 a.m., Paul Kuroda
	Guest Trip to Fort Smith. Bus leaves the Fayetteville Hilton at 9:00 a.m. and the dormitory at 9:05 a.m.
	9:30 - 11:15 a.m., Room 1: Nucleosynthesis and extinct isotope effects
	9:30 - 11:15 a.m., Room 2: Cosmic dust
	Business Meeting, Room 1: 11:15 - 11:45
	1:30 - 5:00 p.m., Room 1: Ordinary chondrites
	1:30 - 4:15 p.m., Room 2: Cosmogenic nuclides and Ar-Ar shock effects
	Evening on Main Campus hosted by the Department of Chemistry and Biochemistry. Shuttle buses leave the Fayetteville Hilton at 6:45 - 7:15 p.m. Museum visit and reception on the Union Terrace, 7:00 - 8:00 p.m., followed by a session in the Arkansas Union Theatre, 8:00 - 9:00 p.m., consisting of a welcome by the Chairman of the Department, presentation of life memberhip to Denis Shaw and Carleton Moore by the President following citations by Michael Drake (Chairman of Publications Committee) and the plenary address by Denis Shaw.
Thursday, July 21	8:30 - 11:30 a.m., Room 1: Asteroids and planets
	8:30 - 11:30 a.m., Room 2: K-T boundary and a fireball
	Guest Trip around historic Fayetteville. Bus leaves Fayetteville Hilton at 9:00 a.m. and the dormitory at 9:05 a.m.
	Medalists' Addresses, Room 1, Klaus Keil, 1:30 - 2:00 p.m.; Michael Dence, 2:00 - 2:30 p.m.
	Award Presentations and Annual Banquet at Eureka Springs. Bus leaves Fayetteville Hilton at 2:30 p.m.
Friday, July 22	Plenary, Room 1, 8:30 - 9:00 a.m., Edward Anders
	9:30 - 12:00 p.m., Room 1: Calcium-Aluminum-Inclusions
	9:30 - 12:15 p.m., Room 2: Differentiated meteorites
	Farewell Reception, Fayetteville Hilton, Sequoyah Atrium, 12:30 - 2:00 p.m.
	Dinner/Passion Play. Bus leaves Fayetteville Hilton at 3:30 p.m. and the dormitory at 3:35 p.m.

PRELIMINARY PROGRAM
51st Annual Meteoritical Society Meeting
July 18-22, 1988 Fayetteville, Arkansas, U.S.A.

* - Indicates Speaker

PLENARY 1
Monday, July 18 Room 1
8:30 - 9:15 a.m.

Chairman: D.W.G. Sears

08:30 - 08:45	Opening Ceremony
08:45 - 09:15	Wasserburg G. W.* **(PRESIDENTIAL ADDRESS)** *Somewhere Over the Rainbow*
09:15 - 09:45	COFFEE BREAK

SESSION A - CARBON
Monday, July 18 Room 1
9:45 - 11:30 a.m.

Chairmen: T. Bernatowicz
J. P. Bradley

A-1	09:45 - 10:00	Bernatowicz T.* Fraundorf G. Fraundorf P. Tang M. TEM Observations of Interstellar Silicon Carbide from the Murray and Murchison Carbonaceous Meteorites
A-2	10:00 - 10:15	Wright I. P.* Ash R. D. Grady M. M. Pillinger C. T. Tang M. The Carbon Components in Murray Residue CF
A-3	10:15 - 10:30	Buseck P. R.* Barry J. C. Twinned Diamonds in the Orgueil Carbonaceous Chondrite
A-4	10:30 - 10:45	Alexander C.M.O'D.* Arden J. W. Gilmour I. Schelhaas N. Ott U. Pillinger C. T. Organic Carbon in the Ordinary Chondrites
A-5	10:45 - 11:00	Ash R. D.* Arden J. W. Grady M. M. Wright I. P. Pillinger C. T. Isotopically Light Carbon in the Allende Meteorite

A-6	11:00 - 11:15	Yates P.* Wright I. P. Prosser S. J. Pillinger C. T. Hutchison R. Carbon Isotopic Measurements of Micrometeorites
A-7	11:15 - 11:30	Bradley J. P. Brownlee D. E.* Schramm L. S. Dietz N. L. The Abundance, Distribution and Chemical State of Carbon in Interplanetary Dust

LUNCH BREAK

SESSION B - EUCRITES, HOWARDITES, DIOGENITES

Monday, July 18 Room 2
9:45 - 11:45 a.m.

Chairmen: H. Takeda
P. H. Warren

B-1	09:45 - 10:00	Kozul J. M.* Hewins R. H. Mafic Mineral Compositions of Igneous Clasts in the Lewis Cliffs 85300, 85302, 85303 Polymict Eucrites
B-2	10:00 - 10:15	Jovanovic S. Reed G. W., Jr.* Thermometry of Eucritic Achondrites
B-3	10:15 - 10:30	Takeda H.* Mori H. Nyquist L. E. Bogard D. Recrystallization of Mesostasis Materials of Eucrites and Late Thermal Events on the HED Parent Body
B-4	10:30 - 10:45	Nyquist L.* Bogard D. Takeda H. Bansal B. Johnson P. Shih C.-Y. Wiesmann H. Comparative Chronologies of Basaltic Clasts in Antarctic Eucrites Y-75011 and Y-792510
B-5	10:45 - 11:00	Warren P. H.* Kallemeyn G. W. Jerde E. A. Reckling Peak A80224: An Anomalous, Ferroan Yet REE-Poor, Eucrite
B-6	11:00 - 11:15	Gosselin D. C. Laul J. C.* Smith M. R. Reid A. M. The Bholghati Consortium: Preliminary Chemical and Petrologic Characterization of the Bholghati Howardite
B-7	11:15 - 11:30	Paul R. L. Sack R. O. Kruse H. Lipschutz M. E.* Simple and Not-So-Simple Mixing in the Howardite-Eucrite-Diogenite (HED) Parent Body
B-8	11:30 - 11:45	Mittlefehldt D. W.* Lindstrom M. M. HED Petrogenesis: View From the Diogenite End

12:30 - 1:30 NOMENCLATURE COMMITTEE MEETING, Albert Pike Room, Fayetteville Hilton

LUNCH BREAK

SESSION C - CHONDRULES

Monday, July 18 Room 1
1:30 - 5:15 p.m.

Chairmen: G. Lofgren
R. Hutchison

C-1 01:30 - 01:45 Prinz M.* Weisberg M. K. Nehru C. E.
Gunlock, A New Type 3 Ordinary Chondrite With a Golfball-Sized Chondrule

C-2 01:45 - 02:00 Weisberg M. K.* Prinz M. Nehru C. E.
Macrochondrules in Ordinary Chondrites: Constraints on Chondrule Forming Processes

C-3 02:00 - 02:15 Nehru C. E.* Prinz M. Okulewicz S. C.
Weisberg M. K.
Glassy, Cryptocrystalline and Radial Pyroxene Chondrules in Type 3 Ordinary Chondrites

C-4 02:15 - 02:30 Radomsky P. M. Hewins R. H.*
Chondrule Texture/Composition Relations Revisited: Constraints on the Thermal Conditions in the Chondrule Forming Region

C-5 02:30 - 02:45 Lofgren G.* Lanier A. B.
Dynamic Crystallization Experiments on Melts of Barred Olivine Chondrule Composition: Origin of Their Textural Diversity

C-6 02:45 - 03:00 Jones R. H.* Brearley A. J.
Kinetics of the Clinopyroxene - Orthopyroxene Transition: Constraints on the Thermal Histories of Chondrules and Type 3-6 Chondrites

03:00 - 03:30 TEA BREAK

C-7 03:30 - 03:45 Hutchison R.* Alexander C.M.O.
A Chondrule Origin for Opaque Rims and Interchondrule Matrices in the UOCs

C-8 03:45 - 04:00 DeHart J. M.* Sears D. W. G. Lofgren G. E.
Sodium Enriched Luminescent Chondrule Mesostasis Rims in the Unequilibrated Ordinary Chondrites

C-9 04:00 - 04:15 Sears D. W. G.* Lu J. Guimon R. K. Morse A. D. Hutchison R. Alexander C. O. Wright I. P. Pillinger C. T.
The Thermoluminescence Properties of Chondrules from Three Low Petrologic Type Ordinary Chondrites

C-10 04:15 - 04:30 Fredriksson K.* Fredriksson B. J.
Chondrule Parents Revisited

C-11 04:45 - 05:00 Mayeda T. K.* Clayton R. N. Kring D. A.
Oxygen and Silicon Isotopes in Ningqiang Chondrules

C-12 05:00 - 05:15 Kring D. A.* Wood J. A.
Why do Allende Chondrules Lie on a Different Oxygen-isotope Mixing Line than Allende CAI's? -- A model

POSTER PRESENTATION

C-13 Fredriksson K. Wlotzka F.
Experiments with a Leitz 1750°C Heating Stage

PRESENTED BY TITLE ONLY

C-14 Kring D. A. Holmen B. A.
Petrology of Anorthite-rich Chondrules in CV3 and CO3 Chondrites

SESSION D - IMPACT STRUCTURES AND MATERIALS

Monday, July 18 Room 2
1:30 - 4:30 p.m.

Chairmen: C. Koeberl
U. B. Marvin

D-1 01:30 - 2:00 McHone J. F. Dietz R. S.* (EXTENDED PAPER)
Arabian Peninsula: Known and Suspected Impact Structures

D-2 02:00 - 02:15 Murali A. V.* Koeberl C. Nazarov M. A. Sharpton V. L. Burke K.
Kara and Ust-Kara Impact Structures, USSR: Geochemical Relationship of the Target Rocks and Ejecta

D-3 02:15 - 02:30 Read W. F.*
Deformation in Soft Ordovician Sediment Produced by Large Masses of Sandstone From a Nearby, but as yet Undiscovered, Impact Crater

D-4 02:30 - 02:45 Sharpton V. L.* Burke K. Lucas L. Horz F.
Reflection Seismic Data From Terrestrial Impact Structures: Evidence of Shallow Penetration?

D-5 02:45 - 03:00 McHone J. F.* Nieman R. A.
Vredefort Stishovite Confirmed Using Solid-State Silicon-29 Nuclear Magnetic Resonance

03:00 - 03:30 TEA BREAK

D-6 03:30 - 03:45 Marvin U. B.* Kring D. A. Boulger J. D.
Petrography of Impactite From New Quebec Crater

D-7 03:45 - 04:00 Bain J. G. Kissin S. A.*
A Preliminary Study of Fluid Inclusions in Shock-metamorphosed Sediments at the Haughton Impact Structure, Devon Island, Canada

D-8 04:00 - 04:15 Meisel T.* Koeberl C.
Geochemical Studies of Impact Glass From the Darwin Crater, Tasmania

D-9 04:15 - 04:30 Wittke J. H. Barnes V. E.*
Multi-Component Source for Muong Nong-Type Bediasite 30775-2

PLENARY 2

Tuesday, July 19 Room 1
8:30 - 9:00 a.m.

Chairman: G. J. Taylor

08:30 - 9:00 Pellas P.* **(INVITED PAPER)**
Foreign OC-Type Clasts in Meteoritic Breccias: What They Tell Us About the Abundance of OC-Type Asteroids in the Main Belt

09:00 - 09:30 COFFEE BREAK

SESSION E - REGOLITH BRECCIAS AND SHOCK

Tuesday, July 19 Room 1
9:30 - 11:30 a.m.

Chairmen: M. W. Caffee
W. L. Manger

E-1 09:30 - 09:45 Olinger C. T.* Garrison D. H. Hohenberg C. M. Goswami J. N. Rajan R. S.
Cosmogenic Neon in Individual Grains From Kapoeta, Pesyanoe and Murchison

E-2	09:45 - 10:00	Caffee M. W.* Fahey A. J. Zinner E. Goswami J. N. Li, B, Mg and Al in Solar-flare- and non-irradiated Kapoeta Grains
E-3	10:00 - 10:15	Grady M. M.* Pillinger C. T. Nitrogen in the Fayetteville Breccia
E-4	10:15 - 10:30	DeHart J. M.* Sears D. W. G. Cathodoluminescence Study of the Fayetteville and Plainview Gas-Rich Regolith Breccias
E-5	10:30 - 10:45	Pellas P.* Clayton R. N. Wieler R. Signer P. Exotism in Fayetteville
E-6	10:45 - 11:00	Sneyd D. S. Nord G. L., Jr. McSween H. Y., Jr.* Origin and Significance of Olivine Dislocations in Chondrites with Documented Strain
E-7	11:00 - 11:15	Dundon R. W.* Shock-induced Fe2+ Disorder in the Pigeonite Phases of Ureilites
E-8	11:15 - 11:30	Wasilewski P.* Identification of Shock Induced Changes in Fe Spheres Using Magnetic Techniques

LUNCH BREAK

SESSION F - ANTARCTIC METEORITES

Tuesday, July 19 Room 2
9:30 - 12:00 noon

Chairmen: J. L. Gooding
D. M. Shaw

F-1	09:30 - 09:45	Wasilewski P.* Huss G. R. Wagstaff J. Thompson C. Ice Patterns and Surface Wind in the Setting of Antarctic Meteorites
F-2	09:45 - 10:00	Hasan F. A.* Sears D. W. G. Cassidy W. A. Evidence for a Relationship Between the Natural Thermoluminescence and the Antarctic Meteorite Recovery Locations
F-3	10:00 - 10:15	Huss G. R.* Wasilewski P. J. Wagstaff J. Thompson C. Do Antarctic Meteorite Concentrations Reflect the Average Infall Rate?

F-4	10:15 - 10:30	Harvey R.* Relative Abundance of Different Types of Meteorites and the Quality of the Antarctic Meteorite Sample
F-5	10:30 - 10:45	Buchwald V. F. Clarke R. S., Jr.* Akaganeite, Not Lawrencite, Corrodes Antarctic Iron Meteorites
F-6	10:45 - 11:00	Velbel M. A.* The Distribution of Evaporitic Weathering Products on Antarctic Meteorites
F-7	11:15 - 11:30	Yates A. M.* Two Methods for Determining Weathering in Equilibrated Chondrites
F-8	11:30 - 11:45	Weber H. W. Schultz L.* Begemann F. Different Interplanetary Source Regions of Antarctic and Non-Antarctic H-Chondrites? The Noble Gas Record
F-9	11:45 - 12:00	Samuels S. M. Lipschutz M. E.* Antarctic and Non-Antarctic Meteorites: Different Populations

POSTER PRESENTATIONS

F-10	Harvey R. Mass and Number Density of H and L Chondrites on the Allan Hills Main Icefield

PRESENTED BY TITLE ONLY

F-11	Mardon A. A. The Detection of Pleistocene Meteorite Placer Deposits Located in North America
F-12	Miyamoto M. Carbonates in Antarctic Meteorites: Infrared Spectroscopy
F-13	Velbel M. A. Gooding J. L. X-Ray Diffraction Evidence for Weathering Products in Antarctic Basaltic Achondrites

LUNCH BREAK

SESSION G - ENSTATITE AND CARBONACEOUS CHONDRITES

Tuesday, July 19 Room 1
1:30 - 4:15 p.m.

Chairmen: A. J. Brearley
M. Prinz

G-1	01:30 - 01:45	Ehlers K.* Woermann E. El Goresy A. Diffusion Experiments in Niningerite Solid Solution and Their Relevance to the Thermal History of EH-chondrites
G-2	01:45 - 02:00	Kimura M. El Goresy A.* Djerfisherite Compositions in EH Chondrites: A Potential Parameter to the Geochemistry of the Alkali Elements
G-3	02:00 - 02:15	Lundberg L. L.* Crozaz G. Enstatite Chondrites: A Preliminary Ion Microprobe Study
G-4	02:15 - 02:30	Steele I. M.* Forsterite Compositions and Cathodoluminescence Within Ornans (C30) Forsterite Grains
G-5	02:30 - 02:45	Scorzelli R. B. Azevedo I. S. Danon J.* Superparamagnetic Component in the Niger (I)C2 Carbonaceous Chondrite
	02:45 - 03:15	TEA BREAK
G-6	03:15 - 03:30	Brearley A. J.* CM2 Carbonaceous Chondrite Matrices: AEM Studies of Matrix Phyllosilicates and Mass Balance Calculations Using a Linear Algebraic Method
G-7	03:30 - 03:45	Zolensky M. E.* Barrett R. A. EET 83334: A CM1 Chondrite With Probable Compaction Textures
G-8	03:45 - 04:00	Kallemeyn G. W.* Metamorphosed Carbonaceous Chondrites
G-9	04:00 - 04:15	Bell J. F.* A Probable Asteroidal Parent Body for the CV or CO Chondrites

SESSION H - LUNAR PETROLOGY AND LUNAR METEORITES

Tuesday, July 19 Room 2
1:30 - 4:00 p.m.

Chairmen: G. Ryder
L. Taylor

H-1 01:30 - 01:45 Dickinson T.* Taylor G. J. Bild R. W. Keil K.
Mantle Metasomatism on the Moon

H-2 01:45 - 02:00 Neal C. R. L. A. Taylor*
Systematics Involved in the Petrogenetic Modelling of Very High Alumina (VHA) and Very High Potassium (VHK) Basalts From the Apollo 14 Site

H-3 02:00 - 02:15 Neal C. R.* Taylor L. A.
Petrogenesis of Very High Alumina (VHA) and Very High Potassium (VHK) Basalts From the Apollo 14 Site by Combined Assimilation and Fractional Crystallization.

H-4 02:15 - 02:30 Ryder G.*
Impact Splashing and Quenching During Crystallization of Volcanic Apollo 15 KREEP Basalts

H-5 02:30 - 02:45 Marvin U. B.* Carey J. W. Lindstrom M. M.
Cordierite-Spinel Troctolite, a New Mg-Rich Lithology From the Lunar Highlands

02:45 - 03:15 TEA BREAK

H-6 03:15 - 03:30 Hawke B. R.* Lucey P. G. Spudis P. D.
Impact Structures as Probes of the Lunar Interior

H-7 03:30 - 03:45 Koeberl C.*
Initial Geochemical Characterization of Lunar Meteorite Y-86032

H-8 03:45 - 04:00 Nishiizumi K.* Reedy R. C. Arnold J. R.
Exposure History of Four Lunar Meteorites

POSTER PRESENTATION

H-9 Ryder G.
Textural Diversity and Chemical Range of Volcanic Apollo 15 KREEP Basalts

PRESENTED BY TITLE ONLY

H-10 Eugster O.*
Yamato-86032 Lunar Meteorite: Cosmic-ray Produced, Radiogenic and Trapped Noble Gases

PLENARY 3

Wednesday, July 20 Room 1
8:30 - 9:00 a.m.

Chairman: M. Rowe

08:30 - 09:00	Kuroda P. K.* **(INVITED PAPER)** The Plutonium-244 Story
09:00 - 09:30	COFFEE BREAK

SESSION I - NUCLEOSYNTHESIS AND EXTINCT ISOTOPE EFFECTS

Wednesday, July 20 Room 1
9:30 - 11:15 a.m.

Chairmen: D. S. Burnett
P. K. Kuroda

	09:30 - 09:45	Chairman's Opening Remarks - D. S. Burnett
I-1	09:45 - 10:00	Clayton D. D.* Magnesium and Oxygen Isotopes in Interstellar Spinel
I-2	10:00 - 10:15	Woolum D. S.* Burnett D. S. Interpretation of Solar System Abundances Around the N = 50 Neutron Shell
I-3	10:15 - 10:30	Hyman M. Rowe M. W.* Fahey A. J. Zinner E. Search for ^{60}Fe in Individual Magnetite Grains From Orgueil
I-4	10:30 - 10:45	Hagee B.* Bernatowicz T. J. Podosek F. A. Burnett D. S. Johnson M. L. Tatsumoto M. ^{244}Pu Abundance in Ordinary Chondrites
I-5	10:45 - 11:00	Lavielle B.* Marti K. Pellas P. Perron C. Search for Extinct ^{248}Cm in the Early Solar System
I-6	11:00 - 11:15	Chiou K. Y.* Manuel O. K. Tests for One Model of the Solar System's Origin
	11:15 - 11:45	BUSINESS MEETING, Room 1

LUNCH BREAK

SESSION J - COSMIC DUST

Wednesday, July 20 Room 2
9:30 - 11:00 a.m.

Chairman: G. J. Flynn
M. E. Zolensky

J-1	09:30 - 09:45	Klock W.* Thomas K. McKay D. S. Bulk Analyses and Mineral Analyses of Extraterrestrial Dust Particles
J-2	09:45 - 10:00	Rietmeijer F. J.* Alumino-Silica Glass: Its Significance for the Mineralogical Evolution of Chondritic Interplanetary Dust
J-3	10:00 - 10:15	Sutton S. R.* Herzog G. Hewins R. Chemical Fractionation Trends in Deep Sea Spheres
J-4	10:15 - 10:30	Thomas K. L.* Klock W. Blanford G. E. McKay D. S. Light and Major Elemental Analysis of Interplanetary Dust Particles: An Update on 26 IDP'S
J-5	10:30 - 10:45	Hartmetz C. P.* Blanford G. E. Gibson E. K., Jr. Comparison of Volatiles Released from Carbonaceous Chondrites and IDPs with the Halley Cometary Volatiles
J-6	10:45 - 11:00	Flynn G. J.* Sutton S. R. Cosmic Dust Particle Densities Inferred from SXRF Elemental Measurements

PRESENTED BY TITLE ONLY

J-7		Walker R. M. Zinner E. Large Chon Particles in the Stratospheric Dust Collection?

11:15 - 11:45 BUSINESS MEETING, Room 1

LUNCH BREAK

SESSION K - ORDINARY CHONDRITES

Wednesday, July 20 Room 1
1:30 - 5:00 p.m.

Chairmen: R. T. Dodd
A. E. Rubin

K-1	01:30 - 01:45	Rubin A. E.* Kamacite in Ordinary Chondrites
K-2	01:45 - 02:00	Wlotzka F.* Fredriksson K. "Exotic" Inclusions in the Study Butte H3-Chondrite
K-3	02:00 - 02:15	Hewins R. H.* Radomsky P. M. Lu J. Hasan F. A. Jarosewich E. L3.7 Chondrite From the Allende Strewn Field
K-4	02:15 - 02:30	Schutt J. W.* Zolensky M. E. Score R. Wells G. L. The Quest for Meteorites: Part One. Two New Meteorites From Deflation Surfaces in Lea County, New Mexico
K-5	02:30 - 02:45	Chickering C. Batchelor J. D. Sears D. W. G. Guimon R. K.* The Thermoluminescence Properties of Mn-Plagioclase Mixtures with Implications for Meteorites
K-6	02:45 - 03:00	Batchelor J. D.* Sears D. W. G. Thermoluminescence in Chondritic Mineral Separates - A Preliminary Report
	03:00 - 03:30	TEA BREAK
K-7	03:30 - 03:45	Morse A. D.* Sears D.W.G. Hutchison R. Guimon R. K. Alexander C. O. Wright I. P. Pillinger C. T. Alteration History of Type 3 Ordinary Chondrites
K-8	03:45 - 04:00	Walker R. M.* Zinner E. Search for Localized Regions of Isotopically Anomalous H in Several Type 3 Chondrites
K-9	04:00 - 04:15	Zhong H.* Jiang L. Yang X. Hu G. Yi W. Wang D. Ouyang Z. Li Z. Elemental Abundances of Ten E, O and C Chondrites Falls From China
K-10	04:15 - 04:30	Larimer J. W.* Fractionation in Chondrites: Major Elements Revisited
K-11	04:30 - 04:45	Wasson J. T.* Kallemeyn G. W. Rubin A. E. Group and Type Compositions of Ordinary Chondrites: Excepting Volatiles, No Relationship Between Type and Composition

K-12 04:45 - 05:00 Dodd R. T.*
Multiple Sources of Young H Group Chondrites

PRESENTED BY TITLE ONLY

K-13 Sipiera P. P. Kawachi Y.
Description of the Pine Dam, South Australia Meteorite

K-14 Steele I. M.
Enstatite Cathodoluminescence: Assignment of Emission Peaks to Cr and Mn and Application to Quantitative Analysis

K-15 Korotev R. L.
Nonuniform Distribution of Ir and Au in the Allende Meteorite Reference Sample

SESSION L - COSMOGENIC NUCLIDES AND AR-AR SHOCK EFFECTS

Wednesday, July 20 Room 2
1:30 - 4:30 p.m.

Chairmen: P.A.J. Englert
K. Marti

L-1 01:30 - 01:45 Nier A. O.* Schlutter D. J.
Helium Isotopic Ratios in Native and Processed Metals

L-2 01:45 - 02:00 Sauvageon H.*
A New Semi-Empirical Formula for High Energy Protons Spallation Cross Sections

L-3 02:00 - 02:15 Lavielle B.* Simonoff G. N.
New Systematics of Nuclear Reactions Induced by Proton or Neutron Bombardment in the Ga to Rh Target Mass Region

L-4 02:15 - 02:30 Zanda B.* Audouze J.
Nuclear Reactions Induced by Galactic Cosmic Rays in Iron Meteorites

02:30 - 03:00 TEA BREAK

L-5 03:00 - 03:15 Englert P.A.J.*
Depth and Size Dependent Production of Cosmogenic Nuclides: Information Content of Meteorite Depth Profiles

L-6 03:15 - 03:30 Graf Th.* Signer P. Wieler R.
Shielding and Size Corrected Exposure Ages of Chondrites

L-7 03:30 - 03:45 Wang S.*
Ordinary Chondrites: How Many Parent Bodies?

L-8 03:45 - 04:00 Stephan T.* Jessberger E. K.
Shock-Induced Disturbance of the K-AR System

L-9 04:00 - 04:30 Bogard D.* Jordan J. Mittlefehldt D. (EXTENDED PAPER)
^{39}Ar-^{40}Ar Dating of Mesosiderites: Evidence for Major Parent Body Disruption Less than 4 GY Ago

PRESENTED BY TITLE ONLY

L-10 Miura Y. Rucklidge J. Beukens R. Nagao K.
Cosmic-Ray Exposure and Terrestrial Ages of Antarctic Meteorites

PLENARY 4

Wednesday, July 20 Arkansas Union Theatre
8:00 p.m.

Chairman: M. J. Drake

Shaw D. M.* **(INVITED TALK)**
To Pergamon and Back: An Account of a Homeric Voyage, With Observations on the Beliefs and Practices of Fellow Travellers and Natives

SESSION M - ASTEROIDS AND PLANETS

Thursday, July 21 Room 1
8:30 - 11:30 a.m.

Chairmen: A. Kracher
E.R.D. Scott

M-1 08:30 - 08:45 Wetherill G. W.*
Accumulation and Fragmentation Model of the Asteroid Belt

M-2 08:45 - 09:00 Scott E. R. D.*
Meteorite Evidence for the Nature and Origin of Primordial Chemical Variations Across the Asteroid Belt

M-3 09:00 - 09:15 Taylor G. J.*
The Role of Impacts in Asteroid Differentiation

M-4	09:15 - 09:30	Jones T. D.* Lebofsky L. A. Lewis J. S. Observational Evidence for Solar Wind Induction Heating of Low Albedo Asteroids
M-5	09:30 - 09:45	Jones J. H.* Treiman A. H. Janssens M.-J. Wolf R. Ebihara M. Core Formation on the Eucrite Parent Body, the Moon and the AdoR Parent Body
M-6	09:45 - 10:00	Drake M. J.* Malvin D. J. Capobianco C. J. Primordial Differentiation of the Earth: Ni, Co, Ir, and Au
	10:00 - 10:15	COFFEE BREAK
M-7	10:15 - 10:30	Kracher A.* Trivedi R. Iron Meteorites and the Physics of Core Formation
M-8	10:30 - 10:45	Broadhurst C. L.* Drake M. J. Hagee B. E. Bernatowicz T. J. Solubilities and Partitioning of Noble Gases in Mineral/Melt Systems: Results for Ne, Ar, Kr and Xe in Anorthite Diopside, Forsterite, and Coexisting Melt with Implications for Terrestrial Planet Atmospheric Evolution
M-9	10:45 - 11:00	Musselwhite D. S.* Swindle T. D. Drake M. J. Mineral/Melt Partitioning of I: Implications for Mantle Outgassing
M-10	11:00 - 11:15	Fang H. Chai C. F.* Mao X. Y. Ma S. L. Ouyang Z. Y. Xie H. S. Implication of Trace Element Distribution During Melting Process of the Jilin Chondrite (H5)
M-11	11:15 - 11:30	Newsom H. E.* Scott E. R. D. Accretion of Planets: Evidence from Meteorites and Asteroids
		PRESENTED BY TITLE ONLY
M-12		Hartmann W. K. Trojan Asteroid Lightcurves: Continuing Work

SESSION N - K-T BOUNDARY AND A FIREBALL

Thursday, July 21 Room 2
8:30 - 11:30 a.m.

Chairmen: F. T. Kyte
U. Krahenbuhl

	08:30 - 08:45	Chairman's Opening Remarks - F. T. Kyte
N-1	08:45 - 09:00	Pugh R. N.* Kraus D. J. Grant County Oregon Daylight Fireball of October 23, 1987
N-2	09:00 - 09:15	Kyte F. T.* Lowe D. R. Byerly G. R. Noble Metal Abundances in Early Archean Spherule Layers from South Africa
N-3	09:15 - 09:30	Gilmour I.* Boyd S. R. Pillinger C. T. Nitrogen Isotope Geochemistry of K-T Boundary Site in New Zealand
N-4	09:30 - 09:45	Krahenbuhl U.* Geissbuhler M. Buhler F. Eberhardt P. The Measurement of Osmium Isotopes in Samples from a Cretaceous/Tertiary (K/T) Section of the Raton Basin, U.S.A.
N-5	09:45 - 10:00	Koeberl C.* Murali A. V. Nazarov M. A. Sharpton V. L. Burke K. The Kara Impact Structure (USSR) and the K/T Boundary Event
	10:00 - 10:30	COFFEE BREAK
N-6	10:30 - 10:45	Hildebrand A. R.* Boynton W. V. Impact Wave Deposits at the Cretaceous/Tertiary Boundary Imply an Oceanic Impact Site Near North America
N-7	10:45 - 11:00	Chai C. F.* Kong P. Chemical Speciation Study of Anomalous Iridium from K-T Boundary
N-8	11:00 - 11:15	Bohor B. F.* K-T Boundary Claystone is a Distal Ejecta Blanket
N-9	11:15 - 11:30	Bohor B. F.* Betterton W. J. Are the Hollow Spherules in K-T Boundary Claystones Altered Microtektites?

POSTER PRESENTATION

N-10 Chai C. F. Ma J. G. Kong P. Zhou Y. Q. Ma S. L. Wang X. F.
Geochemical Anomaly Across the Ordovician-Silurian (O-S) Boundary, Yichang, China, and Their Implications

LUNCH BREAK

PLENARY 5

Thursday, July 21 Room 1
1:30 - 2:30 p.m.

Chairman: S. R. Taylor

01:30 - 02:00 Keil K.* **(LEONARD ADDRESS)**
Enstatite Meteorites and Their Parent Bodies

02:00 - 02:30 Dence M. R.* **(BARRINGER ADDRESS)**
Circular Arguments: Peaks and Troughs in the Crater Game

PLENARY 6

Friday, July 22 Room 1
8:30 - 9:00 a.m.

Chairman: J. W. Larimer

08:30 - 09:00 Anders E.* Tang M. Zinner E. **(INVITED PAPER)**
Interstellar Grains in Meteorites: Diamond and Silicon Carbide

09:00 - 09:30 COFFEE BREAK

SESSION O - CAI'S

Friday, July 22 Room 1
9:30 - 12:00 noon

Chairmen: W. V. Boynton
T. R. Ireland

09:30 - 09:45 Chairman's Opening Remarks - W. V. Boynton

O-1 09:45 - 10:00 Boynton W. V.*
Nebular Processes Associated with CAI Rim Formation

O-2 10:00 - 10:15 MacPherson G. J.* Fahey A. J. Lundberg L. L. Zinner E.
Al-Mg Isotopic Systematics and Metamorphism in Five Coarse-Grained Allende CAIs

O-3 10:15 - 10:30 Caillet C.* Goldstein J. I. Velde D. El Goresy A.
Estimation of Possible Thermal History of a Vigarano CAI

O-4 10:30 - 10:45 Kuehner S. M.* Grossman L.
Relationships Between Compact Type A and Spinel-rich Inclusions Inferred from a Composite CAI

O-5 10:45 - 11:00 Johnson M. L.* Burnett D. S. Woolum D. S.
Relict Refractory Element Rich Phases in Type B CAI

O-6 11:00 - 11:15 Ireland T. R.* Fahey A. J. Zinner E. K.
Petrogenesis of a Hibonite-Pyroxene Spherule from Murchison

O-7 11:15 - 11:30 Brigham C. A.* Hutcheon I. D. Papanastassiou D. A Wasserburg G. J.
Correlated Isotope Fractionation and Formation of Purple Fun Inclusions

O-8 11:30 - 11:45 Davis A. M.* MacPherson G. J.
Further Isotopic and Chemical Investigations of an Isotopically Heterogeneous Vigarano Inclusion

O-9 11:45 - 12:00 Kennedy A. K.* Beckett J. R. Hutcheon I. D.
The Distribution of Trace Elements in an Allende Type B1 Inclusion

PRESENTED BY TITLE ONLY

O-10 Nagahara H. Nagasawa H.
Clinopyroxene in Type B1 CAI

SESSION P - DIFFERENTIATED METEORITES

Friday, July 22 Room 2
9:30 - 12:15

Chairmen: C. A. Goodrich
U. Ott

P-1 09:30 - 09:45 Saito J.* Takeda H.*
"Adsorbed" Oxygen in the Santa Catharina Ataxite

P-2 09:45 - 10:00 McCartney A. P.* Kimberlin J.
The Cape York Meteorite as a Metal Source for Prehistoric Canadian Eskimos

P-3	10:00 - 10:15	Zhang J.* Williams D. B. Goldstein J. I. AEM Investigation of the Plessite Structure of A IIIB Iron Meteorite --- Grant
P-4	10:15 - 10:30	Treiman A. H.* Jones J. H. Janssens M. J. Wolf R. Ebihara M. Angra Dos Reis: Complex Silicate Fractionations
P-5	10:30 - 10:45	McKay G.* Le L. Wagstaff J. Lindstrom D. Experimental Trace Element Partitioning for Synthetic LEW 86010 Analogs: Petrogenesis of a Unique Achondrite
P-6	10:45 - 11:00	Berkley J. L.* Ion Probe Analysis of Melt Veins in Meta78008 Ureilite
P-7	11:00 - 11:15	Goodrich C. A.* Patchett P. J. Drake M. J. Nd and Sr Isotopic Analyses of Ureilites: Evidence for Chemical Activity at 3.74 Ga or Younger
P-8	11:15 - 11:30	Spitz A. H.* Boynton W. V. Trace Element Analysis of Ureilite Meteorites: Extending the Range of Characterized Samples
P-9	11:30 - 11:45	Wiens R. C.* What We Think We Know From Noble Gases in Shergottite EETA 79001
P-10	11:45 - 12:00	Ott U.* Lohr H. P. Begemann F. New Noble Gas Data for SNC Meteorites: Zagami, Lafayette, and Etched Nakhla
P-11	12:00 - 12:15	Wentworth S. J. Gooding J. L.* Calcium Carbonate in Nakhla: Further Evidence for Pre-terrestrial Secondary Minerals in SNC Meteorites

ADJOURN

PLENARY I

PRESIDENTIAL ADDRESS

SOMEWHERE OVER THE RAINBOW

G.J. Wasserburg, Division of Geological and Planetary Sciences, Calfornia Institute of Technology, Pasadena, CA 91125

The study of meteorites has produced a wealth of information about these objects. Petrologic and chemical observations of meteorites have shown the presence of planetary differentiates and of undifferentiated aggregates resulting from nebular condensation and the interaction of these aggregates due to metamorphism. Equilibrium chemistry in a solar gas and in planetary environments has been an excellent guide to our studies. Studies by several groups have yielded remarkable discoveries about the early stages of planetary evolution and of precursor components from the solar nebula and from the interstellar medium (ISM). The isotopic studies have established a rather well defined and short time scale ($\sim 10^6$ y) between some types of nucleosynthesis and the formation of protoplanetary materials and planets. The diverse isotopic anomalies which are unconnected to radioactive parents appear to result from incomplete mixing of debris from different stellar sources before formation of the solar system; some anomalies may come from processes in the early solar system itself. The magnitude of the isotopic effects which have been discovered has grown enormously, and the geometric scales at which they are found have correspondingly decreased to far below optical microscopic dimensions. The number of distinct isotopic effects has increased to populate a zoo of anomalies. We have now found the rainbow of interstellar dust and debries in meteorites. The "earliest" material has been the object of search for over three decades.

The remarkable success of this venture is a testimony to the belief that meteorites are the key to our most ancient past. However, the astonomical sites where the components were produced is quite unclear, the nuclear astrophysical mechanisms are only generally defined (SPQR), and the fundamental processes in meteorites which governed their aggregation and formation are obscure. We have many strong hints of the precursor mechanisms; however, the chemical and physical processes which control the chemistry of the ISM and the collapsing gas and dust mixture and produced chondrules is at best poorly understood. We are in a stage where both meteoritical and astronomical studies are yielding marvelous discoveries and providing a general morphologic guide to the making of solar systems. What we now require is an understanding of the physical and chemical processes and reaction mechanisms which actually control the state of matter that went to make up the early solar nebula. Over the past two decades numerous astronomical observations have been made of dense molecular clouds--the placental medium from which the solar system formed. These clouds contain a rich range of compounds and diverse isotopic compositions. Recently a newly formed solar system has been found. We are rapidly discovering the morphology (fossils) of the phenomena leading to solar system formation and the relicts which are our focus of attention.

Having found the rainbow, we must now seek beyond it, both in theory and experiment, to understand what actually took place. Establishing the relationships of our observations to the basic cosmochemical processes will lead us to real understanding.

TEM OBSERVATIONS OF INTERSTELLAR SILICON CARBIDE FROM THE MURRAY AND MURCHISON CARBONACEOUS METEORITES

T. Bernatowicz, *McDonnell Center for the Space Sciences and the Physics Department, Washington University, St. Louis, MO 63130.*
G. Fraundorf, and P. Fraundorf*, *Monsanto Electronic Materials Company and Monsanto Corporate Research and Development Staff, Monsanto Research Center, St. Louis, MO 63167*
**Also the Physics Department, Washington University*
Tang Ming, *Enrico Fermi Institute and Department of Chemistry, University of Chicago, Chicago, IL 60637.*

We report here results of TEM observations of interstellar SiC grains in dissolution residues from the Murray and Murchison carbonaceous meteorites, which have been subjected to previous isotopic studies (Zinner *et al.*, 1987; Tang *et al.*, 1988). These residues have been shown to have isotopically anomalous noble gas compositions, and to contain grains with isotopically anomalous Si, C, and N.

Darkfield imaging, tilting under brightfield conditions, electron energy loss spectroscopy (EELS) and energy dispersive X-ray spectroscopy (EDXS) show the major constituents of these residues to include crystalline grains in the 0.1 to 3 micron size range whose major elements are Si and C.

Electron diffraction patterns from individual grains and portions of grains invariably show one of the following: (a) single crystal cubic (β) silicon carbide spot spacings and interspot angles, in one case for patterns taken through a 90 degree range of incident electron illumination (Bernatowicz *et al.*, 1987); (b) the reciprocal lattice structure of β-SiC with fcc twinning in one or more {111} direction; or (c) spacings characteristic of β-SiC (and other SiC polytypes) orthogonal to a tetrahedral layering direction (e.g. the cubic {111}), with nearly continuous streaking parallel to that direction. Diffraction patterns from one twinned β-SiC grain from a Murray residue further show 22Å repeats whose explanation, as either a distinct polytype (e.g., the 27R form) or as result of twins upon twins, is still being investigated.

High resolution TEM imaging, using a Philips EM430ST TEM with point resolution near 1.9Å and damping cutoff in that region as well, shows some of the twins to be in the form of {111} laths only about 20Å in thickness. It suggests separately also the existence of "bulk twinning", on a scale comparable to grain dimensions. The habit for these "bulk" twins remains to be determined. We estimate on average between 10^5 and 10^6 cm^2 of twin interface per cm^3 of SiC examined, although (as indicated above) the extent of disordering varies significantly from grain to grain. Finally, periodicity "phase" information in high resolution images down the cubic <110> direction reproduces the triangular symmetry for SiC atom columns expected of a structure consisting of separate interpenetrating fcc lattices of Si and C, offset in the <111> direction by about $\sqrt{3}$ a/4.

β-SiC is a common form for SiC crystals nucleated from the vapor phase, but it is commonly formed under other conditions as well. Identification of coexisting polytypes may provide tighter constraints on formation times and temperatures. Twinning in β-SiC is also common. However, the details of the twinning such as twin lath thickness and number density may put constraints on grain formation rates and temperatures and subsequent thermal history. Since ion microprobe studies (Zinner *et al.*, 1987) point to isotopic differences from grain to grain, an opportunity to correlate these differences with grain structure might prove very interesting. The observations described here also constrain the prior irradiation history of the grains, although the nature of those constraints is still under investigation. For example, the grains certainly are not metamict and we also see no evidence for nuclear particle tracks or other irradiation induced defects.

Bernatowicz T. *et al.*, 1987. *Nature* **330**, 728-730.
Tang Ming *et al.*, 1988. *Lunar Planet. Sci. XIX*, 1177-1178.
Zinner *et al.*, 1987. *Nature* **330**, 730-732.

THE CARBON COMPONENTS IN MURRAY RESIDUE CF; Wright, I.P., Ash, R.D., Grady, M.M., Pillinger, C.T. and Tang, M.*, Planetary Sciences Unit, Department of Earth Sciences, Open University, Walton Hall, Milton Keynes, MK7 6AA, England; *Enrico Fermi Institute, University of Chicago, Chicago, Illinois 60637, U.S.A

A recent ion probe study (1) of individual grains in a chemical/physical separate (CF) prepared from the Murray meteorite has shown there to be two carbon components present: Cδ (diamonds) and a form of SiC. The measurements made by ion probe are consistent with the sampling locations having very low Si/C ratios being diamond with low $\delta^{13}C$ (-38‰; ref 2). Extrapolating the carbon isotopic data from -38‰ to the outliers in the data distribution with Si/C ratios of 1 suggests the presence of SiC of $\delta^{13}C$ between +600 and +1500‰, although no $\delta^{13}C$ values >+1000‰ were measured during the study. Cδ is known to burn at T<550°C (2,3); SiC, even if fine-grained, ought to be more stable. Therefore, an apparently straightforward two-component sample such as CF would appear to be an ideal candidate for analysis by stepped combustion which should resolve the true isotopic compositions of Cδ and SiC. Such an investigation would also greatly facilitate the interpretation of stepped combustion data from less highly processed acid residues. Stepped combustion of CF shows two substantial releases of carbon which are well resolved in terms of combustion temperature (200-550°C and 1000-1200°C) consistent with the two component model (1). The ratio of low/high temperature component is approximately two. Carbon isotopic data for the high temperature component reach a plateau with three consecutive values of $\delta^{13}C$ within ±15‰ of +1370‰, suggestive of a single entity. The combustion temperature of Cδ is known to be low (2, 3), hence the high temperature component is inferred to be SiC; it may be Cβ the host of s-Xe known to be in CF (1). Stepped combustion of commercial SiC polishing powder (F600 grade, 3-19μm) produced a release of carbon at 1100-1200°C, the higher temperature of combustion reflecting a coarser grain size than the mineral present in Murray (*ca.* 0.1 to 0.2μm, ref 4). The $\delta^{13}C$ value of the SiC in CF (+1370‰) is *ca.* 400‰ heavier than any of the grains measured by ion probe, suggesting that the ability of the ion probe to resolve the individual components is compromised by the size of the primary beam, which is far larger than the size of the grains under study.

Over the temperature range at which the low temperature carbon is released no measurements were obtained which would accord with Cδ having a $\delta^{13}C$ of -38‰. The 400-550°C region gave values of +4‰ to +161‰. Assuming Cδ has a $\delta^{13}C$ of -38‰, as indicated by previous investigation of residues rich in this component (2), then the presence of a minor low temperature isotopically heavy carbon component is is inferred which combusts at the same temperature as the diamond. Given that the release profile for carbon during stepped combustion of CF suggests a two-component mixture, and moreover indicates a major difference in the stability of these components to combustion, then a comparatively sharp change in isotopic composition between low and high temperature regimes may be expected. The opposite is, in fact, apparent: $\delta^{13}C$ exhibits a monotonic trend from +4 at 500°C to +1384‰ at 1100°C with clear preferred values of +460 to +500‰ at 600 - 650°C and +970 to +1000‰ at 800 - 900°C. Such a trend is compatible with CF containing several minor heavy components in addition to the low temperature material which obscures Cδ. It is considered unlikely that the stepped combustion process progressively attacks the same generation of SiC (which has, for instance, differing grain size or suffered varying degrees of degradation during the preparation of CF), since this would not produce preferred $\delta^{13}C$ values. Stepped combustion demonstrates that CF is not a simple two component mixture: the scatter in the ion probe data is real rather than an experimental artefact.

References: (1) Zinner *et al.* (1987), *Nature*, **330**, 730-732; (2) Swart *et al.* (1983), *Science*, **220**, 406-410; (3) Ash *et al.*, (1987), *Meteoritics*, **22**, 319; (4) Bernatowicz *et al. Nature* **330**, 728-730.

TWINNED DIAMONDS IN THE ORGUEIL CARBONACEOUS CHONDRITE; Peter R. Buseck, Departments of Geology and Chemistry, and J. C. Barry, Center for Solid State Science, Arizona State University, Tempe, AZ 85287

Tiny diamonds were reported from insoluble residues from the Allende, Murray, Murchison, and Indarch carbonaceous chondrites by Lewis et al. [1], and there have been several confirming studies by other groups. We have have found the first diamonds in residues from the Orgueil CI chondrite,(prepared by Halbout, Robert and Javoy [2]). Such diamonds were not observed *in situ* in the HRTEM study of Orgueil by Tomeoka and Buseck [3], and so they are presumably extremely finely dispersed.

The Orgueil diamonds are from 20 to 50 Å in diameter. The crystal sizes follow close to a log normal distribution. We see no voids, inclusions, or defects that would accomodate trapped gases and so conclude that such gases, if present in the structural fashion implied by [1,4,5], must indeed occur as point interstitials.

Roughly 5 to 10 % of the ~200 Orgueil diamond crystals we have observed are twinned and so are apparently unique among meteoritic diamonds. They have (111) as their composition planes, with both halves of the twins of approximately equal dimensions. Twinning on (111) is common in terrestrial diamonds, although they are usually flattened parallel to the twin plane [6]. The powder patterns of the Orgueil diamonds also appear to be somewhat unusual. In regions where no diamonds or graphite are visible, the powder pattern nevertheless has a ring at 2.1 Å (cf. 111 diamond = 2.06 Å) and a second diffuse ring at 1.2 Å (cf. diamond 220 = 1.26 Å and 311 = 1.08 Å).

Conflicting origins have been proposed for the tiny diamonds in meteorites - (a) that they formed at low pressure, analogous to the way that CVD diamonds are produced [1] or (b) that they formed at high pressures behind supernova shock waves [7,8]. We believe that the twinning in the Orgueil diamonds is more compatible with a high-pressure origin than with free crystallization in unconfined space.

We thank Francois Robert and Jerome Halbout for the Orgueil residues. Supported by NASA grant NAG 9-59.

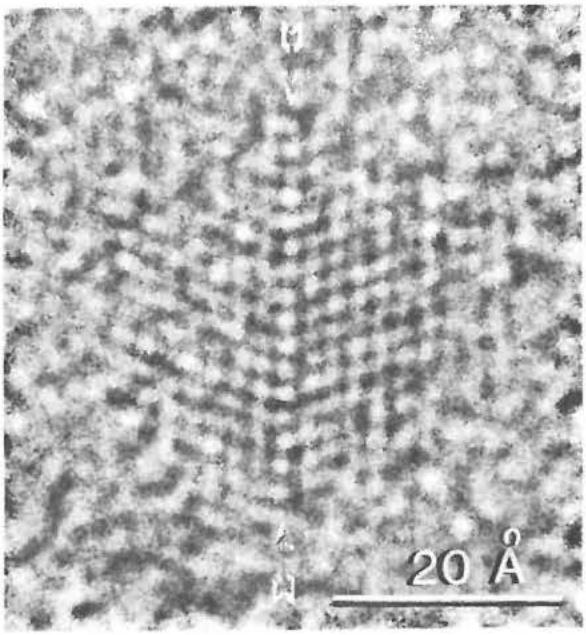

[1] Lewis R.S., Tang M., Wacker J.F., Anders E. & Steele E. (1987) Nature, 326, 160-162. [2] Halbout J., Robert F. & Javoy M. (1986) Geochim. Cosmochim. Acta, 50, 1599-1609. [3] Tomeoka K. & Buseck P.R. (1988) Geochim. Cosmochim. Acta, in press. [4] Anders E. (1987) Phil. Trans. R. Soc. Lond., A 323, 287-304. [5] Ming T. & Anders E. (1988) Geochim. Cosmochim. Acta, in press. [6] Palache C., Berman H. & Frondel C., eds. (1944) The System of Mineralogy, Vol. 1, 7th Edition,p. 147 [7] Blake D., Freund F., Bunch T. & Chang S. (1988) Proc. Lunar and Planet. Sci. Conf. 19th, p. 94-95. [8] Blake D., Freund F., Krishnan K., Echer C., Shipp R., Bunch T., Tielens A., Lipari R. J., Hetherington C. & Chang S. (1988) Nature, in press.

ORGANIC CARBON IN THE ORDINARY CHONDRITES. C.M.O'D Alexander[1], J.W. Arden[2], I. Gilmour[3], N. Schelhaas[4], U.Ott[4], and C.T. Pillinger[1] (1) Open University, U.K. (2) Oxford University, U.K. (3) University of Chicago, USA. (4) Max-Plank-Institut Für Chemie, F.G.R.

The low temperature post accretionary history of the CM and CI chondrites (1) has led to the preservation of organic material within them (*e.g.* 2). The recent identification of hydrous alteration in ordinary chondrites (OCs) suggests the possibility that organic material has also been preserved in these meteorites (3). Based on the comparison of N isotope release profiles obtained by stepped combustion of HF/HCl residues, Alexander *et al.* (4) concluded that an organic material similar to that in CM and CIs is also present in Semarkona (LL3.0). The release profiles of the organic materials are complex. High resolution stepped combustion experiments, for both N and C, are in progress that will enable a better isotopic characterisation of the several components that comprise this material. Other techniques including infra-red spectroscopy and pyrolysis MS are being explored to confirm the organic nature of the carbonaceous material in Semarkona.

Other OCs, including Bishunpur (LL3.1) and Krymka (LL3.1), are being studied to investigate the extent to which organic matter is present in this group. The interpretation of release profiles from most OCs will be complicated by the fact that they have undergone limited metamorphism. It is as yet unclear what effect thermal maturation will have on the organic material but the tendency will be for the organic material to graphitise, resulting in higher combustion temperatures and higher C/N ratios. We have begun to explore this problem by analysing a range of meteorites between petrologic types 3.0 and 4 in order to establish whether systematic trends resulting from metamorphism exist. Stepped combustion of HF/HCl residues of two OCs, ALHA 77214 (L3.4) and Parnallee (LL3.6), shows they do not contain organic matter like that in Semarkona. However, they do have light N releases ($\delta^{15}N \approx -50‰$) between 450 and 650°C. One at present rather speculative possibility is that the light N component in ALHA 77214 and Parnallee is the metamorphosed equivalent of the light N component that dominates the organic material in Semarkona.

If the organic matter in Semarkona is pre-accretionary this raises some interesting problems for models of nebular evolution. Particularly if the organic matter is of an interstellar origin, which may be the case if it is demonstrated to have a high-D abundance (5). Organic material could not have survived high temperature condensation (the best current explanation for the bulk compositions of the chondrites). Indeed complex organic molecules would not have been stable in a nebula of solar composition above 400 K (2). Therefore, it seems the estimated accretion temperatures of the OCs (450-550 K) based on their mineralogy and volatile element contents (*e.g.* 6) are too high. (1) Bunch and Chang (1980) G.C.A. 44, 17. (2) Hayatsu and Anders (1981) Topics in current chemistry 99,1. (3) Hutchison *et al.* (1987) G.C.A. 51, 1857. (4) Alexander *et al.* (1988) Lun. Plan. Sci. XIX, 5. (5) Yang and Epstien (1983) G.C.A 47, 2199. (6) Laul *et al.* (1973) G.C.A 37, 329.

ISOTOPICALLY LIGHT CARBON IN THE ALLENDE METEORITE: R.D.Ash, J.W.Arden*, M.M.Grady, I.P.Wright and C.T.Pillinger. Planetary Sciences Unit, Department of Earth Sciences, The Open University, Milton Keynes MK7 6AA, U.K.
*Department of Earth Sciences, University of Oxford, Oxford OX1 3PR, U.K.

Recent work on the Allende meteorite has shown that it contains at least two components with isotopically heavy carbon (1). A third anomalous phase containing isotopically light carbon was postulated (2). Further work has shown that there is indeed a light component with a carbon isotopic value of at least -261‰ present, combusting between 700-800°C. This is the most ^{12}C enriched component encountered in any meteorite and supplants Cθ, the carbon with a $\delta^{13}C$=-50‰ trapped in spinel in this respect.

An acid residue of Allende was prepared using non-oxidising reagents as harsh reagents, such as $HClO_4$ are known to destroy certain anomalous phases such as Cα (3) and Cθ. Initial results showed that there was heavy carbon present, with a value of +151‰ being recorded over the 700-750°C temperature step. However, 38% of the residue consisted of isotopically normal Cγ ($\delta^{13}C$ =-17‰) and Cδ ($\delta^{13}C$=-38‰), which masked its true isotopic composition due to a tailing effect. This effect was reduced using a repeated precombustion technique (four precombustions were carried out at 400°C producing four precombustion residues, PC(a)-PC(d)) which removed the majority of these problematical phases, leading to a residue containing just 3.3% carbon.

Detailed analysis of the four precombusted residues showed that two forms of heavy carbon are present in the meteorite, one combusting at temperatures *ca.* 700-750°C and a second at *ca.* 1000°C (1). These have maximum $\delta^{13}C$ values of +345‰ for PC(c) and +527‰ for PC(d). We believe that the low temperature heavy carbon phase is a noble gas poor form of Cα, containing little or no NeE-(L) which we have called C.ℵ (C *aleph*). Cα and C.ℵ have identical carbon isotopic signatures. Assuming that the maximum measured $\delta^{13}C$ value of +345‰ represents the true isotopic composition of C.ℵ its concentration is *ca.* 5ppm, the same as the concentration of Cα in the CM2 meteorites as calculated on the basis of noble gas content (4).

The second heavy carbon component may be Cβ, the carrier of s-Xe (5), present in concentrations *ca.* 8ppb, compared with 400ppb in CM2s, although there is no definite data on this point and its isotopic composition cannot be matched to Cβ as previously determined on CM2 residues. In an attempt to measure a limiting $\delta^{13}C$ value for the high temperature heavy C a prolonged, higher temperature (500°C) precombustion experiment was performed on PC(d) to reduce the tailing of the low temperature carbon to a minimum to give PC(e). In addition to reducing the overall carbon content to 0.13 wt%, this extended precombustion also reduced the $\delta^{13}C$ values of both the isotopically heavy components to +248 and +340‰ respectively. This change was affected because a new, isotopically light component, $\delta^{13}C$<-261‰, burning at intermediate temperatures has been revealed. At this point we are unable to decide whether the light component was masked by other carbonaceous material or whether it has been released by degradation of noncarbonaceous minerals in the oxygen associated with the combustion experiment. Because of the similarity of the combustion temperatures of the two heavy carbon components and the new light component, the $\delta^{13}C$ value of -261‰ measured for the latter may well be an upper limit for a substance dramatically enriched in ^{12}C.

(1) Ash *et al.*, 1988. *L.P.S.C.* **XIX**, 15-16. (2) Ash (Oral presentation), *L.P.S.C.*, **XIX** (3) Alaerts *et al.*, 1980. *G.C.A.* **44**,189-209. (4) Anders 1987. *Phil. Trans R. Soc. Lond.* **A323**, 287-304. (5) Swart *et al.*, 1983. *Science* **220**,406-410.

CARBON ISOTOPIC MEASUREMENTS OF MICROMETEORITES; Yates,P., Wright,I.P., Prosser,S.J., Pillinger,C.T. and Hutchison,R.*, Planetary Sciences Unit, Open University, Walton Hall, Milton Keynes, MK7 6AA, England; * British Museum (Natural History), Cromwell Road, London SW7 5BD, England.

A complete understanding of the carbon in interplanetary dust particles (IDPs) should assist efforts to comprehend the relationships of disparate solar system bodies such as comets, meteorites and the terrestrial planets. The nature of carbon in stratospherically-collected IDPs has been elucidated by the use of electron microscopy and infrared spectroscopy with the identification of hydrocarbons (1, 2), amorphous carbon (3), poorly-graphitised carbon (4), lonsdaleite (5), ε-carbide (6) and carbonates (7). Attempts have also been made to determine the stable isotopic composition of carbon in IDPs (8, 9) but the results obtained so far have been inconclusive. The analytical problems stem from the fact that an average-sized IDP is too small to permit carbon isotopic analysis using existing static mass spectrometry and the data acquired by ion probe have errors which are large compared to the apparent variations.

In order to combat problems of sensitivity, Carr *et al.* (10) have tried to gain an insight into the isotopic composition of carbon in IDPs through analyses of individual deep-sea spherules. Although these materials are much larger and therefore stand a better chance of being measurable using stepped combustion/static mass spectrometry, the effects of pulse-heating or melting during atmospheric entry, coupled with contamination problems associated with the sojourn in the oceanic environment conspires to make interpretation somewhat difficult. Regardless, the initial study has shown that for certain samples it is possible to resolve small amounts of indigenous carbon components which are isotopically distinct from terrestrial contaminants (11).

In order to further the study of carbon in IDPs, a new suite of deep-sea spherules have been extracted from Pacific sediments. These have been characterised by XRD, electron probe and electron microscopy. During this process a number of small manganese nodules have been collected which have subsequently been analysed for carbon components by stepped combustion techniques as a control on the likely levels of oceanic contamination. In addition to deep-sea spherules, samples of Greenland cryoconite and found in Antarctic ice (kindly supplied by M. Maurette) are also scheduled for analysis. Higher levels of sensitivity have been achieved by the use of a new static mass spectrometer (12) which is able to make $\delta^{13}C$ measurements on picomole quantities of CO_2 gas to precisions of ±2.5‰.

References:

(1) Fraundorf and Shirck (1979), *Proc. 10th L.P.S.C.*, 951-976; (2) Allamandola *et al.* (1987),*Science*, **237**, 56-59; (3) Bradley *et al.* (1984),*Science*, **223**, 56-58; (4) Reitmeijer and Mackinnon (1985), *Nature*, **315**, 733-736; (5) Reitmeijer and Mackinnon (1987), *Nature*, **326**, 162-165; (6) Christoffersen and Buseck (1983), *Science*, **222**, 1327-1329; (7) Sandford (1986), *Science*, **231**, 1540-1541; (8) McKeegan *et al.* (1985), *Geochim. Cosmochim. Acta*, **49**, 1971-1987; (9) Carr *et al.* (1986), *Meteoritics*, **21**, 344-345; (10) Carr *et al.* (1984), *Lunar Planet. Sci.*, **XV**, 137-139; (11) Wright *et al.* (1988), *in prep.*; (12) Prosser *et al.* (1988), *11th Int. Mass Spec. Conf.*

THE ABUNDANCE, DISTRIBUTION AND CHEMICAL STATE OF CARBON IN INTERPLANETARY DUST; J. P. Bradley[1], D. E. Brownlee[2], L. S. Schramm[2], N. L. Dietz[1], [1]McCrone Associates, Westmont, IL 60559; [2]Dept. of Astronomy, Univ. of Washington, Seattle, WA 98195.

The abundance, distribution and chemical state of carbon in interplanetary dust is poorly known but of considerable interest. Analysis difficultities and various contamination problems have hindered the study of carbon and its compounds. The study of carbon in IDPs is critical for understanding the relationship between dust, meteorites and comets and for evaluation of the processes that formed carbonaceous matter in the primitive solar system materials. A major goal of carbon studies is to determine why carbon is so strongly fractionated among meteoritic materials. Relative to solar composition, meteoritic materials have the following approximate C/Si ratios, Halley dust-.5,IDP's-.15,CI-.06, CM-.03 and L-.001

To better understand carbon in IDP's we have undertaken a study of carbon in chondritic IDP's and carbonaceous chondrites using both X-ray analysis with a thin window energy dispersive SiLi detector and energy loss analysis using a parallel EELS spectrometer. We are investigating bulk 10um particles and microtome thin sections less than 1000A thick. The thin sections are critical for fine scale spatial analysis and for EELS work but they are also critical for bulk carbon measurement. Detected carbon X-rays from a chondritic composition particle are only generated in the outer .1um of the particle skin. True analysis of the bulk carbon content in a 10um particle can only reliably be made from a thin slice that transects the particle interior. A major difficulty in this program is producing microtome slices that are not contaminated carbonaceous matter. We have partly solved this problem by embedding the samples in metal or a polymer that contains a molecular tag that provides a means of distinguishing indigenous carbon from the imbedding medium.

Our bulk carbon abundances for chondritic IDP's are still preliminary but taken at face value they indicate that that the mean C/Si atom ratio is 1.75. If this value is correct it implies that the IDP carbon abundance is intermediate between CI and that indicated for Halley dust from the PIA and PUMA mass spectrometers. Carbon distribution in many IDP's is heterogenous. Similar to the Halley results the IDP's contain submicron areas of pure carbonaceous matter (analogous to the CHONs at Halley) and submicron areas that contain carbon and silicates (analogous to the Halley "mixed"). They also contain single mineral grains with no carbon, analogous to the Halley silicate grains. Qualitatively there is an apparent similarity between Halley and some of the IDP types.

An unusual insight into the carbon problem has come from the analysis of dust particles that were strongly heated during atmospheric entry and particles that were intentionally heated in the laboratory. These particles (the MMS or metal mound silicate) are composed of silicate spheres, FeNi metal mounds and irregular low Z material that was apparently immiscible in the spheres. These particles appear to have been very strongly heated but not sufficiently oxidized to destroy metal or carbon. The irregular low Z masses in these particles appear to be nearly pure elemental carbon. The survival of elemental carbon in particles that have experienced melting and partial evaporation of Si and Fe suggests that a significant fraction of the carbon in IDP's is in a nonvolatile form that is capable of surviving vacuum pyrolysis at high temperature. In connection with the studies of carbon in Halley dust it interesting to speculate that carbon in comet dust may be grouped into two distinct classes. One class is volatile and is lost from small interplanetary particles on time scales of minutes to years while the other is relatively refractory and partly survives extreme heating.

MAFIC MINERAL COMPOSITIONS OF IGNEOUS CLASTS IN THE LEWIS CLIFFS 85300, 85302, 85303 POLYMICT EUCRITES.

Jean Kozul and Roger H. Hewins: Rutgers University, Dept. of Geosciences, New Brunswick, NJ 08903

In the LEW 85300, 85302 and 85303 polymict eucrites, bulk pyroxene and olivine compositions of Mg-rich, selected eucritic and Fe-rich igneous clasts fall within the compositional range of igneous clasts in polymict eucrites (1). All of the clasts studied contain An_{80-100} as a major phase.

The Mg-rich clast, 85302,17, is a granular, coarse-grained, heavily shocked cumulate clast with $En_{55}Wo_9$. Inverted pigeonite exsolved at 675°C (2). REE abundances of this clast (2) are low.

The 85303,63 eucritic clast is sub-ophitic and contains predominantly pigeonite, $En_{36}Wo_{15}$, plus some primary augite, $En_{32}Wo_{40}$. Zoning in some of the pigeonite grains show that this clast has not fully re-equilibrated. REE abundances (2) fall in the normal eucritic range.

The 85302,16 sub-ophitic, coarse-grained eucritic clast contains mostly pigeonite $En_{35}Wo_{10}$ with a few augite $En_{31}Wo_{39}$ grains.

The sub-ophitic to granular, coarse-grained, Fe-rich clast, 85300,45 contains bulk $En_{33}Wo_8$, $En_{30}Wo_{29}$ and Fa_{83}. Olivine is fine-grained, granular and along with minor plagioclase lines the pyroxene-plagioclase grain boundaries and healed fractures in the pigeonite. Augite occurs as small grains, <1mm, in plagioclase. The two pyroxenes crystallized at the same time and the olivine is a late magmatic phase. REE abundances of this clast (2) are higher than the Mg-rich and eucritic clasts, with a negative Eu anomaly.

The finer-grained, granular Fe-rich clast, 85303,67, contains augite $En_{21}Wo_{40}$ and olivine Fa_{88}, which co-crystallized. It has the highest REE abundances (2), of the igneous clasts that have been analyzed.

Discussion: The bulk pyroxene pairs do not plot on single temperature isotherms (3) indicating pigeonite-augite co-crystallization but they may have partially reequilibrated. The igneous history of these clasts may be obscured by sub-solidus and shock history. The sequence of crystallization in the clast suite is pigeonite, pigeonite + augite, pigeonite + augite + olivine and finally augite + olivine but calcium contents of pigeonite and augite and chrome contents of augite do not vary linearly as would be expected in a fractionation trend. The occurrence of small patches of mesostasis in some eucritic clasts and not in the Fe-rich clasts and high chrome in the Fe-rich 85300,45 clast (2) indicate that more than one liquid crystallized to form this suite of rocks.

Pyroxene exsolution for the Mg-rich, eucritic and Fe-rich clasts suggests that all three rock types cooled at similar depths of emplacement to 700° (2). Alternatively, the similarity of exsolution temperatures records a common temperature reached by pyroxenes due to thermal effects of a shock event(s).

(1) Delaney, J.S. et al., 1984. Proc. 15th Lunar Planet. Sci. Conf., Journ. Geophys. Res., 89, C251-C289.
(2) Mittlefeldht,D.W. & Lindstrom,M.M. 1988.(Abstract) Lunar Planet. Sci. Conf., XIX, 790-791.
(3) Lindsley,D.H. and Anderson,D.J. 1983. Proc. 13th Lunar Planet. Sci. Conf., Journ. Geophys. Res., 88, A887-A906.

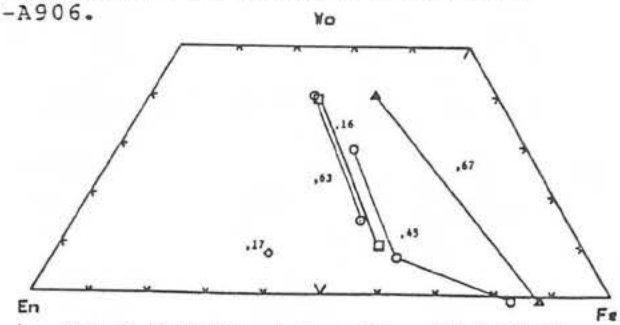

Fig. 1 Mafic Mineral Compositions LEW 85300-03

THERMOMETRY OF EUCRITIC ACHONDRITES; S. Jovanovic and G. W. Reed, Jr., Chemistry Division, Argonne National Laboratory, Argonne, IL 60439

We noted that there appeared to be a significant difference in the thermal conditions experienced by Antarctic achondrites (AA) and non-Antarctic achondrite falls (n-AA) (Jovanovic and Reed, 1987). Meteorites classified as eucrites were the exception; however, only one Antarctic "ordinary" eucrite was measured. Results on additional eucrites confirm this observation.

Thermal equilibration temperatures have been determined for LEW 85303, ALH 81009, ALH 85001, and EETA 79005 based on the amounts of Hg in labile vs retentive sites. The ratio of Hg released in stepwise heating experiments at $\leq 450°C$ and $>450°C \rightarrow 1200°C$ is a measure of the temperature at which Hg had equilibrated in the two types of sites (Jovanovic and Reed, 1985).

Thermometry data on achondrites is sparse and apparently not too reliable. Delaney et al. (1984) discuss the limitations of pyroxene thermometry applied to eucritic systems. These led to potential temperature errors of 50°-200°C using CaO in the low Ca pigeonite (or opx)-augite pair or to a maximum equilibrium temperature of 1000°C using augite lamellae. Takeda et al. (1981) estimated pyroxene closure temperatures of $\gtrsim 850°C$ for chilled lavas or impact melts. Mukherjee and Viswanath (1987) report orthopyroxene-spinel empirical temperatures for the diogenites Johnstown and Y75032 of 687° and 885°C, respectively. We determined Hg equilibration temperatures for Johnstown of 750°C, and for Antarctic diogenites ALH 84001 and ALH 77256 of 870° and 960°C, respectively. Mukherjee and Viswanath (1987) also observed very high temperatures of 1512°-1941°C for three other diogenites (paired?) which are attributed to strong thermal disequilibrium.

Preliminary data are reported for additional Hg equilibration temperatures and concentrations, Table 1. Delaney et al. (1984) paired EETA 79005 with howardite EETA 82600 and ALHA 81009 with polymict eucrite ALHA 78132.

The Antarctic eucrites exhibit both low ($<800°C$) and higher temperature ($>800°C$) histories. In contrast, n-AA aubrites, shergottites and diogenites exhibit lower temperatures by 100°-300°C than AA which gave Hg equilibration temperatures of 860°-1000°C.

If all ALHA eucrites are part of one shower (Freundel et al., 1986) and if the history of the parent body is that suggested by Takeda et al. (1981) in which shock melting followed by recrystallization occurred, then temperatures of $<800°C$ correspond to deep burial, hence, slow cooling of partial melts and $>800°C$ to near surface, rapid chilling of shock melted material. Unbrecciated eucrite PCA 82502, not listed in the table, gives a Hg equilibration temperature of 1100°C. Since this is a fine grained rock, it could be rapidly chilled magma representing original crust that was not cycled through impact melting and burial.

Table 1. Thermometry of Antarctic eucritic meteorites

Sample	EETA 82600	EETA 79005	ALHA 78132	ALHA 81009	LEW 85300	LEW 85303	ALH 85001	Stannern [Hg] in ppm
$[Hg_{ppb}]$	15	111	1.5, 4.8	54	423	423	119	9.3, 18
T°C	-	850	770, 940	985	620	790	990	670, 628

References: Jovanovic and Reed (1987) Meteoritics 22, 423; (1985) GCA 49, 1743-1751. Delaney et al. (1984) JGR 89, Suppl. C251-C288. Freundel et al. (1986) G&LA 50, 2663-2673. Mukherjee and Viswanath (1987) Me . Natl. Inst. Polar Res., Spec. Issue 46, 205-215. Takeda et al. (1981) JGR 12B Suppl., 1297-1313.

RECRYSTALLIZATION OF MESOSTASIS MATERIALS OF EUCRITES AND LATE THERMAL EVENTS ON THE HED PARENT BODY. Hiroshi Takeda and H. Mori, Mineralogical Institute, Faculty of Science, University of Tokyo, Hongo, Tokyo 113, Japan; L. E. Nyquist and D. Bogard, NASA Johnson Space Center, Houston, TX, 77058, U.S.A.

Comparison of degrees of homogenization of Ca-Fe-Mg zoning of eucritic pigeonites revealed that thermal metamorphism at subsolidus temperatures induced by impact events may account for the difference between pristine and monomict eucrites (1,2). Because young ^{39}Ar-^{40}Ar and Rb-Sr ages of Antarctic monomict eucrite Y792510 and the shock sintered polymict eucrite Y792769 (3) may be related to these impact events and because the mesostasis may be easily affected by thermal metamorphism we carried out mineralogical studies of the mesostasis of these eucrites.

Almost unaltered mesostasis has been recognized in the oldest pristine basalt Y75011,84 by Mori and Takeda (4) and Nyquist et al. (1). A coarse-grained subophitic eucrite clast in a polymict eucrite contains abundant dark mesostasis between plagioclase and pyroxene crystals. The boundaries between plagioclase and mesostasis are sharp, but brown-gray subcalcic ferroaugite rims ($Ca_{25.3}Mg_{18.5}Fe_{50.2}$) of pigeonite crystals merge into mesostasis. The mesostasis portion consists of the subcalcic ferroaugite, fayalite (Fa_{72-78}), silica, ilmenite, Ca phosphate, other fine unidentified minor phases, and glassy phases. Silica minerals occur as interstitial patches associated with dark mesostasis. Subcalcic ferroaugite rims show (001) exsolution lamellae 0.2 μm wide alternately of augite and pigeonite. The younger ^{39}Ar-^{40}Ar ages shown by the low-temperature Ar release from the Y75011 clast compared to the higher temperature release (5) may correspond to a record of shock disturbance of the exsolution texture and melting of fayalite of Y75011,84.

Stannern and Y792510 have interstitial areas which are similar to the mesostasis regions in the Y75011,84 clast in their textural relationship to plagioclase and pyroxene. These mesostasis-like areas show fine-grained semi-transparent recrystallized textures with aggregates of ilmenites. In Y792510, the terrestrial staining in these areas is extensive. Mesostasis-like areas, formerly containing unrecrystallized mesostasis, now consist of silica minerals, augite and minor low-Ca pyroxene, sodic plagioclase, ilmenite, troilite, Ca phosphate, and some Fe-bearing minor minerals. Irregular shaped ilmenites are the largest grains in the mesostasis-like areas. Microprobe analyses along lines at 10μm intervals in fine-grained areas devoid of ilmenite masses show that silica is the abundant mineral. Modal abundances (vol %) are: silica 50%, augite 25%, Fe oxide and sulfide 10%, Ca phosphate, plagioclase, and low Ca pyroxene < 5%. It is noted that the compositions of augite $Ca_{44}Mg_{29}Fe_{27}$ and low-Ca pyroxene $Ca_2Mg_{37}Fe_{61}$ in the mesostasis-like areas are identical to the host-lamellae compositions of the main pigeonite crystals. The Y792510, 62 F2 clast used for the age measurements is particularly rich in mesostasis-like areas.

Comparison of the Y75011 mesostasis and the Y792510 mesostasis-like areas suggests that the Y792510 materials might have been originally dark mesostasis areas as are seen in Y75011,84. During impact events and subsequent thermal annealing episodes, the decomposition of metastable Fe-rich pyroxenes in the forbidden region of the pyroxene quadrilateral to fayalite, augite, and silica could have developed. Then, Fe could have diffused into more Mg-rich pyroxenes, and silica and olivine, which lost Fe by diffusion, could form pyroxene again. The diffusion of Fe from the metastable Fe-rich pyroxene into the more Mg-rich pyroxenes in the stable region may also take place without decomposition to fayalite + silica at relatively low temperature. Grain-coarsening also takes place during annealing episodes. The ~3.2 Ga ^{39}Ar-^{40}Ar age of the Y792510 clast may correspond to thermal or shock events or both. The young (~4.1 Ga) Rb-Sr age suggests that this thermal event also disturbed the Rb-Sr system. This would mean a long geological history for the HED parent body, comparable to that of the moon. The geological event recorded by the radiometric systems also may be related to the brecciation events leading to the formation of polymict eucrites and howardites, since they often also show young ages similar to those of the monomict eucrites.

We thank the National Inst. of Polar Res. for the meteorite samples, and one of us (H. T.) gives thanks for an LPI, JSPS/Royal Society fellowship.

REFERENCES: (1) Nyquist L. E. et al. (1986) J. Geophys. Res. 91, B8, 8137-8152. (2) Takeda H. and Graham A. L. (1987) Rept. to Japanese Soc. Promotion of Sci., Tokyo. (3) Aoyama T., Takeda H. and Mori H. (1987) Meteoritics 22, 317-318. (4) Mori H. and Takeda H. (1982) Abstr. 7th Symp. on Antarctic Meteorites, 26-28, Tokyo, NIPR. (5) Nyquist L. E. et al., this volume.

COMPARATIVE CHRONOLOGIES OF BASALTIC CLASTS IN ANTARCTIC EUCRITES Y-75011 AND Y-792510.

L.Nyquist[1], D. Bogard[1], H. Takeda[2], B. Bansal[3], P. Johnson[3], C.-Y. Shih[3], H. Wiesmann[3] ([1]NASA Johnson Space Center, Houston, TX, 77058; [2]Mineralogical Institute, University of Tokyo, Hongo, Tokyo 113, Japan; [3]Lockheed, 2400 NASA Rd 1, Houston, TX, 77058)

We report Ar-Ar, Rb-Sr, and Sm-Nd ages of two eucritic clasts from polymict eucrite Y-75011 and monomict eucrite Y-792510, resp. The clast from Y-75011 (,84) is pristine and represents the least altered basalt type observed among eucrites (1). Unlike monomict eucrites, pyroxenes in Y-75011,84 show a pronounced zoning trend. The clast from Y-792510 (,62) contains pyroxenes of uniform host composition with thick exsolution lamellae of augite (2). Pyroxene exsolution patterns and the partial inversion of pigeonite to opx suggest that Y-792510 was heated at moderate temperatures for a prolonged time. More detailed petrographic descriptions of the mesostasis of the clasts are given in the companion abstract (3).

Ar-Ar Data: The first 50% of the Ar released from the Y-75011,84 clast indicates an age of ~4.0-4.1 Ga in contrast to the older Rb-Sr and Sm-Nd ages of ~4.56 Ga (4). For the last 50% of the Ar release, the ages increase steadily to ~4.6 Ga. The Ar retention age of the matrix adjacent to the clast (sample Y-75011,73) lie in the range 3.9-4.0 Ga between ~20% and ~80% of the gas release and then increase to ~4.5 Ga. These data indicate that an ~4.56 Ga old clast was incorporated into the breccia at ~3.95 Ga ago. The shock event was recorded in disturbance of the exsolved pyroxenes.

The Y-792510,62 clast has a younger Ar retention age than the Y-75011,84 clast. About 80% of the Ar released, including that released at the highest temperatures, yields ages of ~3.2 Ga. Older Rb-Sr and Sm-Nd ages suggest that the Ar retention age is not the crystallization age of the basalt and we conclude that Y-792510 underwent an intense secondary heating event which was distinct from that involving Y-75011. This event may have homogenized pyroxenes in the clast.

Rb-Sr Data: Rb-Sr data for clast Y-75011,84 and matrix Y-75011,73 have been previously reported (4). Internal isochrons give ages of 4.56±0.05 Ga and 4.52±0.06 Ga for the clast and matrix, respectively, for $\lambda(^{87}Rb) = 0.01402\ (Ga)^{-1}$ (5) indicating that the clast has a crystallization age of ~4.56 Ga. The Rb-Sr systematics of the matrix are nearly identical to those of the clast suggesting that the matrix is a mixture of components ~4.5 Ga old and is compositionally similar to the clast.

Rb-Sr data of Y-792510 are complicated by a late disturbance affecting phases with density >3.6 g/cm^3. This is apparently the result of weathering which affected the iron-rich phases in the mesostasis. The lightest phase (<2.65 g/cm^3) and plagioclase define an age of 4.05 Ga for $\lambda(^{87}Rb) = 0.01402\ (Ga)^{-1}$. Silica minerals in the mesostasis were apparently partially isotopically equilibrated with plagioclase during the 3.2 Ga reheating event which reset the Ar-Ar age.

Sm-Nd Data: As reported earlier (4) the Sm-Nd data of the clast and matrix from Y-75011 are indistinguishable. Combined data for clast and matrix give an age of 4.55±0.14 Ga using the York (6) program. The Sm-Nd data are further evidence for an ~4.56 Ga crystallization age of the clast but have been slightly disturbed by the ~3.95 Ga reheating event and/or oxidation of iron-rich mesostasis phases by weathering.

Sm-Nd data for a mineral separate of Y-792510 with density >3.6 g/cm^3 are highly discordant relative to those of plagioclase, pyroxene, and the whole rock, as in the Rb-Sr system. Data for the plagioclase, pyroxene and whole rock define an internal isochron of 4.37±0.17 Ga. We conclude that the crystallization age of the clast is ~4.4 Ga or older but both the Sm-Nd and Rb-Sr data have been affected by the ~3.2 Ga reheating event and/or late oxidation of iron-rich phases.

Discussion: We have suggested that the polymict eucrites were deposited in ejecta blankets following cratering events on the HED parent body whereas the more highly thermally metamorphosed monomict eucrites are probably from the floors or walls of the craters (4). The radiometric ages are consistent with this scenario. We suggest that the ages reflect cratering events on the parent body which left polymict Y-75011 buried near the surface of an ejecta blanket and monomict Y-792510 buried deep beneath its crater floor.

REFERENCES: (1) Takeda H., et al. (1983) Proc. 14th Lunar Planet. Sci. Conf., p.B245-B256. (2) Takeda H. and Nyquist L. E. (1985) Meteoritics, 20, p. 769. (3) Takeda H., et al. this volume. (4) Nyquist L. E. et al. (1986) JGR 91, p. 8137-8150. (5) Minster J.-F. et al. (1982) Nature, 300, p.414-419. (6) York D. (1966) Can. J. Phys., 44, p. 1079-1086.

RECKLING PEAK A80224: AN ANOMALOUS, FERROAN YET REE-POOR, EUCRITE

Paul H. Warren, Gregory W. Kallemeyn and Eric A. Jerde
Institute of Geophysics and Planetary Physics, University of California, Los Angeles, CA 90024

The RKPA80224 meteorite is a lightly-weathered 8.0 g eucrite that appears nearly unbrecciated [1]. We have studied this and other eucrites petrographically and by our standard INAA and fused bead - electron probe analysis techniques. Our data for a 132 mg portion of RKPA80224 indicate an extraordinary bulk composition. A comparable composition had been reported previously for a portion of eucrite ALHA78158 [2], but since ALHA78158 is polymict, its composition is petrogenetically ambiguous. Compared to noncumulate eucrites, RKPA80224 has significantly lower contents of REE (e.g., Sm) (Fig. 1) and other incompatible elements (e.g., Ti = 2.3 mg/g); and much lower Sm/Eu (Fig. 2). On the other hand, RKPA80224 differs from recognized cumulate eucrites in many respects, including lower Mg/(Mg+Fe) and higher Eu/Al (Figs. 1-2). Conceivably RKPA80224 represents an extension of the Stannern Trend, characterized by sharply increasing Sm with constant or moderately decreasing Mg/(Mg+Fe), and putatively formed as primary partial melts. However, the low overall REE, Ti, etc., and especially the low Sm/Eu (positive Eu anomaly — Fig. 2) strongly suggest that RKPA80224 formed as a partial cumulate. Its relatively coarse, largely ophitic texture is comparable to the textures of unbrecciated portions of Pomozdino, a eucrite completely unlike RKPA80224 in composition but also interpreted as a partial cumulate [3,4]. Mass balance calculations, assuming that the K_D(Fe/Mg) for pigeonite = 0.30 [5], indicate that the parent melt of RKPA80224 may have been along an extension of the Nuevo Laredo Trend, characterized by moderately increasing Sm with sharply decreasing Mg/(Mg+Fe), and putatively formed by fractional crystallization of a melt (or melts) similar to relatively magnesian members of the Main Group eucrites [e.g., 2,3,5]. This model requires that the "trapped liquid" content of RKPA80224 be no more than ~40 wt%, because a TL content >>40 wt% would imply a Sm content for the parent melt far lower than any plausible extension of the Nuevo Laredo Trend. The Mg/(Mg+Fe) implied for the parent melt is only about 0.20. Stolper [5] noted that surprisingly ferroan melts, more ferroan than any known eucrite, are required to account for most cumulate eucrites. Meteorites such as RKPA80224 and Pomozdino tend to blur the distinction between cumulate and noncumulate eucrites. However, the putative genetic distinction between Nuevo Laredo (Main-Group-linked fractional crystallization residue) and Stannern (primary partial melt) types of noncumulate eucrites still appears valid, and RKPA80224 appears to strengthen the case for most cumulate eucrites being linked to the Nuevo Laredo Trend.

References: [1] Score R. and Mason B. (1982) *Ant. Met. Newsl.* 5(1), 31. [2] Smith M. R. and Schmitt R. A. (1981) *LPS XII*, 1014-1015. [3] Warren P. H. and Jerde E. A. (1988) *LPS XIX*, 1234-1235. [4] Yaroshevsky A. A. et al. (1988) *LPS XIX*, 1311-1312. [5] Stolper E. (1977) *GCA* **41**, 587-611.

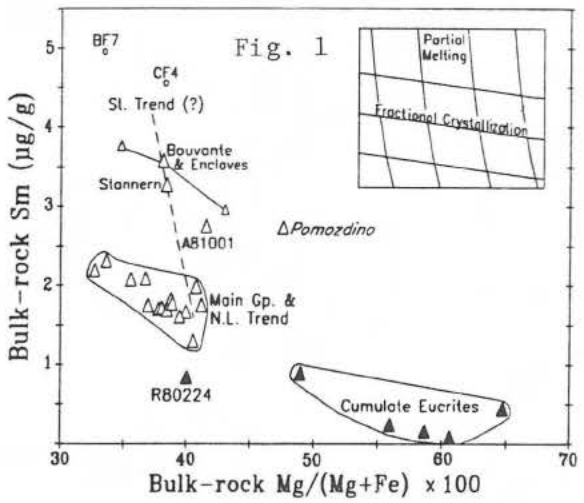

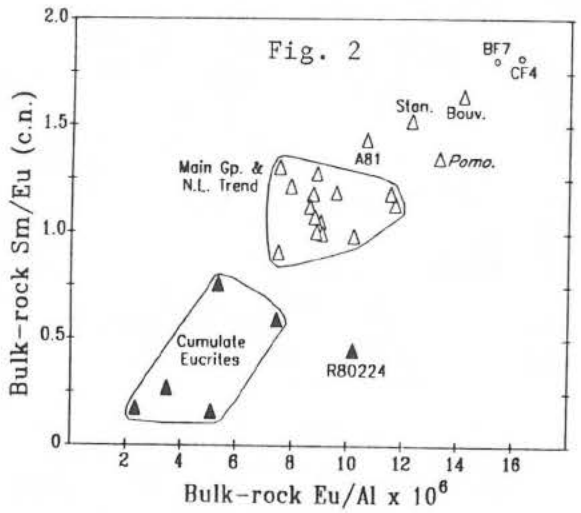

THE BHOLGHATI CONSORTIUM: PRELIMINARY CHEMICAL AND PETROLOGIC CHARACTERIZATION OF THE BHOLGHATI HOWARDITE. D. C. Gosselin, J. C. Laul, M. R. Smith, Battelle Pacific Northwest Laboratory, Richland, WA. 99352; A. M. Reid, University of Houston, Houston, TX

The Bholghati Howardite (10 g), which probably represents a regolith sample of the eucrite parent body (EPB), was obtained through the courtesy of the Geological Survey of India for a consortium study including petrology, chemistry, rare gas, Rb-Sr, Sm-Nd and K-Ar geochrons, thermoluminescence, oxygen isotopes and fission tracks. The purpose of the consortium is to provide insight into the geochemical, petrological, geochronological, and thermal evolution of the EPB. We report preliminary petrologic and chemical data for four bulk samples, two eucrite clasts, and a dark clast.

Bholghati is a polymict breccia composed of small angular lithic and monomineralic clasts, generally less than 2mm in a fine-grained grey matrix. The most abundant lithic clasts are eucrites dominated by intergrown white feldspar and Fe-rich pyroxene. The eucrite clasts are "equilibrated" with unzoned, exsolved Fe-rich pigeonite and ferroaugite. Small dark clasts containing very low Fe pyroxene and olivine, FeS, and Fe-Ni plus secondary alteration products are also prominent. The monomineralic clasts are mostly feldspar and pyroxene that range from Fe-rich eucritic compositions to low Ca and Fe diogenetic compostions.

The four bulk samples have a narrow range of molar FeO/(FeO+MgO)[Fe'= 0.37 - 0.40], FeO/MnO(33 - 36), and atomic Mg/Si(0.41-0.48) that are similar to other howardites (1,2); and indicates a compositionally homogeneous sample of the EPB regolith. Chondrite-normalized REE data indicate a narrow compositional range (La_n = 4.2 - 6.7) and have flat patterns [$(La/Yb)_n$ = 1] with negative Eu anomalies [$(Eu/Sm)_n$ = 0.78 - 1.03)].

The two eucritic clasts (BH-2, BH-5) have noteable differences in TiO_2 (1.74, 0.52 %) and FeO(14.20, 24.50 %). These eucritic clasts are similar to non-cummulate eucrites in terms of their Fe'(0.63, 0.66) and CaO (12.80, 9.62 %). The FeO/MnO ratio (40,45) exceeds that generally observed for eucrites (~35), and can be explained by accessory troilite and ilmenite. The REE patterns are light REE depleted [$(La/Yb)_n$ =.62] with BH-2 having a negative Eu anomaly [$(Sm/Eu)_n$ =.6] and BH-5 having a slightly positive Eu anomaly [$(Sm/Eu)_n$ = 1.3)]. This light REE depletion is unique to normal eucrites, but have been observed in clasts from the Allan Hills polymict eucrites.(3)

The atomic Mg/Si (~1.0), FeO/MnO (114), Ni/Co(21.5), and Ir/Au(3.1) ratios and abundances of Ni, Au, Co and Ir of the dark clast suggest that this clast may represent carbonaceous chondrite-type material that was introduced during regolith formation on the EPB. This clast has a flat REE pattern with a positive Eu anomaly. Similar clasts with positive and negative Eu anomalies have been observed in the Kapoeta Howardite which were interpreted as CI-type materials that did not lose their volatile components during impact or subsequent brecciation.(2)

References: 1) Mittlefehldt, et al., (1979), GCA43, 673-688; 2) Smith M.R., Ph.D. Dissertation. Oregon State University, 193p; 3) Smith, M.R., and Schmitt, R.A., (1981) Lunar Planet. Sci. XII, 1014-1016.

SIMPLE AND NOT-SO-SIMPLE MIXING IN THE HOWARDITE-EUCRITE-DIOGENITE (HED) PARENT BODY, R. L. Paul,* R. O. Sack,† H. Kruse¶ and M. E. Lipschutz* (*Chemistry Department and †Earth and Atmosphere Science Department, Purdue Univ., W. Lafayette, IN 47907; ¶Max-Planck-Institut für Chemie, D-6500 Mainz FRG)

We previously reported data [1] for 15 trace elements (mainly volatile/mobile ones) in Antarctic and non-Antarctic HED meteorites. Here, we report modal analyses and average chemical compositions obtained by microprobe analysis of thin sections representative of these same samples. From these data, we calculated the position of each sample on the eucrite-diogenite join using an "un-mixing" program based upon the howardite data [2]. We also calculated the position of each sample, treating it as a mixture of assumed eucrite and diogenite end-members. With few exceptions (mainly the two cumulate eucrites and Binda) the sample-positions calculated from un-mixing and mixing agree well.

The trace and major element data indicate that our sampling of putative eucrites and howardites form a continuum: there is, however, a distinct hiatus between howardites and diogenites. As found earlier for a much smaller sampling of non-Antarctic HED meteorites [3], contents of at least two trace elements (Ga and U) correlate well with position along the eucrite-diogenite join: notable exceptions are again the cumulate eucrites and Binda. More importantly, contents of mobile trace elements (like Se, Cs, Bi and Tl) in some samples are, at times, very high (approaching Cl levels).

These results confirm earlier work (e.g. [2,3]) indicating that howardites are basically simple mixtures of eucrite and diogenite end-members. However, Antarctic samples extend the end-member ranges in both directions and fill in the previous hiatus between eucrites and howardites. Our trace elements results indicate another component.

This second component seems to be consist of condensed volcanic emanations. The results indicate that <u>after</u> howardite regolith formation early in solar system history, volcanic gases penetrated parent body layers and were deposited in them. Traces from a similar such episode are detectable in lunar samples as e.g. in Yamato 791197 lunar meteorite [4]. There is no evidence in HED meteorites for admixture of a condensed phase, such as, for example, a known type of chondritic component. Traces of a similar volcanic processes may be evident in regolith samples from the H chondrite parent body [5].

Previously, volcanism was thought to be a property of larger planets only. Now, it appears to have taken place in asteroidal-sized objects as well, late enough to post-date regolith formation. Effects of volcanism in meteorites no longer necessarily provide evidence for an origin in a planet-sized body, e.g. Mars.

References: [1] Paul R. L. and Lipschutz M. E., <u>Lunar Planet. Sci. XVIII</u>, 768 (1987). [2] Dreibus G., Kruse H., Spettel B. and Wänke H., <u>Proc. Lunar Sci. Conf. 8th</u>, 211 (1977). [3] Dreibus G. and Wänke H., <u>Z. Naturforsch. 35a</u>, 204 (1980). [4] Kaczaral P. W., Dennison, J. E. and Lipschutz M. E., <u>Proc. Tenth Symp. Antarctic Meteorites (Tokyo)</u>, 76 (1986). [5] Lipschutz M. E., Biswas S. and McSween M. Y. Jr., <u>Geochim. Cosmochim. Acta 47</u>, 169 (1983).

HED PETROGENESIS: VIEW FROM THE DIOGENITE END

David W. Mittlefehldt[1] and Marilyn M. Lindstrom[2] 1. Lockheed EMSCO, C23, 2400 Nasa Rd 1, Houston, TX 77058; 2. SN2, NASA/Johnson Space Center, Houston, TX 77058.

Diogenites are orthopyroxenite breccias from the howardite-eucrite-diogenite (HED) parent body. Although long recognized as cumulates, the petrogenesis of these ultramafic rocks and their relationship to eucrites has remained obscure. The two competing models are 1. diogenites are cumulates from the crystallization of a totally molten asteroid, or 2. diogenites are cumulates from ultramafic partial melts that were formed after basalts parental to eucrites were drawn off. Recent work on the petrology of diogenites has suggested that the major element compositions of the pyroxenes require two separate parent magmas for the diogenites (1). Trace element abundances on whole rocks suggest an even more complex model. Literature HREE (Yb and Lu) vary by an order of magnitude, and show that trace element contents are decoupled from the major and minor element abundances. Using literature La, Sm and Lu data, and internally consistent partition coefficients, calculated REE contents of diogenite parent melts vary from a low of ~0.8 x CI for Shalka to a high of ~8.4 x CI for some analyses of Johnstown. The range in REE contents in diogenites is not due to variation in an included trapped liquid component. Consideration of the La/Sm and Sm/Lu ratios shows that the calculated parent liquid REE content is independent of the calculated amount of trapped liquid.

We are attempting to gain further insight into diogenite, and HED parent body, petrogenesis and are conducting a systematic study of the geochemistry of diogenites. Neutron activation analyses are underway for samples from a suite of 10 diogenites plus orthopyroxene clasts for a howardite and a mesosiderite. To the extent possible, we are analyzing coarse-grained material from the diogenites in order to avoid possible HED parent body contaminants that may be in the matrix. We are also performing petrologic and microprobe studies of grains separated from the INAA samples. Petrologic study on grains from Roda has yielded surprising results. Two 5-10 micron grains of LREE-rich phosphate were found poikilitically enclosed in a diopside grain, which in turn is enclosed in the host orthopyroxene. These phosphates averaged 1.6 wt% La_2O_3 and 3.6 wt% Ce_2O_3, and exhibited an extreme LREE/HREE fractionation. Measured La/Sm ratios are ~10 x CI and the La/Yb ratio is of the order of 100 x CI based on a calculated upper limit for Yb. About 0.003 wt% of these phosphate grains could explain the entire La budget for whole rock Roda measured by (2). However, Roda has a flat REE pattern (2), suggesting that these LREE-rich phosphates are considerably less abundant. Two analyses of Johnstown (3) have shown anomalous LREE enrichments that have not been properly explained. These patterns could reflect the presence of LREE-rich grains in other diogenites. Future work will focus on integrating microprobe data with trace element data in order to understand the petrogenesis of the diogenites and the HED parent body.

References: (1) Harriott and Hewins (1984) Meteoritics 19, 15; (2) Fukuoka et al. (1977) PLSC 8th, 187; (3) Floran et al. (1981) GCA 45, 2385.

GUNLOCK, A NEW TYPE 3 ORDINARY CHONDRITE WITH A GOLFBALL-SIZED CHONDRULE. M. Prinz[1], M.K. Weisberg[1,2], C.E. Nehru[1,2]. (1) Amer. Museum Nat. Hist., NY, NY 10024. (2) Brooklyn College (CUNY), Brooklyn, NY 11210.

The Gunlock meteorite was found by Mr. Don H. Adair on June 22, 1982 while mapping the geology of the Goldstrike Mining District in Washington Co., Utah. Two fragments were found, about 50 m. apart, which fit together nicely indicating they were originally one piece. The larger fragment was cut and AMNH received one half which weighed 3.9kg. The meteorite is black with fresh metal. The outer surface is weathered and tends to exfoliate. A large black (metal-free) mass was found on the edge of the sample, with a beautifully curved contact with the chondrite host. It is rimmed by a thin layer of metal-troilite. This represents about 1/3 of a huge chondrule, most of which is missing. The radius is over 2cm, and the diameter is estimated by reconstruction to be about 5cm. This object is clearly droplet-shaped and is a macrochondrule.

Petrologic data for this chondrite are preliminary, but results indicate some unusual aspects. Texturally, the meteorite is a type 3 chondrite. It has sharply defined droplet chondrules ranging in size up to about 1mm, which contain feldspathic glass. The chondrite host has no opaque matrix. Metal and troilite are present as typical angular grains. The texture of the Golfball chondrule is porphyritic olivine (PO), with a glassy mesostasis containing skeletal olivine crystals. Metal and troilite in the chondrule are in eutectic intergrowths, and are present as small nodules, along fracture surfaces, and as a thin rim surrounding the chondrule. Some metal and troilite grains in the chondrite host have outer margins containing this metal-troilite intergrowth, and the frequency of this added material decreases away from the chondrule-chondrite contact. The chondrule contains darkened areas which have undergone shock melting and blackening. Mineralogically, olivine and pyroxene in the chondrite host has a fairly narrow comp. range, with ol generally from Fo_{75-82}; some as low as Fo_{64} and as high as Fo_{91} is present. Metal is Ni-rich (8-23%) and inhomogeneous within and between grains; these may be kamacite-taenite intergrowths. Olivine in the Golfball chondrule is zoned (Fo_{92-88} and Fo_{88-85}). Chondrule metal is also Ni-rich (7-15%), but less so than in the chondrite host.

Discussion. Gunlock and its Golfball chondrule were analyzed for oxygen isotopes (R.N. Clayton, pers. comm., 1987) and both have the composition of equilibrated L-group chondrites. This is surprising since most Type 3 ordinary chondrites contain heavier oxygen than that of equilibrated ordinary chondrites. Chondrite and chondrule have also been analyzed for thermoluminescence (F.A. Hasan, pers. comm., 1988). These results indicate that the chondrite may be classified as Type 3.4. The natural TL of the chondrite host showed almost no signal and the meteorite may have been reheated during the past 10^5-10^6 years. Some speculations on the significance of macrochondrules are given by Weisberg et al. (this volume).

MACROCHONDRULES IN ORDINARY CHONDRITES: CONSTRAINTS ON CHONDRULE FORMING PROCESSES. M.K. Weisberg[1,2], M. Prinz[2], C.E. Nehru[1,2]. (1) Brooklyn College (CUNY), Brooklyn, NY 11201. (2) Amer Museum Nat. Hist., NY, NY 10024.

Studies of chondrule sizes in ordinary chondrites [1,2,3,4] show that most fall within a specific size range (0.2-3.8mm) and they are moderately sorted. Martin and Mills [2] measured 1265 disaggregated chondrules from the Allegan chondrite and Hughes [3] reported size dimensions on 955 chondrules from Bjurbole and Chainpur. The largest they report are 2.75mm and 3.67mm, respectively. Most are less than 1mm. Based on these studies, chondrules larger than about 4mm are extremely rare in ordinary chondrites. Binns [5] reported one unusually large (4cm) chondrule in Parnallee.

In this study we report on four chondrules (Ca1, Et1, J11, G11) which are at least 1 mm larger than those normally observed in ordinary chondrites. We apply the term "macrochondrule" and define it as any chondrule greater than 5mm in maximum dimension. All four macrochondrules studied have curved surfaces, contain a glassy mesostasis and have chondrule textures. Other possible macrochondrule-type materials are the large masses of cryptocrystalline to barred olivine-textured clasts in the Bencubbin metal-silicate assemblage.

Ca1 is in the Carraweena (L3) chondrite and measures 8.4x6.2mm. It is barred olivine (Fo_{81}) consisting of multiple grouplets [6] of bars in a mesostasis of feld. glass and fine low-Ca pyx. Et1 is in Etter (L5), measures 6.2x10.3mm and is also BO (Fo_{77}). J11 is in Julesberg (L3) and is a compound chondrule pair. The overall dimension is 8.9x8.3mm, and the individual chondrules are 8.3x3.4 and 3.9x5.5mm. Both are BO with coarse low-Ca pyx overgrown on oliv, indicative of resorption. G11 is in Gunlock (L3). Unfortunately it occurs at the edge of the chondrite and only about a third of it is preserved. By reconstruction it is estimated to be about 5cm. It is porphyritic olivine and oliv is zoned (Fo_{90-85}). This is described more fully in Prinz et al. [7].

Macrochondrules in ordinary chondrites are extremely rare and their occurence helps place constraints on chondrule forming processes. They should be considered in all models and experimental work. The BO texture of some macrochondrules indicates that they may have been heated to above liquidus T^o [8,9] and cooled slowly enough for oliv to react with liquid to make pyx. Is it possible for proposed heating mechanisms such as electrical discharge [10] to heat these large objects to above liquidus T^o and maintain that T^o long enough to destroy nuclei? Impact models may have similar problems. No impact-produced cm sized spherules are known. Would radiative cooling allow time for oliv-liquid reactions to occur? Less transient heat sources, such as the sun's T-tauri stage may be more likely.

References: [1] Martin, P.M. and Mills, A.A. (1976) EPSL 33, 239-248. [2] Martin, P.M. and Mills, A.A. (1978) EPSL 38, 385-390. [3] Hughes, D.W. (1978) EPSL 38, 391-400. [4] King, T.V.V. and King, E.A. (1979) Meteoritics 14, 91-98. [5] Binns, R.A. (1967) Min. Mag. 36, 319-323. [6] Weisberg, M.K. (1987) Proc. LPSC 17, E661-678. [7] Prinz et al. (1988), this volume. [8] Nagahara, H. (1983) Mem. Nat. Inst. Polar Res. 30, 61-83. [9] Hewins, R.H. (1988) in: Meteorites and the Early Solar System, in press. [10] Whipple F.L. (1966) Science 152, 54-56.

GLASSY, CRYPTOCRYSTALLINE AND RADIAL PYROXENE CHONDRULES IN TYPE 3 ORDINARY CHONDRITES. C.E. Nehru[1,2], M. Prinz[1], S.C. Okulewicz[1,2], M.K. Weisberg[1,2]. (1) Brooklyn College (CUNY), Brooklyn, NY 11201. (2) Amer. Museum Nat. Hist., NY, NY 10024.

Chondrules have been studied petrologically in many chondrites, but systematic studies of selected textural types are rare. Some of the least studied are the glassy (G), cryptocrystalline (C), and, to a lesser extent, the radial pyroxene (RP). Barred olivine (BO) chondrules were studied previously by us. The types studied here are all complete melts and have cooled very fast. Their bulk compositions may allow determination of the liquidus temperatures attained for these compositions. Unrepresented chondrule compositions may be due to the absence of the appropriate precursors in that environment, or to the lack of temperatures high enough to melt those compositions. With these goals in mind, the bulk compositions of 197 chondrules in H-L-LL3 chondrites were analyzed. Their distribution was: H3 - 31G, 24C, 18RP; L3 - 14G, 10C, 25RP; LL3 - 14G, 20C, 41RP.

Results: (1) The average compositions for each of the 9 groups are relatively similar. They are generally SiO_2-rich (52-55%), with mg nos. from 72-82, indicative of enrichment in normative pyroxene. Na_2O (0.6-1.4%) and K_2O (0.1-0.9%) are relatively low, indicative of non-albitic normative plagioclase components. (2) L3 and LL3 average compositions are indistinguishable, and have lower mg nos. than those in H3 chondrites, except for RP chondrules where they have higher mg nos. (3) C chondrules in L-LL3 chondrites have lower mg nos. (72) than bulk compositions of G and RP chondrules (79). (4) G chondrules in LL3 chondrites are split into two distinct groups, one with high average mg no. (91.4, 5%FeO) and one with low mg no. (61.7, 23%FeO). (5) One subgroup of 5 G chondrules in H3 and L3 chondrites have low SiO_2 (45%) and high FeO (20.5%); they are highly olivine-normative. (6) Chainpur (LL3.4) has 4 C chondrules which also have low SiO_2 (43%) and high FeO (24%), as do 2 RP chondrules in LL3 chondrites. (7) One G chondrule in an H3 chondrite is normatively feldspathoidal, and one G chondrule in an LL3 chondrite is reduced but has high MnO (1.8%).

Conclusions: (1) Whereas most G, C and RP chondrules in H-L-LL3 are normatively pyroxene-rich, there are important exceptions. Some are normatively olivine-rich, feldspathoidal, or reduced. (2) Generally, G, C and RP chondrules are compositionally similar to pyroxene porphyritic (PP) and granular porphyritic (GP) chondrules. (3) Liquidus temperatures for the common pyroxene-rich types are about 1500°C. (4) A main subgroup of olivine-rich compositions represented in G, C and RP chondrules in H3, L3 and LL3 chondrites may be indicative of higher temperatures, but their FeO-rich nature will lower it. These chondrules may have opaque matrix as precursor components, at least in part. (5) Compositional trends of all chondrules studied indicate a relatively uniform temperature upper limit of 1500-1600°C. This may be why more magnesian olivine-rich compositions are scarce and mainly occur as porphyritic chondrules. (6) Ol-rich BO chondrules are also complete melts and had similar liquidus temperatures, but their temperatures may also be lowered because they are more feldspathic.

CHONDRULE TEXTURE/COMPOSITION RELATIONS REVISITED: CONSTRAINTS ON THE THERMAL CONDITIONS IN THE CHONDRULE FORMING REGION.

Patrick M. Radomsky and Roger H. Hewins, Dept. of Geological Sciences, Rutgers University, New Brunswick, N.J. 08903, U.S.A.

Chondrule texture is controlled by the abundance of heterogeneous nuclei (i.e. by % melt). The sequence of chondrule textures (GO,PO,BO,G1) has been obtained by varying T_I for a given composition and by varying composition with fixed T_I (1,2).

Textural/compositional relationships for chondrules indicate a narrow range of initial temperatures as more refractory compositions were melted less. In Figure 1, liquidus temperatures for chondrules calculated by (4) are plotted. NP and P chondrules define low and high temperature end points of this "liquidus curve", respectively, and proportions of NP decreases and P chondrules increase with increasing liquidus temperature. Furthermore, the absence of NP and BO (i.e. textures indicative of total melting) above 1700°C indicates this temperature represents a T max in the chondrule forming events or chondrule forming region of the nebula. This maximum and the narrow range suggested by figure 1 are estimates, as the liquidus temperatures calculated are equilibrium values and do not consider variables such as duration of heating, size and granularity of chondrule precursors which affect the actual disappearance of solids during heating. These results differ from (3) in that T max is a little higher. Furthermore, the gap between T max and T liq for the least refractory chondrules is greater, leading us to expect more totally glassy chondrules than actually observed. We therefore suggest some NP chondrules experienced late nucleation which occurred at temperatures lower than final temperatures of experiments.

CONCLUSION: Chondrules in unequilibrated chondrites experienced a narrow range of conditions with T_I up to 1700°C, time at $T_I \approx .5$ hrs., and cooling rates of 500°C/hr.

REFERENCES: (1) Radomsky and Hewins LPSC XVIII, (1987); (2) Connolly et al. LPSC XIX, (1988); (3) Radomsky and Hewins, Meteoritics 22, 284 (1987); (4) Herzberg GCA 43, 1241 (1979).

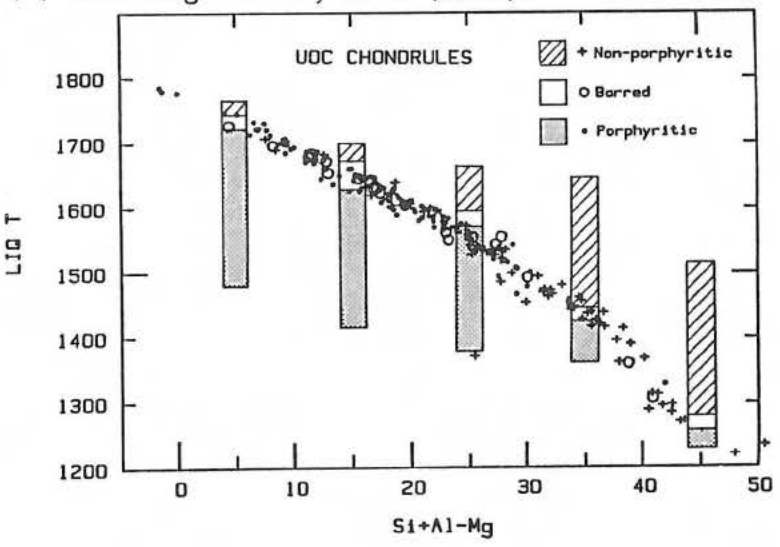

DYNAMIC CRYSTALLIZATION EXPERIMENTS ON MELTS OF BARRED OLIVINE CHONDRULE COMPOSITION: ORIGIN OF THEIR TEXTURAL DIVERSITY. Gary Lofgren, SN-2 NASA Johnson Space Center, Houston, TX 77058; and A. B. Lanier, LEMSCO 1830 NASA Rd. 1, Houston, TX 77258

Dynamic crystallization experiments have been conducted on a starting material which duplicates the average H3 barred olivine chondrule composition [1]. Barred olivine texture consists of olivine plate dendrites (bars) that represent linked parallel growth [2]. The bars develop at cooling rates of 1000 to 2000°C/hr. The melting temperatures were in the range 1600 to 1640°C. Melting times of 15 to 30 minutes produced the appropriate distribution of nuclei; longer melt times reduced the number of nuclei and these runs usually contained spherulites. Each simulated, barred-olivine chondrule consists of several, usually 3 to 5, plate dendrites with different orientations and all are indistinguishable from the natural barred olivine chondrules shown in Weisberg's Fig. 1b [1]. At 2000°C/hr, the plates of the dendrites are 20 to 60 microns across and spaced at comparable dimensions. The plates of individual dendrites vary in width from dendrite to dendrite by as much as an order of magnitude in a single experimentally produced chondrule. As the cooling rates of the experiments are decreased, the plates of the dendrites become larger (in excess of 200 microns) and there are fewer plates per dendrite. At the slowest cooling rates studied, several elongate, skeletal plate olivines are present which are not part of a dendrite. The matrix in all cases is glass, runs were quenched at 1200°C; trace amounts of chrome spinel crystallized in some runs. Slower cooling rates at lower temperatures and, possibly annealing, will be necessary to produce pyroxene.

The plates of the dendrites are nearly homogeneous with a range of Fo contents between 88-85. Some of the larger plates have local, very thin rims (usually less than 5 microns) of Fo 75-70. Late forming olivine microlites occur in some runs and have the same composition as the rims. On average, the experimentally grown olivines are slightly more forsteritic (88-85) than those observed by Weisberg [1], but are not out of the range of observed compositions. A synthetic chondrule with very coarse, plate dendrites has an Fo content between 83-80 which compares well with the observations of Weisberg. Slower cooling rates near the solidus could preserve the barred texture, but allow the olivine to react with the liquid, become less forsteritic, and foster the growth of pyroxene. Similar experiments on a less Fe-rich, porphyritic olivine chondrule composition [3] produced identical textures in the same range of cooling rates. The range of melting temperatures is more restricted, 1590 to 1615°C, but the melting times can be longer, up to 2 hrs.

In these experiments we have duplicated the common type of barred olivine texture; including the variations in the widths of the bars. As the chondrule cools, dendrites will nucleate and grow at different temperatures (i.e. degrees of supercooling) and the variation in plate width is related to the degree of supercooling which existed when a given dendrite started growing. The temperature at which nucleation takes place is more a function of the nature of heterogeneous nucleation sites in the melt that on the cooling rate [4]. Thus the heterogeneous nucleation behavior is more important than the cooling rate in determining many characteristics of the texture. The final texture results from the interplay of cooling rate and the nucleation characteristics which are determined by the grain size of the melted material and the melting temperature and time. The natural equivalents of the barred olivine chondrules of the composition and type crystallized here were melted at temperatures in the range 1590 to 1630°C for times less than 30 minutes, but up to 2 hrs depending on composition and cooled at rates between 1000 and 2000°C/hr.

REFERENCES: [1] Weisberg (1987) *Proc. Lunar and Planet Sci. Conf. 17th,* in *J. Geophys. Res.*, **92**, p. E663-E687. [2] Donaldson (1976) *Contrib. Mineral. Petrol.*, **57**, 187-213. [3] Lofgren and Russell (1985) *Lunar Planet. Sci. XVI*, pp. 499-500. Lunar and Planetary Instit., Houston. [4] Lofgren (1983) *J. Petrol.*, **24**, 229-255.

KINETICS OF THE CLINOPYROXENE - ORTHOPYROXENE TRANSITION: CONSTRAINTS ON THE THERMAL HISTORIES OF CHONDRULES AND TYPE 3-6 CHONDRITES. Rhian H. Jones and Adrian J. Brearley. Institute of Meteoritics, Department of Geology, University of New Mexico, Albuquerque, New Mexico 87131.

Metamorphism in petrologic types 3-6 chondrites is commonly assumed to have taken place during reheating of the meteorite parent body after accretion - prograde metamorphism (e.g. (1)). Less popular is the model of retrograde or autometamorphism, according to which a parent body accretes hot and subsequently cools with cooling rate decreasing with depth of burial (e.g. (2)). Neither model can adequately account for all of the observations from meteorites and available experimental data.

An important argument against a prograde model has arisen from recent studies of the microstructures of the low-Ca pyroxenes of the ordinary chondrites (e.g. (3)). Low-Ca pyroxenes in type 3 chondrites are commonly "twinned clinopyroxenes" which are the product of rapid quenching from the high-temperature protopyroxene polymorph (e.g. (4)). Intermediate petrologic types, 4 and 5, contain "striated orthopyroxene" which consists of a fine-scale intergrowth of ortho- and clino-pyroxene lamellae (5). In type 6 chondrites low-Ca pyroxenes are exclusively orthorhombic. There are two mechanisms which may account for the "striated orthopyroxene" structures in unshocked meteorites: 1) Heating twinned clinopyroxene results in a progressive inversion to orthopyroxene, via a fine-scale intergrowth of the two polymorphs (6), and 2) Upon cooling from the protopyroxene field, a decrease in the cooling rate results in a reaction product with a higher proportion of ortho-lamellae (4). An understanding of the microstructures obtained by the first two of these mechanisms, which the prograde and autometamorphism models invoke respectively, should provide an insight into the thermal histories corresponding to the petrologic series 3-6. For example, the experiments carried out by (3) suggested that compositionally homogeneous striated orthopyroxenes, which are typical of type 4 and 5 chondrites, cannot be formed by prograde metamorphism.

We have begun a systematic experimental and TEM investigation of the clino/orthopyroxene inversion, for compositions En_{100}-En_{80}. We will investigate the effect of cooling rate on the microstructures of pyroxenes cooled from the protopyroxene field, and the effect of annealing on a range of initial microstructures. The kinetics of the reaction will be calculated by measuring the extent of transformation with time.

Experiments have been carried out on a synthetic En_{100} composition. A rapid quench from 1450°C, in the protoenstatite field, gave a reaction product which was 100% twinned clinoenstatite. Slower cooling from the same temperature to 600°C, at a rate of approximately 1000°C/hr, resulted in a product which was predominantly clinoenstatite, but contained approximately 35vol% ortho lamellae. The cooling rate of chondrules containing clinopyroxene with little ortho, i.e. those in type 3 chondrites, must therefore have been greater than 1000°C/hr. When the twinned clinopyroxene product of the rapidly quenched experiment was annealed at 800°C for one week, only very minor inversion to orthopyroxene was observed. This result was not expected, as Ashworth et al. (3) found that many clinopyroxene lamellae in Quenggouk (H4) inverted to orthopyroxene under the same conditions. The difference between these two results may be because either a) Quenggouk already had a substantial proportion of ortho lamellae before the annealing was carried out, thus the reaction rate may be dependent on the initial degree of transformation, or b) the composition of the Quenggouk pyroxene is $En_{83}Fs_{16}Wo_1$, and the presence of the Fs, and/or Wo component, may play an important role in the rate of the inversion reaction. If the reaction rate is very slow for pyroxenes which are predominantly clino, i.e. for pyroxenes of the type found in type 3 chondrites, the formation of striated orthopyroxenes by prograde metamorphism may prove to be reasonable.

Supported by NASA grant NAG9-30; Klaus Keil, principal investigator.

References.(1) Dodd, R.T. (1981) Meteorites: A Petrologic-Chemical Synthesis. Camb. Univ. Press; (2) Heyse, J.V. (1978) EPSL 40, 365-381; (3) Ashworth, J.R. et al. (1984), Nature, 308, 259-261 (4) Smyth, J.R. (1974) Am. Min. 59, 345-352; (5) Ashworth, J.R. (1980), EPSL, 46, 167-177; (6) Boland, J.N. et al. (1974), J. Geol. 82, 507-514.

A chondrule origin for opaque rims and interchondrule matrices in the UOCs. R Hutchison, British Museum (Natural History), London SW7 5BD, and C M O Alexander, Earth Sciences Department, The Open University, Milton Keynes MK7 6AA, U.K.

Opaque rims and interchondrule matrices in highly unequilibrated ordinary chondrites are mainly composed of clastic olivine and low-Ca pyroxene, with a fine-grained component. Clastic grains have compositions consistent with an origin as fragmented crystals from chondrules (1). The finest grained material is mostly in the rims. The mean grain-size is less than 2 μm, and the grains are dominated by Fa-rich olivine that extends to Fa_{80} in Krymka (2). Fayalitic olivine often occurs as overgrowths on olivine clasts. There is also a feldspathic component, rims (and matrices) being richer in bulk Na, K and Al than bulk meteorite. In Bishunpur, this component is amorphous and albitic (1).

The origin of the fayalitic olivine is a problem. Reaction of FeO (from oxidation of metal) with Mg pyroxene yields olivine as Fe-rich as Fa_{50}; exchange of Fe for Mg in magnesian olivine needs an as yet unidentified sink for Mg (3). We propose that the mesostases of pyroxene-olivine chondrules were the precursor of fine-grained rims and matrices. In Semarkona and Bishunpur chondrule mesostases have about 70 wt% SiO_2, 14% Al_2O_3, 6.5% FeO, 1.5 or 4.5% MgO, respectively, and 2% CaO. Reaction with FeO (from metal) and redistribution of Na between chondrules and rim/matrix can produce a molecular normative composition with 55-60% olivine, Fa_{90-96}, and 45-40% plagioclase, $Ab_{75}Or_7An_{17}$, close to the ordinary chondrite mean (4).

Pyroxene-rich chondrules must be prone to spontaneous disintegration because of rapid contraction by 3% along the c axis during transformation of the proto to the clino form. Low-Ca clinopyroxenes have a basal (001) parting that produces fragments elongated perpendicular to the twinning. Such fragments are observed in rim/matrix of UOCs and in chondritic interplanetary dust (1,5). If chondrules accreted as a regolith, by analogy with the Moon (6), the feldspathic component (chondrule mesostases) would be over represented in the finest grained material, as observed in rims and matrices.

We thank Gordon Biggar and Jim Chisholm for discussion.

(1) C M O Alexander et al. (1987) Meteoritics 22, 316-317. (2) H Nagahara (1984) GCA 48, 2581-2595. (3) H Nagahara and I Kushiro (1987) EPSL 85, 537-547. (4) W R Van Schmus and P H Ribbe (1968) GCA 32, 1327-1342. (5) J P Bradley et al (1983) Nature 301, 473-477. (6) J J Papike et al (1982) Rev. Geophys. Space Phys. 20, 761-826.

SODIUM ENRICHED LUMINESCENT CHONDRULE MESOSTASIS RIMS IN THE UNEQUILIBRATED ORDINARY CHONDRITES. J.M. DeHart, and D.W.G. Sears, Cosmochemistry Group, Department of Chemistry and Biochemistry, University of Arkansas, Fayetteville, AR 72701. G.E. Lofgren, SN2 Johnson Space Center, Houston, TX 77058

During the course of our survey of phosphors in the unequilibrated ordinary chondrites (UOC) using cathodoluminescence (CL) petrographic techniques, six chondrules were noted to have their outermost regions of mesostasis luminesce blue while the mesostases in the more interior portions of the chondrule were either nonluminescent (two in Semarkona and one in Krymka) or had red CL emission (the three chondrules noted in ALHA77214). This difference is associated with large differences in sodium content of the mesostases in the chondrules from all three meteorites. The blue luminescent mesostases are from 0.98 to 6.55 weight percent higher in sodium content than the mesostases with different luminescent response in each chondrule. Previous studies indicate these large differences in sodium content are probably not the result of chondrule forming processes (1).

All six chondrules are porphyritic olivine (PO) chondrules and three of the six have rims of sulfide material. In five of the six chondrules, Al_2O_3 is also slightly higher in the luminescent regions. The largest differences in Sodium content are in the chondrule mesostases in Semarkona.

We offer the following interpretation of these compositional and luminescent features. These enrichments in sodium occurred either when these chondrules were exposed to Na-rich gases during their residence in the solar nebula before they acquired their sulfide rims (in the case of the rimmed chondrules), or during their accretionary history prior to being incorporated into their present material. Gases rich in volatile metals are believed to have existed on meteoritic parent bodies as a result of metamorphic heating of the interior materials (2,3). In addition, it is possible that these gases were not only hot enough to contain and implant the sodium, but also to nucleate the phosphor responsible for the luminescent properties, which is probably a Na-rich feldspar. It is also reasonable to suppose that the production of the phosphor was a two step process, with the annealing event that produced the phosphor having occurred as a separate process. These elevated temperatures did not nucleate the phosphor in more interior mesostasis regions because the lower sodium content of these areas would require higher and/or longer exposure to elevated temperatures to produce the phosphor. The greater difference in sodium content in the chondrule mesostases in Semarkona is probably due to the aqueous fluids this meteoritic material has been exposed to. This indicates these fluids could alter the glasses of the interior mesostases but not affect the crystalline material responsible for the blue luminescence, providing another geochemical indicator as to the nature of the fluids that have altered this meteorite.

This research is supported by NASA grants NAG 9-81 and NGT-50064.

(1). Tsuchiyama et al., 1981, GCA, 45, 1357-1367.
(2). Anders, E. and M.G. Zadnik, 1985, GCA, 49, 1281-1291.
(3). Wlotza, et al., 1983, GCA, 47, 743-757.

THE THERMOLUMINESCENCE PROPERTIES OF CHONDRULES FROM THREE LOW PETROLOGIC TYPE ORDINARY CHONDRITES.

D.W.G. Sears[*], Jie Lu[*], R.K. Guimon[+], A.D. Morse[$], R.Hutchison[@], C.O. Alexander[$], I.P. Wright[$], C.T. Pillinger[$].
[*]Cosmochemistry Group, Department of Chemistry and Biochemistry, Univ. Arkansas, Fayetteville, AR. [+]Physical Science Dept., Missouri Valley College, Marshall, MO. [@]Mineralogy Department, British Museum, London. [$]Planetary Science Unit, Open University, Milton Keynes, UK.

As part of a larger project to explore the secondary history of chondrules from low-type meteorites by petrologic, isotopic and TL techniques (1), we have measured the TL properties of separated chondrules from Semarkona (3.0), Bishunpur (3.1) and Chainpur (3.4). Previous work has shown that the TL sensitivity of chondrules is related to the amount of crystalline felspar in chondrule mesostasis and that the peak temperature and width of the induced TL curves are related to the relative amount of feldspar in the high and low temperature forms. This, in turn, is governed by the feldspar's formation temperature and post-formation cooling rate (2).

The chondrules from Semarkona show a 10^6-fold range in TL sensitivity with no correlation between TL sensitivity and peak temperature (1), while Bishunpur and Chainpur show a 10^4-fold range in TL sensitivity with weak correlations between TL sensitivity and peak temperature. In contrast, Dhajala (3.8) shows a strong correlation between TL sensitivity and peak temperature which suggests that 80% of the chondrules contain relatively large amounts of feldspar in the low form while the remainder have small amounts of feldspar in the low-form. Chondrules from all three meteorites show peak temperatures ranging over 80-240°C, but while the spread is uniform for the other, the Chainpur data tend to cluster in the 100-140°C range. The Chainpur chondrules show a correlation between peak temperature and width, similar to that displayed by Dhajala, but with very few chondrules in the cluster corresponding to high-feldspar. In all three meteorites, matrix samples show considerably less spread in TL sensitivity than do chondrules, and they have values 2-3 orders of magnitude below those of the brighter chondrules.

The clustering of peak temperatures for the Chainpur data suggests that feldspar in these chondrules is predominantly in the low-form and the proportion of chondrules with TL sensitivities higher than the highest observed in Semarkona and Bishunpur shows that the amounts of feldspar present are much higher. The simplest interpretation is that Chainpur is more highly metamorphosed than the others, but remained in the low-field throughout metamorphism (<600°C). However, even Chainpur chondrules with low TL sensitivities tend to have peak temperatures corresponding to low-form. Either the low levels of metamorphism experienced by Chainpur converted high feldspar observed in Semarkona and Bishunpur to low feldspar without changing the amount present by devitrification of the mesostases, or the low feldspar in Semarkona and Bishunpur has been preferentially destroyed relative to the high-form. Aqueous alteration has been shown to preferentially attack the low form (3), consistent with several lines of evidence for aqueous alteration in these chondrites (1). Further isotopic and petrologic work will help resolve this point.

1. Sears et al. (1988) LPS XIX, 1051. 2. Keck et al. (1987) EPSL 77, 419. 3.Guimon et al. (1988) GCA 52, 119. (Support: NASA NAG 9-81, NSF INT8612744, SERC GRE 16564).

CHONDRULE PARENTS REVISITED. K. Fredriksson and B.J. Fredriksson, Dept. of Mineral Sciences, National Museum of Natural History, Smithsonian Institution, Washington, D.C. 20560.

As previously reported [1,2] we have analyzed some 400 chondrules from various H, L and LL, Grades 3, 4 and 5 chondrites. Specifically, the distribution of Al, Ca and Ti has been discussed to emphasize the peculiar fact that these elements are positively correlated in the chondrules from so-called unequilibrated chondrites (variable Fe/Mg ratios in olivines and pyroxenes) but anticorrelated in the chondrules from "equilibrated" chondrites, which also have an average Ca content well above the bulk meteorite, particularly at higher SiO_2 contents. Complicating the issue is the discovery of two chondrites, Bjurböle, L4, and Study Butte, H3, [3,4.5] which have both types of chondrules. In any case, this abstract is, in part, a palimpsest [1,2]. However, the interrelation of most major elements have now been evaluated by means of computer graphics; some trace element data, although preliminary, should be available for presentation at the Meeting.

All in all, the extended evaluation of the data seems to reinforce the conclusion that chondrules originated from a "soil" comprised of materials chemically similar to C1 silicates (or CO similar to some Brownlee dust particles), i.e. "unadulterated" C1 aggregates, inhomogenous on a microscale. The chondrules were formed by very, very fast processes involving melting, solidification (quenching) and crystallization with reduction (by carbon) followed by various degrees of modification and induration while accreting into chondrites with the incorporation of more "primitive" materials. This view is strongly supported by melting and crystallization experiments on natural and synthetic chondrite materials [6].

It is implicit that multiple impacts on a low density carbon- (+ H_2O?) containing regolith, gradually becoming more consolidated, is presently the mechanism of choice for the formation of chondrules and chondrites.

References:

(1) Fredriksson, K., 1983. In Chondrules and Their Origin (Ed., E.A. King), Lunar and Planet. Inst., 44-52.
(2) Fredriksson, K., 1988. Lunar and Planet. Sci. XIX, 352-353.
(3) Fredriksson, K. et al., 1984. Meteoritics 19, 225-226.
(4) Fredriksson, K. and F. Wlotzka, 1988. (In preparation).
(5) Wlotzka, F. and K. Fredriksson, 1988. Abstr., this volume.
(6) Fredriksson, K. and F. Wlotzka, 1988. Poster (Abstr. this volume).

OXYGEN AND SILICON ISOTOPES IN NINGQIANG CHONDRULES. T.K. Mayeda,[1] R.N. Clayton,[1] and D.A. Kring.[2] [1]Enrico Fermi Institute, University of Chicago; [2]Harvard-Smithsonian Center for Astrophysics.

Oxygen and silicon isotopic compositions of eight individual chondrules from the C3 chondrite Ningqiang are given in Table 1. The oxygen isotope values fall in the same range as was observed for Allende chondrules, i.e., slightly above the ^{16}O-mixing line defined by Allende refractory inclusions. Four of the chondrules contain anorthite. Two of these, N1 and N5, with abundant anorthite, are at the ^{16}O-rich end of the range of C3 chondrules. Otherwise no systematic relationship is seen between oxygen isotopic composition and mineralogy or texture.

The silicon isotope ratios are mostly higher than those in Allende chondrules (except for N8), and show a larger range than has previously been observed in chondrules. No systematic relationship is observed between silicon isotopes and oxygen isotopes or chondrule mineralogy. The silicon isotopic compositions follow a slope-1/2 mass-dependent fractionation trend with no evidence for nuclear anomalies.

TABLE 1

Ningqiang Chondrules

Number	Mineralogy	δ^{17} (‰ rel.	δ^{18} SMOW)	δ^{29} (‰ rel.	δ^{30} NBS 28)
N1	An, ol, px, sp	-6.7	-2.5	0.0	0.1
N2	An, ol, px	-5.4	-1.6	0.4	0.8
N3	Ol, px	-2.1	1.6	0.1	0.1
N4	Px, ol	-2.2	1.4	1.0	2.0
N5	An, ol, px, sp	-7.1	-2.9	1.1	1.9
N6	Ol, px	-4.0	-0.6	0.8	1.3
N7	Ol, px	-5.6	-2.3	—	0.0
N8	Ol, px	-7.0	-3.4	-0.9	-1.8

WHY DO ALLENDE CHONDRULES LIE ON A DIFFERENT OXYGEN-ISOTOPE MIXING LINE THAN ALLENDE CAI'S? -- A MODEL

David A. Kring and John A. Wood, Department of Earth and Planetary Sciences, Harvard University, and the Harvard-Smithsonian Center for Astrophysics, 60 Garden Street, Cambridge, MA 02138.

The oxygen isotopic compositions of Allende refractory inclusions and matrix define a line that has been interpreted to represent mixing between endmember reservoirs consisting of ^{16}O-enriched dust and ^{16}O-depleted gas. The oxygen isotopic compositions of Allende chondrules do not fall along the CAI mixing line (Figure 1); they seem to require different endmember reservoirs. Clayton et al. [1] propose the existence of a second ^{16}O-depleted gas reservoir, which mixed with solids having isotopic compositions on the CAI mixing line.

However, there is another way to understand the offset of the chondrule line from the CAI line, which this paper explores. The chondrules could have formed from precursor material that had been isotopically mass fractionated from an earlier generation of presolar material that had compositions on the CAI mixing line. Isotopic mass fractionation would have been particularly effective during vaporization and recondensation of the presolar dust. The oxygen from the dust would have mixed with the local gas, producing gas with an intermediate isotopic composition on the CAI mixing line. When the system cooled, dust would have recondensed that was isotopically mass fractionated from the gas. We have modelled this process by considering the vaporization and recondensation of forsterite in a system of cosmic composition at 10^{-5}atm. Forsterite condenses from 1294 to 1169K, at which point 99.9% of the Mg has been removed from the gas. The amount of isotopic mass fractionation has been assessed on the basis of fractionation factors determined by Onuma et al. [2] as a function of temperature and composition. Figure 1 shows the oxygen isotopic composition of the newly condensed, mass fractionated dust. The chondrule line may have been formed by simple mixing of recondensed dust in various proportions with unvaporized dust; or recondensation may have occurred directly onto relic dust, which formed composite grains with bulk oxygen isotopic compositions distributed along the chondrule mixing line. The chondrules themselves were formed by remelting of this precursor dust.

Another effect may have helped establish the distribution of chondrule oxygen-isotope compositions. Vaporization of dust-enriched primordial systems would have produced gas mixtures that lie lower on the CAI line of Fig. 1 than the point shown; recondensation from these gases would yield dust that lies lower on the chondrule line than the point shown.

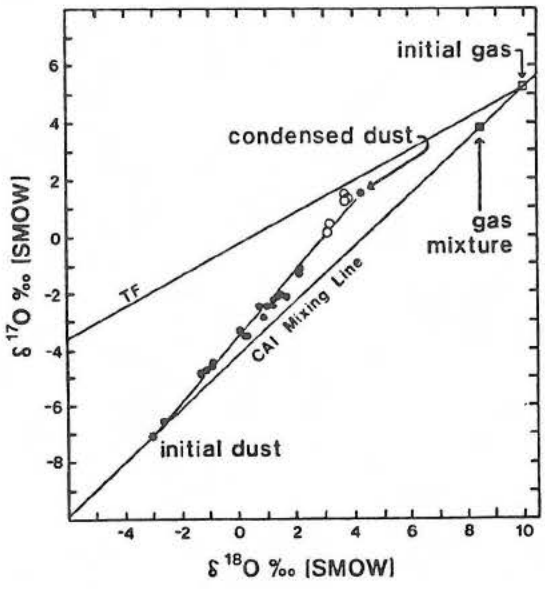

Fig. 1: TF = terrestrial fractionation line, ● = porphyritic chondrules, ○ = barred olivine & radial pyroxene chondrules.

References: [1] Clayton, R.N. et al., 1983, in Chondrules and their Origins, E.A. King (ed.), LPI, Houston, p. 37. [2] Onuma, N. et al., 1972, G.C.A. 36, p. 169.

POSTER SESSION

EXPERIMENTS WITH A LEITZ 1750°C HEATING STAGE.

K. Fredriksson, National Museum of Natural History, Smithsonian Institution, Washington, D.C. 20560 and F. Wlotzka, Max-Planck-Institut für Chemie, Abt. Kosmochemie 6500, Mainz, FRG.

We have extended our melting experiments with the Leitz 1750°C Microscope Heating Stage [1]. A 15- to 20-minute video tape will illustrate these experiments including the structure of the resulting "quench" products, as well as original materials, which were fragments of previously analyzed chondrules, ground chondrules, C3 Allende, C1 Ivuna and synthetic mixes resembling chondrules and CAI's. The poster compares the structure, mineralogy and chemistry of our synthetic "chondrules" with the original chondrules and other spherules of proven impact origin, e.g. micro-Irghizites and Lonar (India) spherules, or suspected impact origin, e.g. many lunar (Moon) spherules. Volatiles emanating from the samples and condensing on the quartz observation window have also been studied.

Our current conclusions are that chondrules must have formed extremely quickly and suffered little modification since accretion together with more "primitive" materials. CAI's, on the other hand, appear to require considerably more time for the formation of, e.g. melilites or plagioclase, while spinel is a "quench" phase. Also, low ambient pressure appears to retard crystallization of CAI materials.

Ref.: Fredriksson, K. 1986. Meteoritics 21, 364.

PETROLOGY OF ANORTHITE-RICH CHONDRULES IN CV3 AND CO3 CHONDRITES

-- David A. Kring and Britt A. Holmén, Harvard-Smithsonian Center for Astrophysics, 60 Garden Street, Cambridge, MA 02138.

Certain chondrules and constituents of chondrules appear to have refractory inclusion affinities. These include relic materials within chondrules [1], Fe,Ca-rich rims around chondrules [2], and Ca,Al-rich fassaite chondrules [3]. A new class of chondrules with refractory inclusion affinities is described, namely anorthite-rich chondrules. Anorthite-rich chondrules are compositionally intermediate between ferromagnesian chondrules and refractory inclusions, and are different from the Ca,Al-rich chondrules of [3]. These types of objects are particularly interesting because they may help determine whether chondrules and refractory inclusions formed in related events or if a real discontinuity exists between the processes that formed these objects.

Anorthite-rich chondrules have been identified in Allende (CV3), Ningqiang (CV3), Kaba (CV3), and Kainsaz (CO3). These objects have the droplet morphology and igneous textures of chondrules. They have abundant anorthite (An_{94-96}), ± spinel, ± olivine, ± pigeonite, ± enstatite, ± augite, ± fassaite, and always contain small amounts of Fe-metal/sulfides. Those chondrules that formed from spinel saturated melts have textures consistent with the crystallization sequence anorthite + spinel, olivine, and clinopyroxene. The chondrules that formed from spinel undersaturated melts appear to have co-precipitated anorthite and enstatite or anorthite and olivine, followed by clinopyroxene. The plagioclase-olivine inclusions (POI's) identified by [4] in Allende are a subset of these anorthite-rich chondrules.

Most of these objects have rims that consist primarily of olivine and Fe-metal/sulfides. The rims occur either as monosilicate layers, or as multisilicate rims with igneous textures. [2] noted that the monosilicate layers appear to be high temperature condensates that formed on previously cooled chondrules, while the multisilicate rims appear to have been molten material that accreted around previously cooled chondrules. The similarity of rims around these anorthite-rich chondrules to rims around ferromagnesian chondrules and refractory inclusions is an indication that all three types of objects could have been processed by similar events.

The refractory lithophile abundances in two anorthite-rich chondrules in Kaba [5] are different from those in ferromagnesian chondrules and most refractory inclusions. In general, these anorthite-rich chondrules are enriched in the elements of moderate volatility, but the abundances are significantly different from the Group II patterns. The REE patterns are similar to those that would remain in the gas phase after partial condensation of refractory condensates ($F_{La} = 0.002$) had occurred [6]. A similar pattern has been found in Allende inclusion EK 1-4-1 [7].

The oxygen isotopic compositions of two anorthite-rich chondrules in Ningqiang, reported in [8], indicate that these objects are similar to refractory inclusions and the most ^{16}O-rich porphyritic chondrules in Allende.

In summary, the anorthite-rich chondrules have petrologic and geochemical properties of both chondrules and refractory inclusions. The similarities among these objects suggests they may have formed in related events.

References: [1] Steele, I.M., 1986, G.C.A. 50, 1379. [2] Kring, D.A. and J.A. Wood, 1987, Meteoritics 22, 432. [3] Bischoff, A. and K. Keil, 1984, G.C.A. 48, 693. [4] Sheng, Y.J. et al., 1988, LPS XIX, 1075. [5] Lui, Y.-G. et al., 1988, LPS XIX, 686. [6] Boynton, W.V., 1975, G.C.A. 39, 569. [7] Nagasawa, H. et al., 1982, G.C.A. 46, 1669. [8] Clayton, R.N. et al., 1988, this volume.

ARABIAN PENINSULA: KNOWN AND SUSPECTED IMPACT STRUCTURES; **J.F. McHone and R.S.Dietz, Dept. of Geology, Arizona State Univ., Tempe, AZ 85287-1604**

Geologists searching for meteorite impact have enjoyed moderate success in arid lands. The Arabian peninsula is a vast area of mostly barren desert and contains, in addition to the well known Wabar craters, several geologic sites of possible impact origin. We report here a recent inventory of these proven and suspected impact structures.

WABAR (al-Hadida), *Saudi Arabia: 21°28'N; 050°29'E, 91 m dia.* A cluster of three craters in live sands of the Rub' al-Khali (empty quarter) first reported by Philby's camel expedition (1). A later motorized group (2) recovered a single iron weighingmore than two tons.

SHAYBAH, *Saudi Arabia: Near 22°N; 53°E. Less than 1 km dia.* Described in unpublished letters from flyers servicing petroleum fields in Saudi Arabia and Oman (3). A handheld photo reveals a small fresh crater with uplifted rim and possible ejecta products. The crater is situated in a zone of distinct "hooked" sand dunes (4) and is near the abandoned Shaybah airfield.

AL-UMCHAIMIN, *Iraq: 32°36'N; 039°25'E, 3.2km dia.* A steep-walled 30 m deep crater in Eocene marls and limestones of the Azraq-Sirhan sedimentary basin (5, 6). On SIR-A shuttle imaging radar the site appears as a brilliant ring of radar beams reflected from blocky rim rocks.

EL-MIRBA, *Iraq-Jordan border: 32°44'N; 039°01'E, 7.2 km dia.* Previously unamed photocircle detected on landsat about 42 km NW of Al-Umchaimin. A multiring feature with a 2 km wide internal disk. Orbital radar renders the site as a dark zone of smooth sediments on the valley floor of Wadi el-Mirba.

AL-MADAFI, *Saudi Arabia: 28°40'N; 037°11'E, 6 km dia.* A miltiring crater situated in sublevel Paleozoic shales and sandstones of the Tabuk sedimentary basin (6, 7) and proposed as impact structure by remote sensors (9, 10).

OMAN RING, *Oman: 19°55'N; 056°58'E, 6 km dia.* First reported as a possible astrobleme (impact feature) on early Landsat images (11). Field observations (12) and aerial photos reveal a subtle sedimentary uplift surrounded by fractured ring of sublevel sedimentary rocks. Recently it has again caught the attention of remote sensors who are studying it as Habhab (10, 13).

WASITA, *Yeman: 14°54'N; 44°12.5'E, 14 km dia.* A circular depression about 4 km wide surrounded by a 14 km dia. concentric structure. Vulcanologists conducting field investigators here inform us they do not regard this site as one of many volcanic features in the region (14). Tentatively named Wasita after nearest mapped town about 5 km to SSE (15).

References: 1) Philby, H., 1933.*Geogr. Journ.*, **81-1**, 1-26. 2) Bilkadi, Z., 1986.*Aramco World Mag.*, **37-6**, 26-33. 3) Murphy, B., 1981.*Pers. Comm.* 4) Holm, D.A.,1960.*Science*, **132-437**, 1369-1379. 5) Merriam, R. and J. Holwerda, 1957.*Geog. Journ.*, **123**, 231-233. 6) al-Laboun, A.A., 1988.*Geol. Soc. Am. Bull.*, **100**, 362-373. 7) al-Laboun, A.A., 1986. *Am. Assoc. Petrol. Geol. Mem.*, **40**, 373-394. 8) Greeley, R. et al., 1987.*Earth,Moon,and Plan*, **37**, 89-11. 9) Garvin and Blodget, 1986.*Meteoritics*, **24-4**, 366-367. 10) Grieve, R. et al., 1988.*LPI Tech Rpt 88-03*, Lunar and Planet. Inst., 89 pp. 11) Dietz et al., 1975.*Meteoritics*, **10**-4, 393, 509. 12) Cain, R., 1982.*Pers. Comm.* 13) Rothery, D. et al., 1988.*EOS* , **69-16**, 391. 14) Orsi, G., 1982.*Pers. Comm.* 15) U.S. Geological Survey, 1978. *Geographic Map of Yemen Arab Republic (San'A')*, Map I-1143-A.

KARA AND UST-KARA IMPACT STRUCTURES, USSR: GEOCHEMICAL RELATIONSHIP OF THE TARGET ROCKS AND EJECTA; **A. V. Murali[1], C. Koeberl[1,2], M. A. Nazarov[3], V. L. Sharpton[1] and K. Burke[1]**
[1] Lunar and Planetary Institute, 3303 NASA Road 1, Houston, TX 77058
[2] Inst. of Geochemistry, University of Vienna, A-1010, Vienna, Austria
[3] Vernadsky Inst. of Geochem. and Analyt. Chemistry, USSR Academy of Sciences, Moscow 117975, USSR.

The Kara and Ust-Kara impact structures in the polar Urals, USSR have been tentatively linked to the K-T event. We have initiated an in-depth geochemical study of the diverse suite of target rocks, impact melts and glasses from these structures to establish their chemical relationships, to constrain compositional variations and the scale of mixing in the impact melting, and also to attempt to characterize the projectile composition.

We analysed 37 samples from the Kara and Ust-Kara impact structures consisting of Permian sandstones and shales (8), shocked magmatic rocks (4), suevites (7), impact melts (5) and the impact glasses (13), for ~30 major, minor and trace elements employing sequential INAA procedure. Preliminary results of our study indicate the following:

1) The shocked magmatic rocks have the highest REE abundances of all the samples of the present study (La=80-100 C1 and Lu=18-25 C1) with distinct negative Eu anomalies (0.6-0.85) whereas the central uplift shows the least fractionated tholeiitic basalt (?) trend with La (10 C1)) and Lu (4 C1) with no europium anomaly. It is likely that the shocked magmatic rocks are genetically related to the rocks exposed in the central uplift by low pressure fractionation of plagioclase and olivine.

2) Although the Carboniferous shale shows LREE enriched trends (La=50 C1 and Lu=6 C1) and is comparable to the Permian sandstones and the shales in its overall REE trends, it has higher negative europium anomaly (0.5) compared to the Permian sandstones and the shales (~0.75). The Carboniferous shale is also distinctly different in that it has the lowest Na_2O (0.71 %), FeO (1.78 %), Sc (3.8 ppm), Co (2.3 ppm), Cr (70 ppm), Ni (56 ppm), Rb (14 ppm), Cs (0.9 ppm) and very high CaO (12.0 %) compared to the Permian sandstones and shales which have higher Na_2O (1.99-3.61 %), FeO (3.2-7.2 %), Sc (12.3-21.8 ppm), Co (15.3-52.9 ppm), Cr (137-420 ppm), Ni (67-271 ppm), Rb (22-71 ppm), Cs (1.3-4.1 ppm) and lower CaO (1.9-9.0 %).

3) All the samples of the present study show LREE enriched trends and negative Eu anomalies (except the sample from the central uplift). The suevites and the impact melts are indistinguishable in their REE abundances and patterns.

4) There are minor differences in the elemental abundances and the ratios between the glasses from Saayakha river (north Kara) and Kara river (south Kara)regions.

Mixing model calculations for the generation of the various glasses and melts and identification of the chemical signatures of the projectile composition are in progress.

DEFORMATION IN SOFT ORDOVICIAN SEDIMENT PRODUCED BY LARGE MASSES OF SANDSTONE FROM A NEARBY, BUT AS YET UNDISCOVERED, IMPACT CRATER. William F. Read, Geology Department, Lawrence University, Appleton, Wisconsin 54912.

A quarry near the east city limits of Madison, Wisconsin, exposes sedimentary rocks of Upper Cambrian and Lower to Middle Ordovician age. The quarry face is about 15 m. high. The lower third is in mostly-white shale, siltstone, and sandstone known from its conodonts to be the Readstown member of the St. Peter formation (Middle Ordovician). The upper two thirds is in yellowish, brown-weathering sandstone which appears to be different from the main (Tonti) member of the St. Peter. A small area of Lower Ordovician Prairie du Chien dolomite is exposed in the quarry floor. Beneath this is a yellowish sandstone of probable Upper Cambrian age.

The upper part of the Readstown contains three conspicuous sandstone layers, each about 0.5 m. thick. On top of these is a rubble bed of variable thickness: roughly 0-1 m. Below them is a considerable thickness of shaly material: at least 1.5 m. The actual thickness is unknown because of a cover of rock fragments which have fallen from above.

The strata in the upper two thirds of the quarry face and those in the quarry floor are, or appear to be, nearly horizontal. But the exposed upper portion of the Readstown shows conspicuous deformation. Where this is most pronounced, the three sandstone layers are abruptly bent, or bent and faulted, downward by as much as 2-3 m. On either side of these downbendings the shaly beds are compressed into numerous small folds with an amplitude of usually less than 10 cm., as if they had been pushed aside to make room for the depressed layers of sandstone.

In my opinion, this is exactly what happened. The slightly more competent layers of sandstone (then unindurated) were pushed down, I think, by the sudden arrival of large masses of rubbly, mainly-Cambrian sandstone from a nearby impact crater. Two such masses are visible in a pair of downbendings in the northeast quarry face. One is about 1.5 m. in diameter; the other quite a bit larger. These masses weather brown like the sandstone above them but differ from it in that they show no distinct stratification and contain fragments of resistant layers in the Readstown. Their apparent absence in other downbendings is due, I think, to the downbent structures' being funnels of considerably larger diameter than the ejecta blocks which caused them. What we see in the quarry face are random cross-sections through these funnels.

I think it likely that the rubble bed at the top of the Readstown was also produced by these ejecta blocks. The yellow sandstone above the Readstown may consist of fine ejecta (individual sand grains and grain fragments from Cambrian sandstone). Petrographic work on this material is in progress.

REFLECTION SEISMIC DATA FROM TERRESTRIAL IMPACT STRUCTURES: EVIDENCE OF SHALLOW PENETRATION? Virgil L. Sharpton[1], Kevin Burke[1], Lynette Lucas[1] and Fred Hörz[2] [1]Lunar and Planetary Institute, 3303 NASA Road One, Houston TX 77058, [2]Solar System Exploration Division, Johnson Space Center, Houston, TX 77058.

There are about 116 impact structures on Earth [1], and it seems likely that some of them may be capable of yielding information about the third dimension of the cratering process in a way that their more numerous and better preserved counterparts on other planets cannot. Reflection seismic profiling offers an important but an as yet apparently underutilized means of exploiting this advantage. We are attempting to compile seismic data as well as other geophysical and borehole information across terrestrial impact structures in an effort to better understand their seismic expression and especially how it varies as a function of scale and gross target characteristics. So far we have obtained seismic data from 4 complex craters and from 2 suspected craters.

Profiling is usually undertaken within sedimentary terrains but seismic data have also provided some information about impact structure in crystalline targets. The ~52 km Siljan structure in Sweden was formed in granitic target rocks intruded by up to seven diabase sills that provide distinct marker horizons spanning the depth of this feature [2]. Truncation and displacement of these horizons provide constraints on morphology and strain paths; weakening of reflector horizons that is observed outward and downward from the crater interior appears to reflect the zone of in situ brecciation and fracturing that surrounds the crater. Reflections from a sill located at ~3 km depth continue at least 8 km inside the mapped crater rim and may extend across the structure as continuous but extremely weak reflections. Although this horizon may not have been totally disrupted, it appears to have sustained severe structural deformation.

We define the structural depth (d_s) of an impact structure as the distance down from the highest horizon affected by the impact to the first subsurface horizon encountered that shows no impact-induced structural displacement. For complex craters d_s encompasses the depth of excavation plus the subjacent depths from which the central uplift is structurally accommodated. As d_s is the depth above which all preserved displacements associated with the cratering process are confined, it also provides a maximum value to the transient cavity depth. Table 1 summarizes values of d_s for the structures we have studied to date. These preliminary results suggest to us a considerable amount of morphological variability in complex structures but clearly support the conclusions of previous workers (based on theory and experiment [3]) that impact craters are relatively shallow features.

Table 1

Structure	Diameter (km)	~d_s (km)	Target	Reference
Probable:				
Red Wing Creek	10	1.5	sedimentary	[4]
Gosses Bluff	22	8	sedimentary	[5]
Ries	24	?	mixed	[6]
Siljan	52	8	crystalline	[2]
Suspected:				
Central Montana	3	0.6	sedimentary	[7]
Oman	6	2.3	sedimentary	[8]

References: [1] Grieve, R.A.F. and Robertson, P.B. (1987) Geol. Surv. of Canada Map 1658A. [2] Castano, J.R. (1988) Lunar Planet. Sci. XIX, 170-171. [3] Melosh, H.J. (1982) J. Geophys. Res. 87, 371-380; O'Keefe, J.D. and Ahrens, T.J. (1987) Lunar Planet. Sci. XVIII, 744-745. [4] Brenan, R.L., Peterson, L., and Smith, H.J. (1975) Wyoming Geol. Assoc. Earth Sci. Bull. [5] Milton, D.J., Barlow, B.C., Brett, R., Brown, A.R., Glikson, A.Y., Manwaring, E.A., Moss, F.J., Sedmik, E.C.E., Van Son, J., and Young, G.A. (1972) Science 175, 1199-1207. [6] Pohn, J., Stoffler, D., Gall, H., and Ernston, K. (1977) in Impact Explos. Crater., 343-404. [7] Plawman, T.L. and P.I. Hagar (1983) in Scis. Express. Structural Styles, vol. 1, 1.4-1 - 1.4-3. [8] Rothery, D.A., Sharpton, V.L., and Francis, P.W. (1988) Eos 69, 391.

VREDEFORT STISHOVITE CONFIRMED USING SOLID-STATE SILICON-29 NUCLEAR MAGNETIC RESONANCE;

J.F. McHone[1] and R.A. Nieman[2], [1]Dept. of Geology,[2]Dept. of Chemistry, Arizona State University, Tempe AZ 85287-1604

South Africa's Precambrian Vredefort Dome, at more than 120 km diameter and nearly 2 billion years age, is one of the largest and oldest circular geologic structures on Earth. Evidence of an extraterrestrial impact origin for this feature was strengthened when Martini (1) reported coesite and stishovite along thin veins of pseudotachylite. These two minerals, pressure phases of silica, are widely accepted as indicators diagnostic of impact-induced shock history and were identified from X-Ray diffractograms of insoluble HF acid residues. This X-Ray technique can be tedious and is subject to misinterpretation due to precipitation of unwanted fluorides during sample digestion. As a result, we are not aware of any successful duplication or confirmation of Martini's experiment. We report here positive recognition of Vredefort stishovite using a separate technique, magic angle sample spinning (MASS) solid-state silicon-29 nuclear magnetic resonance (NMR).

MASS NMR spectra for silica polymorphs have been reported in the literature (references 2-6). Stishovite's short T_1 value allows a very brief recycle time between pulses, less than 5 seconds, enabling rapid data acquisition (3,4). The Si-29 NMR spectrum of concentrated stishovite shows a unique single sharp resonance at about 192 ppm referenced to tetramethylsilane. We have clearly identified this peak in insoluble residues extracted from quartzites containing thin pseudotachylites and thus have confirmed the presence of shock-diagnostic stishovite in rocks of theVredefort structure.

Acknowledgements: We thank Dr. J.E.J. Martini for supplying our Vredefort samples, Dr. A. Yates for repeated X-Ray diffraction identifications, and the Barringer Crater Co. of Princeton, New Jersey for partial funding of our study.

References: 1) Martini, J.E.J., 1978. Coesite and stishovite in the Vredefort Dome, South Africa, *Nature*, vol. 272, p. 715-717. 2) Thomas, J.M., J.M. Gonzalez-Calbert, C.A.Fyfe, G.C.Gobbi, and M.Nicol, 1983. Identifying the coordination of silicon by magic-angle-spinning NMR: stishovite and quartz, *Geophys. Res. Lett.*, vol. 10, no. 1, p. 91-91. 3) McHone, J.F., T.I. Emilsson, W-H. Yang, R.J. Kirkpatrick, N. Vergo, and E. Oldfield, 1984. Coesite and stishovite detected in natural concentrations by solid-state silicon-29 nuclear magnetic resonance, *Meteoritics*, vol. 19, no. 4, p. 268-269. 4) Yang, W-H., R.J. Kirkpatrick, N. Vergo, J. McHone, E. Emilsson, and E. Oldfield, 1986. Detection of high-pressure silica polymorphs in whole-rock samples from a meteor crater, Arizona, impact sample using solid-state silicon-29 nuclear magnetic resonance spectroscopy, *Meteoritics*, vol. 21, no. 1, p. 117-124. 5) Smith, J.V., and C.S. Blackwell, 1983. Nuclear magnetic resonance of silica polymorphs, *Nature*, vol. 303, p.223-225. 6) Dupree, R., D. Holland, and M.G. Mortuza, 1987. Six-coordinated silicon in glass, *Nature*, vol. 303, p. 223-225.

PETROGRAPHY OF IMPACTITE FROM NEW QUEBEC CRATER; Ursula B. Marvin and David A. Kring, Harvard-Smithsonian Center for Astrophysics, Cambridge MA 02138, and James D. Boulger, Jr. Free Lance Photographer, Colraine, MA 01340

As leader of an expedition to the New Quebec Crater in 1986, J. Boulger collected a rounded specimen, 1.75 cm across, of gray, vesicular rock from the shore of Lake Laflamme, about 3 km NNW of the crater rim. Petrographic analyses of a thin section established its identity as glassy impactite containing numerous grains of quartz with shock-induced planar features. Impactite is very rare at New Quebec, as the entire region was stripped of its surficial materials and the bedrock eroded to some depth by post-impact glaciation. Only two loose "pebbles" of impactite were collected previously from the crater rim, and only very small pieces of these remain intact today. The new specimen effectively doubles the world's supply currently available for microanalytical studies.

A detailed petrographic description of the New Quebec impactite has not previously been published. Our thin section shows that the main constituent is glass with an approximate bulk composition of SiO_2 66.89, Al_2O_3 17.49, FeO 3.83, MgO 1.53, CaO 2.98, Na_2O 3.51, K_2O 3.14. This is a siliceous, peraluminous glass with a CIPW normative composition of about 25% quartz, 60% feldspar, 10% hypersthene, 3% corundum, and traces of magnetite, apatite, chromite, and ilmenite. Most of the glass is tawny brown and felty with crystallites of feldspar and pyroxene. Halos of clear glass, with the same composition as the felty, surround some quartz grains. This glass evidently quenched against cold clasts before nucleation of crystallites.

Feldspar laths up to 0.3 mm long, with compositions clustering at andesine ($An_{40}Ab_{54}Or_6$) are the most abundant constituent of the felty glass. Needles of pyroxene up to 0.045 mm long crowd the interstices between feldspar laths. Pigeonite ($En_{68}Fs_{28}Wo_4$) and augite ($En_{47}Fs_{19}Wo_{34}$) are both present. No relict grains of feldspar or pyroxene have been found. Quartz is the main surviving pre-shock constituent, and numerous grains of it display two or three intersecting sets of shock-produced planar features. Silica also occurs in irregular masses with crackled surface textures typical of cristobalite. These masses are partially glassy and isotropic, but they include areas of low birefringence that show progressive optical extinction across bundles of fibers radiating from a point. Rare grains of apatite appear to have survived the impact shock unaltered. Some zircon grains show mosaic texture but retain their SiO_2. To date, we have found no baddeleyite, a common breakdown product of zircon at impact sites. Small, sparse grains of iron oxides (magnetite?) are scattered through the glass, and at least one grain of ilmenite appears to have been decomposed and renucleated *in situ* as a row of irregular crystallites. Special scans for nickel in opaques failed to show any detectable trace.

A geological map of the region (Currie, 1965) shows the crater to be excavated chiefly in Archaen granitoid gneisses and a few small pods of amphibolite breccias. In order to compare the bedrock composition with that of our impactite, we are preparing thin sections of four specimens of granitic gneisses from New Quebec, supplied to us by R. A. Grieve. Microprobe analyses are pending on these sections, but preliminary surveys show all four to consist mainly of feldspar, biotite and granulated quartz. Little, if any, pyroxene occurs in the bedrock. None of the biotite occurs in the impactite. According to the scale of shock-pressure effects compiled by Stöffler (1972), impactite with the characteristics we observe in the New Quebec sample will have undergone minimum pressures in the range of 350 to 450 kb. Some features suggest higher pressures. We are continuing our analyses in an effort to better understand why certain minerals partly or wholly decomposed while others, which should be equally vulnerable, survived intact.

References: Currie, K. L. (1965) Canadian Journal of Earth Sciences, v. 2, No. 3, 141-160. Stoffler, D. (1972) Fortschrift für Mineralogie, v. 49, 50-113.

A PRELIMINARY STUDY OF FLUID INCLUSIONS IN SHOCK-METAMORPHOSED SEDIMENTS AT THE HAUGHTON IMPACT STRUCTURE, DEVON ISLAND, CANADA: J.G. Bain and S.A. Kissin, Dept. of Geology, Lakehead Univ., Thunder Bay, Ont. P7B 5E1 Canada

The Haughton impact structure is a well preserved, 22 ma. old (Miocene), meteorite crater that lies in the Lower Paleozoic shelf-type sediments, overlying gneissic Precambrian basement, on Devon Island in the Canadian Archepelago (1) . A suite of fallback breccias including biotite-granite gneisses from the Precambrian basement and monomict and polymict breccias that represent most of the sedimentary succession from the Haughton region was studied. All of the breccias have been shock metamorphosed. Monomict breccias, which are largely carbonate, show very few shock metamorphic effects. Shock effects, are evident in gneisses and they have experienced pressures up to 25 GPa and temperatures up to 300°C. Polymict breccias, containing thermally melted glass and shocked crystal fragments, display the highest degree of shock metamorphism, in the range of 25 to > 55 GPa and 300 to more than 2000°C. These glass-bearing, polymict breccias are highly vesicular due to the high-pressure vapourization of water and silicate minerals and to the decarbonation of calcite-rich sediments into CO_2 gas and CaO.

Small two-phase, liquid-vapour fluid inclusions are generally abundant in the normal glasses of the glass-bearing, polymict breccias. A thorough microthermometric study of these inclusions revealed that they are water-rich, CO_2-free and of low salinity, in the range 0.3 to 3.37 equivalent wt.% NaCl. Homogenization temperatures are most frequent between 140 and 150°C, although the range spans 137 to 243°C. The glasses are essentially pure SiO_2, and these temperatures could not possibly represent true trapping temperatures. The glasses in these polymict breccias are fresh and unfractured, however, indicating that the fluid in the inclusions was not introduced after solidification of the glasses. The following explanation is proposed.

Wet quartz- and carbonate-rich sedimentary rocks that were shocked to more than 28 GPa, a common occurrence at Haughton, were melted and sometimes vapourized. Water from these rocks was dissolved, forming a superheated solution with the silicate melt. Upon passage of rarefraction waves high-pressure, high-density, superheated water vapour exsolved from the superheated water-silicate melt. Much of this vapour was able to expand to atmospheric pressure, vesiculating the melt in the process. The high-pressure, high-density, superheated water vapours that did not escape before the melt quenched formed submicroscopic to 100 μm long vesicles. These vesicles, filled with high-pressure, high-density vapour, were the precursors to the two-phase, liquid-vapour fluid inclusions that were measured. As the quenched melt cooled below the temperature at which the high-density, high-pressure water vapour was trapped, the water vapour condensed into low-density, metastably stretched water solution. Further cooling caused the stretched water in the inclusion to shrink more than its glass host, creating a non-metastable, two-phase, liquid-vapour inclusion. The homogenization temperatures that have been recorded indicate the temperature range over which the one-phase, metastably stretched water-filled fluid inclusions reverted into the stable, two-phase, liquid-vapour state.

REFERENCES:

(1) Frisch T. and Thorsteinsson R. (1978) Arctic 31, 108-124; Bischoff L. and Ostertag R. (1986) Geowiss. Unserer Zeit, 4, 105-115.

GEOCHEMICAL STUDIES OF IMPACT GLASS FROM THE DARWIN CRATER, TASMANIA. Thomas Meisel and Christian Koeberl*, Institute of Geochemistry, University of Vienna, A-1010 Vienna, Austria. (*)also: Lunar and Planetary Institute, 3303 NASA Road One, Houston, TX 77058.

Darwin Glass has been known since the beginning of the century as was first classified as tektite-like, but later identified as impact glass. The main occurence of the glass in in western Tasmania, SSE of Queenstown, but a definitive outline of the strewnfield is difficult to obtain due to the dense vegetation. Less than 20 years ago, a crater was found to be associated with the glass and was termed Darwin Crater (Ford, 1972; Fudali and Ford, 1979). The crater has a diameter of about 1 km, but is poorly discernable on aerial photographs. There is no field evidence for a crater rim, and large parts of the crater floor are covered by lacustrine sediments; target rocks at the crater have been identified to consist mainly of Siluro-Devonian quartzites and shales (Fudali and Ford, 1979). The geological evidence at the crater is in agreement with the glass age of 0.73 My determined by fission track and K/Ar-dating (Gentner et al., 1973). Although this age puts the Darwin glass close to the Australasian tektites, earlier geochemical studies (Taylor and Solomon, 1964) seem to preclude such a connection.

In our study, 18 individual Darwin Glass samples have been analyzed for about 50 major and trace elements in order to establish a complete geochemical database for the Glass. Numerous other samples have been collected during a recent visit to the crater (T.M.) for additional studies. The glasses are predominantly of irregular shape, ranging in color from translucent white over olive green to dark blackish brown. Some samples show clear evidence of glass flow, a layered structure (with differently colored layers), and abundant vesicles (which sometimes are elongated according to the glass flow). Several samples are highly vesicular, giving them a frothy appearance, which is associated with a change in color (probably due to the foamy structure). A few specimens have shapes similar to teardrops or twisted ropes and wires (very much like slightly larger versions of irghizites), with surficially attached glassy droplets that are probably the remainder of an accretionary process operating during the impact formation of the glass.

Significant geochemical differences between Darwin Glass and commmon tektites and other impact glasses are very low CaO and Na_2O contents, which have been attributed to being due to the lack of plagioclase feldspar in the target rocks (Taylor and Solomon, 1964). This is also found here. Cluster and discriminant analysis of the data from the present samples led to the recognition of three different groups of glasses, which differ in major and trace element abundances and correlations. More than 50% of the samples fall into one group, which contains all olive-green and also compact brownish specimens. This group may be termed "average Darwin Glass" or low Fe, Al-group (LFe,Al). The two other groups are about equally abundant and may be termed high Fe, Al (HFe,Al) and high Mg, Na (HMg,Na) Darwin Glasses, respectively. Most samples show rather high Cr, Co, and Ni abundances, with the highest abundances being present in the HMg,Na group. Trace elements are also useful in defining the groups. REE patterns of the glasses do not allow to distinguish between these groups, but are in perfect agreement with a major shale component. Ni and Cr show a very good correlation with each other and especially with Mg (and Ca). This is indicative of a minor ultrabasic component (at least in the HMg,Na group), which so far has not yet been identified at the crater. The geochemical data thus allow to constrain the type and amount of target rocks that have been mixed to form the impact glass.

MULTI-COMPONENT SOURCE FOR MUONG NONG-TYPE BEDIASITE 30775-2; J. H. Wittke, Dept. Geol. Sci., Univ. South Carolina, Columbia, SC 29208, V. E. Barnes, Bur. Econ. Geology, Univ. Texas, Austin, TX 78713-7508

Bediasite 30775-2 (1) contains spherical and elongate inclusions of light-colored glass enclosed by dark-brown to light-brown glass. Electron microprobe analyses give ranges of values for SiO_2, TiO_2, Al_2O_3, and FeO that are broader than those for 25 bediasites (2) (Table 1). MgO values have a similar range, while CaO, Na_2O, and K_2O values are significantly lower than those in the 25 bediasites. The compositional ranges observed in microtektites (3) are generally broader than those in 30775-2. However, SiO_2, TiO_2, Al_2O_3, and FeO reach higher values in 30775-2 than in the microtektites.

Microprobe data are consistent with production of 30775-2 by melting of a heterogeneous source material. EXTENDED QMODEL (4,5) analysis of the data from 156 determinations for each constituent indicates that 99.24% of the observed compositional variations in 30775-2 can be accounted for using mixtures of five components. These end members (Table 2) represent geologically reasonable source materials: shales and sandstones.

(1) Barnes, V. E., 1940, Univ. Texas Pub. 3945, 477-582.
(2) Barnes, V. E., 1967, Internat. Dict. Geophysics, 2, 1507-1518.
(3) D'Hondt, S. L., et al., 1987, Meteoritics, 61-79.
(4) Full, W. E., et al., 1981, Jour. Math. Geol., 13/4, 331-344.
(5) Full, W. E., et al., 1982, Jour. Math. Geol., 14/3, 259-270.

Table 1. Comparison of bediasite 30775-2 with 25 bediasites and 55 microtektites.

	Bediasite 30775-2	Twenty-five bediasites	Fifty-five North American strewn-field microtektites
SiO_2	68.11-84.86	71.89-81.31	63.52-84.16
TiO_2	0.32-1.17	0.53-1.05	0.30-1.08
Al_2O_3	10.50-19.51	10.96-17.56	8.15-17.75
FeO	1.37-6.86	2.29-5.95	2.06-6.24
MgO	0.37-0.91	0.37-0.95	0-3.26
CaO	0.16-0.48	0.41-0.96	0.27-2.97
Na_2O	0.34-1.22	1.20-1.84	0.17-3.04
K_2O	1.28-1.70	1.60-2.43	1.91-4.03

Table 2. End members derived by EXTENDED QMODEL analysis of data from 156 analyses of bediasite 30775-2.

	Shale 1	Sand 1	Sand 2	Sand 3	Shale 2
SiO_2	48.38	90.82	86.26	85.76	52.20
TiO_2	2.13	0.10	0.01	0.35	1.90
Al_2O_3	31.78	6.12	9.83	11.29	29.16
FeO	12.61				13.09
MnO			0.55		
MgO	1.24	0.05	0.58	0.66	1.14
CaO	0.20		0.33	0.67	0.31
Na_2O	2.85	1.11	0.82		0.12
K_2O	0.78	1.80	1.61	1.28	1.79
P_2O_5	0.03				0.29

PLENARY II

FOREIGN OC-TYPE CLASTS IN METEORITIC BRECCIAS : WHAT THEY TELL US ABOUT THE ABUNDANCE OF OC-TYPE ASTEROIDS IN THE MAIN BELT. Paul Pellas, Laboratoire de Minéralogie du Muséum (CNRS), 61 rue Buffon, 75005 Paris,France

One important question in meteorite research which still gives rise to harsh discussions between spectroscopists and meteoriticists is the identification of the asteroids which are the sources of OCs (73% of total falls).In the past 20 years a huge amount of work has been carried out in order to detect - through spectral studies - possible asteroidal relatives of OCs with, alas ! a rather poor success. For instance,if ~15% of Apollo asteroids could belong to the L-LL classes, not even one example is found among the over 500 main-belt asteroids observed that could easily be related to the OCs (Bell,1986).We need therefore to scrutinize the results of laboratory detections of asteroidal debris which have been trapped by asteroid surfaces and which are found to-day as exotic clasts (xenoliths) in meteoritic (regolith + fragmental) breccias,with the hope that their relative abundance will give us a clue to establish the presence - or not - of OC-like asteroids in the main-belt.

A preliminary inspection of litterature data indicates that at least 30% (26 out of ~70) of xenoliths detected to date in meteoritic breccias are OC-type clasts.Among them, 13 carry oxygen isotopic signatures inside or nearby the H-L-LL fields defined by the data of R.N.Clayton's group.A large majority of the others correspond to carbonaceous chondrite clasts, including some CCs which are not present in our collections (e.g. the CC clast in Krymka : Lewis et al.1979;Grossman et al.1980).Three (maybe 4) xenoliths are of enstatite chondrite parentage, five others achondritic relatives.When judging these results, it is worth noting that CC-like xenoliths are more easily detected by visual inspection, thus possibly leading to an even larger abundance of OC-like clasts.Conversely, the greater friability of C1-C2 materials could decrease their apparent abundance in meteoritic breccias.Finally,to our knowledge, no exotic metal clast has been found yet in those breccias.

There are ample evidences (shock effects, loss of volatiles) that these xenoliths were part of projectiles - ejected by collisions from their original parent asteroids, and subsequently trapped (at rather low velocities) by other asteroidal surfaces in the main-belt,at any time between ~4.6 Byr and present. In this sense,they represent an unbiased sampling of asteroidal debris which were in orbits in the main-belt. They show various degrees of equilibration and textural integration which appear to depend mostly on the time when the trapping has occurred : at early times (4.6-4.3 Byr) metamorphic processes inside host asteroids could have lead to partial equilibration (except for oxygen isotopes) (e.g. H clast in Barwell-L5 : Hutchison et al.1988; L clast in Fayetteville-H : Pellas et al.1988); at later times, after target asteroids cooled down, it leads to a lack of equilibration (e.g. Cumberland Falls, St Mesmin).

The fact that such a large number - statistically significant - of xenoliths belong to OC-like materials (including typical H,L,LL plus many relatives) makes it difficult to believe that there is to-day in the main-belt a total absence of asteroidal counterparts, as stated by Bell (1986),Gaffey (1986a, 1986b) and many spectroscopists. Especially because the larger abundance of CC clasts reflects with a good approximation the observed abundance of C asteroids at 2.5 - 3.0 AU (Gradie and Tedesco,1982). The conclusion seems inescapable : many S asteroids must be OC-type objects as previously suggested (Feierberg et al.1982).

Ref. 1)Bell J.F.1986,LPSC XVII,985. 2)Feierberg et al.1982,Ap.J.257,361.3)Gaffey M.J.1986,Meteoritics 21,365.4)Gradie and Tedesco,1982,Science 216, 1405. 5)Grossman et al.1980,GCA 44,211.6)Hutchison et al.1988,EPSL,prepr. 7)Lewis et al.1979,GCA 43,897. 8)Pellas et al.1988,Meteorit.Soc.Meeting, this volume.

COSMOGENIC NEON IN INDIVIDUAL GRAINS FROM KAPOETA, PESYANOE AND MURCHISON

C. T. Olinger, D. H. Garrison, C. M. Hohenberg, *McDonnell Center for the Space Sciences, Physics Department, Washington University, St. Louis, MO 63130 USA*

J. N. Goswami, *Physical Research Laboratory, Navarangpura, Ahmedabad 380 009, India*

R. S. Rajan, *JPL, California Institute of Oceanography, University of California at San Diego, La Jolla, CA 92093 USA.*

Anomalously large amounts of pre-compaction cosmogenic Ne has previously been reported in separated grains from gas-rich meteorites [1,2]. Apparent regolith exposure ages calculated from these Ne concentrations stretch the limits of constraints on regolith exposures, implying either extremely long regolith residence times, or enhanced fluxes of energetic particles in the early solar system. Unlike the previous work, the results reported here were obtained with a continuous argon-ion laser which provides controlled, continuous heating and near 100% extraction efficiency (97±2%).

We have completed a preliminary survey of 81 grains from the gas rich meteorites Kapoeta, Murchison and Pesyanoe with this new system. The first two are displayed in the graphs below, with similar results from Pesyanoe. Three of the Kapoeta grains were etched and selected on the basis of solar flare heavy ion tracks. We have no track information on the remaining 78 grains, which were not etched. However, one would expect only a few percent of them to contain tracks and pre-compaction spallation. Using the chemical data provided in literature for the minerals in Pesyanoe [3,4] and Kapoeta and Murchison[7], we have calculated exposure ages for the peaks in these histograms (which correspond to the grains exposed only during the conventional cosmic ray exposure period) of 45±8, 3.3±.6 and 2.0±.2 Ma respectively. These ages agree quite well with the literature values of 43, 3-6 and .9-2 Ma respectively [5,6,7]. Note that the double peak in the Kapoeta graph is due to pyroxenes and feldspar grains having different Ne production rates, but yielding the same exposure age.

In addition, the three irradiated Kapoeta grains display *apparent* regolith exposure ages of 170, 220 and 260 Ma (computed as if the particle source is equivalent to that of contemporary GCRs). Note that the apparent pre-compaction exposure times for these three grains are similar to the 6-grain ensemble average of 220 Ma reported by Caffee *et al.*. The Murchison grain off to the right corresponds to an apparent regolith exposure time of 82 Ma. One Pesyanoe grain also has cosmogenic 21-Ne consistent with a 270 Ma regolith exposure.

While none of these grains duplicate the two extreme excesses found in the ruby laser study of 600-700 Ma, the data set is still statistically small considering only a few percent of grains from these gas rich meteorites display significant pre-compaction irradiation effects. By conference time we should substantially increase the amount of information displayed here.

[1] Caffee, M. W. *et al.* (1983), J. Geophys. Res. **88**, B267; [2] Olinger, C. T. *et al.* (1988) Lunar Plan. Sci. XIX, 889; [3] Muller, O. & Zahringer, J. (1966) E. P. Sc. Lett. **1**, 25; [4] Reid, A. M. & Cohen, A. J. (1967) GCA **31**, 661; [5] Marti, K. (1969) Science **166**, 1263; [6] Goswami, J. N. *et al.* (1984), Space Sci. Rev. **37**, 111; [7] Caffee, M. W. (1986) Ph.D. Thesis, Washington University.

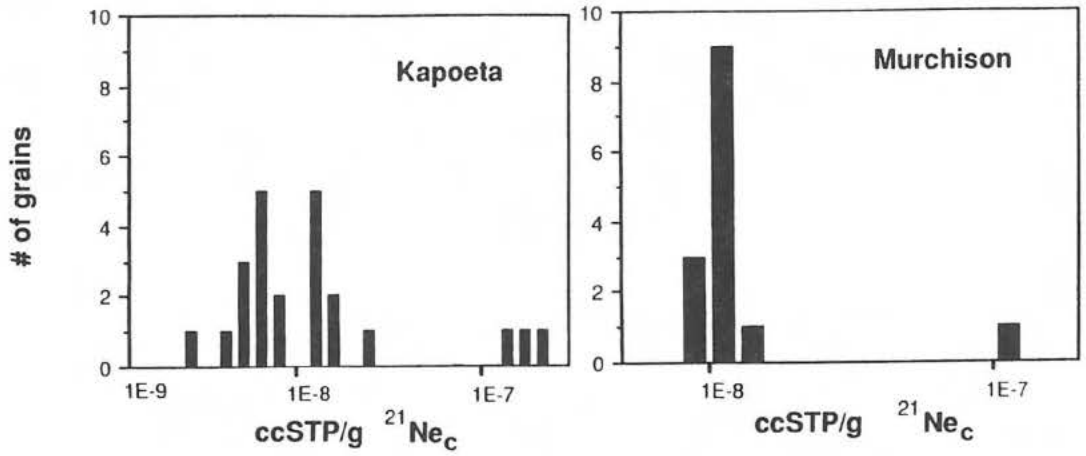

Li, B, Mg AND Al IN SOLAR-FLARE- AND NON-IRRADIATED KAPOETA GRAINS

Marc W. Caffee, *Lawrence Livermore National Laboratory, Livermore, CA 94550 USA.*
Albert J. Fahey and Ernst Zinner, *McDonnell Center for the Space Sciences, Physics Department, Washington University, St. Louis, MO 63130 USA.*
J. N. Goswami, *Physical Research Laboratory, Navrangpura, Ahmedabad 380 009, India.*

A few percent of the mineral grains found in some stoney meteorites contain solar-flare-produced tracks and solar-wind-implanted ions. The presence of these fossil records is evidence that this fraction of grains was exposed to the Sun before consolidation in a breccia. Caffee *et al.* (1,2) observed that grains with solar-flare-tracks also contained far more spallogenic ^{21}Ne than grains without solar flare tracks. To date, the largest ^{21}Ne excess was observed in the Howardite Kapoeta. Production by galactic cosmic rays in the regolith of the Kapoeta parent-body requires exposure of ~ 200 Myr. This long exposure time and the apparent lack of similar excesses of spallogenic isotopes in non-irradiated grains led to propose an alternative hypothesis: production of ^{21}Ne in the track-bearing grains by solar particles from a more active early Sun (1,2). This requires that 1) the exposure occurred ≥ 4.4 Gyr ago, since an active Sun could not remain so for much longer than 100 Myr, and 2) the isotopes of a particular element, such as Ne, can indeed be produced in the proper proportions by protons having considerably less energy than galactic cosmic ray protons.

If the first of these conditions is true then the solar-flare-irradiated grains are an important source of unique material. As such, they deserve close scrutiny by other means. In this initial study we used an ion microprobe to analyze the Al-Mg isotopic system in feldspar grains from the gas-rich meteorite Kapoeta. Regarding the second requirement, it is important to look at reactions other than those producing Ne to possibly set some limits on the flux, or perhaps the energy spectrum of the incident protons. To this end we measured Li and B isotopes in individual grains from Kapoeta. Of the five feldspar grains analyzed one grain (#1) contained solar flare tracks. Lake Co. labradorite (3) was used as a calibration standard for the ion probe measurements.

Al and Mg: Excesses of ^{26}Mg, presumably due to the *in situ* decay of ^{26}Al, are observed in refractory inclusions from meteorites (4). Table 1 shows initial ^{26}Al/^{27}Al ratios inferred from the Mg isotopes and Al/Mg ratios. With the exception of grain #4, all these values are, within errors, zero. The difference for grain #4 is only 2.4 σ and we do not ascribe any significance to it. Spallation reactions also produce ^{26}Al and ^{26}Mg from Al and ^{28}Si, however the production rates are not sufficient to allow the detection of ^{26}Mg effects in feldspar.

Li and B: The abundance of these elements in most rock-forming materials is low, so additions from other sources, such as spallation, may be detectable. Their CI abundance is 1.6 ppm, and 1.0 ppm, respectively (5). These elements are produced by spallation reactions, the principle target being O. Spallation-produced Li and B can be distinguished from naturally-occurring Li and B by their isotopic ratios. For terrestrial materials the isotopic ratios of ^{7}Li/^{6}Li and ^{11}B/^{10}B are 12.33 and 4.03, respectively. In spallation reactions these isotopes are produced in roughly equal proportions, however, the exact ratios are a function of the energy spectrum of the incident protons (*c.f.* 6). Table 1 shows the measured isotopic composition of these elements given as δ-values relative to the Lake Co. standard. None of the grains show any enrichments of ^{6}Li or ^{10}B. By combining the calculated production cross-sections (7) with the measured isotopic ratios we can set some rough limits on the proton fluence. We obtain an upper limit of ~ 5 x 10^{18} protons/cm^2 from the Li and between 6 x 10^{17} protons/cm^2 to 6 x 10^{18} protons/cm^2 from the B data. These results are consistent with the proton fluence based on the production of spallogenic ^{21}Ne, which is ~ 10^{16}-10^{17} protons/cm^2, depending on the shielding conditions under which the irradiation occurred.

Based on this preliminary study it appears that there are no unusual effects in the isotopes of Mg, Al, Li, and B in the solar-flare-irradiated grain and, that excepting the noble gases, this grain cannot be distinguished from the non-irradiated grains or other solar system material.

(1) Caffee *et al.* (1983) *JGR* **88**, B267-B273; (2) Caffee *et al.* (1987) *Ap. J.* **313**, L31-L35; (3) Meyer *et al.* (1984) *Proc. 5th LSC*, 685-706; (4) Gray *et al.* (1973) *Icarus* **20**, 213-239; (5) Anders and Ebihara (1982) *GCA* **46**, 2363-2380; (6) Phinney *et al.* (1979) *Proc. 10th LPSC*, 885-905; (7) Clayton *et al.* (1977) *Ap. J.* **214**, 300-315.

Table 1

Grain	$(^{26}Al/^{27}Al)_0$ (2σ)	Li (ppm)	B (ppm)	$\delta(^{6}Li/^{7}Li)$ (±2σ)	$\delta(^{10}B/^{11}B)$ (±2σ)
1 (irradiated)	$<3.7 \times 10^{-7}$	2.4	1.2	−9 ± 8	11 ± 28
2 (non-irradiated)	$<2.1 \times 10^{-7}$	7.2	0.3	−22 ± 11	26 ± 31
3 (non-irradiated)	$<8.3 \times 10^{-7}$	2.1	0.13	−10 ± 10	0 ± 33
4 (non-irradiated)	$2.8 \pm 2.3 \times 10^{-7}$	6.7	1.1	−17 ± 9	16 ± 23
5 (non-irradiated)	$<1.8 \times 10^{-7}$	4.0	0.38	−16 ± 9	26 ± 25

NITROGEN IN THE FAYETTEVILLE BRECCIA. Monica M. Grady and C.T. Pillinger, Planetary Sciences Unit, Dept. of Earth Sciences, Open University, Walton Hall, Milton Keynes MK7 6AA, U.K.

The Fayetteville H4 ordinary chondrite exhibits the classic light-dark clast-matrix structure associated with regolith breccias. As part of the consortium study of Fayetteville, carbon and nitrogen will be analyzed in separate samples of dark matrix removed from differing depths within the main mass. The aim of the project is to map variation of carbon and nitrogen content and isotopic composition within the chondrite, and to relate any variation to exposure history. It was also hoped that the partitioning of nitrogen between different components (*viz.* solar wind nitrogen (SWN) and spallogenic nitrogen) would allow constraints to be placed on the isotopic composition of the ancient solar wind. Since Fayetteville is the meteorite known to possess one of the highest concentrations of solar wind noble gases (1), it is believed that this is the best sample to study for SWN in a meteorite. Thus far, analysis of nitrogen released by stepped combustion of chips from six matrix separates has been completed.

All the samples analyzed show the same general pattern: a large, low temperature (T<600°C) release of nitrogen with variable $\delta^{15}N$, with decreasing quantities of nitrogen with increasing $\delta^{15}N$ combusting up to 1200°C ($\delta^{15}N$ *ca.* +50 to +100‰). Superimposed on this release profile is a discrete component of nitrogen occurring in the 800 - 900°C temperature increment. At least two of the samples analyzed indicate that the isotopic composition of this additional component is light (< -15‰). The high temperature (T>700°C) nitrogen can be attributed to two components: ^{15}N-enriched spallogenic nitrogen, produced by the interaction of cosmic rays with oxygen in silicates and ^{15}N-depleted nitrogen from the ancient solar wind. Studies of lunar breccias (in which spallogenic nitrogen is believed to be released by pyrolysis at T>1000°C and ancient SWN at 800 - 900°C) indicate that the contribution to total nitrogen content by spallogenic nitrogen is negligible, although total isotopic composition is controlled by this component, since it is highly ^{15}N-enriched (2). The presence of spallogenic nitrogen in Fayetteville accounts for the general drift upwards in $\delta^{15}N$ with temperature. If the same pattern is followed in meteorite regolith breccias as occurs in lunar samples, then the light nitrogen released at 900°C may also be ancient SWN. However, overlapping combustion of spallogenic nitrogen implies that $\delta^{15}N$ of the 900°C step is an upper limit for the $\delta^{15}N$ of ancient SWN. Calculation of $N/^{36}Ar$ ratio using the nitrogen concentration of the 900°C step yields a value close to that derived from lunar studies (3).

In contrast to lunar breccias, over 60% of the total nitrogen inventory in Fayetteville is released below 500°C. After allowing for atmospheric contaminants, the low temperature nitrogen is shown to have $\delta^{15}N$ *ca.* -20 ± 10‰, much lighter than $\delta^{15}N$ of meteoritic organic matter (4,5), and also of common terrestrial contaminants (6). The nature of this component is not understood, but it is weakly-bound by comparison with the putative implanted SWN.

References: (1) Schultz and Kruse (1983) MPI (Mainz) Data Compilation; (2) Becker *et al.* (1976) *PLPSC 7th.* 441-458; (3) Geiss and Bochsler (1982) *GCA* **46**, 529-548; (4) Robert and Epstein (1982) *GCA* **46**, 81-95; (5) Becker and Epstein (1982) *GCA* **4**, 97-103; (6) Heaton (1986) *Chem. Geol.* **59** 87-102.

CATHODOLUMINESCENCE STUDY OF THE FAYETTEVILLE AND PLAINVIEW GAS-RICH REGOLITH BRECCIAS John M. DeHart and Derek W.G. Sears, Cosmochemistry Group, Department of Chemistry and Biochemistry, University of Arkansas, Fayetteville, AR 72701.

The gas-rich regolith breccias provide a unique means of studying the space environment and surface processes on small atmosphere-less bodies. The main questions posed by such meteorites center on the chronology of brecciation and history and origin of the unusual dark matrix which surrounds the normal light chondritic clasts. The matrix is rich in solar wind gases, carbon, highly volatile elements and solar flare tracks. In a recent thermoluminescence (TL) study (1), we found a variety of correlations which suggested that the dark matrix is comminuted clast material to which a non-ordinary chondrite component has been added, rather than being a novel 'primitive' material akin to type 3 ordinary chondrites. We decided to make a cathodoluminescence (CL) study of regolith breccias to explore further the origin of the dark matrix and to try to identify the non-ordinary chondrite component required by the TL data to be present in certain regolith breccias. We chose to look at two samples, Fayetteville and Plainview, which lie at opposite ends of the spectrum of properties we found in our TL study.

If the dark matrix were type 3 material to which clast had been added during the regolith working, a process which must surely have occurred to some degree, then the matrix of Plainview and Fayetteville should consist of about 80-90% type 3 material and 10-20% comminuted clast material in order to produce the TL sensitivity observed. If, on the other hand, the matrix is basically comminuted clast, then type 3 material will be present in minor or trace amounts. The photomosaics of the CL of Fayetteville and Plainview show that little or no type 3 component is present in the dark matrix. Type 3 chondrites have highly characteristic CL properties which include a fine-grained matrix with red or no CL and chondrule mesostases with yellow, red and blue CL. Type 4-6 chondrites show a uniform blue or blue-green CL in all components with only an occassional phosphate grain with red CL. These trends and the factors controlling them have been studied in detail by DeHart et al. (2). The regolith breccias show lower CL in the matrix than in the clasts, as predicted by the TL results, and both clasts and matrix display blue or blue/green CL from the majority of luminescent components. Red, yellow, green or green/brown components are only very occasionally observed and may well be xenoliths acquired during brecciation. The data therefore confirm the conclusion of the TL study that the matrix is comminuted clast material. These results contrast well with those for Ngawi, in which CL imagery shows clearly the existence of type 3.0-3.1 and 3.3-3.4 clasts in a type 3.5 matrix (3).

We could find no evidence in the present data for a luminescent component the TL data require to be present in Fayetteville but absent in Plainview. Presumably the component has CL properties similar to those of 'normal' chondritic material.

(1) Haq et al., (1988) GCA in press (see 49th Ann. Mtg. Meteor. Soc. Abs. vol., p.378). (2) DeHart et al. (1988) LPS XIX 259. (3) DeHart and Sears (1986) LPS XVII 160. (Support NASA NAG 9-81 and NGT-50064).

EXOTISM IN FAYETTEVILLE. P. Pellas, Lab. de Minéralogie du Museum, 61 rue Buffon 75005 Paris, France ; R.N. Clayton, Enrico Fermi Institute, University of Chicago, Chicago, Il. 60637, USA ; R. Wieler and P. Signer, ETH-Zurich, NO C 61, CH-8092 Zurich, Switzerland.

Preliminary results on the irradiation history of light fragments in the gas-rich chondrite Fayetteville have shown that 6 out of 7 clasts present similar Ne_c-21 and He_c-3 concentrations, whereas one (clast "s") contains an excess of $\sim$10% of He_c-3 and $\sim$20% of Ne_c-21, thus possibly indicating a specific pre-exposure in the regolith (1). To be sure that the excess of cosmogenic isotopes are not due to a target effect, chemical and mineralogical analyses were performed on the remaining sample of clast "s". The results are the following :

Fe-Ni : 10.6% (L chondrites : 8-11% ; H ch.: 17-21%)
Fe/Ni : 3.1 (L ch.: $\sim$ 4.8 ; H ch.: $\sim$ 9.3)
Olivines : Fa 18.0-19.1 (L ch.: 22.5-25.5 ; H ch.: 16.5-20.5)
Pyroxenes : Fs 14.8-16.0 (L ch.: 18.5-22.5 ; H ch.: 14.5-18.0)

As the clast presents both an L- (metal abundance, Fe/Ni ratio) and an H-parentage (fayalite and ferrosilite contents in olivine and pyroxene), an oxygen isotopic analysis has finalized the result : clast "s" has an O-17 excess characteristic of L-chondrites (δ 18 = 5.82; δ 17 = 4.58; δ 17 - 0.52 δ 18 = 1.11). It lies, however, somewhat beyond the heavy end of the range of the L-chondrites analyzed in Chicago.

It must be noted that clast "s" appears on the picture of Fayetteville slices slightly less rusty than the others light clasts of typical H composition. It is unfortunate not to have previously detected such a singularity in order to save more material for future studies.

The K-Ar age of clast "s" (assuming a K content of 870 ppm) corresponds to $\sim$ 4.3 Byr, similar to the age data of all other analyzed H-clasts. The near absence of shock effects, the textural integration and chemical equilibration with the H host, suggest that this "L" material was trapped by the Fayetteville parent-body at a time when metamorphic processes were still acting in the H asteroid,, but later than the accretionary stage suggested by the CRISPY inclusion in the L asteroid (2). This would indicate that the oxygen isotope equilibration is a sluggish process compared to Fe diffusion in silicates. A similar clast, with a silicate fraction showing an oxidized iron content close to that of H chondrites but a much lower content of metal, has been described ("clast 2") in Supuhee (H6) breccia (3).

The equilibration of silicates achieved in clast "s" would apparently discard a first pre-exposure before its trapping by the H-asteroid. Fe diffusion in silicates requires indeed an higher activation energy than He-3 diffusion. Its lower metal content does not also seem sufficient to explain the cosmogenic isotope excesses, thus leaving alive the irradiation history scenario suggested by noble gas and track analyses (4).

Actually, based on oxygen isotopes signature, 6 inclusions of H-group chondrites have already been found in L chondrites, and 1 in a LL chondrite, while only 2 LL xenoliths have been found in one H- and one L-chondritic breccias. Fayetteville is the first L-clast found in one H-chondrite (5).

Acknowledgments : We are grateful to Dr. Sears for having initiated the Fayetteville Consortium and for having supplied the samples. We also appreciate the effort of the curatorial staff at JSC for the samples preparation.

References : 1) Wieler et al. 1986, Meteoritics 21 , 538. 2) Olsen E.J. et al. 1981, EPSL 56 , 82. 3) Leitch C.A. and Grossman L. 1977, Meteoritics 12 , 125. 4) Wieler et al. 1988, GCA to be published. 5) Clayton R.N. (personal communication to P. Pellas).

ORIGIN AND SIGNIFICANCE OF OLIVINE DISLOCATIONS IN CHONDRITES WITH DOCUMENTED STRAIN. Deana S. Sneyd, Homestake Exploration, 420 Main St., Lead, SD 57734; Gordon L. Nord, Jr., U.S. Geological Survey, 959 National Center, Reston, VA 22092; Harry Y. McSween, Jr., Department of Geological Sciences, University of Tennessee, Knoxville, TN 37996.

Two different strain gauges, based on chondrule petrofabrics and anisotropy of magnetic susceptibility, have recently been quantified in ordinary chondrites (Sneyd et al., 1988, and references therein). Both strain measurements indicate that chondrites have been deformed to varying degrees by nearly uniaxial compression subsequent to accretion. Although petrofabric strain is based on chondrule shapes and magnetic anisotropy is controlled by the shapes of metal grains commonly situated between chondrules, the axes of strain and susceptibility ellipsoids are correlated in magnitude and orientation.

Analysis of microscopic deformation provides further insight into the process that produced these planar fabrics. TEM analyses of one highly strained chondrite (McKinney, with 15% uniaxial compaction) and one unstrained or minimally strained chondrite (Adrian) have been performed. Olivines in both meteorites contain subgrains, interpreted to have formed during chondrule crystallization, overprinted by dislocations of varying character. In McKinney, dislocation densities of 5×10^9 traces/cm^2 are distributed homogeneously throughout olivine grains. Most dislocations appear to be [001] screw type, which are complicated by the presence of loops, jogs, and curly dislocations. Some unusual [010] dislocations have also been observed. In Adrian, olivine dislocation densities vary from 10^7 to 10^9 traces/cm^2 and are heterogeneously distributed over a scale of several micrometers. Most dislocations have long, straight segments of simple character with [001] Burgers vectors.

The types of olivine dislocations found in both chondrites are indicative of shock deformation by low-temperature plasticity. However, the distinct character of dislocations in McKinney and Adrian indicate different thermal states during and after shock. McKinney experienced higher shock pressure and temperature, which produced more uniformily distributed dislocations and enhanced recovery. These observations are consistent with arguments based on other shock indicators (olivine fracturing, undulatory extinction, and mosaicism; noble gas abundances) which suggest that chondrite petrofabrics and magnetic anisotropy were produced by impacts (Sneyd et al., 1988).

Sneyd D.S., McSween, H.Y., Sugiura N., Strangway D.W. and Nord G.L. (1988) Origin of petrofabrics and magnetic anisotropy in ordinary chondrites. Meteoritics, in press.

SHOCK-INDUCED Fe^{2+} DISORDER IN THE PIGEONITE PHASES OF UREILITES

R. W. Dundon, Chemistry Department, University of Benin, Benin City, Nigeria, West Africa (Marquette University for sabbatical)

Pigeonites were separated from four ureilites. The Fe^{2+} site populations on the M_1 and M_2 sites were determined by Mössbauer spectroscopy at 80K. The pigeonite phases of Novo Urei, Goalpara, Kenna and Dingo Pup Donga all have significant Fe^{2+} disorder. Comparison with the shock intensities required in the laboratory to disorder Fe^{2+} in Bamle enstatite (1,2) suggests that all of these pigeonites were shocked to a higher intensity than 45 GPa. The Dingo Pup Donga pigeonite has far more Fe^{2+} disorder than any of the other ureilites or than Bamle enstatite shocked to 100 GPa in the laboratory. (1,2)

(1) R. W. Dundon and S.S. Hafner, Science 174, 581 (1971)
(2) S. S. Pollack and P. S. DeCarli, Science, 165, 591 (1969)

^{57}Fe MÖSSBAUER ABSORPTION OF DINGO PUP DONGA PIGEONITE AT 80K

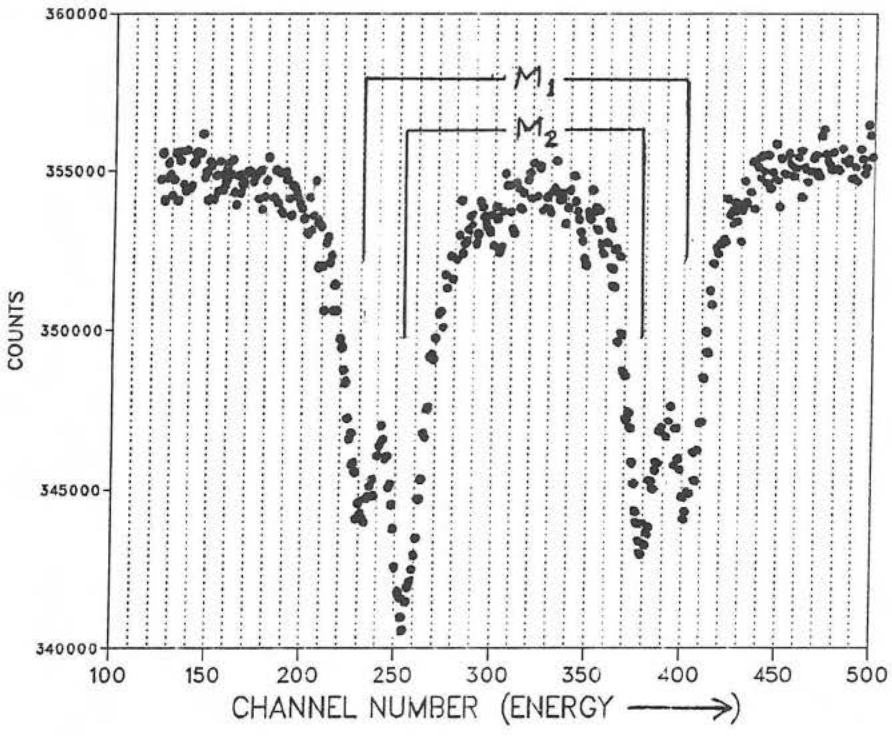

IDENTIFICATION OF SHOCK INDUCED CHANGES IN Fe SPHERES USING MAGNETIC TECHNIQUES

Peter Wasilewski, NASA/Goddard Space Flight Center, Code 691, Greenbelt MD. 20771

Solution annealed Cu (1.5 wt % Fe) alloys were precipitation annealed at 650°C and 750°C to produce size controlled dispersions of non-magnetic fccFe spherical precipitates. Discs of these alloys were then impacted at levels up to 5 GPa and then magnetically characterized after recovery. The impact transforms the fccFe to magnetic bccFe. Substructure in the precipitates before and after shock was characterized. Specimens studied had particle size distributions of 20-35 nm, 40-60 nm, and 80-110 nm. The shock direction was located in the disc by measurement of angular variation of magnetic-coercivity. Magnetization reversal is unique because of the near ideal magnetic properties of fine Fe particles having a narrow size distribution, a mean interparticle spacing dependent on size distribution, no clusters or agglomerates of any kind, the same substructure in all Fe particles, and no significant variation in particle shape.

Magnetic hysteresis analysis is used to follow the magnitude of the shock induced magnetic anisotropy which is impact level dependent. The magnetic anisotropy can be eliminated by thermal anneal, suggesting that not only shape change but the transformation microstructure is dependent on the structure of the shock wave. Alternating field demagnetization before and after anneaal and thermal demagnetization of saturation remanence illustrate the influence of shock impact on the magnetic stability of the spheres. These effects are superimposed on the size dependent properties of the spheres.

These results demonstrate that shock effects can be identified by magnetic techniques, and with calibration, the level of shock can be ascertained. Information about the structure of the shock in the material is also attainable. These results apply directly to lunar samples and are the basis for analysis of the meteorites.

ICE PATTERNS AND SURFACE WIND IN THE SETTING OF ANTARCTIC METEORITES

Peter J. Wasilewski[1], Gary R. Huss[2], Jerry Wagstsff[3], and Carl Thompson[4]

[1]NASA/Goddard Space Flight Center, Code 691, Greenbelt, MD 20771; [2]Enrico Fermi Institute, U. of Chicago, Chicago, IL 60637; [3]Lockheed EMSCO, 2400 NASA Rd. 1, Houston, TX 77058; [4]9 Exmouth Rd., Northcote, Auckland, New Zealand

During the 1987-1988 Antarctic field season, about 370 meteorite pieces were picked up by the reconnaissance team on exposed blue ice patches west and northwest of Elephant Morraine. The ice patches exhibited distinctive surface texture and other features, such as topography, which suggest differences in horizontal and vertical velocities and consequently different ablation rates. In some cases, different velocity vectors and evidence of submergent and emergent patches could be implied by noting the appearance and orientation of the surface texture of the ice and the presence of shear bands and other structural characteristics. It is clear that a considerable differential movement within and between ice patches is characteristic and these dynamics must figure in the appearance of meteorites at the surface.

In one location (Texas Bowl), surface winds appear to locally concentrate meteorites. The size distribution is narrow and the meteorite materials appear localized in an oriented, superimposed texture produced by shear which is subparallel to the prevailing wind direction on a steep slope. At the western end of Meteorite City near a discontinuity marked by pinacles, a few heavily weathered meteorites were found, indicating long surface residence times for this site. On the farthest ice fields we visited, no meteorites were found. The surface of these fields was dominated by a regular and continuous oriented ripple pattern suggesting little or no significant ablation.

From the field evidence, meteorites appear in greatest concentration on blue ice patches that have specific surface textures and related larger scale structural patterns. It is also clear that surface winds may be important locally in concentrating meteorites.

EVIDENCE FOR A RELATIONSHIP BETWEEN THE NATURAL THERMOLUMINESCENCE AND THE ANTARCTIC METEORITE RECOVERY LOCATIONS. Fouad A. Hasan*, Derek W.G. Sears*and William A. Cassidy+. *Cosmochemistry Group, Department of Chemistry & Biochemistry, University of Arkansas, Fayetteville, AR 72701. +Department of Geology and Planetary Sciences, University of Pittsburgh, Pittsburgh, PA 15260.

The discovery of a large number of meteorites in Antarctica poses interesting questions concerning concentration mechanisms, and it also poses a challenge concerning the selection of the most scientifically significant meteorites. Petrographic surveys identify meteorites which are compositionally unusual, but not compositionally normal meteorites with unusual histories. Natural thermoluminescence (TL) measurements, which can be performed on large numbers of specimens, identify meteorites with unusual thermal and radiation histories, such as high temperatures due to recent shock-heating or small perihelion orbits, and they provide an indication of terrestrial age (1-4). In a recent study of 172 meteorites collected during the 1985 season, Lewis Cliff meteorites were found to tend towards lower TL levels compared with those collected at the Allan Hills, inferring a greater proportion of large terrestrial ages for the former site (5).

We now report data for 58 meteorites collected from Lewis Cliff during the 1986 season. The measurements were made in the manner described in ref. 1. The distribution of natural TL for the 1986 collection is significantlly different from the earlier data for the site, having a greater proportion of larger values. The TL sensitivity data for the two years is also different, the 1986 data showing a sharp peak in the histogram at 0.5 (Dhajala=1) suggesting that the 1986 collection contains a number of paired meteorites. These data are related to field relationships, in that the 1986 samples were collected further down field as the ice tongue is systematically searched south to north. There may be a systematic change in terrestrial age along the ice tongue. Additionally, several of the 1986 samples were collected from a gully to the east of the tongue, and these may be paired. It is clear that there are variations in natural TL with location on the ice which are related to pairing and possibly accumulation mechanism. Further study of the present data and, importantly, a completion of the sampling at the site, will surely yield new information on the accumulation mechanism as well as identify unusual meteorites.

Grant support: NASA grant NAG 9-81, NSF grant DPP-8613998. Field work supported by NSF grant DPP-8314496.

REFERENCES: 1) Hasan et al.(1987) J. Geophys. Res. 92, E703. 2) Sears & Hasan (1986) 83-100, LPI Tech. Rept. 86-01. 3) McKeever & Sears (1980) Mod. Geol. 7, 137. 4) McKeever (1982) EPSL 58, 419. 5) Hasan & Sears (1988) LPSC XIX, 457. 6) Hasan et al. (1988) Smith. Cont. Earth Sci. (submitted).

DO ANTARCTIC METEORITE CONCENTRATIONS REFLECT THE AVERAGE INFALL RATE?
Gary R. Huss[1], Peter J. Wasilewski[2], Jerry Wagstaff[3], and Carl Thompson[4], [1]Enrico Fermi Inst., Univ. of Chicago, Chicago, IL 60637, [2]Code 691, NASA Goddard, Greenbelt, MD 20771, [3]Lockheed EMSCO, 2400 NASA Rd. 1, Houston, TX 77058, [4]9 Exmouth Rd., Northcote, Auckland, New Zealand.

Models to explain concentrations of meteorites on blue ice in Antarctica have traditionally assumed a meteorite infall rate of 1-6 km^{-2} $(10^6$ yr$)^{-1}$ (e.g., 1,2). Such a low infall rate requires that meteorites now found on blue ice came from a very large area. The standard model for meteorite accumulation can be summarized as follows (1,2). Meteorites fall on the ice cap and are incorporated into the ice. Usually they are carried to the ocean by the ice. Sometimes the ice encounters a barrier. Stagnant ice behind the barrier ablates, leaving meteorites behind.

Two lines of evidence suggest that the assumed infall rate is in error. In Eastern New Mexico, 153 meteorites from 84 falls have been collected by systematic search of 11 km^2 where the soil had blown away (3,4). From the concentration of meteorites and an estimate of the accumulation time, one can calculate a meteorite infall rate. Two estimates using different accumulation times are 125 km^{-2} $(10^6$ yr$)^{-1}$ (5) and 400 km^{-2} $(10^6$ yr$)^{-1}$ (6) for meteorites > 10 grams. These estimates were based on incomplete data (4) and are therefore lower limits. In addition, meteor observations give a rate of infall for meteorites > 10 grams of 200 km^{-2} $(10^6$ yr$)^{-1}$ (7).

Table 1 shows data for five ice fields near Allan Hills where ice flow has not been stopped by a barrier. Also shown are the accumulation times necessary to produce the observed meteorite concentrations based on the range of infall rates listed above. Direct infall can probably account for the observed meteorite concentrations, provided the snow accumulation rate was low. Numerous blue-ice patches in the Allan Hills area suggest that local snow accumulation is minimal.

It has long been recognized that wind moves meteorites across the ice and modifies the initial concentrations. For example, Texas Bowl is a bowl-shaped area on the downwind side of a large blue-ice patch which, except for Texas Bowl, is largely barren. The meteorites seem to have been blown from most of the ice but were trapped by the rough ice surface and shape of Texas Bowl. At nearby Meteorite City-Upper Meteorite City, meteorites are less abundant, larger, and are often more highly weathered than those at Texas Bowl. The meteorites recovered at Meteorite City seem to be remnants of a larger population that has been depleted by the wind.

Table 1: Meteorite concentrations and sizes on flowing blue ice.

Ice Patch	Meteorites/km^2	Median Size	Falls/km^2*	Accumulation Time (yrs)
Allan Hills Far Western	3.1	41 gr	1.7	4,250 - 13,600
Allan Hills Midwestern	2.2	30 gr	1.2	3,000 - 9,600
Northern†	1.1	103 gr	0.6	1,500 - 4,800
Met. City-Up. Met. City†	7.3	114 gr	4.0	10,000 - 32,000
Texas Bowl†	48.4	43 gr	27	67,500 - 216,000
Texas Bowl and upwind ice†	18		10	25,000 - 80,000

* assuming a ratio of meteorites to falls of 1.8 as seen in Eastern New Mexico (3,4).
† visited during 1987-88 field season; columns 1 and 2 estimated from incomplete collection.

(1) Cassidy (1983), in Oliver, James, and Jago (eds.), Antarctic Earth Science, Canberra. (2) Bull and Lipschutz (1982), LPI Technical Report 82-03. (3) Scott et al. (1986), Meteoritics, 21, 303-308. (4) Huss, G. I, personal communication. (5) Wells and Zolensky (1988), LPSC XIX, 1259-1260. (6) Huss, G. I (1978), Meteoritics, 13, 498; unpublished manuscript. (7) Halliday et al. (1984), Science, 223, 1405-1407.

Relative Abundance of Different Types of Meteorites and the Quality of the Antarctic Meteorite Sample

Ralph Harvey, Department of Geology and Planetary Science, University of Pittsburgh, Pittsburgh, PA 15260

Traditionally the relative abundances of different types of meteorites have been modeled from the Modern Falls. With the inclusion of the collection of meteorites from Antarctica, has the concept of expected relative abundances changed?

The Antarctic finds are comparable to the Modern Falls because they are easily recognized as meteoritic, and have not been highly weathered. The collections differ in two important ways. On one hand, the Modern Falls represent a larger collection area; on the other, the Antarctic finds represent a longer collection time. Both collections are thus important, but in different ways, because they represent samples integrated over different variables: time and space.

The Allan Hills Main Icefield is the only Antarctic meteorite collection site which has been thoroughly searched and from which all the meteorites have been systematically removed and examined. This icefield also shows no strong evidence of being affected by single fall events (1). If we assume that these meteorites are a good sample of what has fallen onto the Antarctic icesheet, we can compare these directly to the Modern Falls. A good test of the similarity of the two samples is the relative abundance of different broad compositional classifications of the meteorites.

Two things must be done in order to compare the relative abundance of different types of meteorites between the Modern Falls and the Antarctic Finds from the Allan Hills Main Icefield. First, we must compare masses, not numbers. There is a strong surplus in number of H chondrites in the Allan Hills population (2). Second, we must remove some of the extremely large meteorites from both collections. The rationale for this is that they are much larger specimens than would be expected to have fallen over the collection area and time represented by the two meteorite collections. When this is done, the relative abundances of different types match within reasonable confidence levels. This match is good only at a broad classification level; rarer class estimates are highly affected by the statistics of small numbers.

If we conclude, due to similarity of relative abundance of masses by type, that the Modern Falls and the Allan Hills Main Icefield samples are equivalent, then we have two samples which can be used to model the meteoritic population which come to the Earth. If we conclude that the two samples are not equivalent, we have to choose which is more representative; integration over time, or integration over geographical area. The choice between the two has bearing on studies of current and ancient meteorite influx rates and size distributions.

1. Harvey, R., 1988. Poster Session, this meeting.
2. Harvey, R., 1987. *Meteoritics*, 22, p.403.

AKAGANEITE, NOT LAWRENCITE, CORRODES ANTARCTIC IRON METEORITES.
Vagn F. Buchwald (1), and Roy S. Clarke, Jr. (2); (1) Department of Metallurgy, Building 204, The Technical University, 2800 Lyngby, Denmark, (2) Department of Mineral Sciences, NHB-119, Smithsonian Institution, Washington, D.C. 20560, U.S.A.

A suite of 12 iron meteorites from various environments and locations in Antarctica was studied, representing a range of chemical compositions, metallographic structures, and degrees of weathering. Polished sections of unaltered metal with adhering corrosion products were examined optically and by electron microprobe, and material was removed from these sections for X-ray diffraction examination. Meteorites selected included 5 from group IA, 2 IIA, 1 IIB, 2 IIIA, and 1 IVA; with a range of Ni values from 5.26% to 18.9%. The major corrosion products observed with general formula and range of Ni and Cl contents are: akaganeite, β-FeOOH, 0.5-19%Ni, 0.3-5.4%C.; goethite, α-FeOOH, 1.0-8.0%Ni, 0-0.5%Cl; lepidocrocite, γ-FeOOH, 0.5-11%Ni, <0.2%Cl; maghemite, γ-Fe_2O_3, 0.4-7.0%Ni, <0.1%Cl. The corrosion products contain small amounts of foreign mineral grains (quartz, olivine, feldspar, calcite, etc.), and the individual oxides contain small amounts of introduced elements (Ca, K, Mg, Al, Si, Na), and occasionally S from the weathering of troilite.

The corrosion reaction is fundamentally electrochemical in nature. Iron goes into solution at the anode ($Fe^0 \rightarrow Fe^{+3} + 3e$). Oxygen is reduced at the cathode ($O_2 + 2H_2O + 4e \rightarrow 4OH^-$). The two reactions may be separated in space, requiring an electrically conducting medium to move electrons from anode to cathode, and an electrolyte to move anions from cathode to anode. Taking into consideration that akaganeite is formed at the reaction front, the total reaction may be expressed as

$$2\ Fe + 3/2\ O_2 + H_2O \rightarrow 2\ \beta\text{-}FeOOH.$$

Corrosion products testify to a more complex process that employs the structural and ion exchange properties of akaganeite. Akaganeite accomodates both Ni^{2+} and Cl in its structure. It forms immediately behind corrosion fronts, with its highest Cl contents next to metal interfaces. A more realistic reaction producing akaganeite from kamacite is:

$$30\ Fe^0 + 2\ Ni^0 + 2\ H^+ + 2\ Cl^- + 47\ O + 21\ H_2O \longrightarrow$$

$$2\ [Fe_{1.5}Ni][O_{12}(OH)_{20}]Cl(OH)_2.$$

Cl^- ion is apparently ubiquitously available in nature to supply electrical neutrality at the corrosion front, even under conditions of meteorite residence within and on Antarctic ice. Akaganeite transforms with time to the other oxides.

No justification for lawrencite, $(Fe,Ni)Cl_2$, has been found in this work. The rationale presented here accounts for the type of observations that have previously been made on similar materials and attributed to lawrencite, a name in the mineralogical literature that has never been adequately defined.

THE DISTRIBUTION OF EVAPORITIC WEATHERING PRODUCTS ON ANTARCTIC METEORITES. *Michael A. Velbel, Dept. of Geological Sciences, Michigan State University, East Lansing, MI 48824-1115*

The present procedure for classifying the weathering of Antarctic meteorites is based on the amount of rust visible to the unaided eye; weathering categories "A", "B", and "C" indicate, respectively, "minor", "moderate", and "severe" rustiness. However, other forms of terrestrial alteration, which do not involve the formation of rust, are also known. The most obvious and widely noted of these "non-rusty" alterations is the appearance of white powders or efflorescences on the surfaces of meteorites. Previous work on the white powdery deposits has been limited to a handful of descriptive mineralogical studies on nine meteorites [1-4] which demonstrated that the deposits consist of various evaporite minerals (hydrous Mg- and Ca-carbonates and sulfates).

To investigate the distribution of evaporite minerals as a function of meteorite composition or weathering class, a census of evaporite occurrences on Victoria Land meteorites was taken. Census results indicate: 1) A strong compositional influence is suggested for carbonaceous chondrites. Carbonaceous chondrites make up only two per cent of the total number of Antarctic meteorites, yet they constitute nearly one-fifth (19.4%) of the described occurrences of evaporite deposits. The widespread occurrence of evaporite mineral deposits on Antarctic carbonaceous chondrites is most likely due to terrestrial redistribution of pre-terrestrial carbonate and sulfate minerals. 2) A weak compositional influence is also suggested for the E chondrites, LL chondrites, and possibly achondrites. 3) For L and H chondrites, and irons/stony-irons, the proportion of meteorites of that group among the evaporite-bearing meteorites is sufficiently similar to their relative abundance among the total population of Victoria Land meteorites to suggest that there is no significant difference in the susceptibility of these meteorite groups to evaporite formation. 4) There are several reports of paired meteorites in which only one individual possesses white deposits. Differences in the weathering behaviors of paired meteorites cannot be due to differences in meteorite composition, and must be due to external environmental factors. 5) Almost two-thirds (65.7%) of the evaporite-bearing stony meteorites are classified as weathering classes A, A/B, or B. Many of these evaporite-bearing but less-rusted meteorites are carbonaceous chondrites and achondrites. 6) Most evaporite-bearing ordinary chondrites are in weathering class B.

The formation of evaporite minerals requires either remobilization of elements from within the sample or addition of elements from outside. The large number of evaporite occurrences on rust-poor meteorites indicates that meteorites of weathering classes B, A/B, and even A may have experienced significant element redistribution and/or contamination as a result of terrestrial exposure. A lower-case "e" should be added to the weathering classification of evaporite-bearing Antarctic meteorites, to inform meteorite investigators of the presence of this potentially significant terrestrial weathering feature, which is not included in the present weathering classification.

References: [1] Yabuki, H., Okada, A., and Shima, M. (1976) *Sci. Papers Inst. Phys. Chem. Res.*, v. 70, p. 22-29. [2] Marvin, U.B. (1980) *Antarct. Jour. U.S.*, v. 15, p. 54-55. [3] Marvin, U.B., and Motylewski, K. (1980) *Lunar and Planetary Sci.* XI, p. 669-670. [4] Gooding, J.L., Jull, A.J.T., Cheng, S., and Velbel, M.A. (1988) *Lunar and Planetary Sci.* XIX, p. 397-398.

TWO METHODS FOR DETERMINING WEATHERING IN EQUILIBRATED CHONDRITES; Ann M. Yates, Department of Chemistry, Arizona State University, Tempe, AZ 85287

X-ray diffraction and a simple loss-on-ignition can be used to indicate the presence of weathering in ordinary equilibrated chondrites.

Buddhue's studies of iron meteorites indicate that, of the minerals present, kamacite is the most susceptible to weathering (oxidation), followed by troilite, and then taenite. This is further supported by the 1970 work of Tackett et.al. on the electrolytic dissolution of iron meteorites.

Magnetite and goethite were the predominant weathering products identified by Buddhue's x-ray diffraction work on iron meteorites. He found less conclusive evidence for the presence of hematite and bunsenite. In chondrites, the situation is complicated by the fact that there are large amounts of olivine, pyroxene, and feldspar contributing diffraction lines to the pattern, and many of the strongest diffraction lines of the potential weathering products lie under these peaks. However, the most intense peak of goethite at 4.18 Angstroms is sufficiently isolated from other peaks in the diffraction pattern of powdered chondrite material to allow it to be diagnostic for weathering of metallic Fe.

Using Mason's values for the average composition of L and H group equilibrated chondrites, one can calculate the expected "loss-on-ignition" as gains of 4.1 and 8.3%, respectively. Since most of the weight gain on ignition is due to oxidation of metallic iron to the oxide, any prior oxidation of metallic iron will cause this observed change to be less and the overall gain in weight to be lower. Thus, low experimental values indicate weathering.

Several equilibrated chondrites have been investigated using x-ray diffraction and loss-on-ignition. In each case, the presence of the diagnostic goethite peak at 4.18 Angstroms correlates with a low observed loss-on-ignition value.

Buddhue, J.D. (1957) The Oxidation and Weathering of Meteorites. University of New Mexico Press

Mason, B. (1965) The chemical composition of olivine-bronzite and olivine-hypersthene chondrites. Am. Mus. Novitates, 2223, 1-38

Tackett, S.L., R.A. Tucker, & F.R. Davis. (1970) Electrolytic corrosion of iron meteorites. Meteoritics, 5, 43-55

DIFFERENT INTERPLANETARY SOURCE REGIONS OF ANTARCTIC AND NON-ANTARCTIC H-CHONDRITES? THE NOBLE GAS RECORD; H.W. Weber, L.Schultz, and F. Begemann, Max-Planck-Institut für Chemie, D-6500 Mainz, FRG.

On the basis of differences in the concentrations of some trace elements it has been suggested that Antarctic and non-Antarctic chondrites have different parent populations (1,2,3), a proposition which is being debated, however (4,5).

Non-Antarctic H-group chondrites have a cosmic-ray exposure age distribution which is characterized by a peak at about 8 Ma. This peak, between nominal ages of 6 Ma and 10 Ma, contains about 45% of all H-chondrites and is interpreted as caused by a major collisional event, which spalled these meteorites off their parent body 8 Ma ago. If Antarctic H-chondrites came from a different source population they might have a different exposure age distribution as well which, in particular, might not show the pronounced 8 Ma peak.

We have measured the concentration and isotopic composition of He, Ne, and Ar in 31 H-chondrites found on the Allan Hills ice fields. Exposure ages were calculated from cosmogenic ^{21}Ne, using the procedures given in (6). The results are shown in the figure together with the exposure age distribution of non-Antarctic meteorites as calculated by the same procedure from literature data. Note, that for such a comparison, possible uncertainties in the absolute values of the production rates are irrelevant.

There is no obvious difference between the two distributions. The 8±2 Ma peak contains 14 out of 31 cases (= 45%), which is in perfect agreement with the result for the non-Antarctic suite of samples. According to mineralogical evidence (metamorphic grade classification) as well as radiogenic and solar wind noble gas data, at least 9 out of the 14 samples in the 8 Ma peak are independent falls, which gives a minimum percentage of 35% (9 out of 26) belonging to this exposure age peak. We conclude that the exposure age distribution does not corroborate the contention of an origin from different parent bodies of Antarctic and non-Antarctic H-chondrites. A similar conclusion, based on 9 Yamato H-chondrites, has been arrived at by Takaoka et al.(7). Of course, the possibility cannot be excluded that the 8 Ma event was not restricted to a single parent body. In this case one would have to explain, however, why only H-chondrite parent bodies should have been affected and why it does not show up for L-chondrites.

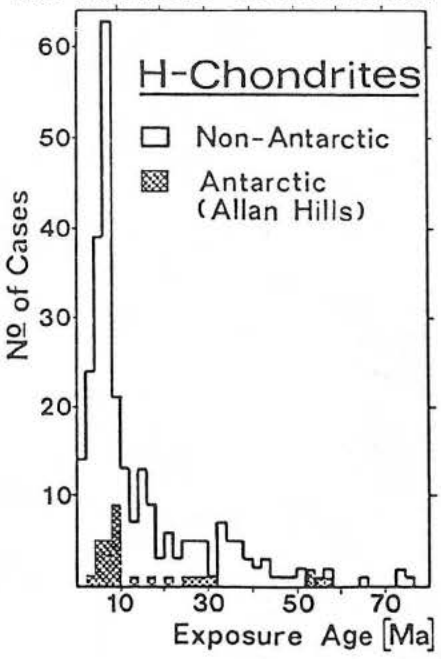

References: (1) J.E. Dennison et al. Nature 319, 390 (1986); (2) D.W. Ligner et al.Geochim. Cosmochim. Acta 51, 727 (1987); (3) J.E. Dennison et al. Geochim. Cosmochim. Acta 51, 741 (1987); (4) G.W. Wetherill, Nature 319, 357 (1986); (5) J. Cashore et al. Lunar Planet. Sci. XIX, 168 (1988); (6) K. Nishiizumi et al. Earth. Planet. Sci. Lett. 50, 156 (1980), (7) N. Takaoka et al. Mem. Natl. Inst. Polar Res. (Tokyo) 20, 264 (1981).

ANTARCTIC AND NON-ANTARCTIC METEORITES: DIFFERENT POPULATIONS, S. M. Samuels† and M. E. Lipschutz*, Depts. of Statistics† and Chemistry*, Purdue University, W. Lafayette, IN 47907

Following a brief summary in a preliminary paper [1], we reported data for 14-16 trace elements, including many of the most volatile/mobile ones, in 44 H4-6 chondrite falls and 45 similar samples from Antarctica [2,3]. In our statistical analysis using a single-sided t-test, we found numerous compositional differences reflecting thermal history differences between the 2 populations. As discussed [1], each population could include samples from the same $\geq$2 regions, but in different proportions.

When Cashore et al. [4] test our data by single parameter techniques, they also find significant differences but invoke weathering that we had previously considered and rejected for ample reason [1-3]. They [4] chide us for modeling the data as we ultimately did, despite the fact that results seem independent of model [1]. They find compositional variations with petrologic type, just as we had earlier [2-3].

When Cashore et al. use multivariate statistical techniques, they claim that the populations do not differ [4]. They assume that the meteorite samples form a closed array, that each meteorite is a closed system.

Meteorites do not form a closed array for volatile/mobile trace elements. When we examine our data by principal component analyses and discriminant analysis, we find ample evidence that Antarctic and non-Antarctic populations differ compositionally. For example, the results of discriminant analysis for H5 chondrites indicate a difference at the 0.0028% test level (99.72% confidence level). These data, in concert with information for H chondrites and other meteorite groups, accord with a previous conclusion that Antarctica sampled a different, near-Earth meteoroid population in the past than is falling today.

References: [1] Dennison J. E., Lingner D. W. and Lipschutz M. E. Nature 319, 390-393 (1986); [2] Lingner D. W., Huston T. J., Hutson M. and Lipschutz M. E., Geochim. Cosmochim. Acta 51, 727-739 (1987); [3] Dennison J. E. and Lipschutz M. E., Geochim. Cosmochim. Acta 51, 741-754 (1987); [4] Cashore J., McKinney M. L. and McSween H. Y. Jr., Lunar Planet. Sci. XIX, 168-169 (1988).

Mass and Number Density of H and L Chondrites on The Allan Hills Main Icefield

Ralph Harvey, Department of Geology and Planetary Science, University of Pittsburgh, Pittsburgh, PA 15260

Using data from ANSMET databases and the literature (1) maps have been produced which show the mass and number density (in g/km^2 and number/km^2) of various types of meteorites collected from the Allan Hills Main Icefield.

If different types of meteorites are found preferentially in given geographical areas, then either a) a significant proportion of the meteorites come from shower falls covering only a portion of the collection area; b) the meteorite influx has had dramatic compositional changes over the age of the stranding surface, and different types are found eroding from ice of differing ages, or c) an unknown agent is sorting meteorites.

The Allan Hills Main Icefield does not show an unequal distribution of differing types. The maps so far produced show distributions that are concentrated in a single area and vary only slightly from type to type. Figure 1 shows two such maps illustrating the number densities of L and H chondrites. Occasional large masses such as ALH76009 (point A on the map) present the only observed deviation from a random distribution across the exposed ice. This is an indication that the Allan Hills Main Icefield represents a sample of sufficient collection time to minimize the effects of single shower falls. Thus use of this icefield as a well-integrated sample of the meteorites which have fallen on the icesheet seems justified.

Figure 1. Maps showing mass density of L and H chondrites on the Allan Hills Main Icefield.

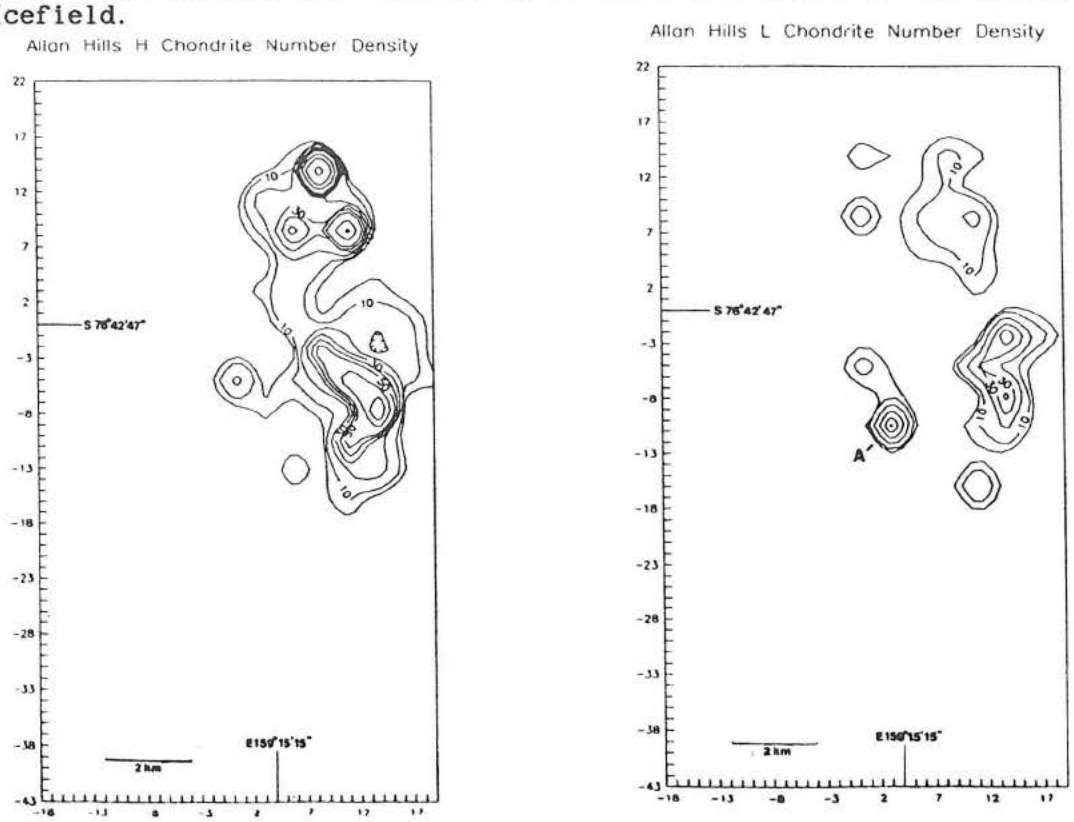

1. Yanai, K., 1982. Antarctic Meteorite Distribution Map, National Institute of Polar Research, Tokyo, Japan.

THE DETECTION OF PLEISTOCENE METEORITE PLACER DEPOSITS LOCATED IN NORTH AMERICA; A. A. Mardon, Texas A&M University, College Station, Texas. 77844.

The Antarctic has been a very fruitful area for the recovery of meteorites since the first discovery of an Antarctic meteorite by Mawson earlier in this century.[1] The volume of annually recovered samples seems to remain at the same level or increase. It has been estimated that thousands meteorites lie on the surface of the Antarctic ice cap beyond the South Pole.[2] The major processes that concentrate meteorites are not completely understood, but we do know that the meteorites arrive at their present sites through a complex interlocking windborne and iceborne transport system. Fall dates for many meteorites are well within the Pleistocene.[3] It has been suggested that placers similiar to Antarctic placers did occur during the last major glaciation of the North American Continent.[4] At the present time the Canadian Government through *The Dept. of Energy, Mines and Resources* and *The Polar Continental Shelf Program* is sponsoring an ongoing program to recover Arctic meteorites deposited through glacial transport systems similiar to those observed in the Antarctic.[5] Dr. Herd leads the annual Canadian field program. What the author is proposing is that meteorite deposits ocurred during the various Peistocene glaciations of North America in more southern latitudes than those being presently looked at in the high Arctic.

Areas of possible deposition of Meteorites might be along the Rocky Mountains. The same processes of concentration of meteorites as we observe in the Antarctic might have occured throughout the Continental Ice Cap. If these concentrations did occur, then where would they have been located? At this point we must refer back to the observed location of recovered meteorites in the Antarctic. They have been associated with extensive ice ablation and a general upwelling of ice at bottlenecks associated with nanutuks along large features such as the Trans-Antarctic Mountain Range. So one might be able to speculate that such physical forces existing during the last glaciation might result in a similiar confluence of natural phenomena that would cause similiar deposits of meteorites to occur in North America. The reason that the author speculates that it would be along the eastern fringes of the Rockies is that similiar upwelling of ice would have occured, combined with Katabatic winds, today locally known as Chinook winds, that occur along this area of the United States and Canada. Other investigators have expressed interest in combining a meteorite search with their already existing Continental programs. The Juneau Icefield program based out of the University of Idaho has expressed an interest in conducting a short search this summer for meteorites at the edge of several ice tongues and some of the moraines surrounding the Juneau Glacier. The extent of the search will be defined by the logistical perimeters of the annual program.[6] In addition to this several amateur meteorite aficionados have expressed some interest in committing some time in hiking around several potential placer sites in Alberta and Montana.[7]

If the Antarctic process of meteorite concentration does occur elsewhere during periods of Continental glaciation, then eventually meteorites transported in a similiar manner to those found in the Antarctic ought to be found.

References:

1.Mawson. Home of the Blizzard.

2.Cassidy, W.; Rancitelli,L. *Antarcitic Meteorites.* American Scientist. Vol. 70,March 1982.

3.ibid.

4.*Meteorites.* Meteor News. Published by the American Meteor Society, #76, January, 1987, page 3.

5.Personal Communication Dr. Herd and Polar Continental Shelf Program.

6. Personal Communication Dr. Carlson and Dr. Miller.

7.Personal Communication with M. Zalciuk.

CARBONATES IN ANTARCTIC METEORITES: INFRARED SPECTROSCOPY.

M. Miyamoto, Coll. of Arts & Sci., Univ. of Tokyo, Komaba, Tokyo 153, Japan

Weathering is one of the important problems involved in studying Antarctic meteorites. Marvin and Motylewski [1] reported the presence of hydrated Mg-carbonates and sulfates that are thought to be produced by terrestrial weathering. Infrared spectra of both interplanetary dust particle (IDP) and the Murchison (C2) meteorite show the 6.8 μm band, which is due to primary carbonates [2,3]. Because infrared spectra of some Antarctic meteorites show faint absorption bands near 1350 cm^{-1} (7.4 μm), we carried out a chemical dissolution experiment to determine whether the 7 μm band could be caused by carbonates.

Spectral reflectance measurements were made with a JASCO FT/IR-3 Fourier transform infrared spectrophotometer in a dry air atmosphere, equipped with a diffuse reflectance attachment. Details of measurements are described in Miyamoto [3]. Powder samples of Antarctic meteorites we used were supplied by the National Institute of Polar Research.

Powder samples of Antarctic meteorites were exposed to 0.5M HCl for 10 minutes at 25°C. Fig. 1 compares the spectrum of the etched sample of ALH-77299 (H3) with that of unetched sample. The 7.4 μm band disappears from the spectrum of the etched sample (curve 2 in Fig. 1). Sulfates and phosphates do not easily dissolve in such weak acid when exposed for short times. In fact, a similar dissolution experiment on gypsum confirmed this. Therefore, we conclude that the 7 μm band of Antarctic meteorites is probably caused by carbonates. Fig. 1 also shows the spectum of an unetched sample of non-Antarctic meteorite Nuevo Mercurio (H5), which fell in 1978, for comparison (curve 3 in Fig. 1). Because the spectrum does not show the 7 μm band, carbonates in Antarctic meteorites are probably formed by terrestrial weathering.

Because infrared spectra of almost all the Antarctic chondrites we measured show faint absorption bands near 7 μm, carbonates which were produced by weathering seem to be common in Antarctic chondrites.

References: [1] U. B. Marvin and K. Motylewski (1980) Lunar Planet. Sci. XI, 669-670. [2] S. A. Sandford (1986) Science, 231, 1540-1541. [3] M. Miyamoto (1987) Icarus 70, 146-152.

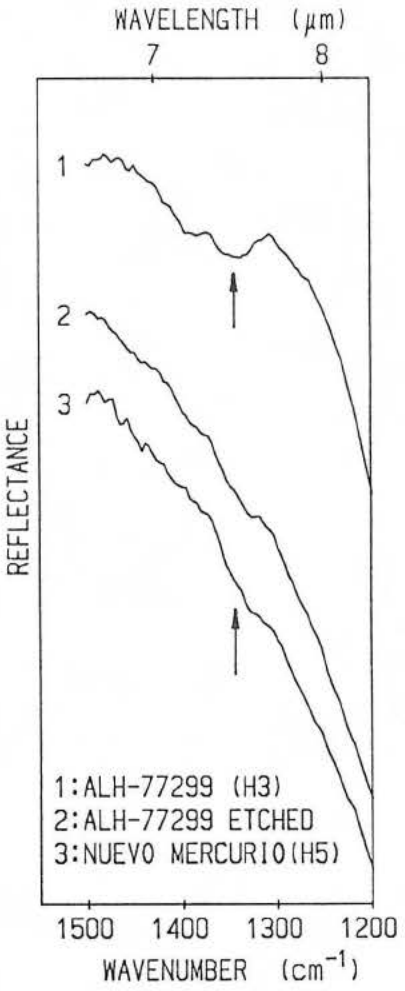

Fig. 1. Comparison of infrared diffuse reflectances of unetched and etched samples of the ALH-77299 (H3) meteorite. 1: unetched sample of ALH-77299, 2: etched sample of ALH-77299, 3: unetched sample of non-Antarctic meteorite Nuevo Mercurio (H5).

X-RAY DIFFRACTION EVIDENCE FOR WEATHERING PRODUCTS IN ANTARCTIC BASALTIC ACHONDRITES. Michael A. Velbel[1] and James L. Gooding[2]
[1] Dept. of Geological Sciences, Michigan State University, East Lansing, MI 48824-1115. [2] SN21/Planetary Science Branch, NASA/Johnson Space Center, Houston, TX 77058.

Introduction. A previous study of terrestrial weathering products in basaltic achondrites from Antarctica [1] found smectite- and mica-like clay mineraloids to be common phases in the exterior portions of diogenites and eucrites. Crystallinities of the clay mineraloids were judged to be poor, based on absence of diagnostic features of phyllosilicates in limited X-ray diffraction (XRD) and differential scanning calorimetry data. Occurrences of jarosite-group and zeolite-group weathering products were also suggested but similarly unconfirmed. The principal difficulty in identifying the weathering products, which tended to occur as fracture fillings and disseminated grains, was in isolating and concentrating sufficient quantities for study by conventional methods of determinative mineralogy.

Samples and Methods. Whole-rock fines from a diogenite (ALHA77256,102), two eucrites (EETA79004,13; EETA79005,83) and a howardite (EETA79006,49) were treated by conventional methods of sedimentary petrology in an attempt to concentrate weathering products. Given previous indications about their grain sizes [1], weathering products were sought by sedimentation of the fine silt- and clay-sized fractions onto oriented slide mounts for subsequent examination in a diffractometer. XRD peaks of weathering products were recognized by comparing the sample patterns with reference patterns of primary meteoritic minerals and with a pattern of bulk Pasamonte, a fresh eucrite.

Results and Discussion. No peaks attributable to well-crystallized clay minerals were found, despite the use of oriented mounts that should have enhanced basal (*00l*) reflections. In fact, preliminary analyses yielded only two peaks from ALHA77256 and three peaks from EETA79004 that were clearly not attributable to primary minerals. For ALHA77256, a 5.12 Å peak is attributable to jarosite whereas, for EETA79004, peaks at 9.02 Å and 2.76 Å are attributable to stilbite. A 2.71 Å peak in ALHA77256 and a 2.27 Å peak in EETA79004 remain unassigned but both would be consistent with goethite.

These results support the earlier conclusion [1] that the clay mineraloids of Antarctic origin are very poorly crystalline. In addition, they corroborate the suspected occurrence of jarosite-alunite and zeolite-group weathering products. Absence of well-crystallized phyllosilicates is also consistent with independent work [2,3] which suggests that crystalline clays form from primary minerals at low temperatures far more slowly than has been previously recognized. Further elucidation of the appropriate rate laws might provide useful information about possible mechanisms for forming clay minerals on meteorite parent bodies through aqueous geochemical processes.

References. [1] Gooding J. L. (1986) *Geochim. Cosmochim. Acta, 50,* p. 2215-2223. [2] Colman S. M. (1982) *Geology, 10,* p. 370-375. [3] Colman S. M. (1982) *U. S. Geol. Surv. Prof. Paper 1246.*

DIFFUSION EXPERIMENTS IN NININGERITE SOLID SOLUTION AND THEIR RELEVANCE TO THE THERMAL HISTORY OF EH- CHONDRITES

K. Ehlers[1], E. Woermann[2], A. El Goresy[1]
1) Max-Planck-Institut f. Kernphysik, Heidelberg, 2) RWTH-Aachen, FRG

Diffusion experiments on members of the niningerite solid solution series were conducted at temperatures between 950°C and 550°C. The aim of the experiments is an attempt to quantify the normal and the reverse diffusion profiles found im niningerites in the EH chondrites family (1). We conducted two sets of experiments in evacuated sealed silica tubes buffered at the Fe/FeS curve: a) Fe - diffusion in pure end members MnS and MgS, and b) Fe - diffusion in MgS-MnS solid solution (10, 35, and 65 mole % MnS, respectively). Calculation of cooling rates were carried out using the following equation (2):

$$r = \frac{D_o \cdot R}{d^2 \cdot A} \cdot T_o^2 \cdot e^{-A/R \cdot T_o}$$

whereby r=cooling rate, D_o=diffusion constant, d=diffusion width, R=gas constant and A=activation energy, T_o=initial temperature. The computed values for D_o (0.1 cm^2/s) and A (201 kJ/mol) were calculated for Fe diffusion in a niningerite solid solution with 10 mole % MnS.
For calculation of the cooling rates we implied that the compositions of the niningerite cores reflect compositions at the initial temperatures for homogenous crystals as equilibrated at the solvus (3) at the given temperature. Estimations of the thermal history were carried out for meteorites displaying normal zoning profiles (Abee, South Oman, St. Marks, and Kaidun III). Data of the cooling rates for South Oman, St. Marks, and Kaidun III are accompanied with uncertainties due to lack of experimental data for the FeS-MnS- solvus below 600°C. We obtained the following preliminary cooling rates (Tab. 1).

Table 1:

T_o(C)	Cooling rates (°C/day)		
	Abee	St. Marks	South Oman
800	122	170	744
700	10	14	60
600	0.5	0.6	3
500	0.01	0.01	6×10^{-2}
400	7×10^{-5}	1.0×10^{-4}	4×10^{-4}

Since the composition of the core lies close to the composition of the niningerite solid solution at the solvus at 800°C (3), a calculated cooling rate of 120°/day for Abee at this temperature appears realistic.
References: (1) Ehlers K. & El Goresy A. (1988) GCA, in press. (2) Kaiser T. & Wasserburg G.J. (1983) GCA 47, 43-58 (3) Skinner B.J. & Luce F.D. (1971) Am. Min. 56,1269-1296.

DJERFISHERITE COMPOSITIONS IN EH CHONDRITES: A POTENTIAL PARAMETER TO THE GEOCHEMISTRY OF THE ALKALI ELEMENTS. M. KIMURA AND A. EL GORESY; MPI Kernphysik P.O. Box 103980, 6900 Heidelberg, FRG.

The abundance of djerfisherite in EH chondrites seems to follow a systematic genetic pattern. It is quite abundant in the least equilibrated EH chondrites, ALHA77295, Qingzhen, Yamato 691 and Yamato 74370. Its amount decreases to Kaidun III and St. Marks, and it appears to be absent in Indarch and Abee. This pattern matches the subgroups arrangements of niningerites [1], except for only South Oman.

For a better understanding of the geochemical behavior of Na and K in EH chondrites, the chemical compositions of djerfisherites in ALHA77295, Yamato 74370 and Kaidun III were examined. The compositions were compared to those in Yamato 691, Qingzhen and St. Marks [2,3,4].

Although each djerfisherite and coexisting kamacite, schreibersite and perryite do not show chemical zoning, the content of Na, K, Fe, Ni and Cu vary from grain to grain. This is distinct especially in ALHA77295 (0.4-1.3 wt.% Na, 7.2-9.2 K, 50.3-53.5 Fe, 0.4-1.9 Ni, 1.3-3.6 Cu). Our results indicate a systematic reverse correlation between Na and K. The average atomic Na/K+Na ratios of djerfisherites decrease in the order of Yamato 691 (0.28), Qingzhen (0.15), ALHA77295 (0.11) and Yamato 74370 (0.02). This relationship is quite intriguing for Qingzhen, ALHA77295 and Yamato 74370, because they belong to the same subgroup with increasing MnS-content of niningerite [1]. The variation in the atomic Na/K+Na ratios is quite large for Yamato 691 (0.19-0.31) and ALHA77295 (0.06-0.26) thus demonstrating the low degree of equilibration of these chondrites.

The bulk Na and K contents of these chondrites are quite similar [5]. Accordingly, the Na/K variation of djerfisherite reflects the partitioning of these elements between glass and/or plagioclase in chondrules and djerfisherite. The glass in Yamato 691 has the highest weight ratio of K/Na (0.13) among the studied EH chondrites (0.03 in Qingzhen; 0.02 in ALHA77295; 0.05 plagioclase in Yamato 74370). This behavior seems to reflect the influence of fO_2 and fS_2 during the formation of these chondrites. Chondrites formed under apparently high fS_2 (high MnS-content in niningerite), e.g., Qingzhen, ALHA77295 and Yamato 74370, display the low Na/K ratios in djerfisherites. K partitioned mostly into djerfisherites as a chalcophile element in these chondrites, whereas into silicate and djerfisherite as lithophile and chalcophile in Yamato 691.

The compositional difference of djerfisherites is also present within Qingzhen, ALHA77295 and Yamato 74370. It seems plausible that the degree of Na fractionation to the chondrules is the main factor for the Na depletion in djerfisherites. This fractionation may have resulted from high fS_2 and low fO_2 during condensation of EH chondrites in the solar nebula. Therefore, the composition of djerfisherite may reflect the redox state and fractionation of Na and K in the nebula.

References:

[1] Ehlers K. and El Goresy A. (1988) GCA (in press).
[2] El Goresy A., Yabuki H., Ehlers K., Woolum D. and Pernicka E. (1988) Mem. Natl. Inst. Polar Res. (in press).
[3] Fuchs L.H. (1966) Science, 153, 166-167.
[4] Boctor N.Z. and El Goresy A. (1986) Meteoritics, 21, 336-337.
[5] Kallemeyn G.W. and Wasson J.T. (1986) GCA, 50, 2153-2164.

ENSTATITE CHONDRITES: A PRELIMINARY ION MICROPROBE STUDY

Laura L. Lundberg and Ghislaine Crozaz, *Earth and Planetary Sciences Department and McDonnell Center for the Space Sciences, Washington University, St. Louis, MO 63130*

The distribution of rare earth elements (REE) among enstatite chondrite minerals is not yet known despite investigations by many researchers. We have started an ion microprobe study to determine the REE abundances of various minerals in enstatite chondrites and, thus, locate the REE host phase(s).

Previous studies have produced conflicting results. Shima and Honda (1) in a dissolution experiment, found that most of the Ca (attributed to oldhamite, CaS) was leached out in one solution while the REE were, primarily, leached out by another solution implying that oldhamite is not the major REE host phase. From a stepwise dissolution experiment, Ebihara (2) reported that oldhamite is not the only host phase for REE in enstatite chondrites. In contrast, from their neutron activation analyses, Sears *et al.* (3) and Frazier and Boynton (4) concluded that oldhamite is the REE host in enstatite chondrites. Kallemeyn and Wasson (5), using factor analysis on INAA trace element and REE data, inferred that La condensed with sulfides that nucleated on the metal while the other REE are in an oldhamite rich component. Larimer and Ganapathy (6) recently succeeded in isolating CaS grains for REE determination by INAA and showed that oldhamite indeed contains a significant proportion of the REE.

The first ion microprobe measurements, reported here, were made on a thin section of ALHA 77156, a type EH3 enstatite chondrite that was reported (7) to have more oldhamite (1.5vol%) than other EH3-4 chondrites. However, oldhamite, so far, has not been located in this thin section and the search has thus concentrated on other minerals. Fig. 1 shows results for enstatite. The three REE patterns illustrate the diversity of REE patterns and abundances observed in this mineral. All REE abundances are less than $1 \times$ C1 chondrite and the heavy rare earth elements (HREE) are enriched relative to the light rare earth elements (LREE). Negative Eu anomalies are common and even a negative Yb anomaly was observed. In this context, it is interesting to note that Ebihara (8) found a yet unidentified phase in EH3 chondrites with a negative Yb anomaly and HREE enrichment. One niningerite grain showing FeS exsolution lamellae was analyzed. The REE pattern decreases from La ($.01 \times$ Cl) to Pr ($<.005 \times$ Cl), then generally increases smoothly from Nd ($\sim .1 \times$ C1) to Lu ($\sim 1.5 \times$ C1) with a dip at Eu and Gd ($\sim .05 \times$ C1). REE enrichments of ~10-100 $\times$ C1 chondrite were observed in 5 areas that were tentatively (but incorrectly) identified as oldhamite grains on the basis of their reflective properties. The REE patterns in these regions, that appear weathered, are relatively flat with small negative Eu anomalies (in one area, the Eu anomaly is positive) and small positive Yb anomalies. In most cases, the REE enrichment seems to be associated with Ca but not with S.

(1) Shima M. and Honda M. (1967), *Geochim. Cosmochim. Acta* **31**, 1995-2006; (2) Ebihara M. (1986), *11th Symposium on Antarctic Meteorites*, 108-109; (3) Sears *et al.* (1983), *Earth Planet. Sci. Lett.* **62**, 180-192; (4) Frazier R. M. and Boynton W. V. (1985), *Meteoritics* **20**, 197-218; (5) Kallemeyn G. W. and Wasson J. T. (1986), *Geochim. Cosmochim Acta* **50**, 2153-2164; (6) Larimer J. W. and Ganapathy R. (1987), *Earth Planet. Sci. Lett.* **84**, 123-134; (7) McKinley *et al.* (1982), *Meteoritics 17, 251. (8) Ebihara M. (1987), Meteoritics* **22**, 368.

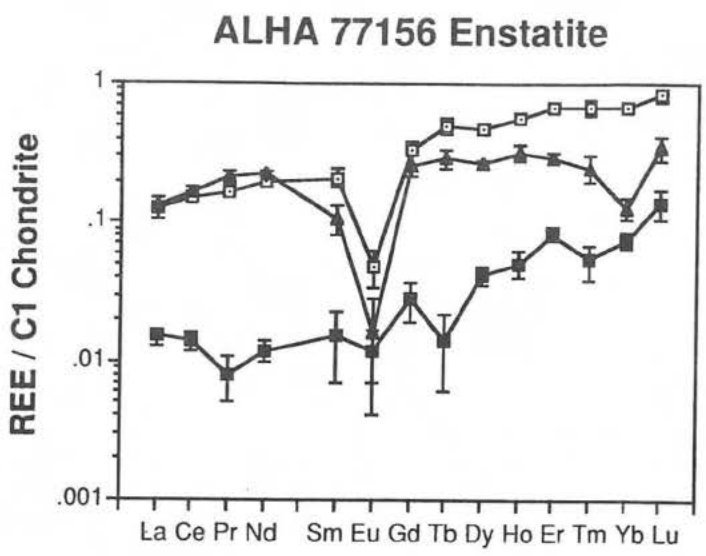

FORSTERITE COMPOSITIONS AND CATHODOLUMINESCENCE WITHIN ORNANS (C3O) ISOLATED FORSTERITE GRAINS. Ian M. Steele, The department of the Geophysical Sciences, The University of Chicago, 5734 S. Ellis Ave., Chicago, IL, 60637.

The recognition of two types of forsterite based on minor elements and cathodoluminescence (CL) was documented by Steele (1). These observations were based on visual CL colors and point analyses from some 15 meteorites including representative C1, C2, C3 and UOC samples. Emphasis was placed on textures within forsterite revealed by CL and the correlation of CL color with minor and trace elements for all forsterites; distinctions were not made for olivines in different textural settings. Present analytical capabilites now include quantitative measurement of CL spectra, rapid scanning CL imaging, and automated point analysis using the CAMECA SX-50 microprobe. A detailed study of forsterites within one meteorite, Ornans, has been initiated with emphasis on the chemical and CL features of forsterites in a range of textural settings including large 300 micron single forsterite crystals and porphyritic chondrules. The features of three large isolated crystals (A,B,C) are described here.

Each of the 3 grains contains a central region of brilliant blue CL with a sharp transition to no CL. Crystal A is euhedral with a euhedral CL core; B is subhedral with an irregular CL core; C is anhedral with an irregular CL core. The irregular CL boundaries correspond with the presence of cracks and tiny Fe-Ni inclusions with associated Fe-rich halos. Traverses with 10 micron steps are shown below for Fe, Al, Ca, Ti, and V for the 3 grains with core (C) and rim (R) indicated. The near constant Fe corresponds in each grain to the blue CL; the minimum Fe values correspond to the core but are not equal in each grain possibly due to the level of the section through the grain. For grains A and C, and possibly for B, the Al, Ca, and Ti tend to decrease from core to rim but within scans the highest values for Al and Ca do not correspond well. Vanadium differs by 4x in the three grains and the Ti/V ratio varies from about 2 to 9. Although not shown, grain B has detectable Sc (60ppm), while the other grains have less than 30ppm. The detailed variation in CL correlates best with Ti suggesting as do synthetic Ti bearing olivines that Ti may be the cause of blue CL.

Many of the observed chemical features parallel those seen in olivine of chondrules (2): 1) decrease of Al and Ca toward rim; 2) increase of Fe toward rim; 3) relatively large variations in some elements with no corresponding variation in Fe. The variation in chemical features among these three grains indicates that they grew from different reservoirs whether liquid or vapor, although otherwise they have similar textural features.

ACKNOWLEDGEMENTS: NASA NAG 9-47 (J.V. Smith); NSF EAR 84-15791.

(1) Steele I.M., 1986. GCA, **50**, 1379. (2) Jones R.H. and E.R.D. Scott, 1988, 1988. LPS XIX, 565.

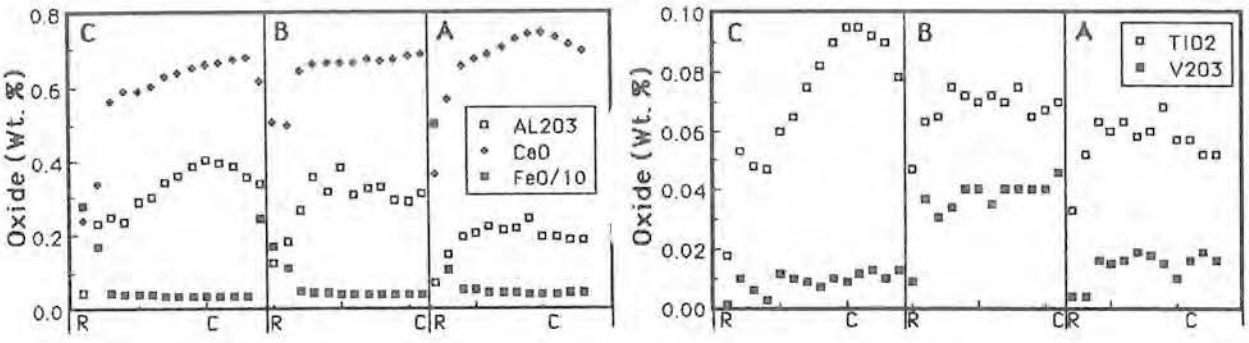

SUPERPARAMAGNETIC COMPONENT IN THE NIGER(I)C2 CARBONACEOUS CHONDRITE

R.B.Scorzelli, I.Souza Azevedo and J.Danon
Centro Brasileiro de Pesquisas Físicas, Rio de Janeiro, Brazil

The Niger(I) carbonaceous chondrite (1) has been investigated by Mössbauer spectroscopy throught the temperature range $4.2K \leq T \leq 298K$ and in applied magnetic field $5KOe \leq H_o \leq 60KOe$. The spectra above 115K indicate the presence of two magnetically aplit components, due to iron in the tetrahedral (A) and octahedral (B) sites of magnetite, and two quadrupole doublets due to paramagnetic Fe^{2+} and Fe^{3+} compounds. The Mössbauer parameters of the Fe^{2+} doublet at room temperature are $IS=0.97mms^{-1}$, $\Delta E=2.69mms^{-1}$, $\Gamma = 0.51mms$ and correspond to ferrous ion in an hydrated silicate form (2).As the temperature is lowered below 80K the intensity of hyperfine split increases and that of the Fe^{3+} doublet decreases progressively. This behaviour is typical of a system containing superparamagnetic microcrystals with a distribution of particle sizes.By taking the total absorption area of all forms of iron we can estimate that about 15% of the iron of the meteorite is in the superparamagnetic subdomain form. The remaining iron is 55% ferromagnetic and 30% paramagnetic.

The Mössbauer spectra at 4.2K in applied magnetic field up to 60 KOe did not lead to the complete disappearance of the $\Delta m = 0$ lines of the magnetic sextets. Broad lines (lines 2 and 5) remain, indicating the presence of an iron containing compound with no significant net magnetization, and probably in the amorphous state.

Superparamagnetic components have been observed in several other carbonaceous chondrites. A detailed study of the Orgueil meteorite has been reported by Mössbauer spectroscopy (3) and the results are similar to those obtained with Niger. It has been possible to identify the phase responsible for the superparamagnetic behaviour from the Mössbauer spectra of the Murchinson meteorite (4). This phase appears to be FESONi, or "FESON", from TEM and electron microprobe analysis (5). The Mössbauer spectra of Niger yield very close parameters to that of Murchinson and Orgueil, which suggest that superparamagnetism in all these carbonaceous chondrites originate from the same "FESON" phase. We are indebeted to Mme.Christophe Michel-Levi for a sample of the Niger meteorite.

(1) C.Desnoyers, EPSL, 47, 223(1980).
(2) J.M.D.Coey in Mössbauer Spectroscopy Applied to Inorganic Chemistry, ed. G.J.Long, pg.443, Plenum Press, New York, 1984.
(3) M.G.Madsen, S.Morup, T.V.Costa, J.M.Knudsen and M. Olsen, Nature, 321, 501 (1986).
(4) M.B.Madsen, S.Morup, T.V.Costa, J.M.Knudsen and M. Olsen, International Conference on the Applications of the Mössbauer Effect, Melbourne,August, 1987.
(5) K.Tomeoka and P.R.Buseck, Geochim.Cosm.Acta, 49, 2149 (1985).

CM2 CARBONACEOUS CHONDRITE MATRICES: AEM STUDIES OF MATRIX PHYLLOSILICATES AND MASS BALANCE CALCULATIONS USING A LINEAR ALGEBRAIC METHOD. Adrian J. Brearley, Institute of Meteoritics, Department of Geology, University of New Mexico, Albuquerque, New Mexico 87131, USA.

The matrices of CM2 carbonaceous chondrites contain a mineral assemblage consisting of phyllosilicates, oxides, sulphides, silicates and carbonates e.g. (1-5). This complex assemblage of phases is widely believed to have formed by aqueous alteration (1,5) of an anhydrous protolith (possibly CV3 matrix material) on the CM2 chondrite parent body. Using textural data (5) have suggested that the phyllosilicate phases, Fe-Mg serpentine and PCP (tochilinite intergrown with cronstedtite (6)) formed by sequential progressive aqueous alteration. This model predicts that the modal abundance of PCP decreases and Mg-serpentine increases a result of increasing alteration. McSween (7) made an important step towards testing this model using a graphical method to obtain modal proportions of phases, but was limited by the compositional data available. In order to more rigorously constrain the proportions of phases in CM2 matrices and identify feasible alteration reactions, AEM studies have been commenced to obtain precise chemical data for the matrix phases, suitable for use in mass balance calculations. At present the results are limited to Murchison, but studies of Murray and Mighei are also in progress.

The data from 90 analyses of individual grains from Murchison show that 3 distinct compositional groups are present within the fine-grained phyllosilicate matrix component. The most abundant phase is an Fe-rich phyllosilicate with a c repeat of 7Å and Si/Fe<1 which is very similar to the cronstedtite in Murray (5) and Cochabamba (8), although it has higher Si and Al contents. This phase coexists with a less abundant phyllosilicate phase with a c lattice repeat of 7Å which can reasonably be described as an Fe-rich serpentine with Si/Fe >1. This phase is intermediate in composition between the yellow and light green phyllosilicates analysed by (1) and has an Mg/(Mg+Fe) ratio between 0.37 and 0.55. Associated with both these phases is a third phyllosilicate phase with high S which is consistent with PCP. The analyses show variable Si, Fe, S and Ni contents, but analyses with the lowest Si contents are essentially identical to analyses of tochilinite from CM clasts in the Jodzie howardite and Murray (1).

These new data have been applied to mass balance calculations for CM chondrite matrices using a linear algebraic method (9). This is a more rigorous method of modal analysis than graphical analysis enabling exact values for the molar proportions of the phases to be calculated simultaneously. A set of linear equations can be written relating the bulk composition in terms of individual elements, to the mineral compositions and their molar proportions. Provided the number of phases present is equal to the number of components needed to describe the phases, the set of linear equations can be solved simultaneously for the only unknown, i.e. the molar proportions, using simple matrix inversion. The results for Murchison and Mighei, solved using the five most abundant phases, tochilinite, cronstedtite, Fe-Mg serpentine, pentlandite and olivine are consistent with the observed modal abundances determined in this study. This procedure was then applied to CM chondrites matrices for which no data on the mineral compositions are available. Phase compositions were assumed to be the same as those in analysed CM chondrite matrices. With few exceptions it was found that it was not possible to calculate realistic modal abundances of the phases because frequent negative modal values were encountered. **Conclusions**: This analysis suggests that considerable caution must be exercised in extrapolating mineral compositions from one CM chondrite to another. It is clear that only when good quantitative data for phases in a large number of CM chondrite matrices become available can realistic constraints be placed on models for the complex alteration processes in CM2 chondrite parent bodies. Supported by NASA grant NAG 9-30 (Klaus Keil, P.I.).

References. 1) Bunch, T.E. and Chang, S. (1980) GCA. 44, 1543-1577. 2) Mackinnon, I.D.R. and Buseck, P.R. (1979) Nature 280, 219-220. 3) McKee, T.R. and Moore, C.B. (1979) Proc.Lunar Planet.Sci. Conf. IX, 921-936. 4) Barber, D.J. (1981) GCA. 45, 945-970. 5) Tomeoka, K. and Buseck, P.R. (1985) GCA 49, 2149-2164. 6) Mackinnon, I.D.R. and Zolensky, M.E. (1984) Nature 309, 240-242. 7) McSween, H.Y. Jr. (1987) GCA 51, 2469-2477. 8) Muller, W.F. et al. (1979). TMPM. 26, 293-304. 9) Spear, F.S. et al. (1982) Revs. in Mineral. 10, 53-104.

EET 83334: A CM1 CHONDRITE WITH PROBABLE COMPACTION TEXTURES

Michael E. Zolensky (1) and Ruth A. Barrett (2). (1) Planetary Science Branch, NASA/Johnson Space Center, Houston, TX 77058; (2) Lockheed/ LEMSCO, 2400 NASA Road 1, Houston, TX 77058.

Grady and co-workers [1] have recently reported that YAMATO-82042 is possibly the first recognized CM1 chondrite. In the course of a survey of the CM and CI populations we have recognized what we believe to be the second known chondrite of the CM1 persuasion: EET 83334.

Petrography and Mineralogy We have examined both of the available thin sections of EET 83334. It is dominated by fine-grained Fe-Mg phyllosilicate matrix, as are all CMs. The most obvious feature of the meteorite in thin-section is the abundant Fe-Mg phyllosilicate aggregates, ranging up to 1 mm in diameter. We have found no anhydrous silicate-containing chondrules or aggregates. Nor have we found anhydrous silicates among the matrix. Fine-grained rims are frequently present about the phyllosilicate aggregates. There are abundant rounded calcite (<1% Fe) grains up to ~90 um in diameter; we have also observed a 900 um-sized aggregate composed predominantly of calcite. The matrix contains many small (up to ~20 um) anhedral grains of high-Ni pentlandite and other low-nickel sulfides. There are a few larger (up to ~60 um) euhedral sulfide crystals in the matrix. Many of the phyllosilicate aggregates contain sulfide and Fe-Ni metal inclusions. There are a few small (<10 um) grains of Fe-Ni metal in the matrix, where they are typically rimmed by Ni-bearing magnetite. Rarer matrix phases include Ca-phosphates and chromite. The entire meteorite is cut by many cracks, often filled with Ca-sulfates, but which are undoubtedly due to deformation and alteration during this meteorite's Antarctic entombment.

Many of the aggregates are elongate, by up to factors exceeding 2. The most elongate aggregates are roughly alligned. We believe that this texture is due to parent body deformation events, possibly impact deformation but most likely burial compaction.

Matrix and Rim Compositions We performed spot analyses of matrix and aggregate rims, as we have done for five other carbonaceous chondrites: Murchison, Bells, Nogoya, EET 83389 and Allende. In all cases the compositional variation for rims was found to be greater than for matrix, as discussed earlier [2]. EET 83334 continues this trend, and its rim analyses fit squarely within the trend defined by all other CM chondrites so analyzed.

Classification Summarizing, EET 83334 contains phyllosilicate-rich aggregates with rims, like CM chondrites, and the bulk matrix and fine-grained rim compositions fit the trends for CM chondrites. However, this meteorite appears to contain no (or at least extremely rare) anhydrous silicates and possibly no true chondrules, like CI chondrites. Finally, EET 83334 appears to contain no pre-terrestrial CI-type veining. Thus, we tentatively classify this meteorite as a CM1 chondrite. It is unfortunate that the total weight of EET 83334 was only 2.5g. It is interesting to speculate about the fact that we now have reports of two Antarctic CM1 chondrites (from opposite sides of the continent) and no non-Antarctic ones.

References [1] Grady et al., Proceedings of the Eleventh Symposium on Antarctic Meteorites, 162-178, 1987; [2] Zolensky et al., Lunar and Planetary Science XIX, 1327-1328, 1988.

METAMORPHOSED CARBONACEOUS CHONDRITES

Gregory W. Kallemeyn, Institute of Geophysics and Planetary Physics, University of California, Los Angeles, CA 90024

Five metamorphosed carbonaceous chondrites (ALH82135, ALH84038, EET83311, Karoonda and PCA82500) were analyzed for 28 elements by INAA. Karoonda is the only fall, but among the finds, only PCA 82500 is extensively weathered. Another chondrite (ALH85151) listed as a C4 chondrite turned-out to be a shocked L3 chondrite upon analyses.

ALH82135, Karoonda and (to a lesser extent) PCA82500 were previously linked by petrographic and compositional data. Cluster analysis of standardized concentration data for 29 grouped and ungrouped carbonaceous chondrites analyzed by this lab support a close relationship between ALH82135, ALH84038, EET83311 and Karoonda.

Refractory lithophile abundances in the five metamorphosed chondrites are intermediate to those in CV and CO (Fig. 1). This suggests that they form their own distinct clan, as previously proposed by this author for Karoonda. The refractory siderophile abundances among the metamorphosed chondrites tend to be at about the same level as the refractory lithophiles, unlike CV chondrites where they are lower.

Volatile element abundances are similar or slightly lower than CV3 chondrites, except for the most volatile elements such as Br, Se and Zn (Fig. 2). The extent of volatile loss does not seem to correlate with petrographic type. Although ALH82135 may be type 5, it has generally slightly higher volatile abundances than type 4 Karoonda. This could result from a small amount of unrepresentative sampling. In general, though, volatile element depletions among these metamorphosed chondrites are significantly less than those seen in the CV4 Coolidge relative to CV3.

It appears that ALH82135, ALH84038, EET83311, Karoonda and PCA82500 probably belong to a clan intermediate to the CV and CM-CO clans. Compostional and petrographic data suggest ALH82135, ALH84038, EET83311 and Karoonda form their own group. PCA82500 may also belong to that group, but its extensive weathering makes classification difficult.

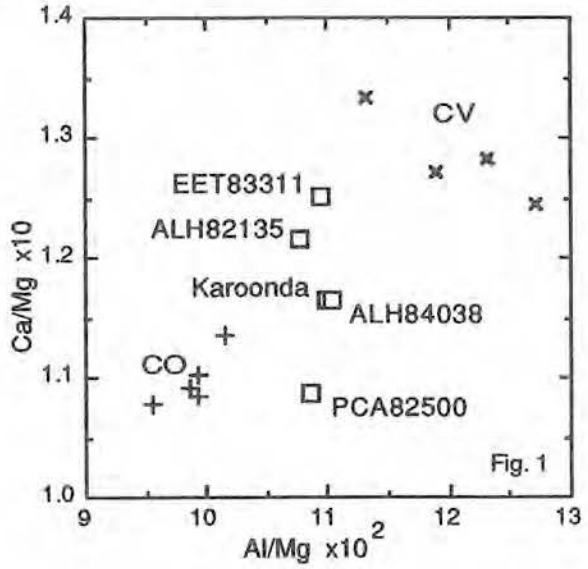

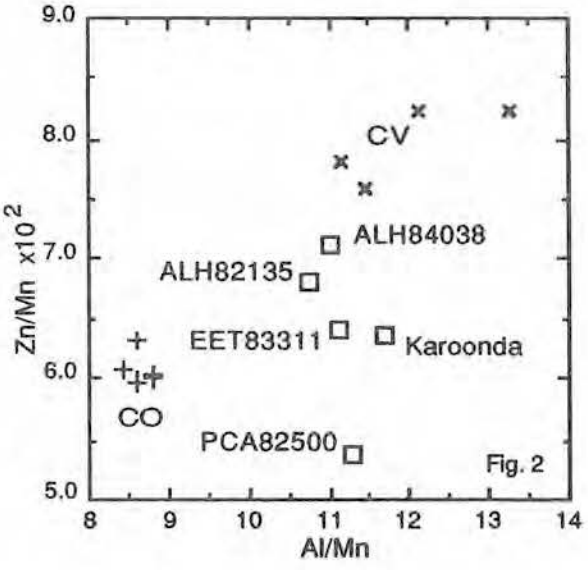

A PROBABLE ASTEROIDAL PARENT BODY FOR THE CV OR CO CHONDRITES.

Jeffrey F. Bell (Hawaii Institute of Geophysics, 2525 Correa Road, Honolulu HI 96822)

"Carbonaceous chondrites" as a class have been traditionally associated with the Class C asteroids. In fact this association only applies to the CI and CM chondrites. The asteroidal affiliations of the anhydrous CV and CO chondrites have been much more mysterious. They have moderate albedos and shallow olivine/pyroxene bands, inconsistent with the low albedos and flat IR spectra of the traditional C-type asteroids. Some workers have associated CV/CO mineralogies with atypical C-type objects, while others have selected certain S-type asteroids as the most likely candidates (e. g. Gaffey and McCord, *Space Sci. Rev.* **21**, 555.) on the basis on visible-wavelength telescopic spectra

This long-standing mystery has been unexpectedly clarified by results from a spectral survey of asteroid families being conducted at the NASA Infrared Telescope Facility at Mauna Kea. "Families" are groups of asteroids on similar orbits which are presumed to be fragments of a common parent body disrupted by a collision in geologically recent time. The Eos family has traditionally posed a difficult problem for asteroid classification schemes. Gradie and Zellner (*Science* **197**, 254-255) found that the UBV colors of the Eos family asteroids clustered tightly on the boundary beween the S and C fields, and that their radiometric albedos were also intermediate to these two classes. This led to the apparently contradictory situation in which the Eos family was thought to be homogenous in composition, while the individual objects were classed as C, S, or U based on very small variations in color and albedo. The classification scheme of Tholen (Ph.D. thesis, 1984) eliminated this discrepancy by putting almost all Eos family objects into an enlarged S class.

The new IR spectral observations have revealed that Eos family asteroids 221 Eos, 653 Berenike, and 661 Cloelia exhibit flat IR reflectance curves with very shallow silicate absorption bands. These spectra are totally atypical of other S-type asteroids, and more closely resemble classical C-type spectra. The visual and IR data as a whole suggest that the Eos family parent body was not a true member of either the C or S class. (The picture is complicated somewhat by 639 Latona, which has a spectrum and albedo very close to the average for "normal" S asteroids, and consequently does not match the rest of the family. This object appears to be an "interloper" or "background object" which existed before the Eos parent body was disrupted.)

Comparison of the spectral and albedo data for "normal" Eos family asteroids with the available meterorite spectra reveals a close similarity with CV and CO chondrites. Other meteorites with similar intermediate albedos such as ureilites and "black chondrites" (highly shocked ordinary chondrites) appear much less likely candidates from both spectral and petrologic grounds. It seems probable that either CVs or COs (but not both) are actually derived from the Eos family. (This family is believed to be the source of the dust responsible for the bright bands in the thermal component of the zodaiacal light which were detected by the IRAS satellite.) If we accept both this compositional interpretation and the Tholen classifications, a new paradox exists: the most common classes of carbonaceous chondrites are derived from Class S asteroids, instead of the Class C asteroids usually associated with dark meterorites. To simplify terminology and properly recognise the unique properties of the Eos family asteroids, a new asteroid class "K" is proposed to incorporate them. This nomenclature phonetically suggests their apparent identity with carbonaceous chondrites, while reminding us that their telescopically observed parameters are intermediate to the classical C and S classes (since K is halfway between C and S in the alphabet). This class is provisionally defined as objects with albedos near 0.09, S-like spectral curvature at visual wavelengths, weak 1-micron absorption bands, and flat reflectance from 1.1 to 2.5 microns. Although the known asteroids of this class to date are Eos family members, the existence of both CV and CO chondrites indicates that some other asteroids currently classed as S-types on the basis of visible spectra will turn out to be K-types as near-IR observations are extended to fainter objects.

MANTLE METASOMATISM ON THE MOON: T. Dickinson, G. J. Taylor, R. W. Bild (1) and K. Keil, Department of Geology and Institute of Meteoritics, University of New Mexico, Albuquerque, New Mexico 87131. (1) Sandia National Laboratories, Albuquerque, New Mexico 87185.

Apollo 15 mare basalts appear to be enriched in Ge compared to Apollo 12 basalts (1,2), suggesting that Ge is not uniformly distributed in the Moon. Based on our final Ge data (3), the Apollo 15 mare basalts are enriched by a factor of 1.6 over the Apollo 12 mare basalts. Ge is also enriched, by factors of 20 to 150, in bulk orange (4) and green glasses, as well as in the surface correlated deposits (5). KREEPy basalts (7-10) and Apollo 14 aluminous mare basalts (3,11-13) show the largest enrichments in Ge, by factors of 10 to 300.

We are investigating the mechanisms of Ge enrichment in lunar samples. In the surface correlated deposits of green glass, volatile elements are enriched in the relative order Cd, Au, Zn and Ge (5). It has been proposed that these elements have been mobilized in a halogen-rich vapor (4). In contrast, the boiling points of these metal chlorides indicate that their relative volatility is in the order (from most volatile to least) $GeCl_4$, $AuCl_3$, $ZnCl_2$, and $CdCl_2$. The orange and green glasses formed by fire fountaining on the lunar surface (4). Pressure release as the magma rose to the surface caused the magma to exsolve volatiles and explosively erupt into the vacuum of the lunar surface. As the droplets fell back to the surface, the vapor recondensed onto the surfaces of the glass spheres. One would expect the most refractory elements to preferentially recondense on the glass spheres, while the more volatile species preferentially remained in the vapor. This explains why the boiling point data and relative enrichment of volatiles on the glass spheres are in approximately reverse order.

Halogen-rich solutions, originating from outgassing of the lunar interior, may have permeated the mantle, preferentially leaching material from the surrounding rocks. These halogen-rich fluids would have come into contact with the more siliceous and Na, K-rich magmas in the upper mantle. Three competing processes affect F partitioning under these conditions. The vapor phase-granite magma partition coefficient for F is generally less than 0.33 (14). However, increasing Si or decreasing K, Na, Ca, or Mg content of the magma causes an increase in the partitioning of F into the vapor phase. Based on terrestrial granites, increases in the $(K_2O + Na_2O)/(CaO + MgO)$ ratio favors retention of F by the magma, despite increasing Si contents. There is also a temperature dependence for F partitioning. Based on the F content of volcanic gases, there is a 23 fold increase in F content of the gases with only a 4 fold increase in the temperature of the gas (15). Thus, when this halogen-rich fluid came in contact with the cooler and more Na and K-rich residual magmas, F was resorbed by the melt. It seems reasonable that the metals associated with the vapor were also resorbed into the melt. In this manner, the source region for KREEPy basalt might have been metasomatized, and enriched in volatiles and Ge. The Apollo 14 aluminous basalts formed by partial melting of a typical mare basalt source region and later assimilated material from these metasomatized areas. Irving (16) proposed previously that halogen-rich fluids may be the source of LIL enrichment in KREEP. The presence of Ge enrichments uncorrelated with abundances of siderophile elements, the inferred existence of halogen-rich fluids, and the volatile enrichments in volcanic glasses indicate that the Moon was not totally melted when it formed. This is consistent with lunar seismic data (17).

(1) Dickinson and Newsom (1985) LPS XVI, 183. (2) Dickinson et al. (1988) LPS XIX, 277. (3) Dickinson et al. (1988) PLSC 19th, in press. (4) Meyer et al. (1975) PLSC 6th, 1673. (5) Chou et al. (1975) PLSC 6th, 1701. (6) Morgan et al. (1974) PLSC 5th, 1703. (7) Warren et al. (1986) PLSC 16th, D319. (8) Warren et al. (1983) PLSC 14th, B151. (9) Gross et al. (1976) PLSC 7th, 2403. (10) Morgan et al. (1975) The Moon 14, 373. (11) Baedecker et al. (1972) PLSC 3rd, 1343. (12) Morgan et al. (1972) PLSC 3rd, 1377. (13) Wanke et al. (1972) PLSC 3rd, 1251. (14) Munoz and Eugster (1969) Am. Min. 54, 943. (15) Sugiura et al. (1963) J. Earth Sci. Nagoya Univ. 11, 272. (16) Irving (1979) Conf. Lunar High. Crust. (17) Mueller et al. (1988) JGR, in press.
[Supported by NASA Graduate Researchers Fellowship NGT 32-004-771 (T.D. and NAG 9-30 (K.K).]

SYSTEMATICS INVOLVED IN THE PETROGENETIC MODELLING OF VERY HIGH ALUMINA (VHA) AND VERY HIGH POTASSIUM (VHK) BASALTS FROM THE APOLLO 14 SITE. Clive R. **NEAL** and Lawrence A. **TAYLOR:** Department of Geological Sciences, University of Tennessee, Knoxville, TN 37996-1410.

The use of computers allows petrogenetic modelling to be rapidly executed. However, there is a tendency to overlook the fundamentals of such modelling. The importance of petrogenetic modelling is illustrated by the genesis of Apollo 14 basalts. Neal et al. [10,11] demonstrated that VHA and VHK basalts are generated through an Assimilation and Fractional Crystallization (AFC) process. The equation 6a of DePaolo [5] is used to model trace element behavior during AFC:

$$C_m / C_m^o = F^{-z} + \frac{r}{r-1} \frac{C_a}{zC_m^o} 1 - F^{-z}$$

where r = mass assimilated/mass crystallized; z = r+D-1/r-1; D = bulk Kd for the crystallizing phase(s); C_m^o = conc. of element in parental magma; C_m = conc. of element in residual magma; C_a = conc. of element in assimilated component; F = proportion of magma remaining. The nature and proportion of crystallizing phases are constrained by plotting major element compositions on an Ol-An-SiO_2 pseudoternary and applying the Lever Rule. Relevant crystal/liquid partition coefficients are required for trace elements in the system being studied (Table 1). Element-element and REE plots demonstrate that KREEP falls at the end of the trends defined by VHA basalts and is taken as the assimilant. The VHK basalts are the products of a VHA basalt assimilating lunar granite, witnessed in the similar chemistries between VHA and VHK basalts, except for the extreme enrichment of K, Ba, and Rb in the latter (e.g., 18). The "r value" is based on the nature of the magma and assimilant. Therefore, if magma and assimilant are both basaltic, the r value will be low. For the VHA basalts assimilating KREEP, r = 0.22. For VHK basalts, where a basaltic magma assimilates granite, r = 0.5. The proportion of magma remaining (F) is varied in order to trace the evolution of the residual magma. In the VHK modelling, three parental VHA magmas and three granite assimilants are used to account for the compositional variability of these rock types (Table 2).

TABLE 1: Crystal/liquid partition coefficients.

	OL	PX	PLAG	CHRN	ILM
K	0.0068	0.014	0.17	0	0
Ba	0.03	0.013	0.686	0.005	0.005
Hf	0.04	0.063	0.05	0.38	1.817
Th	0.03	0.13	0.05	0.55	0.55
Sc	0.4	1.6	0.065	1.5	1.5
La	(0.0001)	(0.012)	0.051	0.029	0.029
Ce	0.0001	0.038	0.037	0.038	0.038
Sm	0.0006	0.054	0.022	0.053	0.053
Eu	0.0004	0.1	1.22	0.02	0.02
Yb	0.02	0.671	0.012	0.39	0.39
Lu	(0.02)	0.838	0.011	0.47	0.47

() = estimated Kd; Chromite REE Kd's taken as those for ilmenite. Refs: 1,2,6,7,8,9,17,21.

The AFC modelling requires a primitive, parental VHA basalt composition, which is an unmodified lunar mantle melt. The inferred parental magma is LREE depleted and compatible element enriched. This parental composition is used to calculate the composition of the lunar mantle source, using the batch melting equation of Schilling [16]:

TABLE 2: Modelling parameters for VHA and VHK basalts (ppm).

	PARENTAL MAGMA	KREEP	Parental Magmas			Assimilated Granite		
			,1161	,1443	,1542	73255c	Av Granite	12033,517
K	249	5561	564	747	2989	62665	58864	24905
Ba	28	837	32	130	230	5470	4490	4540
Hf	1.70	31.6	1.78	5.43	15.4	16.0	15.4	36.8
Th	0.20	10.0	0.20	1.50	7.30	9.50	42.3	40.0
La	3.19	83.5	2.89	13.5	39.7	20.3	50.7	82.0
Ce	9.30	211	8.40	35.0	105	50.0	123	199
Sm	2.10	37.5	2.11	7.59	123	6.74	16.7	27.7
Eu	0.62	2.75	0.56	1.12	1.78	2.71	2.52	3.10
Yb	3.02	24.4	2.89	6.33	12.2	10.3	24.7	36.7
Lu	0.44	3.40	0.47	0.91	1.59	1.50	3.71	5.80

Refs: 3,4,12,14,15,17,20,23,24.

$$C_l / C_o = \frac{1}{[D(1-F) + F]}$$

where F = fraction of melt produced; D = bulk solid/liquid Kd at the time of melt removal (calculated from source mineralogy); C_o = initial conc. of element in the source; C_l = conc. of element in the melt produced. In order to calculate D, a source mineralogy must be assumed. This assumption can be somewhat constrained using the Magma Ocean theory (e.g., 22), and mafic cumulate compositions can be applied. A further constraint is that the source must be LREE depleted. The magma ocean composition can be approximated by dividing the trace element abundance in the source by the bulk distribution coefficient. The cumulate mineralogy and trace element contents must yield a magma ocean with a Sm/Nd ratio 0.89 x chondrite and a La/Lu ratio 2 x chondrite (12,13,19). This approach allows a complete petrogenetic model of basalt generation and evolution at the Apollo 14 site to be developed.

REFERENCES: (1) Arth and Hanson (1975) GCA 39; (2) Binder (1982) JGR 87; (3) Blanchard and Budahn (1979) PLPSC 10th; (4) Blanchard et al. (1977) PLSC 8th; (5) DePaolo (1981) EPSL 53; (6) Drake and Weill (1975) GCA 39; (7) Haskin and Korotev (1977) GCA 41; (8) Irving and Frey (1984) GCA 48; (9) McKay et al. (1986) JGR 91; (10) Neal et al. (1988a) PLPSC 18th; (11) Neal et al. (1988b) PLPSC 18th; (12) Nyquist et al. (1979) PLPSC 10th; (13) Nyquist et al. (1981) EPSL 55; (14) Quick et al. (1977) PLSC 8th; (15) Salpas et al. (1985) LPS XVI; (16) Schilling (1966) PhD Thesis, Mass. Inst. Tech.; (17) Schnetzler and Philpotts (1970) GCA 34; (18) Shervais et al. (1985) JGR 90; (19) Unruh et al. (1984) JGR 89; (20) Vaniman and Papike J.J. (1980) Proc. Conf. Lunar Highlands Crust; (21) Villemant et al. (1981) GCA 45; (22) Warren (1985) Ann. Rev. Earth Planet. Sci. 13; (23) Warren et al. (1983) EPSL 64; (24) Warren et al. (1987) JGR 92.

PETROGENESIS OF VERY HIGH ALUMINA (VHA) AND VERY HIGH POTASSIUM (VHK) BASALTS FROM THE APOLLO 14 SITE BY COMBINED ASSIMILATION AND FRACTIONAL CRYSTALLIZATION. Clive R. **NEAL** & Lawrence A. **TAYLOR:** Dept. of Geological Sciences, University of Tennessee, Knoxville, TN 37996-1410.

Two groups of basalts are present at the Apollo 14 site: VHA is a basalt with 11-14 wt% Al_2O_3, <0.3 wt% K_2O, K/La ≅ 100; and, VHK is a basalt with >0.3 wt% K_2O, K_2O/Na_2O >1, K/La >150. Rb and Ba are also enriched relative to VHA basalts. The major element chemistry of VHK basalts is similar to VHA basalts, except for elevated K_2O.

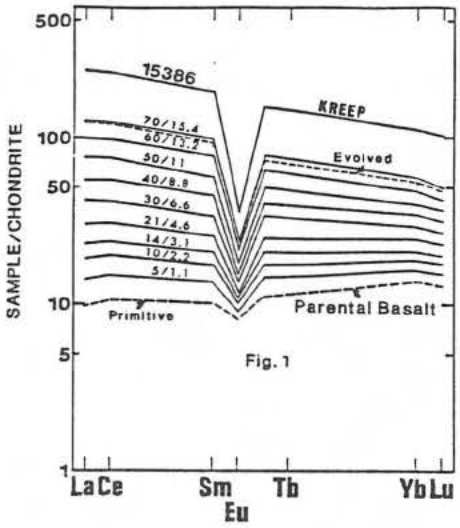

Fig. 1

The VHA basalts show moderate major element variations, but a wide range in trace element abundances. There is a continuum of compositions from LREE depleted (primitive) types [$(La/Lu)_N$ ≅ 0.75; $(Sm/Eu)_N$ ≅ 1.3], to LREE enriched (evolved) types [$(La/Lu)_N$ ≅ 2.5; $(Sm/Eu)_N$ ≅ 4.0]. The evolved types have REE profiles which mirror those of KREEP (Fig. 1). The compatible elements decrease and LIL and HFS elements increase from primitive to evolved types. On element-element plots, the VHA basalts exhibit coherent trends from primitive to evolved, leading towards KREEP. This has led to the formulation of an AFC model between a primitive basalt and KREEP in order to account for the VHA basalt compositions. Fractionating phases are deduced by plotting major element compositions on an Ol-An-SiO_2 pseudoternary (10,11: Table 1). Using published Kd values and applying equation 6a of (1), AFC paths have been constructed between a primitive VHA parent and 15386 KREEP (9). The field of VHA basalt REE profiles (dashed lines) & the evolution of the REE calculated by our AFC method are presented in Fig.1. The LREE enriched nature of the evolved basalts can be generated from a LREE depleted parent.

VHK basalts are produced by VHA basalt assimilation of lunar granite (e.g., 7). However, VHK basalts contain low levels of HFS elements, which appear to be inconsistent with petrogenesis by bulk granite assimilation. A more reasonable approach to VHK basalt petrogenesis, is one of AFC. As VHK and VHA basalts have similar compositions, crystallizing phases are kept the same (Table 1). However, as noted by (4), no one parental magma can generate all observed VHK compositions.

Three parental VHA magmas and three granite assimilants are used. This allows our model to accomodate the compositional variation in VHA basalts (see above) and lunar granites (Fig. 2). The compositions used, with references, are presented by (2). In order to illustrate VHK basalt petrogenesis by AFC, %K is plotted against La (ppm) (Fig. 2: this is divided into three parts so as not to confuse the different AFC paths generated from each parent). Tick marks on AFC paths represent increments of 5% crystallization (2.5% assimilation). Note that all VHK compositions can be generated from a primitive (14321,1161) and more evolved (14321,1443) VHA basalt. This illustrates that VHK basalts can be effectively generated by AFC. Neal et al. (4) demonstrated that the low abundances of HFS elements in these basalts can also be generated by AFC. The necessity of at least two parental VHA magmas, one primitve and one which incorporated a KREEP component (evolved), suggests that VHK basalts with elevated incompatible element abundances, evolved originally as VHA basalts. At some point, granite replaced KREEP as the assimilant. This argues for at least two VHK basalt flows at the Apollo 14 site and supports a type of granite-KREEP relationship (3).

TABLE 1: Proportions of fractionating phases deduced from the "Walker diagram".

% CRYST.	0-14	15-21	22-70
Olivine	90	40	0
Plag.	0	50	30
Pyroxene	0	0	60
Ilmenite	0	0	10
Chromite	10	10	0

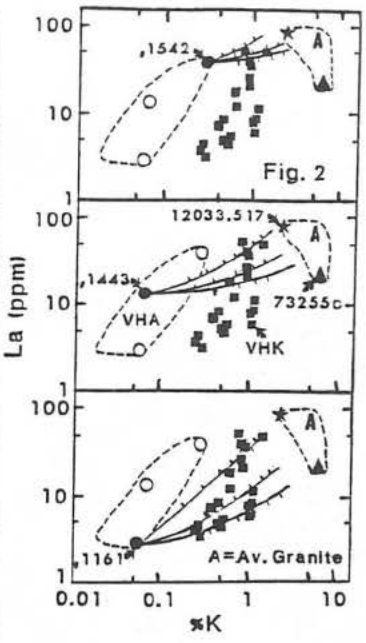

The modelling of Apollo 14 basalts by AFC defines a parental magma (2) composition, which is LREE depleted with a small, negative Eu anomaly, enriched in incompatibles, and has low SiO_2 and a high MG#. This composition is an unmodified mantle melt, and can be used to estimate the composition of the lunar mantle. A source composition is assumed from the magma ocean theory (i.e., melting of mafic cumulates containing a negative Eu anomaly: 12). The trace element composition of the magma ocean can be calculated from this source. The VHA source crystallized from a magma ocean with a $(La/La)_N$ ratio of 2 and a $(Sm/Nd)_N$ of 0.89 (5,6,8). This constrains the degree of partial melting required to generate the primitive parental VHA basalt to 3-5%, although the source can vary (Ol 57-73, Opx 10-20, Cpx 10-15, Plag 2-3, Ilm 5).

REFS: **1)** DePaolo (1981) EPSL 53; **2)** Neal & Taylor (this volume); **3)** Neal & Taylor (1988) LPS XIX; **4)** Neal et al. (1988) PLPSC 18th; **5)** Nyquist et al. (1979) PLPSC 10th; **6)** Nyquist et al. (1981) EPSL 55; **7)** Shervais et al. (1985) JGR 90; **8)** Unruh et al. (1984) JGR 89; **9)** Vaniman & Papike J.J. (1980) P. C. Lunar Highlands Crust; **10)** Walker et al. (1972) PLSC 3rd; **11)** Walker et al. (1973) PLSC 4th; **12)** Warren (1985) Ann. Rev. Earth Planet. Sci. 13.

IMPACT SPLASHING AND QUENCHING DURING CRYSTALLIZATION OF VOLCANIC APOLLO 15 KREEP BASALTS. Graham Ryder, Lunar and Planetary Institute, 3303 NASA Road One, Houston, TX 77058.

Some Apollo 15 KREEP basalt fragments have a clear Ti-rich yellow glass mesostasis, unlike the dark cryptocrystalline mesostasis of most samples. The petrographic characteristics and chemistry of these glasses demonstrate that they are fractionated liquids produced by the crystallization of plagioclase and orthopyroxene/pigeonite from typical Apollo 15 KREEP basalt compositions. However, the yellow glass mesostases were quenched. The yellow glasses show a range of compositions, with Ti, K, and Fe increasing, and Mg decreasing, with evolution (fractionation). Within a sample the glass is fairly uniform in composition; differences among samples are much greater. Samples containing yellow glass show no difference in bulk chemistry from other Apollo 15 KREEP basalts.

Several features roughly correlate with the chemistry of the yellow glass. The less evolved the glass in a sample (lower Ti, K, Fe, higher Mg) then: 1) the more there is of it, and 2) the more limited the silicate mineral compositions are, i.e. the more Fe-rich pyroxenes and more Na-rich plagioclases do not occur. In samples with least evolved glasses (that form perhaps 40% of the rock) neither cristobalite nor ilmenite crystallized, nor did liquid immiscibility set in. These features merely suggest that among Apollo 15 KREEP basalt fragments, for samples with yellow glass sudden cooling and quenching took the place of "normal" crystallization; quenching occurred at varied stages.

Yellow-glass mesostasis KREEP basalts monopolize the clast population in impact melt sample 15358, whose melt matrix is also of Apollo 15 KREEP basalt composition. These basalt fragments have varied grain sizes and textures. In virtually all the 15358 fragments, the silicate minerals have been fractured and the yellow glass forced as a liquid into the fractures prior to incorporation in the matrix melt. In no case do the fractures or the intrusive glasses cut the matrix melt. In some coarse-fines particles, a similar fracture/intrusive relationship occurs. In yet other fragments, the entire basalt texture has been destroyed, such that the appearance is that of an impact melt yellow glass with mineral clasts. Yet their bulk fragment composition is that of an Apollo 15 KREEP basalt and the glass is an evolved, high-Ti,K one. Also, the correlations of % melt and silicate mineral chemistry with glass chemistry are maintained. It is evident that a shock disrupted both the silicates and the residual yellow glass, and that the glass was immediately quenched.

The features of the yellow-glass bearing fragments demonstrate disruption during the original crystallization of the volcanic flows; they are not compatible with impact partial melting of solid interstitial material. Two possibilities are flow tectonization, which does not explain the completely disrupted samples, and impact splashing and quenching during volcanic flow, which is consistent with all the observed features. Both a single impact into a flow or lava pond (with varied stages of crystallization simultaneously occurring) and multiple impacts are consistent with the observations. 15358 is best explained as the product of a single impact, with splashing producing the melt matrix and fracturing and chilling the basalt fragments simultaneously. However, multiple impacts are more consistent with the presence of fragments with yellow glass/fractures at both Stations 6 and 7, and is more consistent with finding such fragments at all (we do not expect to find many fragments of rare events). Thus multiple impacts into complex flows seems most likely. A high impact flux might be expected for the period immediately following the Imbrium impact, which might have triggered the extrusion of these basalts by pressure release.

CORDIERITE-SPINEL TROCTOLITE, A NEW MG-RICH LITHOLOGY FROM THE LUNAR HIGHLANDS Ursula B. Marvin, Harvard-Smithsonian Center for Astrophysics, J. William Carey, Department of Earth and Planetary Sciences, Harvard University, Cambridge, MA 02138, and Marilyn M. Lindstrom, NASA Johnson Space Center, Houston, Texas 77058

We have identified a clast of spinel troctolite containing 8% of cordierite ($Mg_2Al_4Si_5O_{18}$) among the constituents of Apollo 15 soil breccia 15295. Cordierite, has not previously been observed as a principal constituent of a lunar rock. Microprobe analyses show this material to be essentially pure Mg-cordierite with <1% of FeO and no H_2O. The clast mode is approximately 75% anorthite ($An_{94}Ab_{5.5}Or_{0.5}$), 11% olivine (Fo_{91}), 8% cordierite, and 6% spinel (pleonaste) [$(Mg_{0.8}Fe_{0.2})(Al_{0.87}Cr_{0.13})$]. The bulk composition, calculated from the mode, is that of a corundum-normative rock with Mg'= 0.89. This value places the clast among the most Mg-rich of lunar highlands rocks.

The clast broke into several pieces during its excavation from the breccia but, from the fragments in thin section 15295,101, it is possible to reconstruct a well-crystallized mineral assemblage that has been subject to minor *in situ* cataclasis. Streaks of finely crushed anorthite border angular fragments, up to 0.9 mm long, with well-preserved twinning. Red, euhedral crystals of pleonaste, <0.25 mm across, are embedded in anorthite, and tiny grains are also found along boundaries between other mineral pairs. Forsterite grains, <0.4 mm long, have a porous, mosaic texture. Cordierite occurs in grains up to 0.2 mm across, and in thin bands along grain boundaries. Clearly defined, unaltered contacts are observed between corderite and each of the other three minerals. One 0.1-mm crystal of corderite displays 30° sector twinning.

The only previous report of cordierite in lunar samples was published by Dymek *et al.* (1976) who found a single 0.03-mm inclusion of it in spinel in sample 72435. Rock 72435 is a spinel cataclasite, a rare type of lunar lithology first described by Bence *et al.* (1974). Most spinel cataclasites contain spinel and orthopyroxene, a pair that requires pressures of >2.5 kb, equivalent to depths below 50 km in the lower crust or upper mantle of the Moon. However, 72435 is atypical, in that it contains about 20% of olivine (Fo_{72}), which places it among the ferroan anorthosites rather than the Mg-rich suite of highland rocks. It also contains 1% of Al-enstatite as well as the small inclusion of corderite. After calculations of T-P effects on the mineral chemistry of 72435, Herzberg and Baker (1980) concluded that it was a crustal rock formed at <1 kb in the outer 16 km of the Moon, and the minute grain of cordierite was a remnant from a reaction of forsterite plus corderite to enstatite plus spinel.

The clast from 15295 is a highly magnesian cordierite- spinel troctolite, unlike all other spinel-bearing lunar rocks. Liquidus relations within the CaO-MgO-Al_2O_3-SiO_2 system show that the crd-ol-sp-pl assemblage is separated from normal mafic and ultramafic liquids by a thermal divide defined by the an-fo-qtz join (e.g. Gribble and O'Hara, 1967; Presnall *et al.*, 1978). Our clast is corundum-normative in composition, and must, therefore, have originated by some process other than liquid evolution in a mafic system. As this precludes its derivation from a basaltic magma, the most probable mode of origin was as a spinel-rich cumulate that was subsequently metamorphosed and recrystallized into the assemblage we observe. Such an assemblage would be stable at maximum pressures of about 2.5 kb. We conclude that this unique cordierite-bearing Mg-rich lithology formed near the base of the lunar crust at a depth approaching 50 km.

References: A.E. Bence, J.W. Delano, J.J. Papike, and K.L. Cameron (1974), *Proc. Lunar Sci Conf. 5th,* 1:785-827. R.F. Dymek, A.L. Albee and A.A. Chodos (1976), *Proc. Lunar Sci. Conf. 7th*, 2335-2378. C.D. Gribble and M.J. O'Hara (1967), *Nature* 214:1198-1201. C.T. Herzberg and M.B. Baker (1980), *Proc. Conf. Lunar Highlands Crust*, 113-132. D.C. Presnall, S.A. Dixon, J.R. Dixon, T.H. O'Donnell, N.L. Brenner, R.L. Schrock, D.W. Dycus (1978), *Contrib. Min. Petr.* 66:203-220.

IMPACT STRUCTURES AS PROBES OF THE LUNAR INTERIOR; B. Ray Hawke[1], P. G. Lucey[1], and P.D. Spudis[2], [1]Planetary Geosciences Division, Hawaii Institute of Geophysics, University of Hawaii, Honolulu, HI 96822; [2]U.S. Geological Survey, Flagstaff, AZ 86001.

Impact cratering was a major process during early lunar history. Large basin-forming impacts created major bodies of impact melt and excavated crustal material from a variety of depths that was deposited in a systematic fashion. Thus systematic changes in the composition of basin ejecta deposits may reflect changes in the vertical composition of the lunar crust at the target site. The composition of the associated body of impact melt may represent a homogeneous section of the upper crust. Spectral investigations of the mineralogy of basin deposits in different regions of the lunar nearside should allow the determination of the manner in which crustal composition and stratigraphy changes as a function of position on the Moon. In addition, spectral studies of fresh lunar craters provide mineralogical and compositional data concerning the upper levels of the crust as well as insight into the impact cratering process. For a number of years, we have been collecting, analyzing, and interpreting high-resolution near-infrared reflectance spectra (0.6-2.5μm) for lunar crater and basin deposits. The purpose of this paper is to summarize the preliminary results of this effort.

The Orientale basin, on the western limb of the Moon, has long served as the prototype lunar multiring basin. Earth-based spectral reflectance data indicate that Orientale basin ejecta are dominantly anorthositic with compositions ranging from pure anorthosite to anorthositic norite. The composition of the smooth plains unit on the interior of Orientale is very similar to that sampled at the Apollo 16 landing site. Portions of the inner rings of the basin are composed of anorthosite. Deposits of pure anothosite have also been located in the inner rings of Nectaris basin. However, a recent survey of both the internal and external deposits of Nectaris has indicated that they are dominated by norites and anorthositic norites. In contrast, the composition of Imbrium basin deposits is extremely heterogeneous. Both the Apollo orbital geochemical information and Earth-based spectral data suggest that a remarkable diversity of compositions is associated with Imbrium basin. These identified rock types include anorthositic norites, Mg-suite norites and gabbronorites, KREEP basalts, olivine-bearing rocks of the Mg-suite, and exotic, KREEP-rich granitic rocks. A wide variety of compositions was also exposed by the Aristarchus impact event. These include gabbro, mare basalt, and an olivine-rich assemblage. The formation of Tycho crater, on the other hand, exposed only gabbroic rocks. Tycho exhibits a dark halo of impact melt. Spectral studies have shown that this halo is rich in impact generated glass.

INITIAL GEOCHEMICAL CHARACTERIZATION OF LUNAR METEORITE Y-86032

Christian Koeberl, Institute of Geochemistry, University of Vienna, Dr.-Karl-Lueger-Ring 1, A-1010 Vienna, Austria.

Since the first anorthositic breccia was recovered from Antarctic ice in 1982 and identified to be a piece of the moon, several more "lunar meteorites" have been found amongst Antarctic meteorites. One sample (ALHA-81005) is in the U.S. collection, while several more have been identified in the Japanese collection of Antarctic meteorites. Until recently, four additional lunar meteorites from the Japanese collection were known: Y-791197, Y-82192, Y-82193, and Y-793274. All of them were quite small specimens, with a few tens of grams weight at best. In the 1986/7 season the Japanese Antarctic Research Expedition recovered another lunar meteorite from the Yamato Mountains meteorite field. This stone turned out to be the largest of all lunar meteorites, weighing 648.43 g. Like all other lunar meteorites, it is an anorthositic breccia, thus originating from the lunar highlands. Visually the piece is similar to the others, but its size (9.3 x 8.6 x 8.0 cm) indicates that it is larger than what would be expected from its weight. This indicates that the rock has abundant vesicles. A number of large voids are already visible from the outside. A large part of the meteorite seems to consist of impact melt, which is partly glassy. The impact melt is visible in the form of yellowish-brown veins and patches. Numerous white clasts - some are as large as 1 cm in length - are visible from the outside. Some of these clasts may be granulithic breccias. An initial characterization of the mineral phases shows that the plagioclase composition is more uniform (An90.9-97.4) than it is in e.g. Y-82192 (An83.0-98.2) (Yanai et al., 1987) There are, however, some similarities between Y-86032 and Y-82192 and Y-82193. Mineral compositions show closer similarities than if compared to Y-791197. For an initial geochemical characterization, a small sample of Y-86032 was received from the National Institute of Polar Research, consisting of a matrix part and an impact melt part. These samples have been subdivided in oder to get data for the bulk, a large clast, small white clasts, and the impact melt. The samples are currently being measured, and final data will be available at the time of the meeting. Preliminary data show that trace element concentrations are unlike Y-791197, but close to Y-82192. The REE abundances are considerably lower than in Y-791197, and also close to the abundances in Y-82192 and Y-82193. A KREEPy component seems to be completely absent. At the present it is not yet possible, however, to discuss the possibility of pairing with Y-82192 and Y-82193 in a quantitative way. This has to await the final evaluation of the data, which will be available soon.

Reference: Yanai, K., Kojima, H., Koeberl, C., Graham, A.L., and Prinz, M.: Photographic Catalog of the Antarctic Meteorites, National Institute of Polar Research, Tokyo, 298 pp, 1987.

Acknowledgement: This work is part of the Y-86032 consortium study. I am grateful to H. Takeda (Univ.Tokyo, consortium leader) for advice and to H. Kojima (NIPR) for the sample.

EXPOSURE HISTORY OF FOUR LUNAR METEORITES; K. Nishiizumi, R. C. Reedy* and J. R. Arnold, Dept. of Chemistry, B-017, Univ. of Calif., San Diego, La Jolla, CA 92093, *Earth & Space Sciences Div., MS-D438, Los Alamos National Lab., Los Alamos, NM 87545.

Six lunar meteorites have been found in Antarctica. The lunar meteorites are expected to have cosmic ray exposures on the moon (2π irradiation) before their ejection and in space (4π irradiation) during transportation from the moon to the earth. The terrestrial age can also be appreciable for Antarctic meteorites. Although Yamato 82192 and 82193 are believed to be paired, it is not clear whether Yamato 791197 and Allan Hills 81005 were ejected by same impact event. Both meteorites have similar chemical and noble gas compositions. Measurement of cosmogenic nuclides can provide essential constraints. It is necessary to measure three or more cosmogenic nuclides in the same sample to determine such a complex history.

In this study the cosmogenic nuclide ^{53}Mn ($t_{1/2} = 3.7 \times 10^6$ years) was measured by neutron activation in the four lunar meteorites ALHA81005, Y-791197, 82192, and 82193. ^{36}Cl (3.0×10^5 years), ^{26}Al (7.05×10^5 years), and ^{10}Be (1.5×10^6 years) in aliquot samples were previously measured by AMS [1]. The results are shown in Table 1. We combined the cosmogenic radionuclide and noble gas data [e.g. 2-4] to obtain the cosmic ray exposure histories of those objects on the moon and in space and the terrestrial ages in Antarctica. Our results also constrain the ejection depths of the objects from the moon. The production rates of cosmogenic nuclides in lunar meteorites vary in space with the meteoroid's size and the sample's depth and on the moon with the depth and were calculated with existing models.

ALHA81005: The meteorite was irradiated by cosmic rays at a depth of about 130 g/cm^2 in the moon for at least 15 million years before being ejected. The low ^{36}Cl activity can be explained by the terrestrial age of the meteorite. The terrestrial age of the meteorite is about 2×10^5 years and could be as long as 4×10^5 years if there was much neutron-capture-produced ^{36}Cl in the moon. The transportation time from the moon to the earth must have been very short, probably less than 1×10^5 years, which agrees with low TL (thermoluminescence) and almost no cosmic ray tracks.

Yamato 791197: The high ^{26}Al may be explained by solar-cosmic-ray irradiation near the surface of the moon (depth of about 5 g/cm^2) before it was ejected. The meteorite was either ejected directly to the earth and had less than 2×10^5 years terrestrial age or it was exposed in space for about 3×10^5 years and then lay in Antarctica for about 2×10^5 years.

Yamato 82192 and 82193: High ^{10}Be activities indicate that both meteorites were irradiated by cosmic rays in space for at least 5×10^6 years, probably with a small radius of about 15 cm. A lunar exposure is not seen in the record but could be possible over 5×10^6 years ago. The terrestrial ages were about 1-2 $\times 10^5$ years. Those meteorites are very probably a paired fall.

We wish to thank the NIPR and NASA for providing meteoritic samples. We thank R. M. Lindstrom for the neutron irradiation.

Table 1. Cosmogenic nuclides in lunar meteorites

Meteorite	^{36}Cl#	^{26}Al#	^{10}Be#	^{53}Mn
	(dpm/kg meteorite)			(dpm/kg Fe)
ALHA81005,16	8.81 ± 0.44	41.3 ± 4.1	6.33 ± 0.25	176 ± 12
ALHA81005		46 ± 3*	4.1 ± 0.5*	
Yamato-791197,75	12.34 ± 0.86	85.1 ± 8.5	11.61 ± 0.46	253 ± 26**
Yamato-82192,73	18.03 ± 1.07	106.6 ± 7.5	23.96 ± 1.20	384 ± 29**
Yamato-82193,101	18.86 ± 0.66	138.9 ± 9.7	20.10 ± 1.00	306 ± 28**

Nishiizumi et al., (1986) * Tuniz et al., (1983) ** preliminary results

REFERENCES [1] Nishiizumi K., et al., (1986) 11th Symposium on Antarctic Meteorites (Natl Inst. Polar Res., Tokyo) 58-59. ; [2] Bogard, D. D. and Johnson, P.(1983) Geophys. Res. Lett., 10, 801-803. ; [3] Eugster, O., et al.,(1986) Earth Planet. Sci. Lett., 78, 139-147. ; [4] Takaoka, N. (1986) Mem. Natl. Inst. Polar Res., Spec. Issue, 41, 124-132. ; [5] Tuniz, C., et al.,(1983) Geophys. Res. Lett., 10, 804-806.

TEXTURAL DIVERSITY AND CHEMICAL RANGE OF VOLCANIC APOLLO 15 KREEP BASALTS. Graham Ryder, Lunar and Planetary Institute, 3303 NASA Rd. One, Houston, TX 77058.

Apollo 15 KREEP basalts were not recognized as distinct samples by the astronauts in the field, as they are all too small. However, they are important as a chemical component in all soils from the site, and probably are fragments of the Apennine Bench formation, a post-Imbrium light plains unit inside the Imbrium basin (1). They are undoubtedly volcanic (2) and of special importance because of their KREEP chemistry and stratigraphic position. There are many descriptions and reviews of these fragments but a good data base, especially for chemistry, has been lacking. Hence the petrogenesis of these significant basalts has been in a suspended state of infancy. Most studies have concluded that there is a limited range in textures and a wide range of compositions (from fractional crystallization and crystal removal). I have reviewed published data, inspected and made microprobe analyses (px,plag,glass) of many fragments, and made fused bead and INAA analyses of 10 coarse fines fragments. There is a wider range of textures (although most are fine-grained), and a much narrower, but real, range of chemical compositions than previously suggested.

TEXTURAL VARIATIONS: The archetypical varieties are fine-grained subophitic to intersertal, with a network of plagioclase laths (<500 microns long); pigeonites with opx cores partly enclose plagioclases. Dark cryptocrystalline/glassy residue, totalling 10 to 50% occurs interstitially. However, some samples are distinctly porphyritic: one fragment has opx phenocrysts up to 3 mm long, another has a glomeroporphyritc texture with intergrown plag and opx. 15386 has 2-3mm plag and opx, partly intergrown, and a much finer groundmass. At the finer-grain sizes, at least one sample is almost a glass, and many have spherulitic textures with no crystals greater than 200 microns, indicating crystallization from liquids of their own composition. Some samples, from fine spherulites to coarse fragments, contain yellow glass mesostasis instead of the cryptocrystalline dark mesostasis, indicating two-stage cooling and quenching (accompanying abs.). Within a sample the texture, apart from phenocrysts, is quite homogenous, and textures are consistent with a volcanic origin and crystallization in a variety of dynamic environments. Complications are shown by the earliest crystals, which demonstrate that for some opx crystallized slightly before plag, in others plag before opx, in others there was simultaneous crystallization. The opx cores are in some cases complex, with a clearly distinct core overgrown by opx with abruptly distinct Al, Cr, and Ti contents, indicating crystallization in distinct environments.

CHEMICAL RANGE: Analyses for fine-grained samples, including the 10 new ones and some 15358 clasts, show a strong negative correlation between Mg and Sm and between Cr and Sm. Apart from some of the porphyritic samples (either cumulate or unrepresentative analysis), the range in compositions is from mg' .64 to .55, and Sm increases from 29 to 38 ppm. All elements show regular changes from most Mg-rich to most Mg-poor, consistent with fractional crystallization, or with random mixtures of a constant proportion of plag/px and a mesostasis composition. The cotectic fractional crystallization reality is confirmed by a) analyses of two chips of a single sample which show that sampling errors are small, as believed from grain-size considerations and b) the compositions of opx core compositions, which vary reasonably sympathetically with bulk mg'. Fractional crystallization corresponds with about 30% separation of plag+opx/pig, but it is not clear that a single magma was parental, rather than that numerous similar flows have been sampled.

References: (1) Spudis and Hawke (1986) LPI Tech. Rept. 86-03, 105.
(2) Ryder (1986) Proc. Lunar Planet. Sci. 17th, E331.

YAMATO-86032 LUNAR METEORITE: COSMIC-RAY PRODUCED, RADIOGENIC AND TRAPPED NOBLE GASES; O. Eugster, Physikalisches Institut, University of Bern, Switzerland

Yamato-86032 is an anorthositic regolith breccia (648 g) that was recognized by Yanai and Kojima [1] to be similar to the paired lunar meteorites Y-82192 and Y-82193. Sample Y-86032,86 (0.42 g) was obtained for preliminary characterization of the noble gases from the National Institute of Polar Research, Tokyo. First results on bulk samples have been reported previously [2].

Sample (weight mg)	Total	Trapped component					Rad.	Cosmogenic component				Cosmic-ray exposure age [Ma] (4π)
	^{4}He	^{20}Ne	^{36}Ar	$^{20}Ne/^{22}Ne$	$^{38}Ar/^{36}Ar$	$^{40}Ar/^{36}Ar$	^{40}Ar	^{3}He	^{21}Ne	^{38}Ar	$^{22}Ne/^{21}Ne$	
Y-86032,86												
Bulk (1.00)	35	6.8	13.8				677	4.9	1.9	2.0	1.18	9.7
Bulk (1.01)	39	19.1	33.4				653	5.3	2.0	2.2	1.17	10.4
Bulk (20.29)	38	14.5	22.3				682	6.7	2.1	1.9	1.18	9.8
>30μm (20.56)	41	18.8	22.8				710	6.8	2.1	1.9	1.21	9.8
>30μm (12.26)	44	14.7	22.0				734	6.6	2.2	1.9	1.15	10.1
Average	39			11.8	0.194	8.9	691	6.1	2.1	2.0	1.18	10.0
	±3			±0.5	±0.020	±2.0	±30	±0.8	±0.1	±0.2	±0.02	±0.3
Y-82192/3 [3]	48	17.0	12.8	12.02	0.195	8.2	870	7.6	2.3	2.3	1.22	10.7
>25μm B	±3			±0.50	±0.017	±5.2	±80	±0.9	±0.1	±0.2	±0.02	±0.6

The table gives preliminary data for bulk samples and >30μm grain size fractions. The trapped noble gas amounts are low compared to typical lunar breccias and are not homogeneously distributed among the samples. $(^{20}Ne/^{22}Ne)_{tr}$ = 11.8 derived from a $^{20}Ne/^{22}Ne$ vs. $^{21}Ne/^{22}Ne$ plot for the five samples and $(^{40}Ar/^{36}Ar)_{tr}$ = 8.9 from a $^{40}Ar/^{36}Ar$ vs. $1/^{36}Ar$ plot are consistent with solar wind trapped Ne and lunar trapped Ar, respectively. The cosmogenic component is quite constant for the five samples. Galactic cosmic-ray exposure ages were calculated based on the concentrations of ^{21}Ne and ^{38}Ar adopting the average production rates derived for Y-82192/3 valid for 4π exposure [3]. For Y-86032 an exposure age of 10 Ma is obtained; it can not be decided whether this exposure occurred on the lunar surface or in free space before radionuclides are measured. The results for Y-86032 indicate that the lunar meteorite studied in this work is paired with Y-82192/3. The only difference is found for radiogenic ^{40}Ar that is about 20% lower in Y-86032. This difference may be due to a lower gas retention age or to a lower K concentration of Y-86032 compared to Y-82192/3. Determinations of the major and trace element concentrations and of the Kr and Xe isotopic abundances are in progress.

Acknowledgements: Allocation of the valuable sample by the National Institute of Polar Research in Tokyo is greatly acknowledged. This work was supported by the Swiss National Science Foundation.

References: [1] K. Yanai and H. Kojima, Abstr. 12th Symp. Antarctic Meteorites, Tokyo, p. 3 (1987). [2] O. Eugster, Abstr. 13th Symp. Antarctic Meteorites, Tokyo (1988). [3] O. Eugster and S. Niedermann, Earth Planet. Sci. Lett. (1988) in press.

PLENARY III

INVITED PAPER

THE PLUTONIUM-244 STORY: P.K.Kuroda, Environmental Research Center, University of Nevada, Las Vegas, Nevada, 89154(USA).

In 1868,Pierre Janssen went to India to study a total eclipse of the Sun. He observed a strange spectral line and forwarded the data to Sir Joseph Lockyer, who attributed it to a new element he called HELIUM. Since Lockyer's report many strange lines have been discovered in the light of heavenly objects and some have been attributed to new elements named CORONIUM, GEOCORONIUM,NEBULIUM and so on. All of these have turned out to be just old elements under unusual conditions. All,that is,but one. The one exception was HELIUM. Twenty seven years later,the existence of helium was discovered on earth by Sir William Ramsay.

In 1936, Francis Aston went to Japan to study a total eclipse of the Sun and gave a lecture at the University of Tokyo. Most scientists in Japan at that time are said to have failed to understand the connection between the Sun and Aston's mass spectrograph. Twenty seven years after Aston's expedition to Japan,the foundation of a new science called Xenology was being established in the United States by John Reynolds(1) at Berkeley. The discoveries of the Renazzo-type(2) and Pasamonte-type(3) fission xenon then followed in succession in 1964 and 1965. While the latter soon became accepted as the spontaneous fission product of plutonium-244 which existed in the early solar system,the origin of the former became the focus of heated controversies in the 1970's and the 1980's. Manuel et al(4) were the first to recognize it as possible r- and p-products from a supernova. Srinivasan and Anders(5)then followed with their claimof the discovery of s-products from a supernova. These strange xenon components which are now identified variously as CCF,CCFX,X,R,HL and so on remind the speaker of the strange spectral lines discovered in the light of heavenly objects by various investigators in the 19th century. They are not pure substances. Instead,they are mixtures of plutonium-244 fission xenon and mass-fractionated primitive xenon(6).

(1)Reynolds,J.H.:J.Geophys.Res.68,2939-2956(1963).
(2)Reynolds,J.H.,and Turner,G.:J.Geophys.Res.693263-3281(1964).
(3)Rowe,M.W.,and Kuroda,P.K.:J.Geophys.Res.70,709-714(1965).
(4)Manuel,O.K.,Hennecke,E.W., and Sabu,D.D.:Nature240,99-101(1972).
(5)Srinivasan,B., and Anders,E.:Science 201,51-56(1978).
(6)Kuroda,P.K.:Nature 230,40-42(1971).

MAGNESIUM AND OXYGEN ISOTOPES IN INTERSTELLAR SPINEL; Donald D. Clayton, Rice University, Houston, TX 77251

Refractory spinel ($MgAl_2O_4$) is a good candidate for a component of refractory interstellar dust for three district causes: (a) the primary thermal condensate of new supernova-synthesized Al into SUNOCONs (1) during expansion of supernova interior; (b) thermal condensate of old Al into STARDUST (1) during mass loss from giant stars; (c) concentration of superrefractory interstellar atoms into grain cores during interstellar evolution owing to sputtering, fragmentation, and episodic heating of interstellar dust (2). Each spinel source should have distinctly different isotopic compositions of both Mg and O. I here discuss expectations of case (c), which will dominate if spinel condensation in stars is not efficient so that elements are ejected in gaseous form, leaving only dust evolution to produce refractory cores (designated "phase-A" by Liffman and Clayton (3)).

Interstellar Al is observed to be tenfold less gaseous than other refractory cations (Mg and Si). A likely explanation is that Al is volatilized tenfold less efficiently during sputtering and fragmentation owing to Al's refractory nature and to its gradual concentration into superrefractory cores that are more shielded from those disruptions. If so, Al atoms reside tenfold longer in grains than do Mg and Si. Sputtering and reaccretion-cycle studies (3) confirm this; phase-A superrefractory cores have mean lifetime against sputtering $\tau_A = 1.2 \times 10^9$ yr even though bulk refractory grains have sputtering lifetime $\overline{\tau}_{sput} = 2.6 \times 10^8$ yr. Thus phase-A superrefractory cores may be expected to have an age greater than that of bulk dust by about 10^9 yr, or about 15% of the galactic age at the time the sun formed. That age difference generates isotopic differences.

Because $^{17,18}O$ and $^{25,26}Mg$ are both secondary nucleosynthesis products, their bulk interstellar abundances increase quasilinearly with respect to ^{16}O and to ^{24}Mg respectively (2). If interstellar Al is primarily in oxidized phase-A cores rich in $MgAl_2O_4$ units (representing only small fractions of bulk O and Mg), and if the isotopic composition of those units is taken to be that of the bulk ISM at the time they were formed, it would follow that interstellar spinel would carry isotopic excesses of about 15% in ^{16}O and in ^{24}Mg. The former could be the reason that meteoritic CAI were initially enriched in ^{16}O by about 5%; i.e. correlation with aluminum.

Such large ^{24}Mg excess has never been seen; but suppose some exchange process has diluted Mg much more than oxygen. The small residual ^{24}Mg excess could be mistaken for negative mass fractionation within Mg, which, if corrected to solar 25/24 ratio, might then appear instead to be a ^{26}Mg excess. Conservative reasoning has thereby produced an "apparent ^{26}Mg excess" in Al without benefit of ^{26}Al decay! Its potential role as a contributor to Mg isotopic systematics correlated with Al needs careful investigation.

I briefly describe also the contrasting Mg behavior within $MgAl_2O_4$ SUNOCONs and the hope that infrared observations of Supernova 1987a can strengthen or weaken the case for the older SUNOCON mechanism (1). Because they are young, these ^{16}O-pure SUNOCONs carry instead $^{25,26}Mg$ excess, emulating positive fractionation with "apparent ^{26}Mg deficit."

Supported by NASA and the Robert A. Welch Foundation.

REFERENCES: (1) Clayton, D. D. (1978), Moon and Planets, 19, 109-137.
(2) Clayton, D. D. (1988), Astrophys. J. Letters, (submitted).
(3) Liffman, K. and Clayton, D. D. (1988), Proc. Lunar Planet. Sci. Conf. 18th, p. 637-657.

INTERPRETATION OF SOLAR SYSTEM ABUNDANCES AROUND THE N=50 NEUTRON SHELL; D.S. Woolum, Physics, Calif. State Univ., Fullerton, CA 92634; D.S. Burnett, Geol. & Planet. Sci., Caltech, Pasadena, CA 91125.

New measurements [1] of CI chondrites for Ni-Ru show a high degree of smoothness for the odd-A solar system abundance curve (SSAC) through the region of the N=50 closed neutron shell (Fig. 1). The resolved s- and r-process peaks at the N=82 and 126 neutron shells [2] are not apparent for the N=50 region. Our data confirm (Fig. 1) the necessity for a single element ^{89}Y SSAC peak, presumably of s-process origin. If the total SSAC is smooth but made of contributions from more than one nucleosynthesis process, then at least the major contributing processes must also have smooth abundance curves. Within errors, a smooth s-process abundance (N_s) curve can be drawn (Fig. 1) using N_s from Beer and co-workers. For A=75-85 there are strong "non-s" contributions which could be flat or show a shallow maximum at mass 79-81 (Fig. 1; N-N_s; suppressed scale). This maximum would be analogous to the "r-process" peaks at A=129 or 195. The reason that the two-peak structure for N=50 is not apparent in the total abundance curve is that the lower mass peak is relatively broad, leading to unresolved s and non-s peaks in the total SSAC. The rise in the N-N_s curve below mass 75 is probably an error in the theoretical N_s, so the "non-s" peak is better defined than at first glance. Below mass 69 it is hard to separate the contributions of n-capture nucleosynthesis from the high-mass tail of the iron group nuclei, the origin of which is not well understood.

In the mass 70-100 range the even-A SSAC is not smooth (Fig. 2), showing a sawtooth structure. From the point of view of identifying CI abundances with the average solar system it is not necessary that the even-A curve be smooth. It is sufficient that the odd-A curve be smooth. For even-A the N_s show similar structure to the total SSAC. The product of N_s and stellar-temperature neutron capture cross section (σ) is a slowly varying function of mass number except near neutron shells. The inset in Fig. 2 shows that the sawtooth structure is found in σ for even-A nuclei on the s-process path. There is thus a strong suggestion that the sawtooth structure is an s-process feature. However, quantitatively, the literature N_s are insufficient to account for the sawteeth. One possibility is simply that the calculated s-process abundances are low, but a speculative alternative is that n-rich nuclear statistical equilibrium nucleosynthesis contributes significantly to SSAC in this region. This previously has been invoked to explain the relatively frequent occurrence of meteoritic isotopic anomalies in ^{48}Ca, ^{50}Ti and ^{54}Cr [3].

References: [1] D.S. Burnett et al., submitted to *Geochim. Cosmochim. Acta;* [2] D. Woolum, Chap. 14 in *Meteorites and the early solar system,* Kerridge & Matthews, ed., 1988; [3] D. Papanastassiou, *Ap. J.*, **308**, L27, 1986.

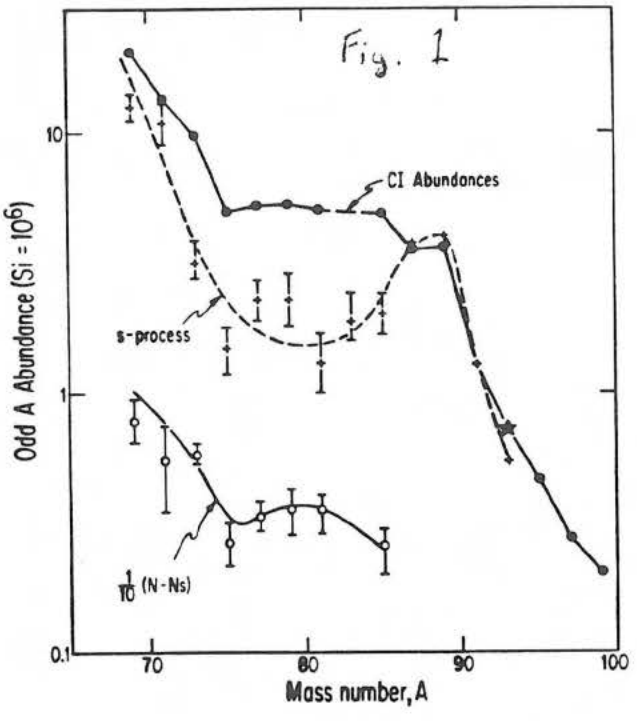

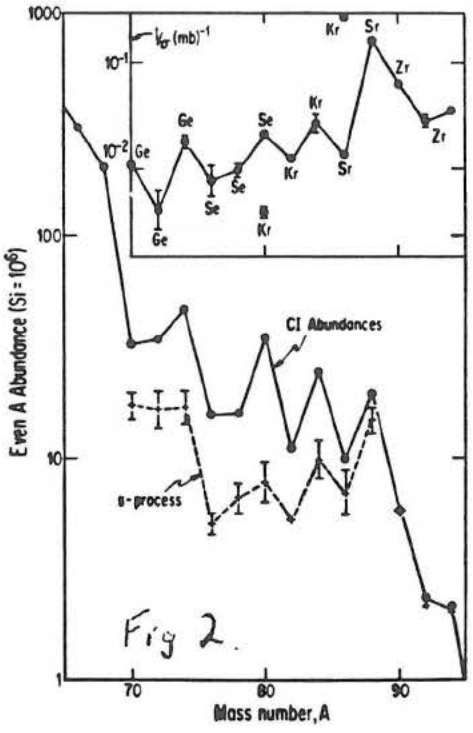

SEARCH FOR ^{60}Fe IN INDIVIDUAL MAGNETITE GRAINS FROM ORGUEIL

Marian Hyman and Marvin W. Rowe, *Department of Chemistry, Texas A&M University, College Station, TX 77843*
Albert J. Fahey and Ernst Zinner, *McDonnell Center for the Space Sciences and the Physics Department, Washington University, St. Louis, MO 63130.*

^{60}Fe is thought to be produced by either the classical r-process or a neutron-rich e-process in nucleosynthesis. Calculations indicate expected production rates of $^{60}Fe/^{56}Fe = 3.9 \times 10^{-5}$ and 3.4×10^{-5}, respectively (Cameron, 1979), though with considerable uncertainty. Its half-life of 1.5×10^{6} years (Kutschera *et al.*, 1984) makes ^{60}Fe a promising candidate for having produced ^{60}Ni excess by *in situ* decay in primitive meteorites. However, four previous studies (Morand and Allegre, 1983; Shimamura and Lugmair, 1983; Hinton et al., 1984; Birck and Lugmair, 1988) have not seen enirchments of ^{60}Ni in meteoritic materials compared to terrestrial nickel.

Since magnetite in CI chondrites occurs in several distinct morphologies, we decided to isolate magnetite grains of a given morphology and examine the isotopic composition of nickel in each individual grain. In this study we measured the isotopic composition of nickel in a number of individual magnetite plaquettes, 8-μm to 20-μm in diameter, which were extracted from the Orgueil CI chondrite. These grains, identified by optical and scanning electron microscopy, were initially mounted on Nuclepore polycarbonate filters attached to 2.5-cm glass slides for analysis in a CAMECA IMS-3F ion microprobe mass analyzer. Most of the grains for this study, however, were mounted on a standard gold foil grid (McKeegan et al., 1985). Ion probe isotopic measurements were made at high mass resolution. Iron isotopes were measured along with ^{60}Ni, ^{61}Ni, ^{62}Ni. The positions of the ^{54}Fe, ^{56}Fe and ^{57}Fe peaks were used to extrapolate to those of the Ni isotopes whose count rates were often too low for automatic peak centering. Nickel-rich stainless steel, magnetite and olivine were used as terrestrial standards. The measurements on the Orgueil magnetites consistently yielded Ni isotopic compositions which are indistinguishable from terrestrial Ni compositions. Table 1 shows our isotopic data along with the measured upper limits of the $^{60}Fe/^{56}Fe$ for each of the samples.

Table 1.

Sample	$^{56}Fe+^{62}Ni+$ (10^4)	Fe/Ni	$\delta(^{60}Ni/^{62}Ni)$ ($\pm 2\sigma$)	$^{60}Fe/^{56}Fe$ (2σ limit)
43-6a	1.63	180	49 ± 50	$0.8 \pm 0.8 \times 10^{-4}$
43-6a	3.70	407	19 ± 82	$0.1 \pm 0.6 \times 10^{-4}$
56-2	7.51	827	-70 ± 120	$<0.2 \times 10^{-4}$
56-3	2.10	228	66 ± 108	$0.8 \pm 1.4 \times 10^{-4}$
56-4	2.95	324	-21 ± 192	$<1.5 \times 10^{-4}$
56-5	13.9	1533	<200	$<0.4 \times 10^{-4}$
56-9	0.87	95	-18 ± 62	$<1.5 \times 10^{-4}$
56-10,1	1.18	130	16 ± 136	$0.4 \pm 3.0 \times 10^{-4}$
56-10,2	1.23	135	39 ± 50	$0.8 \pm 1.1 \times 10^{-4}$
56-10,3	5.40	596	100 ± 378	$0.5 \pm 1.8 \times 10^{-4}$

Cameron A. G. W., 1979, *Astrophys. J.* **230**, L53-L57.
Kutschera W. *et al.*, 1984, *Nucl. Instr. and Meth.* **B5**, 430-435.
Morand P. and Allegre C.J., 1983, *Earth Planet. Sci. Lett.* **63**, 167-176.
Shimamura T. and Lugmair G. W., 1983, *Earth Planet. Sci. Lett.* **63**, 177-178.
Hinton R. W. *et al.*, 1984, *Lunar Planet. Sci. XV*, 365-366.
Birck J. L. and Lugmair G., 1988, *Earth Planet. Sci. Lett.*, submitted.
McKeegan K. D. *et al.*, 1985, Geochim. Cosmochim. Acta **49**, 1971-1987.

^{244}Pu ABUNDANCE IN ORDINARY CHONDRITES

B. Hagee, T. J. Bernatowicz and F. A. Podosek, *McDonnell Center for the Space Science, Washington University, St. Louis, MO 63130*
D. S. Burnett and M. L. Johnson, *Geological Sciences, Cal Tech, Pasadena, CA 91125*
M. Tatsumoto, *U.S.G.S., Federal Center, Denver, CO 80225*

The cosmic abundance of ^{244}Pu is an important parameter in models of nucleosynthetic chronology and as a reference value in studies of solar system chronology. Experimental determination of this abundance is a long-standing problem which has still not been fully solved. Two different approaches have been used, both based on measuring ^{244}Pu via its fission product Xe, but in two different classes of meteoritic material. One class consists of samples relatively rich in Pu and relatively poor in Xe components, especially trapped Xe, which interfere with identification of fission Xe. Such materials, e.g. achondrites, phosphates, refractory inclusions, are, however, chemically fractionated, and lacking a stable or long-lived isotope of Pu the ^{244}Pu measurements must be translated to cosmic abundance by assuming geochemical coherence with another element, typically Nd. By this approach the best estimate (1) of cosmic ^{244}Pu abundance, stated relative to co-produced (r-process) ^{238}U, is ^{244}Pu/^{238}U = .004. The other class of material is bulk chondrite, believed to be an unbiased sampling of non-volatile elements. We believe that this is the best approach to determining the cosmic abundance of ^{244}Pu, since assessing whether Pu is geochemically coherent with Nd or another element requires independent knowledge of the unfractionated abundance of ^{244}Pu. The whole-rock chondrite approach is experimentally difficult, however. For some time the best estimate of ^{244}Pu abundance by this approach was ^{244}Pu/^{238}U = .015, based on an analysis of the LL6 chondrite St. Severin (2). More extensive and sophisticated analyses of St. Severin (3,4) led to an improved estimate ^{244}Pu/^{238}U = .007, sharply lower than the previous value but still substantially higher than the value based on differentiated samples.

While it is important to determine ^{244}Pu abundances in whole-rock chondrites other than the single meteorite St. Severin, previously available data on other meteorites have not been usefully precise. We have determined fission Xe concentrations (Table) by stepwise heating analysis of a group of (unirradiated) ordinary chondrites selected to facilitate identification of fission Xe. Isotope dilution measurements of U, Th, Nd and Ce on aliquots of the samples used for gas analysis are under way. These samples were prepared from alternating cut slabs; the remaining slab faces have been examined for general petrological characterization and for distribution of phosphates, the principal hosts of Pu. The data available so far indicate fission Xe concentrations and ^{244}Pu/^{238}U ratios consistent with those in St. Severin.

The fission Xe calculations require assumption of trapped Xe composition and are sensitive to this assumption. The tabulated fission concentrations are minima in that they assume trapped ^{130}Xe/^{136}Xe equal to the lowest observed value. The trapped ^{130}Xe/^{136}Xe ratios for all these meteorites are similar and, as previously noted for St. Severin (4), are significantly different (lower) from AVCC.

Sample	$^{136}Xe_f$ (10^{-13}cc/g)	U (ppb)	$\frac{^{244}Pu}{^{238}U}$
LL5 Olivenza	7.1 ± 2.9	10.88	.006
L6 Barwell	7.6 ± 4.2	9.24	.006
H5 Pultusk	12 ± 7		
H6 Guarena	20 ± 8		
LL6 Marion	6.9 ± 2.6		
LL6 St. Severin (3,4)	6.9 ± 0.6		.007

1) Marti K., Lugmair G. W. and Scheinin N. B. (1977) *Lunar Planet. Sci. VIII*, 619-621.

2) Podosek F. A. (1972) *Geochim. Cosmochim. Acta* **36**, 755-772.

3) Hudson G. B., Kennedy B. M., Podosek F. A. and Hohenberg C. M. (1982) *Lunar Planet. Sci. XIII*, 346-347.

4) Hudson G. B., Kennedy B. M., Podosek F. A. and Hohenberg C. M. (1988) *Proc. Lunar Planet. Sci. Conf. 19th*,, submitted.

SEARCH FOR EXTINCT ^{248}CM IN THE EARLY SOLAR SYSTEM. B. Lavielle[1,3], K. Marti[1], P. Pellas[2] and C. Perron[2]. [1]Chem. Dept., B-017, Univ. of Calif., San Diego, La Jolla, Calif. 92093, [2]Museum National d'Histoire Naturelle Mineralogie 61, Rue de Buffon, Paris 53, [3]CENBG, Bordeaux, France.

^{244}Pu ($T_{\frac{1}{2}}$ = 82Ma), like U and Th, was produced in r-process nucleosynthesis and has the shortest half-life of the transbismuth nuclides whose presence in the early solar system has been established. The solar system $^{244}Pu/^{238}U$ ratio provides a benchmark for the history of r-process synthesis. Furthermore, ^{244}Pu may be used as an important chronometer in early solar system history, if the initial abundance can be established.

We report the results of our study of the fission fragment record in the chondrite Forest Vale (H4). The mineral merrillite of this chondrite reveals exceedingly high track densities ($\gtrsim 5 \times 10^{8} cm^{-2}$). On the other hand, the relatively track-poor mineral apatite ($\sim 10^{7} cm^{-2}$), which borders and often surrounds merrillites, does not reflect the track density gradient that is commonly observed in other H4 chondrites in the 6 μm wide contact region. This evidence suggests the possible presence of extinct 3.4×10^{5}a ^{248}Cm in the early history of this chondrite [1]. Our detailed study of the fission xenon isotopic signatures uniquely identifies the extinct progenitor as ^{244}Pu. No evidence is obtained from the phosphate study for extinct ^{248}Cm, and an upper limit $^{248}Cm/^{244}Pu < 1.5 \times 10^{-3}$ is calculated at the time of fission xenon retention. A significant fraction of the total fissiogenic xenon in Forest Vale phosphates is released at 1700°, which may, in part, be due to the release of recoil fission fragments in spinels, which occur as minor inclusions in the phosphates. It is interesting to note that a coarse (>2μm) spinel fraction from Murray [2] was found to contain a large amount of ^{244}Pu-derived fissiogenic Xe. This again may indicate that this component represents fission fragments from phosphates which were in contact with spinels during the ^{244}Pu decay interval. Information from radiogenic $^{129}Xe_r$, coupled with neutron capture effects in $^{128}Xe_n$ (from ^{127}I), suggest that system closure for Xe in the phosphates postdates the closure times of other phases in the Forest Vale chondrite. Studies of the Xe_f records in other phases are in progress; an interesting distinct component appears to be present in the metal.

References:

[1] P. Pellas, C. Perron, M. Bourot-Denise, C. Fiéni, M. Ghelis (1987), Lunar and Planet. Sci. Conf., XVIII, Lunar and Planet. Inst., 772-773.

[2] T. Ming and E. Anders (1988), "Isotopic anomalies of Ne, Xe and C in meteorites III. Local and exotic noble gas components and their interrelations. Geochim. Cosmochim. Acta, in press.

TESTS FOR ONE MODEL OF THE SOLAR SYSTEM'S ORIGIN. K. Y. Chiou and O. K. Manuel, Department of Chemistry, University of Missouri, Rolla, MO 65401 USA

We have interpreted isotopic anomalies of solar-wind-implanted elements and the correlations of chemical and isotopic heterogeneities of elements trapped in meteorites (1-5) as evidence that the Solar System was produced from the debris of a single supernova (SN). According to this view, (i) the Sun formed on the collapsed SN core, (ii) iron meteorites and the inner portions of the Sun and the inner planets formed primarily from elements in the central Fe-rich region of the SN debris, (iii) the giant Jovian planets formed primarily from elements in the outer portions of the SN, (iv) accretion of matter on a central black hole produces most of the Sun's energy, and (v) intrasolar diffusion enriches light elements like H and He and the lighter isotopes of individual elements, e.g., Xe, at the solar surface. When solar surface abundances are corrected for the fractionation seen across the isotopes of elements in the solar wind, the major elements of the bulk Sun appear to be (in decreasing order): Fe, Ni, O, Si, S and Mg. These are also major elements in the group of planets closest to the Sun.

The following tests are proposed for this model:

1. In meteorites, isotopically anomalous Xe-X is always accompanied by planetary-type He and Ne (He-A and Ne-A). Our suggestion that this represents material from the outer portion of the parent SN implies that Xe-X is dominant in the outer planets. Isotopic analysis of Xe in the He-rich atmosphere of Jupiter can conclusively test this prediction in the upcoming Galileo mission to Jupiter. The "W"-shaped anomaly pattern of Xe-X cannot be obscured by physical fractionation.

2. Our suggestion that intrasolar diffusion is responsible for the enrichment of light noble gas isotopes in the solar wind can be experimentally tested. Diffusion of ions in a plasma will not depend on the chemical properties of the elements. The light isotopes of a refractory element like Mg will be enriched in the solar wind in the manner observed for Ne, if this enrichment is produced by intrasolar diffusion. Calculations indicate that for mineral separates of Apollo 16 soils the ratio, (Solar-wind-implanted Mg)/(Indigenous Mg) $\simeq$ 0.07, in the outer 0.1μ of 40μ feldspar grains containing 0.05% Mg. This mixture of SW and indigenous Mg should show about a 2% depletion of the Mg-26/Mg-24 ratio if intrasolar diffusion is responsible for the enrichment of light noble gas isotopes in the solar wind.

3. The use of detectors other than Cl-37 will indicate whether the flux of neutrinos from the Sun is indeed much lower than that expected if H-fusion is its source of energy (6). Preliminary data on recoil electrons in the Kamiokande II water detector (7) seem to confirm the low flux of solar neutrinos.

1. Manuel O. K. and Sabu D. D. (1975) Trans. MO Acad. Sci. **9**, 104-122.
2. Manuel O. K. and Sabu D. D. (1977) Science **195**, 208-209.
3. Sabu D. D. and Manuel O. K. (1980) Meteoritics **15**, 117-138.
4. Manuel O. K. and Hwaung G. (1983) Meteoritics **18**, 209-222.
5. Manuel O. K. and Sabu D.D. (1988) in Nuclear, Geo- and Cosmochemistry, Proceedings of Symposium 1987 SW Regional Meeting of ACS, Little Rock, December 2-4, 1987.
6. Bahcall J. N. and Davis R. (1976) Science **191**, 264-267.
7. Koshiba M. T. (1987) Physics Today **40**, 38-42.

BULK ANALYSES AND MINERAL ANALYSES OF EXTRATERRESTRIAL DUST PARTICLES

W. Klöck, (1), K. Thomas (2) and D.S. McKay (1); (1) Code SN4, NASA JSC, Houston, Tx, 77058; (2) Lockheed-EMSCO, Houston, Tx, 77058

Chondritic porous extraterrestrial dust particles collected in the stratosphere are considered to be micrometeoritic material different from any class of meteorites because of their fine-grained textures and high porosities. We analyzed 25 of these "chondritic" particles for major elements by energy dispersive X-ray analysis. Microtome sections were made from 11 particles. The average composition of the bulk particles is close to carbonaceous chondrite composition. All the chondritic extraterrestrial dust particles are clearly enriched in carbon by factors 2-5 compared to C1 chondrites. This seems to indicate that "chondritic" IDP's were formed in a different environment compared to carbonaceous chondrites, and the composition of the dust particles is more "solar"-like than C1.

Seven particles out of the 11 particles which were sectioned had olivine and/or pyroxene compositions (Fig.1) significantly different from compositions of olivine and pyroxene of chondritic meteorites. MnO contents in olivines and pyroxenes of the seven IDP's range from 0.7% to 1.5% and some values reach 3-4%. Our data are in qualitative agreement with data from relic olivines of stratospheric particles (1). Olivines and pyroxenes of equilibrated ordinary chondrites contain usually about 0.4% MnO. MnO contents of forsteritic olivines in C1, C2 and C3 carbonaceous chondrites range from < 0.05.% MnO to about 0.1 % MnO (2). The lowest FeO/MnO ratios in forsterites of C2 meteorites are about 5 at a FeO/MgO ratio of about 0.02 (3), but the average FeO/MnO ratios of Belgica (C2) and Murchison (C2) are 23 and 37 (2). Olivine data from Deep Sea Particles (DSP) seem to be in the same range as the olivine data from C2 meteorites (3). The compositions of relic olivines of two DSP particles reported by (3) are very close to our forsterites with FeO/MnO ratios < 1.0, but most of the DSP olivines have FeO/MnO ratios from 5-35. Two relic blue olivines from Orgueil plot very close to forsteritic compositions of stratospheric dust particles at FeO/MnO ratios of 1.5 and 2.25, however, another blue Orgueil forsterite plots at a FeO/MnO ratio of 180, in the range of Allende "blue" olivines. Blue olivines are considered to be vapour condensates rather than melt products (2). We suggest two possible explanations to explain the variable Fe/Mn ratios of forsterites in carbonaceous chondrites and IDP's:

1. The first condensing olivines contain very small amounts of Mn (e.g. Allende) but Mn increases in the gas phase as indicated by the decreasing Fe/Mn ratios of forsterites going from C3 to C2 and ordinary chondrites to C1 and finally to IDP's (4).

2. The second scenario implies simultaneous condensation of forsterites with variable Fe/Mn ratios and these grains were subsequently sampled by the chondrite parent bodies.

References: (1) Steele I.M. et al., (1985) Nature, 313, 294; (2) Steele I.M. (1986) Geochim. Cosmochim. Acta, 50, 1379; (3) Steele I.M. (1985) Nature, 313, 297; (4) Wai C.M. & Wasson J.T. (1977) EPSL, 36, 1-13;

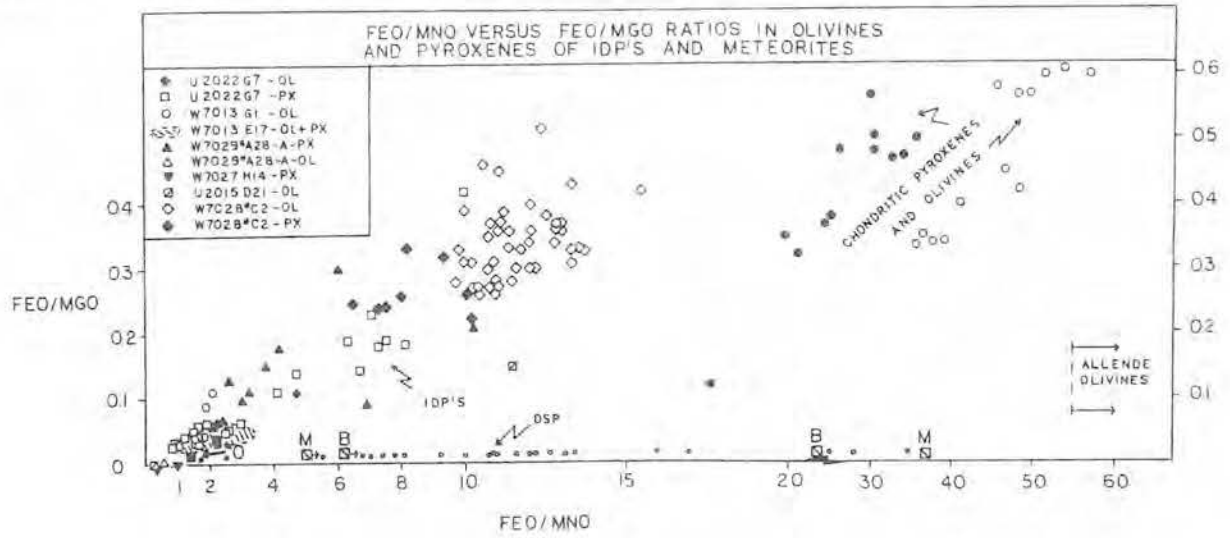

ALUMINO-SILICA GLASS: ITS SIGNIFICANCE FOR THE MINERALOGICAL EVOLUTION OF CHONDRITIC INTERPLANETARY DUST.

Frans J. M. Rietmeijer, Department of Geology, University of New Mexico, Albuquerque NM 87131, U.S.A.

Alumino-silicate glass is an important constituent of olivine-rich chondritic interplanetary dust particles (IDPs)[1,2]. This glass may form during pulse heating on atmospheric entry or through particle-particle collisions in space although evidence in support of either origin is lacking[2]. Another possibility is solid state annealing of chondritic amorphous precursor material for which evidence is present in the mineralogy and texture of IDPs[3,4]. Assuming that chondritic IDPs are solid debris of short-period comets, it has been suggested that thermal regimes in comet nuclei (~200 <T(K)< ~400) are conducive to extensive mineralogical activity[5,6]. A major contributor to the driving force for these diagenetic alterations[7,8] is the excess Gibbs free energy stored in high-temperature minerals and which may include a glass phase. A glass phase will be highly reactive during diagenesis including low-temperature aqueous alterations.

I used a JEOL 2000FX Analytical Electron Microscope equipped with a Tracor Northern 5500TN energy dispersive system (EDS) for thin-film analyses of ultra-microtomed sections of chondritic IDPs W7029E4&E5, U2011C2 and U2022C7&C8. EDS data have been reduced using a SMTF program. Selected area electron diffraction data have a relative error <1.5%. Here, I report only on data that plot above the "pyroxene line" in a ternary diagram Si-Mg-Fe[2]. Structural formulae for layer silicates are calculated assuming ideal amounts of H_2O (wt%) for the appropriate layer silicate types.

RESULTS. A major portion of data for IDP W7029E4&E5 is consistent with plagioclase (Plag) (An = 23-94; Or < 9.5 mole%) and Ca-free alkali-feldspar (Kfs), Or = 47-100. All Kfs, and to a lesser extent Plag, is non-stoichiometric with either excess [ ]Si_4O_8 or excess $(Na,K)_4Al_4O_8$ components[9]. For Kfs, the amount of [ ]Si_4O_8 is ~30 mole% and amounts of the excess Al-component are ~13-43 mole%. The remainder of data is consistent with layer silicates. The Al/Si ratios of almost pure peraluminous (Al/Si > 1.0) layer silicates and Plag/Kfs with excess $(Na,K)_4Al_4O_8$ are similar. Peraluminous layer silicates contain (MgO+FeO) < 1.0 wt% or (FeO+CaO) < 0.5 wt% plus Na_2O < 1.0 wt%. Also, Al/Si ratios of layer silicates (Al/Si < 1.0) closely mimic this ratio in Kfs and Plag containing excess silica. These layer silicates are predominantly Na-rich beidellite-saponite [Mg/(Mg+Fe) ratio = 0.55-0.99] and minor beidellite and montmorillonite. Increased Na-contents in beidellite and saponite are accomodated via a coupled substitution $Si^{4+} = Al^{3+} + Na^{+}$.

DISCUSSION. It seems plausible that during low-temperature annealing of IDPs (T < 525K)[10] an alumino-silica glass will decompose into non-stoichiometric feldspars as the difference in gibbs free energy between the glass and these feldspars will be small (cf. Ostwald Step Rule). The resulting non-stoichiometric Plag and Kfs will add considerably to the potential Gibbs free energy budget of IDPs in low-temperature environments. I contend that non-stoichiometric Plag and Kfs are conducive to layer silicate formation in chondritic IDPs, probably even at very low water pressure. The most conspicuous property of resulting layer silicates will be the inherited high Na and Al contents. I conjecture that a high alkali content will be intrinsic to layer silicates in the least altered, fine-grained Solar System materials. Higher Na/(Na+K) ratios in layer silicates compared to precursor Kfs suggest that fractionation of alkalies occurred during aqueous alteration between circa 273-373K at pH > ~8.0. Finally, I suggest that Mg,Fe-poor, high Na,Al layer silicates will be common constituents of anhydrous[5,9] IDPs.

REFERENCES. 1. Bradley JP & DE Brownlee, 1986. Science 231, 152; 2. Bradley JP et al., 1988. LPSC XIX, 126; 3. Rietmeijer FJM, 1986. Meteoritics 21, 492; 4. Rietmeijer FJM & DS McKay, 1985. Meteoritics 20, 743; 5. Rietmeijer FJM & IDR Mackinnon, 1985. JGR 90 Suppl., D149; 6. Rietmeijer FJM & IDR Mackinnon, 1987. ESA SP-278, 363; 7. Rietmeijer FJM, 1985. Nature 313, 293; 8. Mackinnon IDR & FJM Rietmeijer, 1987. Rev. Geophys. 25, 1527; 9. Longhi J & JF Hays, 1979. Am. J. Sci. 279, 876; 10. Rietmeijer FJM, 1986. Meteoritics 21, 492.

CHEMICAL FRACTIONATION TRENDS IN DEEP SEA SPHERES:

S. R. Sutton[1,2], G. Herzog[3], and R. Hewins[4]; [1]Department of the Geophysical Sciences, The University of Chicago, Chicago, IL; [2]Department of Applied Science, Brookhaven National Laboratory, Upton, NY; [3]Department of Chemistry, Rutgers University, New Brunswick, NJ.; [4]Department of Geology, Rutgers University, New Brunswick, NJ.

Elemental fractionation studies on deep sea spheres may be useful in determining the effects of rapid heating and quenching and thereby establish the importance of these effects in chondrule formation. Previous work on major elements using EDX [1] showed that the deep sea spheres in general are nearly CI for lithophiles but depleted in siderophiles and alkalies. These depletions have been attributed to physical segregation effects and to volatilization, respectively. We have made some exploratory analyses of 9 deep sea spheres (kindly supplied by D. Brownlee) using synchrotron x-ray fluorescence (SXRF) [e.g., 2] in an attempt to define chemical fractionation effects in minor and trace elements due to atmospheric heating.

All of the particles studied exhibited barred olivine (Fo70-86) textures. One particle was mounted whole on double-stick tape while the remaining eight were mounted with epoxy on ultrapure silica slides and polished with diamond paste to expose the interiors for analysis. Each sphere was excited with continuum synchrotron radiation (beamline X26C at the National Synchrotron Light Source, Brookhaven National Laboratory, NY) filtered by 275 micrometers of Al and collimated to a 40 micrometer spot with Ta slits. SXRF spectra were obtained in air with a Si(Li) detector equipped with a 170 micrometer Al filter to suppress the intense fluorescence from Fe. Acquisition times were typically 10 minutes. We will report the Fe, Ni, Cu, and Zn contents of the nine spheres. Elements with lower atomic number were eliminated by filters; the sensitivity for higher atomic number elements was reduced by intense scattered background from the silica substrate. These elements represent a range of volatility and chemical character (siderophile to chalcophile). Sampling depths were between 20 and 50 micrometers.

Three element plots, Cu/Fe vs. Ni/Fe and Zn/Fe vs. Ni/Fe, reveal the presence of two compositional clusters. One cluster with 6 members falls on an apparent tie line between the compositions of CI or CM meteorites and the origin. The second cluster with 3 members lies close to the compositions of ordinary chondrites (OC) and also possesses a linear character but a positive Ni/Fe intercept. These data are consistent with the conclusion from previous EDX studies [3,4] that most deep sea spheres derive from CI/CM meteoroids but also provide evidence for the existence of a small group of OC fragments in the collection. The spheres nearest to the origin in these plots, i.e., those with the lowest Cu, Ni and Zn contents relative to Fe, show the greatest depletions relative to CI. The implication is that these trends result from greater degrees of Cu, Ni and Zn loss relative to Fe. The similarity in slope for the CI/CM and OC trends implies coupled loss of Ni, Cu and Zn during entry heating. More analyses are needed, particularly on high Ni particles, to sharpen the definition of these apparent trends.

REFERENCES: [1] D. E. Brownlee, B. Bates and R. H. Beauchamp (1983) in *Chondrules and their Origins*, ed. E. King, p. 10-25; [2] S. R. Sutton and G. J. Flynn (1988) *Proc. Lunar Planet. Sci. Conf. 18th*, p. 607-614; [3] I. M. Steele, J. V. Smith and D. E. Brownlee (1985) Nature 313, p. 297-299; [4] M. B. Blanchard et al. (1980) Earth Planet. Sci. Lett. 46, p. 178-190.

LIGHT AND MAJOR ELEMENTAL ANALYSIS OF INTERPLANETARY DUST PARTICLES: AN UPDATE ON 26 IDP'S

K.L. Thomas (Lockheed-EMSCO, Houston, Tx 77058), W. Klöck (NASA, Johnson Space Center, Houston, Tx 77058), G.E. Blanford (U. Houston-Clear Lake, Houston, Tx, 77058), and D.S. McKay (NASA Johnson Space Center, Houston, Tx 77058)

We analyzed ten stratospheric dust particles for major and minor elements including carbon and oxygen. These particles were chosen due to their identification in the catalog (1) as chondritic. In combination with 7 previously analyzed interplanetary dust particles (IDP's) (2), we report here the bulk compositions of all 17 particles. During transfer to substrates and subsequent washing, 5 particles broke apart into 14 subparticles of acceptable size for analysis. Therefore our results include the analyses for a total of 26 particles including these subparticles. Technique is described in (2).

These particles are generally chondritic in composition with the exception of carbon which is significantly higher in the dust particles (2,3). It has been argued that our high carbon concentrations do not reflect the true bulk composition of the particles because most of the detected carbon x-rays come from the outer few hundred Angstroms of the particle being analyzed and therefore may only represent a carbon-rich surface coating on a chondritic core, a model similar to (4). However, results from the 5 particles which broke apart into subparticles suggest that we are really determining a bulk carbon content. These particles broke apart during rinsing so it is highly unlikely that only the original surface remained exposed. Particles W701316 and U2015D22 split into 3 subparticles each. In both cases, two of the three subparticles contain approximately 12% carbon and the third subparticle contains approximately 6%. In both cases the subparticle with the lower carbon is dominated by a large grain (olivine in the first case and iron-rich sphere in the other, respectively.). Particle U2015E3 broke into 3 subparticles each containing roughly 8% carbon. Particle W7029*A28 broke into 2 subparticles containing 10% and 16% carbon. The particle with 10% C is rich in Fe,S. Particle W7013B17 broke into 3 subparticles containing 6% C in two and 12% C in the third subparticle. It is clear from these that the carbon is fairly evenly distributed in the analyzed IDP's. That is, random interior sections of the original particle always show significant carbon abundances, and where lower carbon is found, it can usually be explained by the presence of a particularly big mineral grain. Furthermore, detailed work on carbon on a split of one of our particles (W7029*A) has previously shown that the carbon is distributed throughout the particle as small clumps consisting of sheets, granules, and fibers of poorly graphitized carbon (5). A simple model in which the carbon is all found on a mantle covering the silicate grains is not supported by these data.

Histograms of the Fe/(Fe+Mg) atomic ratios of these particles are a valid method of comparing IDP's to other extraterresterial material, in particular, with comet Halley dust (6). Our Fe/(Fe+Mg) ratios for 26 particles range from 0.2-0.6 with a mean at 0.4. One particle very rich in Fe is at 0.8. Of these 26 particles, 4 have been thin-sectioned. Three of the 4 thin-sectioned particles primarily contain anhydrous grains, with the Fe/(Fe+Mg) ratios in the range 0.3-0.36 for the bulk (~20 micrometer) grains. The spread of these ratios for all particles will depend on the presence and amount of iron sulfides, but in the anhydrous particles there is not a wide spread and no concentration of ratios near 0 or 1 for the bulk particles, although smaller volumes and individual minerals within the bulk grain may show ratios which spread throughout the entire range. The fourth thin-sectioned particle is primarily layer-lattice silicates, probably hydrous, and the Fe/(Fe+Mg) ratio is for this particle 0.5. These ratios are unlike those for Halley dust (7) which have a maximum at <0.1 and centers at 0.2 and 0.5. More data from thin-sectioned particles will be necessary before this ratio can be used to define hydrated vs. anhydrous IDP's.

References: (1) E.g.: M.E. Zolensky, R.A. Barrett, D.S. McKay, K.L. Thomas, J.L. Warren, and L.A. Watts, *Cosmic Dust Catalog, NASA, Johnson Space Center, Pub. No.77, 9, 1* (1987). (2) G.E. Blanford, K.L. Thomas, and D.S. McKay, *LPSC XIX*, 102-103 (1988). (3) W. Klöck, K. Thomas, and D.S.McKay (this volume). (4) J. Kissel and F.R. Krueger, *Nature, 326*, 755-760 (1987). (5) F.J.M. Rietmeijer and I.D.R. Mackinnon, *Nature, 315*, 733-736 (1985). (6) D.E. Brownlee, M.M. Wheelock, S.Temple, J.P. Bradley, and J. Kissel, *LPSC XVIII*, 133-134 (1987). (7) E.K. Jessberger, A. Christoforidis, and J. Kissel, *Nature, 332*, 691-695 (1988).

COMPARISON OF VOLATILES RELEASED FROM CARBONACEOUS CHONDRITES AND IDPs WITH THE HALLEY COMETARY VOLATILES. C.P. Hartmetz[1], G.E. Blanford[2] and E.K. Gibson, Jr.[1]. [1]SN2, Planetary Sciences Branch, NASA Johnson Space Center, Houston, TX 77058. [2]University of Houston Clear Lake, Houston, TX 77058.

The composition of the volatiles associated with cometary objects has recently been measured by instruments aboard the Vega-1 spacecraft during the encounter with Halley comet (1). The study of volatile contents in primitive extraterrestrial materials is important to the understanding of the origin and subsequent evolutionary histories of the organogenic elements (H, C, N, O, S, and P). Equally important is the comparisons of the volatile compositions of interplanetary dust particles (IDPs) and carbonaceous chondrites with the dust analyzed by the comet flyby missions. We are carrying out direct analysis of volatiles associated with IDPs and individual fragments of carbonaceous chondrites and comparing the abundances and distributions of these with information from the Halley encounter. If chondritic IDPs are in fact cometary dust particles, many types of analyses can be performed on samples that can be collected relatively easy.

A laser microprobe-quadrupole mass spectrometer system has been used to extract volatiles from IDPs and the Orgueil CI, Murchison CM, and Allende CV carbonaceous chondrites. The individual particles have been "zapped" with a Q-switched, Nd-glass laser (energy input of 0.1 to 1 Joule) to extract the volatiles from the samples. The released volatiles are fed directly into a benchtop quadrupole mass spectrometer and detected by an electron multiplier. Spectral information has been obtained from individual 1 mm grains of Orgueil CI meteorite (mounted on Torr Seal®) along with bulk samples (approximately 1 cm^2 in cross-section) of the Murchison CM (2) and Allende CV (2) meteorites. Three IDPs [W7013B13 (3), W7013C16, and 4 fragments of W7013B17 (3)] have also been analyzed for their volatiles.

The major volatiles released from the carbonaceous chondrites include (m/z): C (12), N (14), O (16), H_2O (18), CN (26), CO with minor N_2 (28), O_2 (32), H_2S (34), hydrocarbons (39 and 41), CO_2 (44), COS (60), CS_2 (76), and C_6H_6 (78). Allende contained less H_2O than Murchison and Orgueil, and as expected the CI Orgueil released a factor of approximately 1.5 and 4.0 more volatiles than the CM Murchison and CV Allende meteorites, respectively. The volatiles released from the IDPs varied quite widely in composition and abundance.

The W7013B17 particles released CH (13), N (14), O (16), m/z=20, O_2 (32), H_2S (34), HCl (36), hydrocarbons (23, 51, and 77) mass 61 and 74 possibly related to C_2H_5S or $C_2H_5O_2$ and C_3H_6S or $C_3H_6O_2$, respectively, and Silicon oil (132). The W7013B13 IDP particle released similar volatiles, however, W7013B13 released an order of magnitude more N than W7013B17 and its spectra also contained NH_3 (17), hydrocarbons (27, 39, 41, 49, 51, 55, 56, 62, and 67), COS (60), and CS_2 (78). From the recent data of Blanford *et al.* (4) it is clear that the abundances of carbon vary widely for IDPs. Their data showed that for several "chondritic" IDPs the carbon abundances varied between 2 and greater than 40 percent. Jessberger *et al.* (1) have shown that the mean composition of five groups of dust particles identified by cluster analysis of the data from 40 "short" spectra from PUMA-1 aboard the VEGA spacecraft range from 2.7 to 65 atom percent carbon and the hydrogen abundances range from between 2.6 and 94.1 atom percent for the five compositional groups.

The spectral information obtained from the analysis of volatiles within IDPs suggests that their compositions are related to those reported by Kissel and Krueger (5) for cometary dust analyzed during the Halley encounter. From the available information on the analysis of IDPs in the laboratory and the cometary encounter analysis it is clear that the compositions and abundances of organogenic elements and their simple compounds vary over a wide range. Analysis of additional IDPs in the laboratory should further assist with the characterization of the CHON compositions associated with both cometary and meteoritic materials.

1) Jessberger, E.K. et al. (1988) Nature, 332, p.691. 2) Blanford, G.E. and E.K. Gibson Jr. (1988) LPS XIX, p.98. 3) Blanford, G.E. and E.K. Gibson Jr. (1988) LPS XIX, p.100. 4) Blanford, G.E. et al. (1988) LPS XIX , p.102. 5) Kissel, J. and F.R. Krueger (1987) Nature, 326, p.755.

COSMIC DUST PARTICLE DENSITIES INFERRED FROM SXRF ELEMENTAL MEASUREMENTS. Flynn, G. J.[1] and Sutton, S. R.[2]. 1) Dept. of Physics, SUNY-Plattsburgh, Plattsburgh, NY 12901, 2) Dept. of Applied Science, Brookhaven National Laboratory, Upton, NY 11973.

Particle density is important in calculating the time scale for orbital evolution (or solar flare track density) and the peak temperature reached on atmospheric entry. Both track density (1) and peak temperature (2) have been used to distinguish between asteroidal and cometary sources of stratospheric cosmic dust. Fraundorf et.al. (3) measured the mass and volume of 7 small (all but one $\leq$ 11 μm) chondritic particles. They reported densities from 0.7 to 2.2 gm/cm^3. Sandford (1) and Flynn (2) used this density range in modeling orbital evolution and atmospheric entry for 10 to 20 μm particles. Much lower densities (~0.1 gm/cm^3) are inferred from radar meteor deceleration (4). Mackinnon et.al. (5) also report cosmic dust porosities suggesting low densities. Such densities would significantly alter the time scales calculated by Sandford (1) and peak temperatures by Flynn (2).

We measured elemental abundances in 3 large chondritic cosmic dust particles by Synchrotron X-Ray Fluoresence (6), and obtained the absolute mass of iron in each particle. Densities were then computed using the % Fe estimated from JSC EDS spectra and volumes determined from SEM photos. U2022G1 and W7029*A27 have Fe/Si peak heights in the JSC spectra consistent with CI (ie, 18% Fe), while U2015G1 has Fe/Si = 0.5 CI (see 6). Two particle dimensions were measured from the JSC photograph. The third (thickness) was estimated from apparent particle depth in the JSC photo. Optical observations during particle transfer for SXRF showed all three particles are roughly equidimensional, consistent with estimated thicknesses. Volumes assume the particles are rectangular boxes (except W7029*A27 whose cross-section in the JSC photo is triangular).

Particle densities range from 0.7 to 1.6 gm/cm^3, consistent with the smaller particles (3). Using optical volumes and SXRF Ni masses, we inferred densities of 2.0 and 3.8 gm/cm^3 for two standard glass fragments of known density (2.2 gm/cm^3). Our major uncertainty is in the thickness. However a density of 0.1 gm/cm^3 would require the particles to be from 7 to 16 times as thick as we estimated, inconsistent with optical shape observations. Low density particles (~0.1 gm/cm^3), if they exist in interplanetary space, are rare or do not survive atmospheric entry/collection in the 5 to 50 μm diameter size range.

REFERENCES: 1) Sandford, S.A. (1986) Icarus, 68, 377-394. 2) Flynn, G.J. "Atmospheric Entry Heating..." (submitted to Icarus). 3) Fraundorf, P. et.al. (1982) LPSC XIII, 225-226. 4) Verniani, F. (1966) J. Geophys. Res., 71, 2749-2761. 5) Mackinnon, I.D.R. et.al. (1987) Meteoritics, 22, 450-451. 6) Sutton, S.R. and Flynn, G.J. (1988) Proc. Lunar Planet. Sci. Conf. 18th, 607-614.

TABLE I: PARTICLE DENSITIES FROM SXRF Fe MASS DETERMINATIONS

Particle	Fe Mass	% Fe	Total Mass	Size (μm)	Vol.(cc)	Density
U2022G1	1090 pg	18	6.0 ng	30x20x15	9.0×10^{-9}	0.7 g/cc
W7029*A27	300 pg	18	1.8 ng	15x15x10	1.1×10^{-9}	1.6 g/cc
U2015G1	780 pg	9	8.7 ng	25x20x15	7.5×10^{-9}	1.2 g/cc

LARGE CHON PARTICLES IN THE STRATOSPHERIC DUST COLLECTION?

R. M. Walker and E. Zinner, *McDonnell Center for the Space Sciences, Physics Department, Washington University, St. Louis, MO 63130.*

The Comet Halley PIA-PUMA dust analyzer experiments (1,2) showed that many cometary particles ~ 1000Å in size consist primarily of H, C, N, and O (CHON particles). Regions rich in low Z elements have also been found in interplanetary dust particles (IDPs) that have overall chondritic compositions (3,4). We report here hydrogen isotopic measurements of several large ($\geq$ 10 μm) low-Z particles found in the stratospheric dust collection. The objective was to see if these predominantly low-Z particles could be identified as interplanetary dust by virture of their hydrogen isotopic compositions. Because the basic EDS characterization does not include measurements of elements with $Z \leq 11$, the low-Z nature of the particles was inferred by the presence of low energy bremsstrahlung radiation. Measurements were made on samples W7027H17 and W7027C3, selected from the JSC catalogs, and on U214M3-5, a particle found by us on a collection flag allocated to our laboratory. W7027H17 has a fine-grained, aggregate structure reminiscent of the chondritic porous aggregate morphology of particles that are known to be extraterrestrial (5). In addition to bremsstrahlung the EDS spectrum also shows minor peaks at Al, Si, and S, and it was characterized as TCA? Particle W7027C3, which was classified simply as ?, also has an aggregate structure but exhibits only a low energy bremsstrahlung spectrum with no elemental peaks. Particle U214M3-5, which was more compact, has a relatively large Si peak accompanied by small Al, Ca, and Fe peaks. None of the particles has a δD that was significantly different than terrestrial values within the precision of the measurements (~ ± 100 ‰). About 50% of chondritic IDPs, which are known to be extraterrestrial from other measurements (such as the presence of solar flare tracks), have normal hydrogen isotopic compositions. Thus, our results neither prove nor disprove the existence of CHON type IDPs in the stratospheric dust collection. We report the measurements here simply to inform other investigators of these negative results, and to emphasize the necessity of <u>proving</u> the extraterrestrial nature of unusual particles in the stratospheric collection before drawing conclusions as to the nature of interplanetary dust.

(1) Kissel J. *et al.*, 1986a. *Nature* **321**, 280.
(2) Kissel J. *et al.*, 1986b. *Nature* **321**, 336.
(3) Walker R. M., 1987. In *Infrared Observations of Comets Halley & Wilson and Properties of the Grains*, in press.
(4) Blandford G. E. *et al.*, 1988. *LPS XIX*, 102.
(5) Bradley J. P. *et al.*, 1988. In *Meteorites and the Early Solar System*, in press.

KAMACITE IN ORDINARY CHONDRITES. Alan E. Rubin, Institute of Geophysics and Planetary Physics, University of California, Los Angeles, CA 90024, USA.

The H, L and LL chondrites form a sequence of decreasing siderophile abundances and increasing degree of oxidation. The proportion of oxidized Fe increases at the expense of metallic Fe. Because Fe oxidizes more readily than Ni or Co, bulk metal becomes increasingly rich in Ni and Co. Equilibrated LL chondrites are thus characterized by high FeO/(FeO+MgO) ratios in olivine and low-Ca pyroxene, low abundances of metal, high taenite/kamacite ratios and Co-rich kamacite.

I analyzed kamacite by electron microprobe in 36 ordinary chondrites to search for systematic changes in composition and to better characterize extremely Co-rich, Ni-poor metal in highly oxidized LL chondrites. Ten of the chondrites contain aberrant kamacite grains with Co concentrations significantly different from the mean. These chondrites must be fragmental breccias that incorporated xenolithic grains during brecciation events subsequent to peak metamorphism.

Through the H-L-LL sequence, kamacite becomes systematically richer in Co and poorer in Ni [cf., 1,2]; H: 4.5-5.1 mg/g Co, 65-73 mg/g Ni; L: 6.7-9.1 mg/g Co, 53-64 mg/g Ni; LL: 15.8-370 mg/g Co, 12-53 mg/g Ni. Co is readily accommodated into the kamacite crystal structure, but the reason for the decrease in kamacite Ni is not clear; it appears that Co replaces Ni.

H3 and L3 kamacite has less Ni than H4-6 and L4-6 kamacite; L3 and LL3 kamacite has less Co than L4-6 and LL4-6 kamacite. The lower Ni and Co contents of kamacite in type-3 chondrites may be due to the presence of a relict nebular metal component with correlated Ni and Co concentrations.

Appley Bridge, LL6 (Fa 31.4), Jelica, LL6 (Fa 32.4), Manbhoom, LL6 (Fa 31.3), Parambu, LL5 (Fa 32.0) and Ngawi, LL3, all contain numerous tiny (≤1-10 μm) grains of high-Co, low-Ni metal (200-370 mg/g Co; 12-16 mg/g Ni). A large (40-μm-size) Co-rich grain was previously found in a clast in Ngawi [2]. In virtually every case, the Co-rich metal grains occur at the boundaries between sulfide and Ni-rich metal, i.e., troilite-tetrataenite boundaries in most of these meteorites, and troilite-awaruite and pentlandite-awaruite boundaries in Parambu.

Equilibration of the highly oxidized LL chondrites above 600°C would yield taenite as the sole metal phase. After post-metamorphic cooling to low temperatures (≤325°C), Ni partitioned into tetrataenite and awaruite. Because the crystal structures of these Ni-rich metal grains apparently could not accommodate >22 mg/g Co, an additional low-Ni, high-Co phase nucleated at metal-sulfide interfaces. It is not known if this phase has the body-centered-cubic crystal structure of kamacite; it may be ordered [2].

References: [1] Sears D.W. and Axon H.J. (1976) Nature **260**, 34-35; [2] Afiattalab F. and Wasson J.T. (1980) Geochim. Cosmochim. Acta **44**, 431-446.

"EXOTIC" INCLUSIONS IN THE STUDY BUTTE H3-CHONDRITE.

Frank Wlotzka, Max-Planck-Institut für Chemie, Abt.Kosmochemie, Mainz FRG, and Kurt Fredriksson, Department of Mineral Sciences, National Museum of Natural History, Smithsonian Institution, Washington, D.C. 20560.

Study Butte is a complex accretionary breccia consisting of chondrules, matrix, and crystal and lithic fragments (1). In addition it contains inclusions, which are here called "exotic", because they show little relation to the other components. There are two types:

1. Al-rich inclusions. They consist of a fine-grained intergrowth of Al-rich silicates (often close to sodalite) and spinel, usually surrounded by a clear diopside rim. One of the inclusions contains melilite (Ak 4 to 15) and in addition to spinel small grains of perovskite. The inclusions have diameters between 50 and 200 microns and resemble the CAI's of carbonaceous chondrites.

2. Magnetite inclusions. Magnetite occurs as single, sometimes euhedral grains in the matrix, but also in complex intergrowths with other phases, i.e. metal (kamacite and taenite), sulfide, cohenite and graphite. The grain size is 10 to 100 microns. Often metal forms the core and magnetite the outer part of an inclusion, suggesting formation of the magnetite by oxidation.

Magnetite and graphite are also found as magnetite-graphite aggregates in some unequilibrated ordinary chondrites, but on a much finer, submicron scale (2). However, coarse-grained magnetite-carbide assemblages were observed by Taylor et al. (3) in "two of the least metamorphosed" LL-chondrites, Semarkona (type 3.0) and ALH 77278 (type 3.6). Study Butte is, in contrast, a breccia, which contains equilibrated components (H-type chondrules, lithic clasts of higher petrologic type, differentiated lithic fragments) and unequilibrated components (chondrules with low and variable Fe/Fe+Mg and clear igneous glass, and the described exotic inclusions).

All components were apparently assembled on the surface of a parent body, as Study Butte is gas-rich (4). Al-rich and magnetite-carbide inclusions are usually considered to be condensates from the solar nebula. This implies that these primary components were still available and were mixed with processed, equilibrated material from the parent body, when Study Butte formed. It is difficult to understand, however, how the primary material survived the multiple compaction, equilibration, break-up and reworking processes, which must have occurred. It seems likely that the "exotic" inclusions were also altered in this process.Or were they produced on the surface of the parent body ?

References:

(1) K.Fredriksson, R.S.Clarke, R.Pugh (1984) Meteoritics 19, 225.
(2) E.R.D.Scott, G.J.Taylor, A.E.Rubin, A.Okada, K.Keil (1981) Nature 291,544.
(3) G.J.Taylor, A.Okada, E.R.D.Scott, A.E.Rubin, G.R.Huss, K.Keil (1981) Lunar and Planetary Science XII, 1076.
(4) H.Weber (1987) Private communication.

L3.7 CHONDRITE FROM THE ALLENDE STREWN FIELD.
Roger H. Hewins, P.M. Radomsky, Geological Sciences, Rutgers U., New Brunswick, N.J. 08903; Lu Jie, F.A. Hasan, D.W. Sears, Chemistry, U. of Arkansas, Fayetteville, AR 72701; and E. Jarosewich, Mineral Sciences, National Museum of Natural History, Washington, D.C. 20560.

A group of meteorites collected in the Allende strewn field for Alan Langheinrich included an unequilibrated ordinary chondrite. A minority of its chondrules contain brown glass, and some contain clouded relict olivine or forsteritic grains as well as normal ferroan olivine. The range of olivine compositions is Fo99-63. A minority of the chondrule olivine grains show strong zoning in BSE, but this is relatively patchy rather than sharply concentric. Olivine grains can be classified as Ca-rich (0.2-0.6 wt% CaO) or Ca-poor (0-0.1 wt% CaO). The Ca-rich grains, which include the most magnesian olivine crystals, show marked depletion in Ca and enrichment in Fe towards the rims. The Ca-poor grains show minor Fe enrichment at rims or are homogeneous, and show little variation in Ca. These grains correspond to olivine types B and D of Miyamoto et al. (1986), which we interpret as partially and completely reequilibrated crystals. The question of whether the reequilibration is nebular or planetary is of major interest.

Thermoluminescence sensitivity data (Dhajala=1) are given below:

Mass (mg)	TL Sensitivity	Peak Position (°C)	Peak Width (°C)
150	.35 ± .10	171 ± 18	177 ± 13
150	.35 ± .14	178 ± 17	193 ± 12
20	.63 ± .20	135 ± 15	159 ± 11

The small sample is atypical, possibly being dominated by a silica-bearing chondrule. The petrologic type is 3.7/3.8.

Chemical analysis yielded the following composition:
SiO2 39.30, TiO2 0.15, Al2O3 2.37, Cr2O3 0.42, FeO 16.06, MnO 0.32, MgO 24.54, CaO 1.86, Na2O 0.87, K2O 0.10, P2O5 0.19, Fe 5.30, Ni 1.19, Co 0.06, FeS 5.81, H2O+ 0.67, H2O- 0.24, C 0.21, Total 99.66. This is an L chondrite, with FeO a little higher than average because of weathering.

Reference Miyamoto, M. et al. (1986), J. Geophys. Res. 91, 12804.

THE QUEST FOR METEORITES: PART ONE. TWO NEW METEORITES FROM DEFLATION SURFACES IN LEA COUNTY, NEW MEXICO

JOHN W. SCHUTT[1], MICHAEL E. ZOLENSKY[2], ROBERTA SCORE[3] AND GORDON L. WELLS[4], [1]Box 767, Ferndale, WA 98248, [2]SN2/NASA, Johnson Space Center, Houston, TX 77058, [3]Lockheed, 2400 NASA Road 1, Houston, TX 77058, [4]Lunar and Planetary Institute, 3303 NASA Road 1, Houston, TX 77058.

Deflation surfaces in Roosevelt Co., New Mexico, have been found to be prolific sources of meteorites [Huss and Wilson, 1973]. This area is characterized by (1) low rainfall, (2) low input of alluvial and colluvial material, (3) prevalent high winds, and (4) areas of local deflation. By extrapolating this mode of occurrence to other areas two of us (JWS and MEZ) found two new meteorites on interdunal deflation surfaces near Jal, Lea Co., New Mexico.

We made foot searches of deflation basins in active dune fields in Quaternary sand sheets. The deflation basin floors are slightly indurated aeolian sedimentary units. In the Jal region these basins generally do not exceed 300 m in length and 50 m in width. We discovered two new meteorites on deflation surfaces, in relative proximity, approximately 5 miles south of the Jal metropolitan area. These are tentatively named Jal(a) and Jal(b) ($32^{o}02'N$, $103^{o}09'W$ and $32^{o}02'N$, $103^{o}10'W$, respectively).

Jal(a) is a H5 chondrite found in two fragments which fit together (11 x 5 x 5 cm), to form a total mass of 489 grams. Thin black fusion crust covers approximately 60% of the otherwise highly weathered surface; a weathering rind extends 2 mm into the interior of the stone. Approximately one third of the stone appears to be missing. Olivines vary in composition from Fa_{18} to Fa_{19} (Fa_{19} avg); pyroxene varies from Fs_{15} to Fs_{21} (Fs_{16} avg). We observed some small grains of plagioclase (An_{41} avg). Chondrules in this stone are poorly defined, ranging from approximately 0.5 to 1 mm in diameter. Fragments of chondrules and lithic clasts are abundant.

Jal(b) is an LL3 chondrite which has a mass of 11 grams (3.0 x 1.3 x 2.0 cm). No fusion crust remains on this weathered specimen. The abundant chondrules contrast sharply with the highly oxidized matrix. These chondrules are dominantly porphyritic, and range in size from 0.5 to 2.5 mm. Olivines vary in composition from Fa_{1} to Fa_{47}; pyroxene varies from Fs_{2} to Fs_{4}. We observed interstitial glass in chondrules, with an average composition of An_{76}. Fragments of chondrules and lithic clasts are abundant. Oxidation staining and veining of this stone is severe.

Based upon our preliminary meteorite discovery rate, we suggest that coordinated searches of other deflation basins in the western U.S. (and elsewhere) will result in the recovery of many new meteorites. We are currently identifying additional promising areas for future expeditions.

Reference: Huss and Wilson, 1973, Meteoritics, 8, 287-290.

THE THERMOLUMINESCENCE PROPERTIES OF Mn-PLAGIOCLASE MIXTURES WITH IMPLICATIONS FOR METEORITES. Clark Chickering*, J. David Batchelor+, Derek W.G.Sears+ and R. Kyle Guimon*
+Cosmochemistry Group, Department of Chemistry and Biochemistry, Univ. Arkansas, Fayetteville, AR 72701. *Physical Science Department, Missouri Valley College, Marshall, MO 65340.

The thermoluminescence (TL) properties of meteorites have provided unique insights into several aspects of their history, most notably metamorphism and shock (1). Through a number of laboratory experiments and measurements on natural samples, it has been shown that TL sensitivity reflects the amounts of feldspar, and the peak shape (peak temperature and width) relate to the relative amounts of high and low feldspar (2). However, certain properties remain poorly understood; for example, TL sensitivity decreases strongly along the plagioclase series as Ca increases (3), and the peak temperature of the high form seems to vary in a poorly understood fashion (4). Important in our attempts to explain some of these properties are data of Geake et al. (5), who observed that plagioclase showed a 17-fold increase in blue/green cathodoluminescence (CL) when annealed with $MnSO_4$ for 30 minutes at 1050°C. Based on these data and arguments involving the ligand field of Mn in $CaSiO_3$ and feldspar, Geake et al. argued that Mn was the activator for CL in lunar and terrestrial plagioclase. CL and TL are closely related phenomena, and presumably this implies that Mn is an important activator for TL in meteoritic feldspar. We have therefore repeated the Geake et al. experiments, extending the annealing to much longer times, in an attempt to confirm their finding.

Samples of bytownite and mixtures of bytownite and $MnSO_4$ (2 wt.%) were annealed at 1050°C for 30 minutes and 50 hours and the induced TL measured. We found that after annealing for 30 minutes the TL sensitivity decreased by about 50%. The peak temperature also increased from 80 to 140°C. In contrast, after annealing for 50 hours we did find a significant increase in TL sensitivity, but the increase was shown by both the bytownite and the bytownite-$MnSO_4$ mixture and is clearly associated with the thermal treatment and not any doping effect on the part of the Mn; in fact, the mixture showed a much smaller increase than the pure bytownite. We also observed very large increases in peak temperature similar to those previously reported by Hartmetz and Sears (4). These data have several implications for CL and TL studies of meteorites. For instance, thermal treatments in a closed system can cause increases in TL sensitivity, as well as peak shape changes, in certain cases, without the need to invoke chemical changes. Also, the often-reported association between Mn and feldspar CL may not be causative.

(1) Sears and Hasan (1986) LPI Tech. Rpt. 86-1, 100. (2) Guimon et al. (1985) GCA 49, 1515. (3) Hasan et al. (1986) J. Lumin. 34, 327. (4) Hartmetz and Sears (1987) LPS XVIII, 395. (5) Geake et al. (1971) Proc. 2nd Lun. Sci. Conf. 2265. (Support: NASA NAG 9-81).

THERMOLUMINESCENCE IN CHONDRITIC MINERAL SEPARATES - A PRELIMINARY REPORT. J.David Batchelor, and Derek W.G. Sears, Cosmochemistry Group, Department of Chemistry and Biochemistry, University of Arkansas, Fayetteville, AR 72701.

It has been shown that plagioclase feldspar is the predominant thermoluminescence (TL) phosphor in chondritic meteorites. Van Schmus and Wood (1967) recognized the presence of secondary feldspar in chondrites of type 4 and higher, and specified the presence of well developed plagioclase as a defining characteristic of type 6. Van Schmus and Ribbe (1968) found plagioclases ranging from An 8 to An 16 in type 6 chondrites. Their X-ray diffraction studies showed a moderately high degree of disorder with [20(131)-20(131)] about 1.75 and with little spread. They saw no evidence for crystallographically distinct K-feldspar. Lalou et al. (1970) examined mineral separates from Saint Séverin (LL6), and found that about three-fourths of the TL signal (71% for the induced TL and 78% for the natural TL) was due to plagioclases, with about 10% from Merrillite/Whitlockite. They reported that 8% of the induced TL and 3% of the natural TL was in the olivine fraction. McDougall (1968) reported only a very weak TL signal from olivine at temperatures above 425°C. Pasternak (1978) reported that the TL peak temperature (Tmax) of albite increased with thermally induced Al/Si disorder, and Guimon et al. (1984) showed that annealing of a type 3.5 ordinary chondrite caused the peak to broaden and move to a higher Tmax.

We are attempting to demonstrate a correlation between Tmax and degree of ordering of feldspar in ordinary chondrites. We have performed mineral separations by heavy liquids on Bruderheim (L6), Dhajala (H3.8), and ALHA 77214,55 (L3.4). Each sample was ground, and the magnetic fraction separated. Density separation was by float/sink in heavy liquids. Each split was acetone washed, and its natural and induced TL measured. Each fraction was then further ground, and X-ray diffraction patterns obtained.

The bulk material showed TL levels of 1.4 for Bruderheim and 0.069 for ALHA 77214 (Dhajala = 1), consistent with their petrologic types. Peak temperatures were at 198°C for Bruderheim, 160°C for Dhajala, and 128°C for ALHA 77214, as expected for their petrologic types. The first separation was done in CH_2I_2 with a measured density of 3.30g/cc. Each meteorite showed 12 to 20% light material. ALHA 77214 and Dhajala both showed a 3-fold enhancement in the TL of the light fraction, but Bruderheim showed an 11-fold enhancement, consistent with feldspar being the major phosphor and its larger feldspar crystal size. X-ray diffraction showed the presence of olivine and pyroxene in all fractions, but only the 040 line for oligoclase. Further separations will be done at densities of 2.6 and 3.0 g/cc to extract the plagioclase component.

This research is supported by NASA grant NAG 9-81.

GUIMON R.K. et al. (1984) Nature 311, 363-365.
PASTERNAK E.S. (1978) Dissertation, Univ. of Pennsylvania.
LALOU C. (1970) C. R. Acad. Sc. Paris 270, Série B 1706-1708.
VAN SCHMUS W.R. and RIBBE P.H. (1968) GCA 32, 1327-1342.
VAN SCHMUS W.R. and WOOD J.A. (1966) GCA 31, 747-765.

Alteration History of Type 3 Ordinary Chondrites.

Andrew D. Morse*, Derek W. G. Searst, Robert Hutchison+, R. Kyle Guimont, Conel O. Alexander*, Ian P. Wright*, and C. T. Pillinger*.
*Planetary Sciences Unit, Open University, Milton Keynes MK7 6AA. U.K. ; †Cosmochemistry Group, University of Arkansas, Fayetteville, AR 72701, U.S.A.; +British Museum (Natural History), London, SW7 5BD, U.K.

Metamorphism has obscured the nebula record of most of the type 3 ordinary chondrites, however a few of the type 3 ordinary chondrites show little metamorphism (1). Thermoluminescence (TL) has been used to define a scale of metamorphism for the type 3 ordinary chondrites ranging from 3.0, least metamorphosed to 3.9, most metamorphosed (2). Semarkona (type 3.0) and Bishunpur (type 3.1) show the least degree of metamorphism. Semarkona has many other unusual properties as determined by thermoluminescence, cathodoluminescence (CL) (3) and isotopes (4). These unusual properties could reflect nebula processes, not obscurred by metamorphism, or have been later imparted by other secondary processes.

Aqueous alteration has been observed by petrographic analysis in Semarkona and to a lesser extent in Bishunpur (5). This could explain the unusual properties of these two meteorites. Many of these properties are associated with chondrules and these two meteorites are heteregenous, so to explore the relationship between these properties a combined study was performed of three different techniques on individual chondrules ; thermoluminescence, petrology and mass spectrometry.

Chondrules and matrix samples were hand picked under a low powered binocular microscope from Semarkona, Bishunpur and as a link with other type 3 ordinary chondrites Chainpur (type 3.4). Each sample was split into three fragments, one fragment each for TL, petrology and isotope analysis. Fragments used for TL have been retained as reserve material for othe studies.

Mass spectrometry was used to determine the water content and the D/H ratios of the water released by stepped pyrolysis at 200°C and 1100°C. The 200°C step was an attempt to remove terrestrial contamination. The water released from the pyrolysis was reduced to hydrogen by a zinc furnace at 320°C or uranium furnace at 620°C and the entered directly into the mass spectrometer to increase sensitivity. The amount of water released by each chondrule fragment was ~1μg for each step (< 1% by wt.). For the chondrules the water released during the low temperature step had δD ranging from -600‰ to +3200‰ and the water released during the high temperature step had δD ranging from 0‰ to + 7800‰. The matrix fragments released a greater amount of water for both steps 2-4 wt%. The δD values for the matrix samples were around terrestrial values for the low temperature step and ranged from +1000‰ to +3000‰ for the high temperature step.

There is a suggestion of a relationship between TL and δD measurements. Chondrules with δD < +3800‰ tended to have a lower TL sensitivity than those with δD > +3800‰. Petrographic studies indicate the chondrules with low TL sensitivity and low δD values may be contaminated by matrix fragments attached which would reduce the D/H ratios.

Due to the small sample size and instrument technique used there were large errors in determining the δD values and water content of the samples. Recently a new inlet system has been built for the mass spectrometer. The water released from pyrolysis is converted to hydrogen in a zinc capillary furnace and then injected into the mass spectrometer by helium using a capillary flow technique. Using this technique it is hoped that more accurate measurements can be obtained using the posterity samples of particularly interesting chondrules where necessary. We intend to use the petrographic description to allow similar chondrules be grouped to obtain a larger sample size.

1. Dodd *et al.* (1967) GCA 31, 921 - 951
2. Sears *et al.* (1980) Nature 287, 791 - 795
3. DeHart *et al.* (1986) LPS XVII, 160 - 161
4. McNaughton *et al.* (1983) Proc 13LPSC, A297 - A302
5. Hutchison*et al.* (1987) GCA 51, 1875 - 1882
6. Morse*et al.* (1987) 50th Meteor. Soc. Mtg.
7. Sears *et al.* (1988) LPSC

SEARCH FOR LOCALIZED REGIONS OF ISOTOPICALLY ANOMALOUS H IN SEVERAL TYPE 3 CHONDRITES

R. M. Walker and E. Zinner, *McDonnell Center for the Space Sciences, Physics Department, Washington University, St. Louis, MO 63130.*

It has been demonstrated that D-enrichments in at least some interplanetary dust particles are due to the presence of localized "hot spots" of highly anomalous material (1). We report here the results of a search for similar anomalous regions in fragments of Semarkona (Sm), Clovis (Cl), and Mezö-Madaras (MM), all of which are petrologic type three chondrites. Approximately 30 fragments ~ 10 to 50 μm in size from each meteorite were pressed into sputter-cleaned Au foils and analyzed by the ion probe techniques previously described. Measurements on terrestrial amphibole standards were used to correct for instrumental mass fractionation effects. In MM, 14 of 15 fragments gave normal compositions within measurement errors ($2\sigma \approx 60^0/_{00}$); one fragment with a $\delta D = -297$ was found. In contrast, 17 fragments of Cl all gave δD in the range from -190 to -300 ($\pm 50^0/_{00}$) relative to SMOW. Confirming previous results, almost all of the 36 fragments of Sm studied showed enrichments of D ranging up to $\delta D \geq +4100$. A notable exception was a C-rich particle (28A) ~ 18 μm in size, whose isotopic composition was normal. Although we cannot rule out contamination, 28A is probably an indigenous fragment of Sm. (similar C-rich fragments have been found by us in X-ray maps of polished sections of type three meteorites.) Ion images of four particles that had high δD values failed to show D-rich "hot spots" similar to those seen in the IDP, Butterfly. Previous pyrolysis work (2) indicated that the heaviest hydrogen in Sm is released above 450°C. In an attempt to remove terrestrial water contamination, which would dilute the isotopic effects, we heated the Sm mount for two hours at 448°C in an Ar atmosphere. Relative to Si (which was apparently retained), the samples lost ~ 50 to 80% of H, 50 to 90% of C, and 80 to 95% of N (measured as CN^- ions). With two exceptions, the δD values were systematically lower in the heated samples than in the unheated materials (see fig. 1). Although these results are consistent with the existence of a volatile, organic, D-rich carrier phase in Sm, the newest data set show no correlation between δD and C, as had been found by us in our earlier work (3). This fact, coupled with the absence of a D-enrichment in the C-rich fragment, 28A, thus leaves the nature of the D-rich material removed by heating in doubt. We further note that Cl, which exhibits systematic depletions in D, has about as much C relative to Si as Sm (MM in contrast, is relatively low in C). Images of three Sm particles after heating, again failed to show "hot spots" of D-rich material. Clearly, more work is needed to characterize the carriers of hydrogen anomalies in Sm and and other similar meteorites.

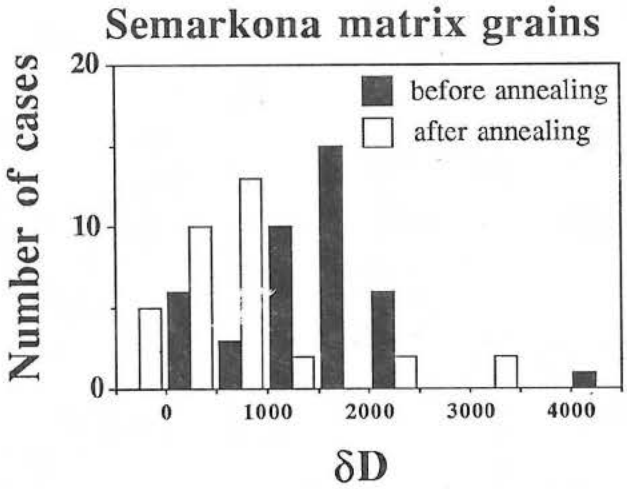

Fig. 1. δD measurements of the same fragments of Semarkona before and after heating to 450°C in an Ar atmosphere. Although there is a systematic reduction of D-enrichments, two particles had higher D values after heating than before.

(1) McKeegan K. D. *et al.*, 1987. *LPS XVIII*, 627. (2) McNaughton N. J. *et al.*, 1982. *Proc. 13th LPSC, JGR* **87**, A297. (3) McKeegan K. D. and E. Zinner, 1984. *LPS XV*, 534.

ELEMENTAL ABUNDANCES OF TEN E, O AND C CHONDRITES FALLS FORM CHINA

Zhong Honghai Jiang Lijin Yang Xiaohui Hu Guohui
(Chinese National Analytical Centre, Guangzhou)

Yi Weixi Wang Daode Ouyang Ziyuan Li Zhaohui
(Institute of Geochemistry, Academia Sinica)

We report data for 41 major and trace elements determined by FNAA and INAA in 10 E, O and C chondrites falls from China with an attempt to discuss and to classify in 10 chondrites. On the basis of characteristic of elemental abundances these chondrites are classified into E4(Qingzhen), H5(Zaoyang), H6(Nantong and Wuan), L4(Zhaodong), L6(Guangnan, Nanyangpao and Suizhou), LL6(Dongtai) and C3(Ningqiang).

E4 is characterized by high content of iron. From E4 through H5 to LL6 siderophile elements (as Fe, Co, Ni, Ru and Ir etc.) and sulphophile elements (as Au, Cu and Se etc.) decrease gradually, to C3 increase, while silicophile elements (as Si, Mg, Al, Ti, V and REE etc.) regular increase gradually. These meaning results show that these regularity variation have a connection with the aggregation temperature and the formation space of meteorites in Solar nebular disk. In other words a general decrease in the order of E--H--L--LL--C in the aggregation temperature at the time of formation, while the environment of formation of E group may be nearer Solar than H, L, LL and C groups.

The elemental fractionation (depletion) in all chondrites tends to increase with increasing elemental volatility and this trend is similar, indicating that the fractionation in all chondrites is controlled mainly by elemental volatility. The degrees of elemental abundances concentration in chondrites tend to increase gradually in the order of E4--O--C1--C3 chondrites, while loss of volatility elements (as Ga, Cs, Zn and Br etc.) in H5, H6, L4, L6 and LL6 chondrites may by more than E4 and C3 chondrites.

The degrees of metamorphism of all chondrites depend on the contents of Br and Se. The atomic ratios of Br/Se in E4, H5, H6, L4, L6, LL6 and C3 chondrites there are obvious difference, reflecting that the different degrees of thermal metamorphism. The abundances of mobil trace elements (as Co, Au, As, Cs, Sb, Se, Br and Zn etc.) in E4, H5, H6, L6, LL6 and C3 chondrites show that these chondrites all exhibit signs of low to mild impact metamorphism, reflecting impact-induced heating and thrmal metamorphism of chondrites.

The distribution characteristics of elemental abundances in E4, H5, H6, L4, L6, LL6 and C3 chondrites also show that chondrite of each chemical family has its own formation and evolution history, and chondrites of different chemical families may have originated from parent bodies of different compositions. Or, owing to the differentiation of thermal metamorphism, different kinds of meteorites may by derived from a common parent body.

FRACTIONATION IN CHONDRITES: MAJOR ELEMENTS REVISITED

J.W. Larimer Dept. of Geology and Center for Meteorite Studies Arizona State University Tempe AZ 85287

The elements Fe, Mg, Si and O account for 80 to 90% by mass of chondritic material. All are fractionated among the various groups of chondrites and O displays isotopic fractionations which may be related to the elemental fractionations. Recent data have been combined with previous high quality data in an attempt to establish new constraints, and obtain some fresh insights, on the nature of these fractionations.

In CI chondrites (within solar value uncertainties) Fe(±20%), Mg(±40%) and Si(±20%), as well as most other elements, occur in solar proportions which is generally accepted as evidence that planetary material evolved from this composition. Additional evidence is obtained from mixing diagrams where the fractionation trends intersect at, or point to, CI composition. It is possible to quantify the fractionation: the amounts of Fe, Mg and Si and all the more refractory elements in the materials that accreted to form the chondrites varied by more than a factor of two. The fractionation of the lithophile elements apparently involved a component that compositionally resembled amoeboid olivine inclusions, which contain all the refractory elements in more or less solar proportions diluted by variable amounts of olivine. Relative to CI material, ordinary and enstatite chondrites accreted only a fraction of their Mg and Si. Since these elements are commonly used for normalization, the implication is that all elements are more severely depleted in the accreted material than previously considered. This means, for example, that E-chondrites should not be regarded as being as rich in volatiles as C-chondrites, instead they are better described as being depleted in Si. In addition metal/silicate fractionation is more extensive than thought; we are currently in the midst of reviewing and re-evaluating the data on siderophile elements.

When the information drawn from the fractionation patterns is combined with other observations some general conclusions can be drawn. Individual chondrules from unequilibrated chondrites vary markedly in their proportions of Fe, Mg, Si and O as well as in their proportions of O isotopes yet when blended together in the meteorite the average elemental and isotopic composition falls within the narrow ranges displayed by their more nearly equilibrated counterparts. Moreover, in carbonaceous chondrites where there are not only variations in composition between chondrules but also in the proportions of chondrules to matrix, the Mg/Si ratio remains remarkably constant. This indicates that the chondrules and matrix in each group of chondrites evolved from a parental material whose composition was already fixed by prior fractionation. Chondrule formation must post-date the fractionation processes and cannot itself be a process that tends to remix the various batches of material from which each chondrite group evolved.

GROUP AND TYPE COMPOSITIONS OF ORDINARY CHONDRITES: EXCEPTING VOLATILES, NO RELATIONSHIP BETWEEN TYPE AND COMPOSITION

John T. Wasson, Gregory W. Kallemeyn and Alan E. Rubin,
Institute of Geophysics, University of California, Los Angeles, CA 90024, USA

We have determined 25 elements in replicate samples of 66 ordinary chondrites. Group compositions are in good general agreement with those determined in earlier studies. We observed some Mg-normalized abundance trends not previously defined: Na and K abundances are about 9% lower in H chondrites than in L and LL; LL Ga abundances are about 10% lower than in H and L. We confirm earlier reports that refractory-lithophile/Mg ratios are about 2% higher in H than in L or LL.

Considerable interest attaches to the question of compositional differences among petrographic types, since the common interpretation that types 4-6 reflect different degrees of metamorphic alteration of type-3 starting materials implies that, within each group, the different types should be isochemical except for highly volatile elements outgassed during metamorphism. With the exception of highly volatile Br, our data show no significant differences among petrographic types of L and LL chondrites. There is also no significant difference among H-group types 4-6. Our set of H-related type-3 chondrites included Dhajala and Sharps which show no significant compositional differences from H4-6 chondrites, and Bremervörde and Tieschitz, which have siderophile abundances intermediate between H and L levels. The kamacite Co content and O-isotope composition of Tieschitz show it to be more closely related to L than H, and the O-isotope composition of Bremervörde is also L-like. It seems probable that these latter meteorites are rare representatives of nebular materials intermediate in properties between H and L, and did not originate on either of these parent bodies. Our data also show that Albareto, Bjurböle, Cynthiana and Qidong have olivine and kamacite compositions and siderophile abundances between the upper L and lower LL limits.

Siderophile abundances in the L3 falls Hedjaz and Khohar and LL3 falls Bishunpur, Manych, Ngawi and Semarkona fall within the ranges defined by the type 4-6 members of the respective groups. We conclude that nebular accretion processes were the same for all types of each ordinary chondrite group. This is comforting, since even if mechanical processes late in nebular history led to a gradual fractionation in planetesimal compositions, asteroids appear to have formed somewhat later by the accretion of planetesimals and smaller asteroids. This process would have lead to the incorporation of such fractionated bodies at all levels in asteroid-size parent bodies. If degree of metamorphism was directly related to the radial depth within the asteroidal parent body, the early- and late-formed planetesimals should occur at all depths and show all degrees of metamorphism.

MULTIPLE SOURCES OF YOUNG H GROUP CHONDRITES: R.T. Dodd, Department of Earth and Space Sciences, SUNY at Stony Brook, N.Y. 11794. (1)

Systematic variation of fall time (year, day, and hour -- [Figure 1]), petrologic type, and radiogenic argon content with CRE age in the 2 to 7 m.y. range (2) suggests that the prominent 4.45 m.y. peak identified by previous workers (3) is complex and records either several closely-spaced meteoroid-forming events or continuous stripping of the H chondrite parent body in the recent past.

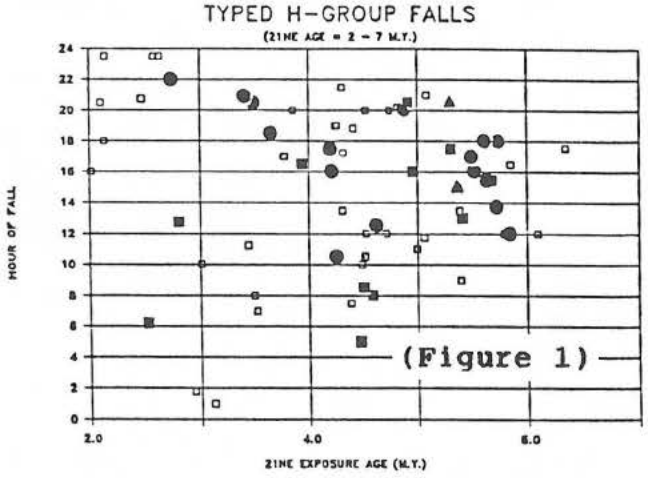

(Figure 1)

Evidence in support of this view of the age spectrum for young H chondrites is shown in Figure 2, which compares solar longitude and ecliptic latitude for H chondrites with ages within 1σ (3) of the peak, and in which the northern limit of fall recovery is shown as a solid line. With few exceptions, H4 and H6 chondrites in this age range (filled squares and circles) fall on different, well-constrained (R > 0.95) linear trends, indicating that the two types sample objects in different orbits. H5 chondrites (open squares) form a complex but different pattern.

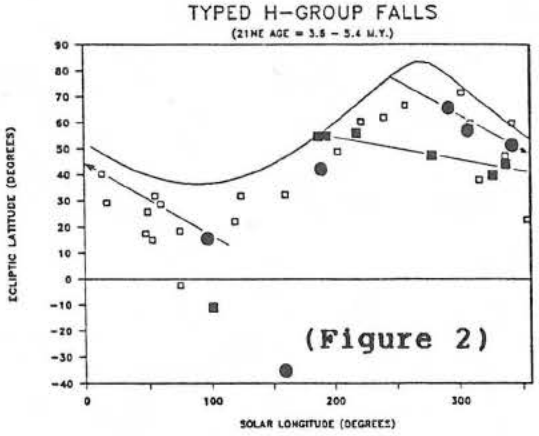

(Figure 2)

Similar patterns for other parts of the CRE age spectrum suggest: 1) that we can identify H chondrites that sample the same object and establish the orbital properties of that object; and 2) that H chondrite source objects are both numerous and less thoroughly mixed by petrologic type than heretofore supposed (3).

References:

1. Also American Museum of Natural History and National Museum of Natural History.
2. CRE ages for this study were calculated according to procedures outlined in (3).
3. Crabb, J. and Schultz, L. (1981) Geochim. et Cosmochim. Acta 45, p. 2151 to 2160.

DESCRIPTION OF THE PINE DAM, SOUTH AUSTRALIA METEORITE;
P.P. Sipiera, Meteorite Research Group, Harper College, Palatine, IL 60067, and Y. Kawachi, Dept. of Geology, Univ. of Otago, New Zealand.

A small weathered stone meteorite was found near Pine Dam, Myrtle Springs Station, north-west of Leigh Creek, South Australia, by a local aborginal. The location of find is noted at Lat. 30° 25' S , Long. 138° 00°E. The circumstances of find are somewhat vague, but the date of find is given as 30 March, 1976. The meteorite was acquired shortly thereafter by a local mineral dealer. The main mass now resides in the DuPont collection, Watchung, New Jersey.

The individual stone is a well-rounded, 200.4g (original weight) mass, which exhibits a rusty-red coloration indicative of a moderate to advanced weathering state. Minor amounts of remnant fusion crust are noted, with occasional metallic grains protruding from the surface. On a cut surface, a mottled appearance is apparent, with small amounts of metal clearly seen.

Mineralogically, microprobe analyses of the principal silicate phases give the following compositions: Olivine Fa 24.2, PMD=1.61 (N=10), pyroxene Fs 20.4, PMD=0.89 (N=10), and plagioclase Ab 85.1, (N=10). The accessory minerals noted are kamacite, taenite, troilite, and chromite. Petrographically, the numbers of whole chondrules are small, with partial chondrules and lithic fragments being more numerous. Metallic grains are common, but in relatively smaller numbers. On the basis of phase compositions and petrographic features, a classification of L 5 is assigned to the Pine Dam chondrite.

ENSTATITE CATHODOLUMINESCENCE: ASSIGNMENT OF EMMISSION PEAKS TO CR AND MN AND APPLICATION TO QUANTITATIVE ANALYSIS. Ian M. Steele, The Department of the Geophysical Sciences, The University of Chicago, 5734 S. Ellis Ave,, Chicago, IL, 60637.

Cathodoluminescence (CL) is a well known feature of enstatite from the enstatite chondrites and achondrites, but little attempt has been made to obtain quantitative interpretation of its intensity and textures. It has long been recognized that the 'redness' of the enstatite CL correlates with Mn content (e.g. 1) but the correlation between Mn and Cr and the presence of at least two CL emissions in the red as well as one in the blue complicates interpretation (2) but at the same time allows greater chemical information to potentially be derived from the CL spectra. To assign peaks to specific substituents in enstatite, I describe below CL spectra from synthetic enstatite and compare with CL of natural enstatite from the enstatite meteorites.

Typical spectra obtained using an optical multichannel analyzer (OMA) for enstatite from Cumberland Falls were shown in (3); spectra from the ALHA 77295 enstatite chondrite as well as synthetic Cr and Mn doped enstatite are shown below. This detector maintains good sensitivity up to 900nm allowing spectrum acquisition into the near infrared. Synthetic trivalent Cr-enstatite shows peak CL emission centered at 752nm while Mn-enstatite emission is centered at 664nm with wavelength values determined by extrapolation of a Ne calibration spectrum. For Cumberland Falls, CL peaks are at 658nm with a shoulder at 741nm (estimated) and for A-77295 shown below, red peak positions are 742 and 664nm. Shallowater, in which Cr and Mn are not detectable by electron probe (<30ppm), shows no CL peaks in these two regions.

The good correspondence for CL peak positions in synthetic Cr and Mn doped enstatites with peaks observed in natural enstatites strongly suggests that these peaks result from these elements; in addition, the linear correlation between peak intensity of the 660nm peak and Mn concentration in enstatite supports this assignment (3). Although the 740 and 660nm peaks have comparable intensities in some enstatites, the 740nm peak does not affect the visible CL. For near Fe-free enstatite, the CL intensities provide a sensitive measure of Mn content with detection levels below that of the electron probe; a similar linear relation qualitatively holds for Cr. With measurement times on the order of a second, Cr and Mn concentrations or spatial distributions can readily be determined.

ACKNOWLEDGEMENTS: NASA NAG 9-47 (J.V. Smith); NSF EAR 84-15791.

(1) Reid A.M. *et al.* , 1967. GCA, **31**, 661. (2) Steele, I.M. and J.V. Smith, 1987. Meteoritics, **22**, 507. (3) Steele, I.M., 1988. LPS XIX, 1121.

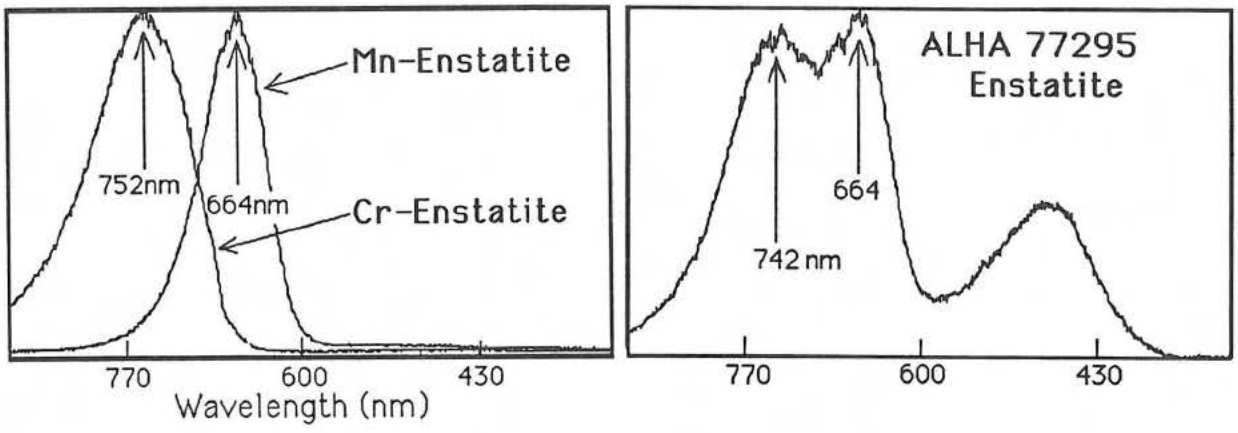

NONUNIFORM DISTRIBUTION OF Ir AND Au IN THE ALLENDE METEORITE REFERENCE SAMPLE. Randy L. Korotev, Dept. of Earth and Planetary Sciences, Washington University, St. Louis, MO 63130.

We have analyzed by instrumental neutron activation (INAA) twenty 50 mg subsamples from a single bottle of the Allende Meteorite Reference Sample (AMRS) [1] to test chemical uniformity. Other INAA labs have used the AMRS as a standard for Ir and Au because of the powdered meteorite contains high concentrations of the two elements compared to most other geochemical reference samples used in INAA. We have sought such a standard for our studies of lunar samples. An additional requirement is that subsamples in the 10-50 mg range have relatively constant concentrations of Ir and Au.

In each of 5 irradiations, 4 different samples (A,B,C,D) each were analyzed. During radioassay, sample A was counted 4 times alternated with the counts of the other samples (A1,B,A2,C,A3,D,A4). The total relative standard deviation (RSD, based on counts A1,B,C,D in the 5 experiments) was 7.2 % for Ir and 3.9% for Au (Table 1). This total RSD has 3 components, a "sample" component resulting from true differences in concentations among the samples, a "radioassay" component resulting from uncertainty in measurement of the analytical signal ("counting statistics", peak area measurement), and a "flux" component resulting from differences in neutron flux received by the samples (also includes some geometry effects during radioassay). An upper limit for the flux component is 0.6%, which is the total RSD observed for the elements Cr and Fe in the 20 samples (Cr and Fe are carried by major mineral phases and the radioassay RSD is small, 0.1-0.2%). The radioassay component for each element is the combined RSD of the 4 counts of sample A in the 5 experiments.

Table 1. Relative Standard Deviations (RSD, %) and Mean Concentrations.

	total		radioassay		flux		sample	conc.
Ni	0.81^2	=	0.37^2	+	0.6^2	+	0.4^2	1.415 %
Co	0.70^2	=	0.13^2	+	0.6^2	+	0.3^2	664 µg/g
Ir	7.2^2	=	0.52^2	+	0.6^2	+	7.1^2	777 ng/g
Au	3.9^2	=	1.11^2	+	0.6^2	+	3.7^2	145 ng/g

The sample component to the total RSD was calculated by difference using the formulas in Table 1. For Ir and Au, most of the observed scatter results from sampling. We conclude that distribution of Ir and Au in the AMRS is not sufficiently uniform for 50-mg subsamples of the powder to be good standards for these two elements.

REFERENCES

[1] Jarosewich E., Clark R.S. Jr., & Barrows J.N., eds. (1987) The Allende Meteorite Reference Sample, SCES no. 27, Smithsonian Inst. Press.

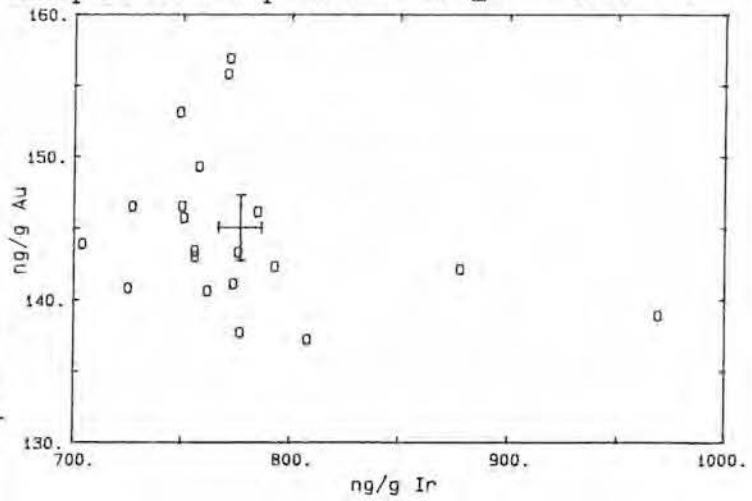

Fig. 1. There is no correlation between Ir and Au concentrations in the 20 subsamples. The error bars represent typical 1-σ uncertainties from analytical sources (flux + radioassay, see text).

HELIUM ISOTOPIC RATIOS IN NATIVE AND PROCESSED METALS;

A.O. Nier and D.J. Schlutter, School of Physics and Astronomy, University of Minnesota, Minneapolis, MN 55455

We have reported on mass spectrometrically-determined isotopic abundance ratios in helium and neon extracted from deep Pacific magnetic fines believed to be of extraterrestrial origin, and from individual stratospheric particles [1]. Samples studied are placed at the center of a square of tantalum foil, approximately 6 x 6 x 0.025 mm, which is folded to form a filament and heated by passing an electric current directly through it. Extraction temperatures of up to 1600^0 C. are employed. We have observed, as did Craig and co-workers [2], that the small amount of helium released when tantalum is heated has a $^3He/^4He$ ratio which may be hundreds of times greater than the atmospheric value, 1.39×10^{-6}, and in the range expected for extraterrestrial particles. Pre-heating of the tantalum to 1800^0 C. greatly reduced this source of contamination.

We have examined other processed metals such as nickel, iron, tungsten, Nichrome, and stainless steel, and in some cases observed similar enhancements. While some of the high ^3He observed could conceivably be due to contamination from the re-cycling of metals used in tritium diffusion experiments, this would not explain all of our results, since some of our metals pre-dated the "nuclear" age. High isotopic ratios for helium in metal foils have been reported in Russian experiments [3].

Our studies have been extended to native metals [4] -- copper, iron, gold, platinum, silver, $FeNi_3$ (Awaruite), and others. In some cases high isotopic ratios were also observed. The highest ratio found to date, over 0.01, was in a sample of copper from the upper peninsula of Michigan. For the $FeNi_3$, both the amount of ^3He and isotopic ratio fell in the general range reported by Bochsler, et al [5] for Josephenite. Craig, et al [6] reported much lower values for similar material. More extensive isotopic studies in metals are clearly of geological, and almost certainly of cosmological interest.

REFERENCES: [1] Nier, A.O., D.J. Schlutter, and D.E. Brownlee, 1987, LPSC XVIII, 720; 1988, LPSC XIX, 858; 1987, Meteoritics, **22**, 472. [2] Harmon Craig, U. of CA, La Jolla, private communication. [3] Helium Isotopes in Nature, Mamyrin and Tolstikhin, Elsevier. 1984. [4] Provided by E. J. Olsen, Field Museum of Natural History, Chicago. [5] Bochsler, P., A. Stettler, J.M. Bird, and M.S. Weathers, 1978, EPSL **39**, 67. [6] Craig, H., J.E. Lupton, K.M. Marti, and S. Regnier, 1979, EOS **60** 970.

A NEW SEMI-EMPIRICAL FORMULA FOR HIGH ENERGY PROTONS SPALLATION CROSS SECTIONS

H. Sauvageon, Centre d'Etudes Nucléaires de Bordeaux-Gradignan, UA 451 - 33170 GRADIGNAN - FRANCE

Spallation reactions have a crucial importance in the interaction between cosmic rays and extraterrestrial matter, particularly meteorites. Consequently, the knowledge of spallation cross sections presents a great interest for many astrophysicists and cosmochemists.

From the great amount of experimental results relative to proton spallation cross sections measured since more than twenty years, we have performed a calculation to obtain spallation cross sections of products formed in natural targets of mass A ~ 40 to ~ 200 by high energy protons (E_p > few hundred MeV).

The general principle of the calculation is the same that already used to calculate deep spallation cross sections in uranium which lead to very good results (1). It consists to fit experimental isotopic distribution of spallation products by a gaussian curve of which the expression is :

$$\sigma = (\sigma_{max})_{Ep} \exp [-(A-A_M)^2)/ 2S^2]$$

where σ is the cross section of the nuclide of mass A obtained in the interaction and index M refers to the maximum of the distribution. S is related to the FWHM (Full-Width at Half-Maximum), ΔA, of the gaussian $S=\Delta A/2.35$; $(\sigma_M)_{Ep}$ is the cross section of the maximum of the isotopic distribution for a given incident energy. $(\sigma_M)_{Ep}$, A_M and ΔA have been directly obtained from experimental results.

This formula is simple, of easy use, concerning a rather large mass range and needing only very few parameters of purely experimental origin.

The results are in good agreement ($0.7 \leq \sigma_{calc}/\sigma_{mes} \leq 1.5$) with experimental values, principaly in the region of middle mass targets (from V to Ag) which presents great interest for astrophysical applications and cosmogenic nuclides studies.

Référence

(1) H. Sauvageon, Z. für Phys. A 326 (1987) 301

NEW SYSTEMATICS OF NUCLEAR REACTIONS INDUCED BY PROTON OR NEUTRON BOMBARDMENT IN THE Ga TO Rh TARGET MASS REGION. Bernard Lavielle and Gabriel N. Simonoff, UA 451 CNRS, CENBG 33170 Gradignan, France.

Cosmic-ray-produced nuclides provide sensitive tools for studying exposure histories of terrestrial or extraterrestrial materials. A knowledge of the excitation functions for the nuclear reactions induced by protons and neutrons is essential for production rate calculations which take into account the shielding depth of the samples within a meteoroid and the meteoroid size. However, these excitation functions have been measured for only a few proton-induced reactions, and most of them are completely unknown for neutron-irradiated targets. For proton-induced reactions, the missing cross-sections may be calculated using semi-empirical formulae (1,2,3). Generally, calculated cross-sections are within a factor of two of the experimental values for well-documented targets and product mass ranges. These formulae can be utilized for neutron-induced reactions. We elaborate on new systematics of nuclear reactions which allow cross-section calculations for incident protons or neutrons.

We compiled 420 cross-section measurements for (p or n, xn)-type nuclear reactions and 243 for (p or n, pxn)-type nuclear reactions in the Ga to Rh target mass region ($x \geq 1$).

For the two considered types of nuclear reactions, the experimental data clearly show that the excitation functions have a maximum at low energy. The position E_p (in MeV) of this maximum is correlated with the threshold energy E_s. Its height (in mb) varies from one excitation function to another, but can be well fitted using an analytical expression of the parameters E_s and $(N/Z)_{cn}$, the ratio of the numbers of neutrons and protons of the compound nucleus in the considered nuclear reactions. The utilization of E_s and $(N/Z)_{cn}$, which can be defined for proton- as well as for neutron-induced reactions, allows us to describe the different types of excitation functions, independently of the nature of the incident particles.

Two different semi-empirical formulae have been obtained using the (p or n, xn) set and the (p or n, pxn) set of experimental data, respectively.

In the Ga to Rh mass region, our two formulae give better results than published formulae (1,2) which cover a larger range of data.

Using our formulae and considering 383 cross-sections of proton-induced nuclear reactions, the average of the calculated to measured ratio R is $0.96 \begin{smallmatrix} + 0.46 \\ - 0.33 \end{smallmatrix}$. The compiled 105 (n, 2n) cross-sections give $R = 0.96 \begin{smallmatrix} + 0.47 \\ - 0.32 \end{smallmatrix}$ and the 49 (n,p) cross-sections $R = 1.11 \begin{smallmatrix} + 0.21 \\ - 0.18 \end{smallmatrix}$.

Other comparisons of our calculated and experimental cross-sections from high energy neutron irradiations (with a nearly flat spectrum between 40 and 180 MeV (4)) show also a good agreement.

References:

(1) Rustam, G., Z. Naturf. 21a, 1027 (1966).
(2) Silberberg, R., Tsao, C. H., Astrophys. J. Supp. 220, 315 (1973).
(3) Lavielle, B., Regnier, S., J. Physique 45, 981 (1984).
(4) Katcoff, S., Cumming, J. B., Godel, J., Buchanan, V. J., Susskind, H. and HSU. C. J., Nucl. Instru. and Methods, 129, 473 (1975).

NUCLEAR REACTIONS INDUCED BY GALACTIC COSMIC RAYS IN IRON METEORITES

B. Zanda and J. Audouze
Institut d'Astrophysique de Paris- 98,bis Bd Arago - 75014 Paris. FRANCE

After being ejected from their parent body, meteorites travel in the interplanetary space and are irradiated by the Cosmic Ray particles. The study of nuclear reactions induced inside meteorites yields information both on the irradiation history of these bodies (duration of the exposure, geometry constraints...) and on the history of the particle fluxes. The abundance of a produced nucleus in a given sample (which is the quantity that can be measured) results of the integration over time of the production rate. This production rate itself comes from the integration over energy of the flux of the incident particles on the sample, multiplied by the cross section that describes the probability of the production reaction. As the particles propagate inside the solid meteoritical matter, the charged ones are slowed down by electromagnetic interactions, the ones that induce reactions are captured and secondary particles are produced. The particle flux thus changes with depth inside the meteorite, and so do the production rates. To make the link between a measured abundance and the incident Cosmic Ray flux at the surface of the meteorite, it is necessary to calculate production rates as a function of depth inside solid bodies. An additionnal difficulty relies in the fact that, due to the ablation in the atmosphere, the geometry of the meteorite during the exposure is not known, and the irradiation conditions of the sample have to be deduced from the measurements: this geometry problem has to be solved and one has to be able to estimate the incident flux at the surface of the meteorite to determine the exposure age and study the possible time variations of the Cosmic Ray fluxes.

We have developped a method to compute production rates as a function of depth inside spherical bodies. Through an analysis of the physical processes at work, the transport equations for protons and neutrons have been established. The results of Monte Carlo intranuclear cascade calculations have been used to describe the distribution of the emitted secondary particles that are responsible of most of the reactions induced. The two transport equations are linked (through the source term of secondary particles), and have been solved simultaneously by the use of an iterative method. The resulting fluxes have been used together with semi-empirical formulae [1] for the production cross sections in order to derive the production rates at different depths inside iron meteorites of various radii. A method is proposed to use these computed production rates to study the pre-atmospheric geometry of meteorites. The correlation between ^{21}Ne and ^{10}Be production rates that was determined experimentally by Graf et al [2] in the iron meteorite Grant has been computed: this allows to derive an exposure age for this meteorite. Being related to the abundance of a stable nuclide produced by the present Galactic Cosmic Ray (GCR) flux, this age is analogous to the one determined by Lipschutz et al [3]. It is discrepant with the age determined by Voshage and Feldmann [4] through the use of ^{40}K data. If significant, this discrepancy can be interpreted in terms of a GCR flux variation either in intensity or in spectrum, due to a change of the solar modulation. A method is proposed to distinguish between these two types of possible variation.

[1] Silberberg,R., and Tsao,C.H.: 1972. *Astrophys. J. Suppl. series* **220**, 315
[2] Graf,T, Vogt,S., Bonani,G., Herpers,U., Signer,P., Suter,M., Wieler,R., and Wölfli,W.: 1987, *Nucl. Instr. Meth. Phys. Res.* **B29**, 262
[3] Lipschutz,M.E,, Signer,P. and Anders,E. : 1965 *J. Geophys. Res.* **70** No6, 1473
[4] Voshage,H., and Feldmann,H. : 1979, *Earth Planet. Sci. Lett.* **45**, 293

DEPTH AND SIZE DEPENDENT PRODUCTION OF COSMOGENIC NUCLIDES: INFORMATION CONTENT OF METEORITE DEPTH PROFILES

Peter A.J. Englert, San Jose State University, San Jose, CA 95192

In the past two decades a considerable number of depth profiles of cosmogenic nuclides in stony meteorites have been studied in some detail [1]. While in some meteorites only a few isotopes were considered, in others a large number of cosmogenic nuclides have been measured in aliquot samples of cores and cross sections, i.e. meteorite slabs.

Though the quantity of data is huge, the interpretation in general is not always simple. Suitable model meteorites - from the standpoint of cosmogenic nuclide research - namely those that cover the entire size range from micrometeorite to a three to five meter diameter boulder, even in the most common meteorite class, have not yet been identified in the collections. A great number of meteorite cores and cross sections that were investigated in L, LL, H-chondrites, and other stony meteorites cluster around a certain size, the size of St. Severin core AIII, which is assumed to represent a preatmospheric spherical meteoroid of about 23 cm diameter; the actual preatmospheric shape of St. Severin is not spherical. Very few cross sections were analyzed from preatmospherically small meteorites [2,3]. A few cores or cross sections were analyzed of very large meteorites [4,5,6]. Ablation, obviously, presents the most important obstacle to a complete coverage.

In the process of investigating a meteorite depth profile the first cosmogenic nuclide, cosmic ray track, and/or thermoluminescence results obtained are those that indicate as to wether further investigation of a specimen is a worthwhile endeavour. These measurements may indicate the value of the meteorite for further studies but do not preclude production and/or reduplication of results that do not provide new insight into the subject studied.

The paper will present a review of measured cosmogenic nuclide depth profiles in stony meteorites as well as new data especially on Estacado's ^{53}Mn and - possibly - light noble gas content. The problematic of depth profile studies will be discussed using the example of Estacado's cosmogenic nuclide results.

REFERENCES: [1] References until 1985 in: Reedy R.C. and Englert P. Workshop on Cosmogenic Nuclides, LPI Tech. Rpt. 86-06. Lunar and Planetary Institute, Houston. [2] Michel R., et al. (1985), Proc. of the International Conference on Nuclear Data for Basic and Applied Science, Santa Fe, NM, USA. [3] Finkel R.C., et al. (1978) Geochim. Cosmochim. Acta 37, 197. [4] Heusser G., et al. (1985). Earth Planet. Sci. Lett. 72, 263-272. [5] Barton J.C., et al. (1982) Geochim. Cosmochim. Acta 46, 1963- 1967. [6] Englert P. and R. Sarafin (1984). Meteoritics 19, 223-224.

Shielding and Size Corrected Exposure Ages of Chondrites

Th. Graf, P. Signer, R. Wieler. ETH-Zürich, 8092 Zürich, Switzerland

To deduce reliable exposure ages from chondritic samples from unknown positions in meteoroids of unknown size, the depth dependence of the production of cosmogenic nuclides should be well known. To this goal, we measured He, Ne, Ar and 10-Be in adjacent samples from the L5 chondrite Knyahinya as a function of sample position (1). With this data base we determined the free parameters in the production equation used to model the production of cosmogenic nuclides in iron meteorites (2). The validity of the model was tested by comparing the predictions with experimental data on Keyes (3), St. Severin (4,5) and ALHA78084 (6). The exposure ages based on 3-He, 21-Ne, 22-Ne and 38-Ar agree within 5% for each of the meteorites.

Fig.1 shows the production rates of 21-Ne versus the 22-Ne/21-Ne ratios for spherical meteoroids of various radii and the line corresponding to the shielding correction of the 21-Ne production rate according to Nishiizumi et al. (7).

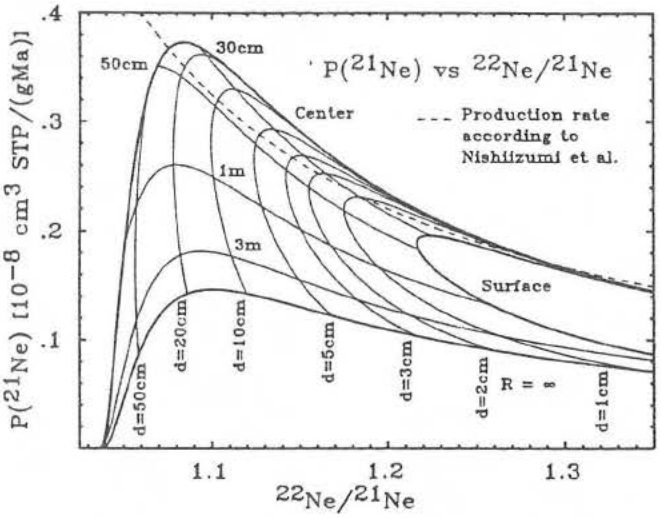

As in iron meteorites, the model does not allow to deduce meteoroid size and sample position from the noble gases in a given sample only (8). Because the 10-Be production is also modeled, this situation is remedied. The 3-isotope correlation between the ratios of the production rates of 10-Be/21-Ne and 22-Ne/21-Ne is linear (8). It can be used to compute size and shielding corrected exposure ages in chondrites:

$$\frac{t}{1-\exp(-4.33*10^{-7}*t)} = \frac{(^{10}Be/P(^{21}Ne))\{1.11\} + (0.053 \pm 0.030)(^{22}Ne/^{21}Ne - 1.11)}{(^{10}Be/^{21}Ne)\{m\}}$$

The production rate ratio (10-Be/P(21-Ne)){1.11} is given in atoms/atom and for a 22-Ne/21-Ne ratio of 1.11 and the index {m} denotes the measured ratio. With an exposure age of Knyahinya of 40 Ma according to Nishiizumi et al. (7), we determined (10-Be/P(21-Ne)){1.11} = 0.141 ± 0.002

The large uncertainty of the coefficient of the 22-Ne/21-Ne ratio reflects the comparatively large errors of the Be determinations. Improvements of the counting statistics as well as interlaboratory calibrations of 10-Be and the noble gas determinations would reduce this uncertainty. Exposure ages of St. Severin and ALHA78084 derived by this method agree to 5% with those based on noble gas profiles mentioned above.

References: 1) Graf et al., 1988. in prep. 2) Signer and Nier, 1960. JGR 65, 2947. 3) Wright et al., 1973. JGR 78, 1308. 4) Schultz and Signer, 1976. EPSL 30, 191. 5) Tuniz et al., 1984. GCA 48, 1867. 6) Sarafin et al., 1985. EPSL 72, 171. 7) Nishiizumi et al., 1980. EPSL 50, 156. 8) Voshage, 1984. EPSL 71, 181.

Ordinary Chondrites: How Many Parent Bodies? Sichao Wang, Institute of Geophysics and Planetary Physics, University of California, Los Angeles, CA 90024 and Purple Mountain Observatory, Academia Sinica, Nanjing, P.R. China

The ordinary chondrites (OC) account for 80% of observed falls. With minor exceptions they can be classified into three groups on the basis of their bulk chemical and phase compositions. A relatively large compositional hiatus separates the H from the L group, whereas there is some overlap in most taxonomic parameters between L and LL. The distinct compositional modes and differences in cosmic-ray (CR) or gas-retention age patterns indicate that each of these groups originated on a separate body. Recent neutron activation data of G. Kallemeyn and olivine and kamacite compositional data by A. Rubin have revealed the existence of small OC clusters that lie distinctly outside the highly populated cores of the H, L and LL groups. A series of plausible arguments indicates that the OC parent bodies formed and are mainly still located in the asteroid belt. Reflection spectroscopy studies show that there are no main-belt asteroids having spectra that resemble OC powders. If it should develop that considerably more than 3 parent bodies are required to account for the entire spectrum of ordinary chondrites, the "missing OC asteroids" problem will be aggravated.

To help determine whether these minor OC sets originated in separate bodies, we have examined the available cosmic-ray and gas-retention ages. We do find some clustering of ages in the minor sets: H/L Bremervörde and Tieschitz show similar cosmic-ray ages of ~25 Ma and low-Fa L-an Saratov and Tennasilm are similar both in terms of cosmic-ray ages (ca. 20 Ma) and U,Th-He ages (ca. 3.8 Ga). On the other hand, only about 25% of our H chondrites show CR ages in the 7-Ma peak that should include 46% of H, and only ~14% of the L core shows U,Th-He ages <0.9 Ga, not the acticipated 44%. We are providing samples of these OC sets for rare-gas investigations, and reviewing the literature to confirm that recent data confirm the large abundance of outgassed L chondrites reported by D. Heymann two decades ago.

SHOCK-INDUCED DISTURBANCE OF THE K-AR SYSTEM

Thomas Stephan and Elmar K. Jessberger
Max-Planck-Institut für Kernphysik
P.O.Box 103980, 6900 Heidelberg, F.R.G.

Shock metamorphism by impact events is a widespread phenomenon observed in lunar, meteoritic, and some terrestrial rocks. To study the chronology of such rocks, the response of radiometric clocks to impact has to be known. If components of these rocks have been totally molten, the age of such components dates the impact (1, 2). If, however, the shock strength was insufficient to melt, isotopic clocks still may be disturbed. This is a report of first results from a study on the response of the K-Ar clock to experimental shock, which continues our earlier work (3). It is part of a more comprehensive investigation also involving the Rb-Sr system (*A. Deutsch* and *D. Stöffler, Münster, FRG*).

Whole rock samples of a gneiss from NW-Argentina (~ 55 vol-% quartz, ~ 15 vol-% oligoclase, ~ 25 vol-% biotite (4); age ~ 450 Ma (5)) were shocked to 47.5 and 60 GPa in vacuo (10^{-3} Torr) at the *Ernst-Mach-Institut, Weil am Rhein, FRG*. Here we report the argon release behavior and ^{40}Ar-^{39}Ar ages for mineral separates - biotite and quartz-plagioclase - from shocked as well as from unshocked material.

Biotite: For unshocked biotite two major argon releases at temperatures of 750 and 1050 ^{o}C, possibly indicating two distinct argon reservoirs, are apparent. The argon release behavior of the two shocked biotite samples is almost identical with only one release maximum at about 900 ^{o}C independent of the shock pressure. The integrated $^{40}Ar_{rad}$-concentrations do not vary systematically, indicating no observable Ar-loss by shock up to 60 GPa. Thus the change of the argon release seems to be the major shock effect in biotite.

Quartz-plagioclase: The unshocked sample shows a broad distribution in argon release. In contrast, the shocked samples exhibit major low temperature release maxima. Their height increases and their width decreases with increasing shock pressure.

These preliminary data demonstrate that the K-Ar clock may be disturbed by shock, at least in some minerals and certainly depending on the shock pressure. We will discuss the results of a ^{40}Ar-^{39}Ar study of aliquots of the above samples which are performed to understand in more detail the effects of shock on the K-Ar clock.

References: **1.** Staudacher Th., Jessberger E.K., Flohs I., and Kirsten T. (1979) *Proc. Lunar Planet. Sci. Conf. 10th*, p. 745-762. **2.** Staudacher Th., Jessberger E.K., Dominik B., Kirsten T., and Schaeffer O.A. (1982) *J. Geophys. Res.* **81**, p. 1-11. **3.** Jessberger E.K. and Ostertag R. (1982) *Geochim. Cosmochim. Acta*, **46**, p. 1465-1471. **4.** Deutsch A. (1987) *Lunar Planet. Sci. Conf. 18th*, p. 237-238. **5.** Bachmann G. et al. (1985) Zbl. Geol. Paläont., Teil 1, p. 1257.

39Ar-40Ar DATING OF MESOSIDERITES: EVIDENCE FOR MAJOR PARENT BODY DISRUPTION LESS THAN 4 GY AGO

Donald Bogard, Jim Jordan (1), & David Mittlefehldt, NASA Johnson Space Center, Houston, TX 77058 (1-Also Lamar University, Beaumont, TX)

Mesosiderites are basaltic regolith breccias which experienced metal-silicate mixing, probably when the metal was molten. Nickel zoning in the metal and the abundance of tetrataenite suggests that this phase cooled slowly, about 0.5-1°C per million years (My), suggesting burial depths of up to tens of kilometers in a relatively large, asteroidal parent body. Several theories have been offered for mesosiderite origins. Most assume that brecciation and silicate-metal mixing occurred early in solar system history, and that the slow metal cooling rates were produced by deep burial processes such as crust-core mixing, material still accreting to the parent object, or burial in deep ejecta layers. The apparent incompatible characteristics of slow cooling of the metal, suggesting deep burial, and brecciated nature, suggesting a surface origin, are not readily explained by any one model for mesosiderite origin. A chronology of events should be valuable in understanding mesosiderite origin and history. However, only a modest amount of published chronological data is available on mesosiderites. Among these data are a 4.24 ±.03 Gy Rb-Sr isochron for Esterville, several classical K-Ar ages (with K and Ar not measured on the same sample) that ranged 3.2-4.25 Gy, and 244Pu fission track ages for six of ten measured mesosiderites of 3.9-4.2 Gy.

We have determined 39Ar-40Ar ages for 11 samples of 9 mesosiderites, which include all four of the classified metamorphic groups (modestly recrystallized to melted matrix) and both of the mineral groups (pyroxene or feldspar dominant). 39Ar-40Ar ages for all samples indicate Ar loss by one or more events more recently than 4.0 Gy ago. A few samples gave reasonably well-defined plateau ages of approximately 3.6 Gy. A few other samples gave ages that start at approx. 3.6 Gy at low extraction temperatures and increase to ages of 3.8-4.0 Gy. One sample indicates major loss of Ar by an event approx. 2.7 Gy ago, but Ar released at higher temperatures suggests an age of ~3.6 Gy. None of the 11 analyses show significant evidence for 39Ar-40Ar ages older than 4.0 Gy. Most analyses, however, are consistent with one or more heating events approx. 3.6-3.8 Gy ago. Ar was released from these samples at relatively high temperatures. Closure temperatures calculated from our diffusion data indicate that Ar diffusion loss would have ceased at ~350-500°C for cooling rates of ~1°C/My, which is the same temperature region where Ni diffusion profiles were established. The Ar ages thus determine the time of establishment of Ni cooling rates to have been ~3.6 Gy ago.

The ~3.6-3.8 Gy 39Ar-40Ar ages found for mesosiderites would appear to rule out those models that form mesosiderites at ~4.5 Gy, followed by relatively rapid cooling to ~600°C, then cooling at ~1°C/My through the ~500°C region to establish Ni cooling rates. The 39Ar-40Ar ages could be interpreted in one of two other ways. After mesosiderite formation ~4.5 Gy ago the metal-silicate mixture cooled slowly deep inside a parent planet, until both the Ni cooling rate textures and K-Ar ages were established at ~500-350°C, ~3.6-3.8 Gy ago. This interpretation suffers several disadvantages: it would require slow cooling of silicate at higher temperatures (>700°C), counter to petrographic observations; it would require deep burial in an unusually large parent body to sustain slow cooling over ~1Gy; and it probably would be difficult to account for the significantly older Rb-Sr ages if mesosiderites were held at high temperatures for millions of years. A second model to explain available data is that a catastrophic collision of two asteroids ~3.6-3.8 Gy ago caused disruption of the mesosiderite parent body and subsequent deep burial when the material gravitationally reassembled. A similar model has been offered to explained observed thermal histories of chondrites. With this model, mesosiderite cooling would have been rapid at high temperatures, but post-assembly cooling at a rate of ~1°C/My below ~550°C would have caused resetting of K-Ar ages and would have established the Ni cooling rates. Although we favor the latter model, either of these two models of mesosiderite origin requires a complex history involving deep burial in a parent body and establishment of the Ni cooling rate at a time dated by the 39Ar-40Ar ages.

COSMIC-RAY EXPOSURE AND TERRESTRIAL AGES OF ANTARCTIC METEORITES.

Miura, Y., Rucklidge, J.*, Beukens, R.* and Nagao, K.**

Dept. of Min. Sci. and Geol., Fac. of Sci., Yamaguchi Univ., Yamaguchi, 753, Japan. *) IsoTrace Lab., Univ. of Toronto, Toronto, M5S1A7, Canada. **) Inst. Earth's Interior, Okayama University, Misasa, Tottori, 682-02, Japan.

Cosmic-ray exposure and ^{14}C terrestrial ages in the same ten Antarctic meteorites are discussed in various chemical groups and petrologic types; that is, Y-791500 (H3), Y-74647 (H5), Y-74014 (H6), Y-74191 (L3), Y-791630 (L4), Y-75271 (L5), ALH-77231 (L6), Y-790448 (LL3), Y-74097 (Diogenite) and Y-791717 (C3) for meteorite ages. The Bruderheim (L6) and Nio-3 (H3) chondrites are used as comparison references [1].

The exposure ages of the meteorites are calculated from the ^{3}He and ^{21}Ne isotopic data [2]. Carbon-14 terrestrial ages of the Antarctic meteorites have been measured by the IsoTrace accelerator mass spectrometry (AMS) [1]. The ^{14}C terrestrial age of 1 gram sample was determined from ^{14}C concentrations collected at melt and re-melt temperatures, compared with the ^{14}C concentration of the known falling-time chondrites. The Yamato chondrites have wide range of terrestrial age, though Allan Hills meteorite of the ALH-77031 chondrite shows older age of about $30x10^{3}$ years. Among various chemical groups of H, L, LL and C, there are no regular relationships in ^{14}C terrestrial age data. This indicates that Antarctic meteorites are mixtures of the various falling-times which are concentrated to several regions in the Antarctica.

The two meteorite ages between types 3 and 6 are completely different in the Antarctic chondrites. Type 6 chondrites show the longest cosmic exposure ages, whereas the type 3 chondrites have relatively the shortest cosmic exposure ages. The types 4 and 5 chondrites show the shortest exposure and terrestrial ages with younger (i.e. the most metamorphosed) gas-retention ages. Thus the tentative formation model of these chondrites is that the types 3 and 6 chondrites are the fragments from the core and margin, respectively, in the the meteoroids if these fragments came from the similar parent body [3,4].

References

1) R. P. Beukens, J. C. Rucklidge and Y. Miura (1987): Mem. Natl Inst. Polar Res., Spec. Issue, pp. 5 (in press).
2) K. Nagao, K. Ogata, N. Takaoka and K. Saito (1983): Mem. Natl Inst. Polar Res., Spec. Issue, 30, 349-361.
3) Y. Miura (1987): Lunar Samples and Antarctic Meteorites (Tokyo), 1-6.
4) Y. Miura, J. Rucklidge, R. Beukens, K. Nagao and H. Koga (1988): 13th Inter. Symp. Antarctic Meteorites (NIPR, Tokyo), pp.3 (in press).

PLENARY IV

TO PERGAMON AND BACK. AN ACCOUNT OF A HOMERIC VOYAGE, WITH OBSERVATIONS ON THE BELIEFS AND PRACTICES OF FELLOW TRAVELLERS AND NATIVES; Denis M. Shaw, Department of Geology, McMaster University, Hamilton, Ontario, Canada, L8S4M1.

Many undertake the journey to Pergamon, and live to tell their grandchildren of privations suffered, hardships overcome, brigands repelled and the like.

Few comment on the reasons why they chose to make the voyage, what investment was made to ensure the seaworthiness of the vessel, what time was spent in detached reflection to guarantee the quality of the goods carried, what outcome in spiritual fortification was hoped for, what gifts were prepared for the benefit (in fruitful intercourse) of other voyagers, natives and sailors.

Using the premise that (with apologies to Plato) "the unexamined voyage is not worth taking", some cheerful discourse will be offered for past and future travellers.

In accordance with one of the few truths in science, namely that "all meeting abstracts are bad abstracts", the reader is left to muse on what might really be presented.

ACCUMULATION AND FRAGMENTATION MODEL OF THE ASTEROID BELT; G.W. Wetherill, DTM, Carnegie Institution of Washington, Washington, D.C. 20015

Recent advances in understanding the physical principles of planetesimal accumulation provide the opportunity of developing self-consistent quantitative models of asteroid formation that can be compared with observational data on asteroidal meteorites, and telescopic and spacecraft observations of asteroids themselves. By iteration of theory and observation one can thereby make more complete use of the unique record of early solar system history preserved in meteorites.

It is plausible to assume that the solar nebula filled the asteroid belt in a continuous manner. A straightforward application to the asteroid belt of the planetesimal accumulation model proposed for the terrestrial planets (1) then leads to a reductio ad absurdum because runaway accumulation predicts formation of $\sim$1/3 Earth-mass planet-size bodies in $\sim 3 \times 10^5$ years. Merger of these bodies will then lead to at least one "terrestrial" planet in the asteroid belt.

An alternative is quenching the asteroidal runaway by perturbations by an early-formed Jupiter, possible models for which have been obtained (2,3). These same models still permit runaway growth at 1 A.U. and formation of the terrestrial planets in the manner described earlier (1,4,5). If modest external perturbations lead to eccentricities $\sim 10^{-3}$ to 10^{-2}, asteroidal growth will be satisfactorily limited to formation of $\sim 10^{24}$ g bodies in $\sim 10^6$ years. During the growth of these larger asteroids, the smaller members of the planetesimal swarm will be destroyed by mutual collisions, leading to loss of material by fragmentation with an initial characteristic time scale of $\sim$2 m.y. The largest bodies will be nearly invulnerable to destruction. During this period of growth, much of the material in the larger bodies will consist of breccias, formed by low velocity impact, as well as by reaccumulation of fragments of smaller bodies, derived from limited regions of the asteroid belt, $\sim$0.03 A.U. in width.

Further gradual increase in eccentricity to present asteroidal values on a $\sim 10^7$ year time scale, (presumably externally driven) is then found to cause collisional destruction of >99.9% of the asteroidal material within 150 m.y., after which time asteroidal evolution resembles that observed today. This model is amenable to future comparison with observational evidence obtainable from petrography of meteorites, evidence for a "late veneer" on the terrestrial planets, their cratering history, and asteroidal observation.

References:

(1) Wetherill, G.W. and Stewart, G.R. (1988) Accumulation of a swarm of small planetesimals, submitted to Icarus.

(2) Lissauer, J.J. (1987) Time scales for planetary accretion and the structure of the protoplanetary disk. Icarus 69, 249-265.

(3) Wetherill, G.W. (1988) Origin of the asteroid belt. Submitted to Asteroids II, R.P. Binzel, ed., University of Arizona Press, Tucson.

(4) Wetherill, G.W. (1986) Accumulation of the terrestrial planets and implications concerning lunar origin. In Origin of the Moon, ed. Hartmann, W.K. et al, pp. 519-550, Lunar Planet. Inst., Houston.

(5) Wetherill, G.W. (1988) Accumulation of Mercury from planetesimals. In Press, Mercury, C. Chapman and F. Vilas, ed. Univ. of Arizona Press, Tucson.

METEORITE EVIDENCE FOR THE NATURE AND ORIGIN OF PRIMORDIAL CHEMICAL VARIATIONS ACROSS THE ASTEROID BELT; Edward R.D. Scott, Institute of Meteoritics and Department of Geology, University of New Mexico, Albuquerque, NM 87131.

The chemical and mineralogical purity of chondrites belonging to the same chondrite class, the relative homogeneity of their chondrule oxygen isotopic compositions and the low volume (1%) of foreign clasts suggest that each chondrite class is composed of solids that accreted in a narrow nebular zone <0.1 AU wide, between 2 and 3 AU from the sun [1]. Although some asteroid types are concentrated in specific zones of the asteroid belt [2], there are considerable overlaps between these zones even for large asteroids, suggesting that reflectance spectra are controlled as much by geological processing within asteroids as by primordial chemical variations across the solar nebula. Thus neighboring, large C, S, P, B and G asteroids may have been derived from a single chondritic class of material, as it is unlikely that their relative locations have altered much since they accreted.

The best estimate for the order of increasing distance of formation of chondrite classes from the sun is E, H-L-LL, CV, CO, CM and CI [3]. This sequence is very approximately the order of increasing refractory content and FeO/(FeO+MgO) ratio. However, elemental abundances, chondrule sizes and abundances, refractory inclusion, metal and matrix abundances are not well correlated, as might be expected if chondrites formed in a homogeneous nebula of monotonically varying density and temperature. If a single, monotonic, chemical sequence existed, the position of a new chondrite class in the sequence and all of its properties could be determined from a single parameter. Instead, the ungrouped chondrites, Kakangari [4] and Allan Hills 85085 [5], cannot be comfortably fitted into the E-CI sequence, and their components have properties far outside the known ranges. Thus it is likely that neither the bulk properties of chondrites, nor the properties of chondritic components varied monotonically with distance from the sun. The complete chondritic sequence from 2 to 3 AU is probably vastly more complicated and extensive than our sample of nine classes would suggest; our sample may represent only a small fraction of the whole sequence.

The diverse chemical properties of chondrites reflect the diverse proportions and properties of their chondrules, metal, refractory inclusions and matrices. These properties may be controlled to a limited extent by presolar elemental heterogeneities, but the components have all been affected by one or more brief, local, high temperature events in the nebula. It is possible that these local, energetic events together with differential settling of particles to the nebular midplane largely controlled the size, composition and abundance of all components. Thus the chondrite properties suggest that chaotic conditions existed at 2-3 AU, albeit briefly, prior to the accretion of chondritic components.

Although Jupiter prevented a planet from forming around 2.8 AU, it is unlikely to be responsible for the formation or existence of a rich menagerie of chondrite classes at 2-3 AU. Thus chaotic conditions may have prevailed over a large proportion of the solar nebula, producing diverse but relatively homogeneous planetesimals within all planetary feeding zones [6].

References. [1] E.R.D. Scott and G.J. Taylor (1987) Meteoritics 22, 497. [2] J. Gradie and E. Tedesco (1982) Science 216, 1405. [3] J.T. Wasson (1985) Meteorites; Their Record of Early Solar System History, W.H. Freeman. [4] A.J. Brearley (1988) Lunar and Planetary Science XIX, p. 130. [5] E.R.D. Scott (1988) Lunar and Planetary Science XIX, p. 1049. [6] H.E. Newsom and E.R.D. Scott, this volume.

THE ROLE OF IMPACTS IN ASTEROID DIFFERENTIATION G. Jeffrey Taylor, Institute of Meteoritics and Department of Geology, University of New Mexico, Albuquerque, NM 87131.

Many properties of individual groups of differentiated meteorites, such as trace-element concentrations, homogenization of zoned minerals, and ages, cannot be explained by simple, one-stage heating of an asteroid. Although impact is unlikely to play a major role in providing heat to drive asteroid igneous activity, it might interact significantly with magmatic processes to produce products that magmatism alone could not. This paper considers how impact complicates igneous processes in two ways: formation of thick regoliths and direct excavation of melts.

Regolith formation Regoliths begin to develop almost as soon as a body begins to accrete. An incoming projectile with the strength of basalt breaks up if it arrives at > 25 m/sec, the escape velocity of a chondritic object about 20 km in radius. Allowing for compaction and sintering of the interior, the outer 10 km of an asteroid 100-200 km in radius will be a rubble pile as a consequence of accretion. An increase in relative velocities to a few km/sec soon after accretion will ensure this. The presence of a thick regolith will affect the migration of magma. It would have a lower density, perhaps as low as 2.5 g/cm^3, than the magmas moving through it (about 2.8 g/cm^3 for eucritic magmas); this could arrest magma ascent, leading to the formation of intrusions rather than basalts. The lower temperature and blocky nature of the regolith would lead to rapid cooling of rising magmas, also causing arrested migration. Consequently, the earliest magmas to erupt probably formed intrusions, both dikes and plutons. Continued magmatism would heat the crust and increase the average density, leading to eruptions. However, because impact rates were high early in solar system history, the upper crust would have continued to be reworked and fractured, causing magmas to engulf fragments of preexisting rock and possibly thermally metamorphosing them. Finally, craters could contain thick accumulations of lavas; individual flows might be exceptionally thick because flow thicknesses on planets vary inversely with gravitational acceleration. Thick flows or lava lakes in craters could provide the setting for equilibration of many eucritic basalts such as Juvinas, which need to be buried a few hundred meters; such metamorphism could also take place near dikes beneath the surface.

Melt excavation Magmas could be excavated by impacts over a wide range of depths on asteroidal bodies. Small impacts would excavate flows or lava lakes, mixing these lavas with solid rocks; this might provide another opportunity to equilibrate eucrite basalts. Larger impacts (craters 50 km across) could excavate magma chambers crystallizing at depths up to 10 km. This could eject or expose crystal mushes to the surface, thereby quenching in their high-temperature characteristics (e.g., the high Ca in olivine and unexsolved pigeonites present in ureilites). Such impacts could also mix more fractionated and less fractionated magmas existing within a chamber or nearby chambers, or possibly mix impact-produced melt into a cumulate containing trapped liquids. Still larger impacts, those near the limit of an asteroid's strength, might excavate to the zone of partial melting; an asteroid 400 km in diameter might survive formation of a 200 km crater, which would be 40 km deep. This could mix partial melts formed under a variety of conditions (source composition, percent of melting) or quench them. Finally, an extremely large event might disrupt an asteroid undergoing magmatism. If reassembled by gravitational forces, the newly-formed megabreccia would contain at great depth both surface lavas and cumulates formed in shallow intrusions. Hot, partially molten rock from the interior would cool partly during the several hours it would take to reaccrete the body, but fragments > 5 m in radius would cool negligibly. Subsequent melting of the reassembled but disorganized body, either by ^{26}Al returned to the interior in the buried basalts or by electromagnetic induction, might account for the lithologies that appear to have formed by partial melting of previously-formed cumulates.

OBSERVATIONAL EVIDENCE FOR SOLAR WIND INDUCTION HEATING OF LOW ALBEDO ASTEROIDS; T.D. Jones, L.A. Lebofsky, J.S. Lewis, Univ. of Arizona.

Since the late 1970's, the decay of the short-lived radionuclide ^{26}Al has been the favored heat source for producing igneous differentiation and milder aqueous alteration in some meteorite parent bodies [1]. Our 3-μm reflectance observations of asteroidal hydrated silicates [2] now indicate that their orbital distribution is inconsistent with ^{26}Al heating . Solar wind induction heating [3,4] may better explain the observed "primitive" asteroid distribution.

We combined our 1986-88 3-μm observations of 19 low albedo asteroids with earlier results from Lebofsky [5] and Feierberg et al. [6,7], all from the NASA Infrared Telescope Facility. Of the 32 C and C-subclass objects observed, 66% display the 3-μm hydrated silicate absorption feature caused by structural hydroxyl and interlayer and adsorbed H_2O. We see no correlation between clay mineral abundance (represented by 3-μm band depth) and asteroid diameter, albedo, orbital inclination or eccentricity. However, a linear fit to the 39-object sample shows a significant (> 95% confidence) negative correlation between hydrated silicate abundance and heliocentric distance. The distribution by asteroid type is largely bimodal: The C,B,F,G, & T classes exhibit the full range of 3-μm band depths, but primitive outer belt minerals appear to be anhydrous (only 1 of 7 CP-, P-, and D-class objects shows even a weak 3-μm feature). Apparently, volatile-rich, "ultracarbonaceous" outer belt asteroids [8] are not composed of hydrated silicates.

A wealth of evidence indicates that meteoritic and asteroidal hydrated silicates are secondary products of aqueous alteration [9]. Their presence on an asteroid, then, implies an alteration episode extensive enough to produce hydrated silicates in quantities sufficient to survive collisional evolution and still be spectrally prominent today. Thermal models for volatile-rich parent bodies [10,11] can produce such mild alteration episodes. However, if ^{26}Al furnished the required heat, it is difficult to see how an initial endowment of ^{26}Al in the C region could have produced the variety of alteration outcomes observed: 3-μm band depths of 0 - 40% over narrow orbital ranges (0.1 AU), and anhydrous asteroids as large as 300 km in diameter. By contrast, electrical induction heating accounts for the igneous differentiation of inner belt asteroids [2,4], the apparent decline in hydrated silicates with solar distance, and the variety of C-class alteration states. Electrical conductivity variations among the carbonaceous chondrites [4] suggest that different thermal outcomes are possible in asteroids with only slight compositional differences. The original outer belt asteroid composition (dominated by anhydrous silicates, water ice, and organics [12,13]) may survive in P and D asteroids beyond the effective range of early inductive heating.

REFERENCES: [1] Lee (1979) Rev. Geophys. Space Phys. 17, 1591-1611. [2] Jones et al. (1988) LPSC XIX, 567-8. [3] Sonett et al. (1968) Nature 219, 924-926. [4] Lebofsky et al. (1988) in Planetary and Satellite Atmospheres: Origin and Evolution, U. Az. Press, in press. [5] Lebofsky (1980) Astron. J. 85, 573-585. [6] Feierberg et al. (1985) Icarus 63, 183-191. [7] Feierberg et al. (1985) Bull. Amer. Astron. Soc. 17, 730. [8] Gradie and Veverka (1980) Nature 283, 840-842. [9] Kerridge and Bunch (1979) in Asteroids, U. Az. Press, 745-764. [10] Gaffey (1979) Bull. Amer. Astron. Soc. 11, 708. [11] Grimm and McSween (1988) LPSC XIX, 427-8. [12] McSween (1987) GCA 51, 2469-2477. [13] Bunch and Chang (1980) GCA 44, 1543-1577.

CORE FORMATION ON THE EUCRITE PARENT BODY, THE MOON AND THE AdoR PARENT BODY. J.H. Jones[1], A.H. Treiman[2], M.-J. Janssens[3], R. Wolf[3] and M. Ebihara[3]. [1]NASA Johnson Space Center, SN21, Houston, TX 77058; [2]Dept. of Geology, Boston U., Boston, MA 02215; [3]Enrico Fermi Institute, U. of Chicago, Chicago, IL 60637.

The Moon, the Eucrite Parent Body (EPB) and the AdoR Parent Body (APB) are all presumably small bodies within the inner solar system and all three, to varying degrees have experienced core formation events. Refractory elements which are more siderophile than P show good correlations between depletions and degree of siderophility. Depletions are also relatively consistent, for a given element, between different parent bodies. Taken at face value, this observation appears to imply that the primary determining influence on the abundances of siderophile elements in the silicate portions of these bodies is the separation of solid Fe-Ni metal under similar redox conditions. For some elements such as P and Ag, depletions due to volatility may be more important than those attributed to core formation. Solutions to detailed models (after Newsom [1]) indicate possible variations in styles of core formation. Unfortunately, systematic differences between the experimentally determined partition coefficients (D) of different authors [2,3,4,5] preclude strong conclusions.

EPB. EPB models are sensitive to calculations of elemental depletions and to the exact redox conditions that are assumed. Estimates of the redox conditions during core formation on the EPB range from 1-1.5 log units below the Fe-FeO buffer. The D values of [5] for Ni, Co, Au and Mo imply that the core was 45-15% of the mass of the planet and that core formation occurred after 65-90% silicate partial melting -- depending on whether conditions were oxidizing or reducing, respectively. The D's of [5] for W and P cannot be fit into this model. However, under oxidizing conditions, W agrees with the other elements if the D value of [3] is used instead. P can be fit into the model only if P was severely depleted prior to core formation and some liquid metal was present. If, for example, P is required to agree with the other elements, then a D value of ~7.5 (bulk metal/silicate liquid) is necessary if P is already depleted by a factor of 5. Regardless, models which require such large degrees of silicate partial melting are petrologically suspect.

The Moon. If the same type of model is applied to the Moon, a much different solution is obtained. The D values of [5] for Ni, Co, W and Mo indicate a much smaller core on the Moon (3-4 wt.%) and that the degree of partial melting was also smaller (~15 - 30 %). Re can also be made to come into acceptable agreement if Re behaves incompatibly in silicate systems (D_{ss} ~0.05). Again, P is too severely depleted, compared to experimentally determined D values, to fit into this model -- unless P was initially depleted ~10X by volatility. If the terrestrial upper mantle is used as a starting composition, there is no well-defined solution, but the size of the lunar core would be trivial (~0.01 - 0.1 wt.%). Note that the degree of silicate partial melting is too low to produce a 500 km deep lunar magma ocean. However, there is no guarantee that partial melting did not continue after the lunar core had segregated. Thus, with "chondritic" starting materials, models for the Moon seem consistent with geophysically-constrained core sizes and with inferred amounts of silicate differentiation -- in contrast to the EPB.

APB. Detailed models have not been performed for the APB, for which we have new data. The Delano method for determining the Ni and Co depletions of a planetary body are only calibrated for planetary compositions that are peridotitic [6]. The compositions of AdoR and LEW86010 are so remarkable that there is no certainty that the APB is indeed peridotitic. Also, the severe depletions in volatile elements in AdoR make it unclear that Mg, Co and Ni initially existed in chondritic proportions. Consequently, it appears premature to speculate on core formation processes on the APB -- except to note (as above) that the AdoR siderophile depletions mimic those of the Moon and the EPB. A cautionary note should be added. If the calculated Co and Ni depletions are correct, then Co and Ni, although depleted, are in chondritic relative proportions. The likelihood that this could be solely due to core formation seems remote.

References. [1] Newsom H. E. (1985) *Proc. Lunar Planet. Sci. Conf. 15th.* C613-C617. [2] Rammensee W. (1978) Ph. D. Thesis, Mainz. [3] Newsom H.E. and Drake M.J. (1982) *G. C.A.* **46**, 2483-2498. [4] Newsom H.E. and Drake M.J. (1983) *G.C.A.***47**, 93-100. [5] Jones J.H. and Drake M.J. (1986) *Nature* **332**, 221-228. [6] Delano J.W. (1986) In, *The Origin of the Moon*. pp. 231-248.

PRIMORDIAL DIFFERENTIATION OF THE EARTH: Ni, Co, Ir, and Au

MICHAEL J. DRAKE, DANIEL J. MALVIN, AND CHRISTOPHER J. CAPOBIANCO
(Lunar and Planetary Laboratory, University of Arizona, Tucson, AZ 85721, U.S.A.)

Theoretical considerations of planetary accretion suggest that terrestrial planets should begin to melt by the time they achieve about one tenth of an Earth mass [1]. Hypotheses for the origin of the Moon involving giant impacts suggest that the Earth would have been substantially melted or even vaporized as a result of the impact [2]. Recent high pressure experimental phase equilibrium studies [3,4] have shown a convergence of the liquidus and solidus for candidate upper mantle compositions, and may be interpreted in terms of a substantially molten Earth during and subsequent to accretion. In contrast, experimental trace element partitioning studies [5] have shown *that at* most minor amounts of majorite and perovskite fractionation are consistent with the approximately chondritic ratios of most refactory lithophile elements inferred for the upper mantle. It has also been proposed that the superchondritic Mg/Si ratio of 1.12 relative to CI in the upper mantle [6] is a consequence of flotation of olivine at high pressure on a buried magma ocean, with subsequent mixing of that olivine into the upper mantle [7]. Mixing of approximately 20% olivine is required.

This proposal may be tested against the approximately chondritic ratios of Ni/Co and Ir/Au in the upper mantle. Under all experimental conditions [e.g. 8,9], olivine/liquid partition coefficients for Ni, D(Ni), are greater than for Co, with D(Ni) > 2 X D(Co). Experiments conducted in this laboratory investigating the solubility of Au in silicate melts indicate that maximum solubilities of about 30 ppm Au are achievable. Thus, experimental determinations of Au partitioning are in progress as these solubilities should be high enough to permit analysis of both phases by a proton-induced X-ray emission trace element microprobe (PIXE). In the meantime, estimates of partition coefficients obtained from abundances [10] of Au and Ir in mantle nodules and basalts indicate that Ir is compatible and Au indifferent in magmatic processes. Whether these contrasting geochemical behaviors are due to silicate mineral/silicate melt partitioning or to sulfide mineral/silicate melt partitioning is presently uncertain. However, estimates of D(Ir) and D(Au) from olivine fractionation in komatiites also suggest that Ir is compatible and Au incompatible [11]. Absolute values of partition coefficients are not known under appropriate mantle conditions. Calculations have been carried out for a variety of partition coefficient values. For example, using arbitrary (but plausible) values of D(Ni) = 7, D(Co) = 2.6, D(Ir) = 50, D(Au) = 1, mixing of 20% olivine into the upper mantle will raise the Ni/Co ratio by about 35% and the Ir/Au ratio by about 75%, the exact values being dependent on the details of the calculation. If D(Ni) = D(Ir) = 2 and D(Co) = D(Au) = 0.6, upper mantle ratios will be raised by about 12%, again, the exact values being dependent on the details of the calculation. In fact, Ni/Co and Ir/Au ratios in the upper mantle appear to be slightly subchondritic [12]. Thus, it seems difficult to reconcile extensive melting of the Earth's upper mantle with siderophile element systematics.

[1] Stevenson D.J. (1981) Science 214, 611-619.
[2] Kipp M.E. and Melosh H.J. (1987) Lunar Planet. Sci. XVIII, 491-492.
[3] Takahashi E. (1986) Jour. Geophys. Res. 91, 9367-9382.
[4] Ito E. and Takahashi E. (1987) Nature 328, 514-516.
[5] Kato T., Irifune T., and Ringwood A. (1987) Geophys. Res. Lett. 14, 546-549.
[6] Palme H. and Nickel K. (1985) Geochim. Cosmochim. Acta 49, 2123-2132.
[7] Agee C.B. and Walker D. (1987) Meteoritics 22, 314.
[8] Seifert S., O'Neill H., and Brey G. (1988) Geochim. Cosmochim. Acta 52, 603-616
[9] Irving A. (1978) Geochim. Cosmochim. Acta 42, 743-770.
[10] Chou C., Shaw D., and Crockett J. (1983) Jour. Geophys. Res. 88, A507-A518.
[11] Brügmann G., Arndt N., Hofmann A., and Tobschall H.J. (1987) Geochim. Cosmochim. Acta 51, 2159-2169.
[12] Newsom H. and Palme H. (1984) Earth Planet. Sci. Lett. 69, 354-364.

IRON METEORITES AND THE PHYSICS OF CORE FORMATION; Alfred Kracher, and Rohit Trivedi, Department of Earth Sciences and Department of Material Science and Engineering, Iowa State University, and Ames Laboratory, USDOE, Ames, IA 50011.

The majority of iron meteorites originated by fractional crystallization of a metallic melt, probably in the cores of asteroids. At least three cores (parental to iron meteorite groups IIAB, IIIAB, and IVA) are sampled well enough to allow inferences about the physical conditions of their formation[1]. Attempts to model the fractionation behavior of trace and minor elements in these cores have confirmed a fractional crystallization origin, but in detail discrepancies remain between laboratory measurements and observations[2]. In order to improve our understanding of core formation, we are developing a model to investigate the physical parameters of this process.

A major uncertainty is the extrapolation of laboratory measurements to very low cooling rates and very long time scales. Cooling rates at the $\gamma \rightarrow \alpha + \gamma$ transition (near 800 K) are thought to be on the order of 10^{-13} to 10^{-11} K/s (Ref. 3). If there is no active heat source, cooling should be controlled by conductive heat loss through the silicate mantle. During the early stages of solidification (about 1800 K), the silicates are partially molten, increasing heat loss. However, the heat source that led to melting in the first place might still be active, and slow down cooling. Thus any model has to consider a range of cooling rates.

At least two major sources of deviation from simple Rayleigh behavior need to be considered: back diffusion in the solid and incomplete mixing in the liquid. Diffusion in solid can be significant when the solidification rate is very slow. Concentration gradients observed in the Agpalilik specimen of the Cape York shower provide constraints on the effect of back diffusion. Liquid mixing is controlled by convection and "surface roughness" of the solid. This is probably about the size scale of secondary dendrite arms, assumed to be tens of cm. Because this is small relative to the size of primary convection cells, slower cooling rates do not necessarily lead to more ideal fractionation.

Density driven convection during the directional solidification of alloys may lead to the formation of freckles with much smaller grain size than the primary dendrites and compositions of solid-liquid mixtures. The primary grain size of freckles is of the order of 10x the secondary dendrite spacing. The phenomenon should be rare when temperature gradients are low, but it may explain the existence of iron meteorites whose compositions lie on a solid-liquid mixing line, e.g., Agpalilik.

The various size scales such as core diameter, primary and secondary dendrite arms, freckles, liquid convection cells, typical meteorite size, and grain size of γ-(Fe, Ni) as reflected in uniformity of Widmannstätten pattern will be considered so that a reasonable model for non-ideal trace element fractionation can be developed.

1. J. T. Wasson (1974), "Meteorites", Springer Verlag.
2. J. H. Jones and M. J. Drake (1983) GCA 47, 1199-1209.
3. V. Saikumar and J. I. Goldstein (1988) GCA 52. 715-726.
4. A. F. Giamci and B.H. Kear (1970) Met. Trans. 1, 2185-2192.

SOLUBILITIES AND PARTITIONING OF NOBLE GASES IN MINERAL/MELT SYSTEMS: RESULTS FOR NE, AR, KR, AND XE IN ANORTHITE, DIOPSIDE, FORSTERITE, AND COEXISTING MELT WITH IMPLICATIONS FOR TERRESTRIAL PLANET ATMOSPHERIC EVOLUTION. C.L. Broadhurst, M.J. Drake (Lunar and Planetary Laboratory, University of Arizona, Tucson, AZ 85721), B.E. Hagee, and T.J. Bernatowicz (McDonnell Center for the Space Sciences, Washington University, St. Louis, MO 63130).

Introduction: The atmospheres of the terrestrial planets provide accessible, homogeneous reservoirs, which we can sample for noble gases. These samples can be used to detect any primordial heterogeneity in the material which accreted to form the planets, as well as to investigate the atmospheres themselves, *provided that* we know the relation between the measured atmospheric abundances and the bulk planet inventories. This relation is determined by the interplay of the degassing mechanisms which are operational on each individual planet. In particular, magmatic transport is the only mechanism, catastrophic or non-catastrophic, that can be shown to be important on Earth, Mars, and Venus [1]; therefore it is the focus of our experiments.

Experiments: Noble gas solubilities in basaltic melts are reasonably well known [2], but only one set of mineral/melt partition coefficients was previously available [3]. To provide the necessary information we have developed a technique for the determination of equilibrium partition coefficients through (a) synthesis experiments in which phase separation is not required, and (b) reversal experiments and diffusion rate studies in which the equilibrium solubilities of noble gases in minerals and melts are established. Here we report on results from synthesis experiments for Ne, Ar, Kr, and Xe in anorthite-melt, diopside-melt, and forsterite-melt systems. Two experiments were performed in which mineral melt equilibrium pairs were held at 1300°C for 18 days in a one bar atmosphere nominally composed of 5% Ne, 93% Ar, 1% Kr, and 1% Xe. The mix is commercial and has not yet been reanalyzed by us.

All mineral samples show a clear trend of increasing solubility with increasing atomic number, however the *absolute solubilities* are extremely variable. This variation is real, and indicates that prior sample history affects solubility. For example, two subsamples of anorthite WU-617 run separately agree with one another and with past Ar synthesis results within a factor of two, yet differ from sample anorthite HO-228 by a factor of 100. Among the anorthites, HO-228 has the highest concentrations of all the noble gases, but is internally self-consistent: previously this anorthite sample yielded a much higher Ar concentration than four others run simultaneously [1]. Work in progress should help to determine which factors control solubility variations and which sites in the minerals are accomodating the gases.

In contrast, the melt solubilities show a clear trend of decreasing solubility with increasing atomic number and very little variation over a relatively large compositional range. Results are consistent with [2] and [3]. The spread in solubilities affects greatly the *absolute values* of partition coefficients, but is not significant in terms of partition coefficient *patterns*. These patterns show a clear trend of increasing compatibility with increasing atomic number.

Conclusions: Consideration of these results in concert with [1,2,3] indicates strongly that the noble gases as a group are not uniformly incompatible in anorthite, diopside, and olivine, thus will be fractionated by igneous processes. If this partitioning and solubility behavior is characteristic of other common crustal and mantle minerals, planetary atmospheres will contain the bulk planetary inventory of noble gases only if the planet is substantially outgassed. A more general conclusion is that the noble gas abundance patterns should not be interpreted in terms of the bulk planet inventories without a detailed understanding of planetary differentiation.

[1] Broadhurst, CL, Drake, MJ, Bernatowicz, TJ, and Hagee, BE (1987) *Meteoritics* **22**, 342. [2] Lux, G (1987) *GCA* **51**, 1549-1560. [3] Hiyagon, H and Ozima, M (1986) *GCA* **50**, 2045-2057.

MINERAL/MELT PARTITIONING OF I: IMPLICATIONS FOR MANTLE OUTGASSING. Donald S. Musselwhite, Timothy D. Swindle and Michael J. Drake (Lunar and Planetary Laboratory, University of Arizona, Tucson, AZ 85721)

Introduction: Noble gas concentrations in atmospheres, mantle materials and mantle-derived materials are important constraints on models of planetary formation and evolution. Several isotopes of Xe are the decay products of now extinct radioactive species. ^{129}I decays to ^{129}Xe ($t_{1/2}$ = 17 m.y.) and ^{244}Pu decays to $^{131\text{-}136}Xe$ ($t_{1/2}$ = 82 m.y.)[1,2].

The excess ^{129}Xe found in mantle-derived materials is often assumed to be primordial. Based on the Xe systematics of MORBs, gas wells, OIBs and other mantle-derived materials, Allègre *et al.* [1] proposed a two layer mantle. In this scheme, one layer (upper mantle as sampled by MORBs) degassed early in Earth history while ^{129}I was still alive, thereby enhancing its I/Xe ratio. The other layer (lower mantle, as sampled by OIBs) is undegassed and therefore has a low I/Xe ratio. A problem with this model is the lack of enhanced $^{131\text{-}136}Xe$ in MORBs over atmosphere as would be expected from concomitant decay of ^{244}Pu.

Alternative models have been proposed. Caffee and Hudson [3] proposed that fission of ^{238}U can produce enough ^{129}I to account for the ^{129}Xe excess in the MORB source if a plausible method for separation of ^{129}I from the fission $^{131\text{-}136}Xe$ can be found. Ozima *et al.* [4] suggested that the excess ^{129}Xe in MORBs originated in a reservoir that accreted earlier than the atmospheric source region and had different I-Pu-Xe systematics.

A poorly constrained factor in discussions of this problem has been the partitioning of I relative to Xe and Pu in mantle melting events. This work reports the first mineral/melt partitioning results for I.

Methods: I partitioning experiments are being carried out in the system Di-An-Fo at 1 atm following the approach of [5]. 100 mg aliquants of oxide mixtures with 2 wt. % I (as KI) are sealed into platinum capsules, suspended in a muffle furnace and brought up to superliquidus temperature (1380°C), held there for one half to one hour, then brought down to the crystallization temperature (1300°C) for 24 to 120 hours, then quenched in air. The resulting crystal/glass assemblage is analysed by electron microprobe. Samples with measurable I in the glass are then analysed by the Proton Induced X-ray Emission (PIXE) probe.

Results and Discussion: We measure a value of D(I) for the diopside/melt pairs of less than 0.0055. The concentration of I in the diopside is below the detection limit for the PIXE (15.5ppm at 2 σ). The charges analysed by PIXE also contain trace amounts of Sr, giving a diopside/melt D(Sr) of 0.11, within the range of published values [6]. This close agreement and the fact that I is distributed homogeneously throughout the glass leads us to believe that equilibrium was attained in the experiment. D(Xe) for diopside/melt pairs is 0.73 [7] and D(Pu) for diopside/melt is 0.17 [8]. These data indicate that I is much less compatible than Xe or Pu.

The fact that I is less compatible in diopside than Xe casts doubt on the 2-layered mantle model of Allègre *et al.* [1], since the enrichment of I over Xe in a degassed upper mantle would be very difficult to achieve if the relative partitioning behavior of I and Xe for other relevant mantle mineral/melt pairs is similar to diopside. The partitioning data available for other halogens [9] leads us to believe that this will be the case.

References: (1) Allègre, C.J. *et al* (1983) *Nature* v. 303, 762-766. (2) Swindle, T.D. (1986) In Origin of the Moon (W.K. Hartmann, R.J. Phillips and G.J. Taylor, eds), 331–357 LPI, Houston. (3) Caffee, M.W. and G.B. Hudson (1987) LPS XVIII, 145–146. (4) Ozima *et al.* (1985) *Nature* v.315, # 6019, 471-474. (5) Malvin, D.J. and M.J. Drake (1987) *GCA* v.51, 2117–2128. (6) Arth, J.G. and G.N. Hanson (1975) *GCA* v.39, 325-362. (7) Broadhurst, C.J. *et al* (1988) LPS XIX, 138–139. (8) Jones, J.H. (1982) *GCA* v.46, 1793-1804. (9) Kortinig, S. (1972) In Handbook of Geochemistry (K.H. Wedepoll, ed.) 9-F-1 to 5, Springer-Verlag, New York.

IMPLICATION OF TRACE ELEMENT DISTRIBUTION DURING MELTING PROCESS OF THE JILIN CHONDRITE (H5); H.Fang, C.F.Chai, X.Y.Mao, S.L.Ma, (Institute of High Energy Physics, Academia Sinica, P.O.Box 2732, Beijing, China), Z.Y.Ouyang and H.S.Xie (Institute of Geochemistry, Academia Sinica, Guiyang, China)

We carried out a series of melting experiments of the Jilin chondrite (H5) in high temperature-low pressure (HTLP) and high temperature-high pressure (HTHP), respectively, in order to simulate chemical fractionation of the core, the mantle and the crust of the earth and to study the meteorite-ablated cosmic dust, etc.

The HTLP experiments were done in two conditions: one at vaccum and the other at 1 atm argon-filled with the same temperature range (1400-1600^{o}C). In first case all the chondrite samples were melted and the Fe-Ni metal was well separated from the silicate without forming sulfide phase. The siderophile elements of Os, Ir, Ru, Re, W, Au and Ni were aggregated in the metal phase with enrichment factors of 5 to 10 relative to the source chondrite. The chalcophile elements of As, Se and Sb, etc., also exhibited more or less riched, while the lithophile elements of Sc, REE and others were significantly depleted. The elemental compositions of the silicate phase formed in the vaccum melting were quite different from those of the raw silicate of the Jilin chodrite.

The melting products (silicate, sulfide and metal) of the argon-filled HTLP experiments were well arranged from the top to the bottom in the melts in the order of density increase, similar to the fractionation character proposed by the uniform accretion.

We used the silicate material from the HTLP experiment as a representative of the primitive mantle. The partial melting under the HTHP (20 to 50 atm; 1400 to 1760^{o}C) produced 1 to 5 % of two non-mixed melts: the light melt and the dark melt in colour. The former concentrated the large ion imcompatible elements of REE, Sc, U, Th, Ta and Hf, while repulsed the compatible elements of Fe, Co and Ni. In chemistry and petrology the light melt was close to the basic and intermediate rocks, e.g. basalt and andesite. The residue materials after melting mainly consisted of the olivine, a main constituent of the earth's mantle.

ACCRETION OF PLANETS: EVIDENCE FROM METEORITES AND ASTEROIDS;
H.E. Newsom and E.R.D. Scott, Institute of Meteoritics, Univ. of New Mexico, Albuquerque, NM 87131

The compositions of the planets vary relatively smoothly with heliocentric distance. This was reflected in early models of solar system formation that predicted a monotonically changing composition of the nebular solids that accreted to form the planets [e.g., 1]. In contrast, the compositions of meteorites and asteroids, which were probably derived from a small region of the solar system at 2 to 3 A.U., are remarkably varied. It is likely that a fifth terrestrial planet would have formed from a mixture of E, O, C and other chondritic material, if not for Jupiters gravitational influence. We suggest that the terrestrial planets may have accreted from locally formed planetesimals with similarly variable compositions, thereby eliminating the need for widespread transport of material across large heliocentric distances.

The varying compositions of meteorites and asteroids were partly inherited from the interstellar cloud and mainly produced by nebular and parent body processes. Meteorites display a wide range of chemical and physical characteristics (e.g. abundances, oxidation state, isotopes, chondrule size, amount of melting). Eight groups of primitive chondrites are known, along with the unique primitive meteorites Kakangari and Bencubbin. Discoveries of new types of primitive chondrites (e.g. ALH 85085 [2]) are expanding the range of primordial asteroid characteristics. The metal content of chondrites, for example, varies from 0 to 35 wt%. Spectral observations of asteroids reflect the diversity of materials in the asteroid belt, with 14 distinct classes concentrated in different regions of the main belt. The melting of asteroids was also highly variable, even for similar materials such as the E chondrites and E achondrites. The distribution of ^{26}Al, which was heterogeneous in some meteorites, may have resulted in variable amounts of melting, or played a role in heating asteroids to temperatures conducive for melting by electromagnetic induction heating. Such heterogeneities, including the amount of melting, may have extended into the inner solar system.

Most evidence indicates that the asteroids formed in nearly their present relative positions, although this is also disputed by a few authors [3,4,5]. The low abundance of foreign inclusions in meteorite regolith breccias argues against significant mixing across the asteroid belt. Based on the abundance of asteroidal cores and basaltic crusts, and the number of Hirayama families (thought to be broken up asteroids), modelling of asteroid collision rates suggests that the initial asteroid population was only modestly larger than it is today, implying that large scale transfer of mass out of the asteroid belt due to orbital stirring did not occur after Vesta's basaltic crust formed, presumably early [6]. These results are consistent with Patterson's [7] model of asteroid belt formation, which invokes trapping of planetesimals into resonances as they spiral toward the sun in the presence of a gas phase. The cratering record indicates separate or local populations in the inner solar system, the Jovian satellite system, the Saturnian system, and the Uranian system [8]. These separate populations argue against significant stirring across the solar system in the late stages of planetary formation. S.R. Taylor [9] argues against mixing of materials throughout the inner solar system because the chemical and isotopic compositions of the Earth and Mars do not closely match any group of primitive meteorites.

The evidence against widespread transfer of material through the solar system [10] appears to contradict many current theories of planetary formation that call upon sequential accretion of material of different compositions, such as those with diverse metal and volatile contents [11,12,13]. These models require the late accretion to the Earth of volatile-rich planetesimals, from material scattered into the inner solar system. The solution may be that the material in each nebular zone from which an inner planet formed also varied in composition. Planetary formation may involve the stochastic order of assembly of the components available in the vicinity of each planet. This could, for example, explain the evidence from siderophile elements that the SNC parent body (Mars) accreted homogeneously, while the Earth accreted heterogeneously [11].

CONCLUSIONS: The planets in the inner solar system may have accreted from locally derived planetesimals which had widely varying compositions and thermal histories, similar to the mix of asteroids observed in the present asteroid belt. The accretion of different zones may have in some cases emphasized the local structure, resulting in heterogeneous accretion, and in other cases resulted in homogeneous accretion.

References: [1] Lewis (1973) Ann. Rev. Phys. Chem. 24, 339 [2] Scott (1988) Lunar Sci. XIX, 1049 [3] Wetherill (1985) Science, 877 [4] Wasson (1985) Meteorites, Freeman [5] Hartmann (1987) Lunar Sci. XVIII, 389 [6] Davis et al. (1985) Icarus 62, 30 [7] Patterson (1987) Lunar Sci. XVIII, 766 [8] Strom (1987) Lunar Sci. XVIII, 966; Lunar Sci. XIX, 1141 [9] S.R. Taylor (1988) in Meteorites, U. Ariz. [10] Drake (1987) J. Geophys. Res. 92, E377 [11] Dreibus & Wanke (1987) Lunar Sci. XVIII, 248 [12] Newsom & Palme (1984) Earth Planet. Sci. Lett. 69, 354 [13] Pepin (1987) Eos 68, 1337. Supported by NASA grant NAG 9-30 (K. Keil, P.I.).

TROJAN ASTEROID LIGHTCURVES: CONTINUING WORK; William K. Hartmann, Planetary Science Institute, Tucson, AZ 85719

Last year, Hartmann, Tholen, Cruikshank, and Goguen (1) reported the unexpected discovery that Trojan asteroid lightcurves appear to contain more high amplitudes than among main belt asteroids. This result is important because it may imply information about Trojans' origins and histories. We hypothesized that because of the low collision frequency among the Trojans, more primordial bodies may be preserved, and they may have more irregular shapes. This work has now been published by Hartmann, Tholen, Goguen, Binzel, and Cruikshank (2).

Further observations are underway to attempt to confirm these results. Coordinated, complimentary work is being done by our group and by Linda French and co-workers. Figure 1 shows the status of our current set of data. This new figure includes recent three additional asteroids observed by Tholen, subsequent to our earlier work. More observations are needed to enlarge the sample, but the peculiarity of the Trojan-Hilda sample remains prominent. We need to understand its cause!

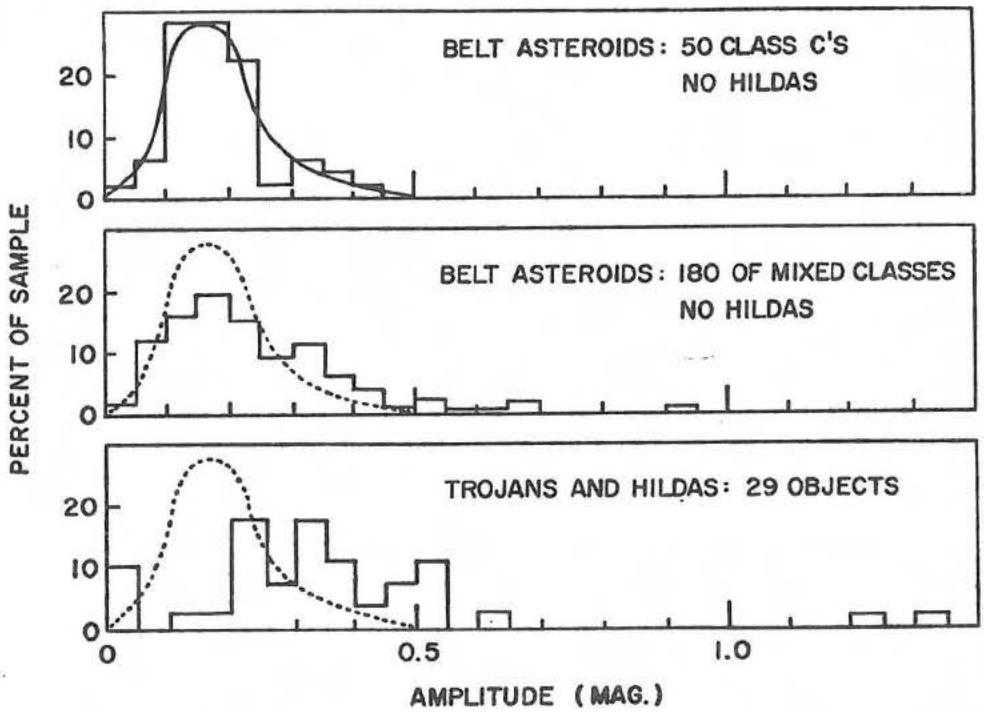

Figure 1. Comparison of distributions of maximum observed amplitudes among belt asteroids (top, center) and Trojans and Hildas (bottom). All samples are for the same diameter range, 42 - 188 km. Dotted lines repeat the distribution sketched in the top figure, for reference.

References

(1) Hartmann, W., D. Tholen, D. Cruikshank, and J. Goguen (1987). Meteoritics 22, 399-400.

(2) Hartmann, W., D. Tholen, J. Goguen, R. Binzel, and D. Cruikshank (1988). Icarus 73, 487-498.

GRANT COUNTY OREGON DAYLIGHT FIREBALL OF October 23, 1987

Richard N. Pugh, Science Department, Cleveland High School, Portland, Oregon and
Daniel J. Kraus, Chief Research Assistant, Pine Mountain Observatory, University of Oregon

A very large daylight fireball occurred at approximately 2:35 P.M. Pacific Daylight Time, October 23, 1987. The fireball was seen over about 186,000 sq. km of Washington and Oregon. It entered the atmosphere over south central Washington at a shallow angle. The angle became steeper as the object fell, until the fireball reversed direction just before it exploded. The end point of the fireball was 24 km, south of Monument, Oregon, latitude 44 degrees 30', longitude 119 degrees 24'. The fireball was very bright casting shadows in the daylight. Observers in front of the fireball reported it having a diameter of up to 10 times that of the sun. Most observers report a multi-colored bolide with a long tail producing flames, sparks, and smoke.

The fireball blew up at an altitude of about 24 km producing a large blue-white cloud with a black to brown center. The dust cloud appears to have fallen through a thin overcast that was at 6 km. One observer directly under the explosion reported seeing dark specks fall out of the center of the cloud. The dust cloud persisted for over 30 minutes.

Rumblings and sonic booms were heard over about 25,000 sq. km at central Oregon. Most observers heard or felt from one to three very heavy sonic booms, followed by up to 35 pops or cracks like large firecrackers.

There were two reports of people smelling the event. One reported the smell of sulfur, the other the odor of "hot metal". There were several reports of anomalous sound. The furthest was 300 km from the end point of the fireball.

There were three reports of strange animal behavior shortly before the fireball was seen or heard; two were horses acting up, the other was the reaction of dogs just prior to the event.

This information is based on two hundred interviews of people who saw or heard the fireball.

NOBLE METAL ABUNDANCES IN EARLY ARCHEAN SPHERULE LAYERS FROM SOUTH AFRICA

Frank T. Kyte, Institute of Geophysics and Planetary Physics, University of California, Los Angeles, CA 90024
Donald R. Lowe and Gary R. Byerly, Louisiana State University, Baton Rouge, LA 70803

Layers of altered spherules in Early Archean (3.2 to 3.5 Ga) sedimentary deposits from the Fig Tree Group, Barberton Greenstone Belt, South Africa and the Warrawoona Group, Eastern Pilbara Block, Western Australia have been interpreted as the oldest known impact deposits on Earth (1). Three spherule layers have been identified in South Africa and one in Australia. These layers contain high concentrations of spherules, some of which have relict quench textures. Individual layers can be identified in outcrops separated by distances of up to 50 km.

Recent analyses of these spherule beds (2) have shown that all four layers contain high concentrations of Ir relative to surrounding sediments. The excess Ir is particularly anomalous in the youngest two spherule beds from South Africa. Samples from bed S3, the uppermost Fig Tree layer have been observed to contain Ir concentrations as high as 162 ng/g and samples from Fig Tree bed S2 have yielded Ir concentrations as high as 76 ng/g. Iridium concentrations of 5 to 10 ng/g in the other two layers are an order of magnitude higher than in surrounding sediments, but not much greater than in hi-Mg komatiites (0.5 to 5 ng/g Ir) found elsewhere in the section.

As a test of the hypothesized impact origin for these spherule beds, we have begun to analyze a suite of noble metals - Ir, Au, Pt, Os, and Pd in the most Ir-rich samples. In our first experiment, we have found that all of these elements are easily detectable in a sample from bed S3 and preliminary data for Ir, Au, Pt, and Os all show element/Ir ratios within a factor of two of those ratios in CI chondrites. Chemical yield data are not yet available for Pd, but we estimate that this element also has a roughly chondritic abundance relative to Ir.

These spherule beds and most of the other rock units in the Fig Tree Group have been heavily altered by metasomatic processes, primarily resulting in removal of most of the mobile elements and replacement of most minerals by quartz and phyllosilicates. However, relatively immobile elements (e.g., Al, Ti, REE) appear to reflect the original concentrations of the precursor rocks. The high concentrations and roughly chondritic abundances of 4 or 5 noble metals are unlikely to be an artifact of alteration and probably reflect the composition of the source material.

References:

(1) Lowe D.R. and Byerly G.R. (1986) Geology 14, 83-86.
(2) Lowe D.R., Asaro F. and Byerly G.R. (1988) Lun. Plan. Sci. XIX, 695-696.

NITROGEN ISOTOPE GEOCHEMISTRY OF A K-T BOUNDARY SITE IN NEW ZEALAND

Iain Gilmour*, Stuart R. Boyd† and C.T. Pillinger†
*Enrico Fermi Institute and Dept. of Chemistry, University of Chicago, Chicago, IL 60637;
†Dept. of Earth Sciences, The Open University, Milton Keynes MK7 6AA, U.K.

Nitrogen in the basal layer of the K-T boundary clay at Woodside Creek, New Zealand, has an abundance of 1100 ppm, a 20-fold enrichment over Cretaceous and Tertiary values (figure). The enrichment parallels that for Ir and elemental carbon (soot) (1); all decrease over the next 6 mm of the boundary clay. The C/N ratio, assuming the nitrogen to be associated with organic rather than elemental carbon, is approximately 5 for the basal layer compared to 20-30 for the remainder of the boundary clay. The correlation between N and Ir abundances appears to persist above the boundary, implying that the N is intimately associated with the primary fallout and remained with it during the secondary redeposition processes that kept the Ir abundance relatively high into the lowermost Tertiary.

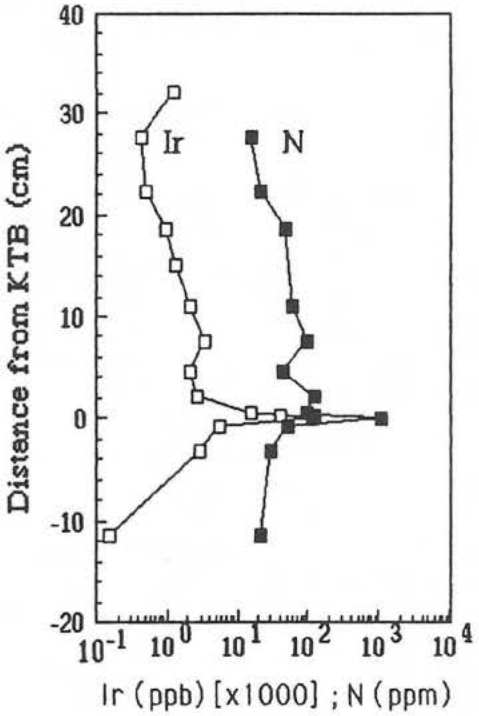

$\delta^{15}N$ is +2.0‰ in the basal layer, but decreases to -4.4‰ at the top of the boundary and -8.2 ‰ in the lowest Tertiary sample, compared with -8.1‰ for the sample immediately below the boundary. Apparently the basal layer of the boundary clay represents the accumulation of a substantial quantity of nitrogen with an isotopic composition approximately 10‰ heavier than background $\delta^{15}N$ values. It is conceivable that this shift in $\delta^{15}N$ may represent an influx of nitrogen from a different source, perhaps deposited contemporaneously with the impact ejecta. An interesting possibility is that it may be derived from nitrate, produced from the combustion of atmospheric nitrogen as proposed by Lewis *et al.* (2). However, it is unclear whether such nitrogen could be biologically assimilated or otherwise rendered insoluble in the presumably short time prior to the fallout of ejecta or before a decrease in pH killed surface water planktonic species.

References.

1. Wolbach W.S. *et al.*(1988) Nature (in press). 2. Lewis J.S. *et al.* (1982) GSA Spec. Publ 190.

THE MEASUREMENT OF OSMIUM ISOTOPES IN SAMPLES FROM A CRETACEOUS/TERTIARY (K/T) SECTION OF THE RATON BASIN, U.S.A.

U. Krähenbühl[1], M. Geissbühler[1], F. Bühler[2] and P. Eberhardt[2];
1 Laboratorium für Radiochemie, University of Bern, Switzerland;
2 Physikalisches Institut, University of Bern, Switzerland.

The ^{187}Os / ^{186}Os ratio in geochemical samples is influenced by the decay of ^{187}Re and the degree of fractionation of Re and Os during the formation of the material of interest. Osmium from meteorites and from the earth mantle have ^{187}Os / ^{186}Os ratios close to unity, whereas material from the crust of the earth manifests a ratio of about 10 (1). Our technique for separation of nanogram quantities of Os out of up to 5 g of material will be presented. Good yields and negligible blank contributions were obtained in the two OsO_4 distillations necessary for the purification.

The measurements of the Os isotopes were made on a modified Cameca ion probe using the high mass resolution mode.

Results for samples of a section across the K/T boundary at the Raton Basin will be presented. They indicate the admixture of non-crustal material.

(1) Science 222 613 (1983)

THE KARA IMPACT STRUCTURE (USSR) AND THE K/T-BOUNDARY EVENT.

C. Koeberl[1,2], A.V. Murali[1], M.A. Nazarov[3], V.L. Sharpton[1], and K. Burke[1]
(1) Lunar and Planetary Institute, Houston, TX 77058 (2) Inst. of Geochemistry, Univ. of Vienna, A-1010 Vienna, Austria (3) Vernadsky Inst. of Geochem. and Analyt. Chemistry, USSR Academy of Sciences, Moscow 117975, USSR.

The Kara impact structure is located north of the Ural mountains at the shore of the Kara Sea at about 69° 10' N and 65° 00' E and consists of two adjacent impact craters, the Kara crater (55 km diameter) and the Ust-Kara crater (25 km diameter). The Ust-Kara crater is mostly underwater and just grazes the shore at Cape Polkovnik (at the Kara estuary) where the only outcrops of Ust Kara-impactites and suevites are found. Although suevites and impactites from the Kara crater have been known since the beginning of the century, they have been mistaken for glacial deposits. Only about 15 years ago the impact origin nature of the structure was recognized. In 1987 a Soviet expedition of four scientists (including one of us, M.A.N.)spent about two months in the area collecting samples of target rocks and impactites. The Kara crater is situated in a marshy tundra environment and is poorly discernable. It has a central uplift (with diabasic rocks) and a ring syncline structure. The area features a number of small lakes and several rivers, the largest of which is the Kara river. All impactite outcrops are situated at places where the rivers cut across the crater rim. Impact melts occur in the form of large intrusive bodies and dykes, not unlike normal basalt flows. Numerous suevite deposits are also present in places exposed by the rivers, often accompanied by large (up to > 1m) shattercones.. The target rocks of the Kara crater that have been collected at the Saayakha river (and Ust Kara target rocks from the Kara Sea shore) consist mainly of Permian shales and sandstones, while a few places near the Kara river expose also Paleozoic limestones and diabases. The target rock variations are mirrored by the composition of the clasts present in suevites. Shocked magmatic rocks are of diabasic or dioritic composition, although most samples are heavily shocked, so the rocks are not easily identified. Impact glasses are heterogeneous, and show layering, inclusions, and colors ranging from translucent white over brown to black, not unlike some zhamanshinites. About 50 samples of target rocks, shocked country rocks, suevites, impact melts and impact glasses are currently analyzed for major and trace elements in order to establish a geochemical relationship between target rocks and impactites, the degree of impact mixing, and the presence of possible cosmic component. Preliminary K-Ar ages of impact glasses range from 65-68 My, thus being close to the K/T-boundary. Ar-Ar analyses of shocked country rocks, suevites, impact melts,and impact glasses are currently being made and will hopefully constrain the ages of the two craters in relation to the K/T boundary. If the Kara impact structure is of the correct age, the possibility of a connection with the K/T boundary event should be considered.

IMPACT WAVE DEPOSITS AT THE CRETACEOUS/TERTIARY BOUNDARY IMPLY AN OCEANIC IMPACT SITE NEAR NORTH AMERICA; A.R. Hildebrand and W.V. Boynton, University of Arizona, Tucson, AZ 85721

An array of chemical, physical and isotopic evidence indicates that an impact of a comet or asteroid in the terrestrial ocean terminated the Cretaceous Period. Simulations of such an oceanic impact indicate that giant waves would have radiated from the impact site, washing onto adjacent continents (1). We have performed a stratigraphic analysis and INAA study of the Brazos River, Texas K/T locality (2) and suggest that this site contains an example of a giant wave deposit produced by a nearby impact.

We examined and sampled this marine section and found two clay layers with thicknesses corresponding to the fireball and outgassing layers as preserved at other North American K/T boundary sites. Two confirmed Ir anomalies, separated by 20 cm, which apparently correspond to these two layers, have been reported for this section (3). We have analyzed the section using INAA, discovering Au and Re anomalies associated with the fireball and outgassing layers. The 2 mm fireball layer also has associated weak chalcophile element anomalies (e.g. As,Sb,Se) consistent with its composition at other localities. Therefore, we tentatively interpret the two layers as the outgassing and fireball layers which are here interbedded with coarse giant-wave deposits.

Paleontological evidence indicates this K/T boundary section which was deposited in 100-150 m of water. The boundary section lies on an irregular surface, eroded into the Cretaceous marl; the initial deposits are coarse skeletal sands, overlain by rippled calcarenite. The 20 mm outgassing layer then occurs containing abundant well-preserved Cretaceous microfossils, which may represent an initial kill from lethal effects of the impact. The interval between the two impact layers is barren of all macrofossils and only a few poorly preserved microfossils are present in the upper half of the interval. The 6 cm micrite immediately overlying the ejecta layer is enigmatic in that it is a limestone layer that contains no fossils of any sort, and it is uniform in thickness over the region in contrast to the coarser units. The remainder of the barren interval is similar to the underlying micrite, although it contains several percent of opaque organic material and a significant clay fraction. The 2 mm fireball layer was apparently deposited contemporaneously, at least in part, with a pulse of sand which formed an immediately overlying 20 mm unit. In the marl above this unit the first Danian (Tertiary) fossils appear.

Similar coarse deposits with associated Ir anomalies have been described from marine K/T boundary sections in Alabama and Haiti (4,5). These data suggest the K/T impact site was near southern North America. An impact site near North America is also indicated by the restricted geographic distribution of the outgassing layer, the gradation of shocked mineral grain sizes and proportions, the gradation of spinel phase compositions, and local severity of floral extinctions.

References. (1) Ahrens, T.J. and O'Keefe, J.D., 1983, Proceedings of the Thirteenth Lunar and Planetary Science Conference, Part 2. Journal of Geophysical Research 88: Supplement, A799-A806. (2) Jiang, M.J. and Gartner, S., 1986, Micropaleontology 32:232-255. (3) Ganapathy, R., Gartner, S. and Jiang, M.J., 1981, Earth and Planetary Science Letters 54:393-396. (4) Jones, D.S., Mueller, P.A., Bryan, J.R., Dobson, J.P., Channell, J.E.T., Zachos, J.C. and Arthur, M.A., 1987, Geology 15:311-315. (5) Maurrasse, J.-M.R., 1986, Geological Society of America, Abstracts with Programs, p. 686.

CHEMICAL SPECIATION STUDY OF ANOMALOUS IRIDIUM FROM K-T BOUNDARY; C.F.Chai and P.Kong (Institute of High Energy Physics, Academia Sinica, P.O.Box 2732, Beijing, China)

By means of a newly-developed chemical dissociation procedure, we studied the distribution patterns of Ir, Au, Ni, Co, Fe, As and Sb in the Cretaceous-Tertiary(K-T) boundary samples taken from the Stevns Klint, Denmark, and Montana, USA, the Ningqiang chondrite (CV3) and the Baoxian chondrite (LL4), and ultrabasic rock from the Saltohai, Xinjiang, China, in order to reveal the origin of excess iridium. The samples were chemically divided into 6 phases, i.e. carbonate, Fe-Ni metal, sulfide, oxide, silicate and insoluble residue in strong HF medium. The weight fractions (%) of each phase in the K-T boundary is 25.7 (carbonate), 9.1 (Fe-Ni), 22.5(sulfide), 12.2 (oxide), 25.7(silicate) and 4.7 (HF-insoluble residue), while its Ir relative abundance (%) is 4.3, 25.0, 0, 12.3, 0 and 58.6, respectively. It implies that although the residue phase only constitutes less than 5 % of its parent sample in weight, it contains over 50 % Ir of total, with an enrichment factor of above 40 relative to the source material.

The Ir speciation results of the K-T boundaries including marine and continent sediments are similar to those of the Ningqiang chondrite, but show large discrepancy with those of the ultrabasic rock, which seems to favour the extraterrestrial origin of the anomalous iridium.

This work is supported by National Natural Science Foundation of China (NSFC).

K-T BOUNDARY CLAYSTONE IS A DISTAL EJECTA BLANKET; B.F. Bohor, U.S. Geological Survey, Box 25046, MS 901, DFC, Denver, CO 80225

Nonmarine claystones at the Cretaceous-Tertiary (K-T) boundary at two sites in Wyoming (1,2) display visual evidence of ballistic ejecta products (glass bombs and lithic clasts) not previously recognized at other sites in the Western Interior. A strong color contrast between bombs and matrix in the basal kaolinitic layer at these two sites is due to selective replacement and staining by secondary goyazite. The massive quenched glass bombs were replaced by light tan to white kaolinite before the goyazite mineralization of the spherules and reddish-brown staining of the porous, fine-grained matrix occurred. Depression of matrix layers beneath the bombs and clasts indicates ballistic emplacement of these latter elements into the kaolinitic layer.

Identification of the kaolinite masses as altered glass bombs was enhanced by the discovery within them of relict vesicles and "threads" of mineral glass, along with quartz and other mineral grains in bands showing flow structure. Quartz grains displaying shock lamellae occur in the surrounding matrix. The bombs occur as ovoid masses and pancake-shaped "fladen". These shapes and textural features are similar to impact glasses and lithic clasts found in the Ries crater suevite (3,4) and the Late Eocene distal ejecta blanket layer at DSDP Site 612 (5,7). The hollow goyazite spherules in the basal layer are probably altered microtektites (8).

The presence of altered glass bombs, lithic clasts, probable microtektites, and shock-metamorphic features in mineral grains in the basal kaolinitic layer of these boundary claystones strongly suggests that it is part of an ejecta blanket. Together with the thin overlying layer composed of high-angle ejecta and vaporized bolide components, the claystone unit comprises a distal ejecta blanket similar in almost all respects to known blankets at the Ries crater and Site 612. The relatively greater thickness of this claystone unit in the Western Interior compared to other sites worldwide helps confirm the hypothesis of a North American continental impact site that was previously based only on the maximum size and mineralogy of shocked quartz grains (9).

REFERENCES: (1) Bohor, B.F. et al. (1987) Geology 15, p. 896-899; (2) Wolfe, J.A. and Izett, G.A. (1987) EOS 68, p. 1344; (3) Stahle, V. (1972) Earth Planet. Sci. Lett. 17, p. 275-293; (4) Horz, F. (1965) Beitr. Mineral. Petrog. 11, p. 621-661; (5) Bohor, B.F. et al. (1988) Lunar Planet. Sci. Conf. XIX, p. 114-115; (6) Glass, B.G. (1987) Lunar Planet. Sci. Conf. XVIII, p. 328-329; (7) Thein, J. (1987) In Poag, C.W., Watts, A.B. et al., eds. Init. Repts. DSDP, Leg 95 XCV, p. 565-579; (8) Bohor, B.F. and Betterton, W.J. (1988) this volume; (9) Bohor, B.F. and Izett, G.A. (1986) Lunar Planet. Sci. Conf. XVII, p. 68-69.

ARE THE HOLLOW SPHERULES IN K-T BOUNDARY CLAYSTONES ALTERED MICROTEKTITES?; B.F. Bohor and W.J. Betterton, U.S. Geological Survey, Box 25046, MS 901, DFC, Denver, CO 80225

At two Cretaceous-Tertiary (K-T) boundary sites in the southern part of the Powder River basin in Wyoming (1,2), hollow goyazite spherules occur in the basal kaolinitic layer of a dual-layered claystone unit that comprises a distal ejecta blanket (3). Prior to the identification of the basal layer as part of an ejecta blanket containing ballistically emplaced altered glass bombs, lithic clasts, and shocked quartz grains (3), it was hypothesized that the spherules were analogous to hollow fly ash spherules and were formed by the devolatilization of lower crustal rocks exposed at the base of the impact crater (4). This hypothesis may be no longer tenable because of problems of timing and spherule forms.

Microtektites are common components of known ejecta blankets, such as the Ries fallout suevite (5) and the Late Eocene distal ejecta layer in a core at DSDP Site 612 in the northwest Atlantic Ocean (6). Because all the other identified components of the basal layer are similar to those found in known ejecta blankets, the spherules should correspond to microtektites--the one major component not previously recognized as common between the basal layer and the known ejecta blankets.

The sizes, shapes (rotational splash forms), and surface features of microtektites and K-T spherules are exactly the same. Infolded surfaces or cracks can be recognized in both forms. However, the microtektites are solid glass and the Wyoming K-T spherules are hollow, with goyazite walls. One scenario explaining the hollow aspect of the spherules invokes transportation of the glassy microtektites from the crater in a hot, turbulent cloud through the lower atmosphere. Suspension in this hot cloud over significant distances from the crater site would allow enough time for devitrification to commence on the perimeter of the spherules, forming a thin wall of crystalline material surrounding a glass core. Alternatively, the microtektites may have been ballistically emplaced and annealed during reentry heating. After deposition of the spherules, diagenetic solutions dissolved the glassy cores and replaced the crystalline walls with goyazite. The wall structures also resemble artificial weathering rinds on some natural and artificial glasses (7). In some ways, the K-T spherules resemble cpx-type spherules as much as they do ordinary glassy microtektites. Thus, the hollow goyazite K-T spherules may have been originally glassy microtektites or cpx spherules that have been modified by devitrification and/or weathering, dissolution over time, and replacement and partial filling by phosphatic solutions.

REFERENCES: (1) Bohor, B.F. et al. (1987) Geology 15, p. 896-899; (2) Wolfe, J.A. and Izett, G.A. (1987) EOS 68, p. 1344; (3) Bohor, B.F. (1988) this volume; (4) Bohor, B.F. and Triplehorn, D.M. (1987) Lunar Planet. Sci. Conf. XVIII, p. 103-104; (5) Graup, G. (1981) Earth Planet. Sci. Lett. 55, p. 407-418; (6) Thein, J. (1987) In Poag, C.W., Watts, A.B. et al., eds. Init. Repts. DSDP Leg 95, XCV, p. 565-579; (7) Malow, G. et al. (1984) J. Non-Cryst. Solids 67, p. 305-321.

GEOCHEMICAL ANOMALY ACROSS THE ORDOVICIAN-SILURIAN (O-S) BOUNDARY, YICHANG, CHINA, AND THEIR IMPLICATIONS;

C.F.Chai, J.G.Ma, P.Kong, Y.Q.Zhou, S.L.Ma (Institute of High Energy Physics, Academia Sinica, P.O.Box 2732, Beijing, China) and X.F.Wang (Yichang Institute of Geological Sciences, P.O.Box 275, Yichang, China)

We studied elemental abundance variations across a O-S boundary(440 m.y. ago) at Fengxiang, Yichang, Eastern Yangtze Gorges, China, where the paleontological work has been carefully done for many years, to examine whether the Ir anomaly similar to that at the Cretaceous-Tertiary boundary is present.

The Fengxiang O-S section is well exposed and yields abundant graptolites, comprising a complete graptolite succession from the latest Ordovician (Wufengian) to the earlist Silurian (early Longmaxian).

We determined the contents of Ir and other 40 elements across the O-S section by radiochemical and instrumental neutron activation. The Ir contents from 0.05 ppb at the late Ordovician increase to 0.64 ppb just at the O-S boundary, then decline to about 0.10 ppb at the upper Longmaxi Fm. The evident Ir anomaly is different from that across the Dob's Linn section reported by Wilde, et al.(1986). The reason may be rarity of fossils in the Dob's Linn sequence, which makes it difficult to define the exact O-S boundary.

Wilde et al.(1986) indicated that correlation of Ir with other elements, except for Cr, was not found to be significant. Our results do not agree with theirs. Ir of the Fengxiang section exhibits positive correlation with the siderophile elements (Au, Ni and Co), as well as with the chalcophile elements (As and Sb), besides Cr. The contents of Au, Ni, Co, As and Sb at the O-S boundary are (ppm) : 0.0166, 527, 20.1, 54.5 and 27.2, respectively. Our results do not support the conclusion that the high Ir background abundances may be from erosional contribution from chromium-bearing minerals.

The geochemical anomaly, supported by carbon isotope excursion and paleomagnetic evidence, of the O-S section implies a sudden event happened at the end of the Ordovician.

Finally, it should be emphasized that the O-S boundary should be placed between the Hirnamtia-Kinnella Zone and G. persculptus Zone, where the geochemical anomaly, isotope excursion and paleomagnetic variation occur, instead of the base of the P. acuminatus.

This work is supported by National Natural Science Foundation of China (NSFC).

Wilde, P., et al., (1986) Science, v.233, p.339.

PLENARY V

LEONARD ADDRESS

ENSTATITE METEORITES AND THEIR PARENT BODIES. Klaus Keil, Dept. of Geology, Institute of Meteoritics, Univ. of New Mexico, Albuquerque, N.M. 87131, USA.

Enstatite chondrites (E) and achondrites (aubrites, A) have identical oxygen isotopic compositions, indicating formation from similar starting materials in the same general region of the solar nebula. Here I discuss their properties and the nature and number of their parent bodies.

Conclusions: 1. EH and EL show bulk compositional differences that were established by nebular, not planetary processes. Occurrence of abundant breccias among them but lack of clasts of EL in EH (and vice versa) suggests that EH and EL represent two separate parent asteroids.

2. (A) were not derived from known (E) by melting and fractionation on the same parent body (1). Arguments by (2) to the contrary are not convincing [e.g., there is insufficient (≈0.5%) CaS in (E) to produce abundant (up to 20%) diopside in (A) by an oxidation reaction with enstatite, and thermal metamorphism of (E), which contain carbon, is reducing, not oxidizing; there is no evidence that (A) formed from (E) in large asteroids where high pressure could have caused the En-Fo peritectic line to be displaced away from SiO_2 rel. to 1 atm., to crystallize the abundant Fo in (A)].

3. Shallowater (S) is the only unbrecciated, igneous (A) (3). It contains 80% large (up to 4.5 cm) opx crystals poikilitically intergrown with small opx; the large crystals contain xenoliths (X) of ol-low-Ca cpx-plag-Fe,Ni-FeS-schr (20%). a) (S) is of igneous origin, as is indicated by the poikilitic texture, corroded ol, melt inclusions and +Eu anomaly. b) Presence of (X) within opx suggests that (S) is an impact, not internally derived melt. c) High abundance of opx suggests that the target was essentially pure pyroxenite and not material of (X) composition, because a melt of (X) would not crystallize pure opx. Presumably it also requires that the (S) body had large volumes of pure opx. d) (S) cannot be an impact melt from the EH or EL bodies, because an essentially pure opx target and, thus, a differentiated body is required, and because high-T quench of (S) melt would prohibit extensive fractionation. Also, (S) has a +Eu anomaly but lower plag (2.5 vs. up to 16%) and only a trace of CaS (vs. 0.5%) than known (E). Furthermore, (E) contain only kam, whereas (S) has abundant kam + tae, incompatible with an origin of (S) from (E). e) The (A) body cannot be the parent asteroid of (S) because most (A) contain abundant diopside and have negative Eu anomalies, and impact melts of (A) would not crystallize pure opx nor would they have +Eu anomalies. Thus, (S) probably formed on a fourth enstatite asteroid. f) (S) experienced a 3 stage cooling history. Stage 1, quench, thousands °/hr of (S) melt from ≥1580° C to somewhere above 712° C, as indicated by preservation of twinned low-Ca cpx in major opx, lack of reaction of plag, and presence of abundant Fe,Ni and FeS that did not segregate from the melt. Stage 2, very slow cooling: Calculations (courtesy A.D. Romig) for Fe,Ni of 9.2% Ni, 0.1% P indicate kam nucleation at 712° C and cooling to 680° C at <7.5° C/my. Uncertainties due to ≈1% Si in Fe,Ni may make this rate at most 3-5x faster. Stage 3, fast cooling: Kam-tae compositions indicate cooling rates of >0.5/day from 680-600, > 0.4/day from 600-400, >0.1/day from 400-300 (in ° C). g) This complex cooling history suggests the following origin for (S). Model 1: A partly molten asteroid of nearly pure opx composition was broken up by low-velocity impact with a solid E-like object. Fragments were quenched due to their small sizes and incorporation of cold (>20%) projectile debris (X). That the projectile was E-like is indicated by mineral compositions and chondritic Ni/Ir [(S) 22; Hvittis 24; CI 23; x10³]. Fragments reassembled into the (S) asteroid while T >712° C, and deeply buried objects cooled very slowly from 712-680° C. Excavation by impact(s) accounts for fast cooling from 680° C. Model 2: Impact into pure opx on solid (S) asteroid produced an opx melt that quenched due to incorporation of cold regolith (X), cooled very slowly due to deep burial under hot, thick ejecta blanket, and subsequently cooled fast due to impact excavation(s). This model is unlikely because a cooling rate of ≈7.5° C/my, even when assuming a lunar regolith thermal diffusivity of the ejecta blanket, requires burial at the center of a ≈14 km thick blanket. This is unrealistically thick for an asteroid-sized object.

4) It is unknown what caused some enstatite meteorite parent asteroids to melt (A, S), whereas others remained unmelted (EH, EL). Potential reasons may be differences in accretionary heating due to mass differences and rate of accretion, which may or may not result in sufficiently high initial temperatures conducive for melting by induction heating; or time of accretion relative to decay of ^{26}Al.

Supported by NASA grant NAG 9-30. References: (1) Keil, K. (1969), EPSL 7, 243-248. Brett, R. and Keil, K. (1986), EPSL 81, 1-6. (2) Fogel, R.A. et al. (1988), LPSC XIX, 342-343. (3) Ntaflos, Th. et al. (in prep.).

PLENARY VI

BARRINGER ADDRESS

CIRCULAR ARGUMENTS: PEAKS AND TROUGHS IN THE CRATER GAME.

M.R. Dence
Royal Society of Canada, Ottawa, Ontario, Canada

While there has been considerable progress in understanding and modeling the early stages of impact crater formation, there is little evidence of consensus in the analysis of the later stages, particularly those which result in morphologically and structurally complex craters. For example, craters on various planetary bodies continue to be analyzed in terms of slow yielding following initial formation of deep bowl-shaped cavities. Those workers who accept the alternative of rapid modification of crater form are divided on the interpretation of the physical process involved and the structural significance of morphological features such as peaks, rings and troughs. A review of the structural, geophysical and petrographic evidence from terrestrial craters underlines the consistency of the evidence in favour of rapid modification, low strength late into the modification stage and the secondary role played by structural discontinuities. Intriguing complexities in the centres of large craters may help explain some outstanding enigmas of Sudbury, the ultimate challenge in the understanding of craters on Earth.

From another perspective, structural variation in impact craters is a metaphor for abrupt change in many natural systems.The possibility of surprising, possibly devastating changes, due to human activity as well as nature, is now gaining international attention under the Global Change program, possibly the ultimate challenge to science and humanity.

PLENARY VII

INVITED PAPER

INTERSTELLAR GRAINS IN METEORITES: DIAMOND AND SILICON CARBIDE

Edward Anders and **Tang Ming**, Univ. Chicago, Chicago, IL 60637-1433, USA
Ernst Zinner, Washington University, St. Louis, MO 63130, USA

Matrices of primitive chondrites contain grains of diamond ("Cδ"; ~25 Å and ~400 ppm; *1*) and several kinds of SiC ("Cβ", "Cϵ"; ~0.03-4 μm and ~7 ppm; *2,3*). These grains apparently are interstellar, being tagged with isotop-ically anomalous noble gases [Xe-HL, Xe-S, and Ne-E(H)], and showing large anomalies in C, N, and Si (*4,5,6,7*). The survival of noble gases indicates that these grains were not heated appreciably on or after arrival in the solar system--in contrast to the presolar components in CAI and chondrules--and thus are well-preserved samples of interstellar matter.

Both minerals can condense from stellar atmospheres, but only at C/O >1, well above the solar ratio of 0.6 (*8*). SiC is a stable phase under these conditions, and has actually been observed in circumstellar shells. Diamond is metastable relative to graphite, but can form preferentially under special conditions (*1,8*). On the ion probe, SiC shows large isotopic variations for Si, C, and N, suggesting that it comes from several stars rather than one (*6,7*).

The SiC grains are older than the solar system, but apparently not by much (*3,10*). Cϵ-SiC, the carrier of Ne-E(H), contains some Ne^{21}, of which ≤5% comes from the recent cosmic-ray exposure of the meteorite. The rest, if cos-mogenic, corresponds to a presolar exposure age of 50 (+75,-30) Myr (*10*), much shorter than the estimated mean lifetime of refractory interstellar grains, 500-1000 Myr. Either this lifetime has been overestimated or the solar system formed in part from atypically young material (*10*).

The isotopic anomalies of SiC and diamond are 10^1-10^3x larger than those for anomalous oxide minerals (*6*). One reason is the resistance of SiC and diamond to alteration by heat and liquid water. Another is the low C/O ratio of the solar system, which precludes formation of "local" SiC and diamond that might dilute their "exotic" counterparts. A third reason is that SiC and diamond occur in matrix, whereas anomalous oxide minerals occur--or at least are sought--in more strongly heated parts of chondrites, i.e. CAI and chondrules. Thus meteoritic SiC and diamond are two rather transparent windows--or at least peepholes--on the galaxy, which may provide a few glimpses of the prehistory of the solar system.

(*1*) Lewis R. S., Tang M., Wacker J. F., Anders E., and Steel E. (1987) *Nature* 326, 160-162.
(*2*) Tang M. and Anders E. (1988) *Geochim. Cosmochim. Acta*, in press.
(*3*) Tang M. and Anders E. (1988) *Geochim. Cosmochim. Acta*, in press.
(*4*) Swart P. K., Grady M. M., Pillinger C. T., Lewis R. S., and Anders E. (1983) *Science* 220, 406-410.
(*5*) Lewis R. S., Anders E., Wright I. P., Norris S. J., and Pillinger C. T. (1983) *Nature* 305, 767-771.
(*6*) Zinner E., Tang M., and Anders E. (1987) *Nature* 330, 730-732.
(*7*) Tang M., Anders E., and Zinner, E. (1988) *Lunar Planet. Sci.* 19, 1177-1178.
(*8*) Larimer J. W. and Bartholomay M. (1979) *Geochim. Cosmochim. Acta* 43, 1455-1466.
(*9*) Saslaw W. C. and Gaustad J. E. (1969) *Nature* 221, 160-162.
(*10*) Tang M. and Anders E. (1988) *Nature*, submitted.

NEBULAR PROCESSES ASSOCIATED WITH CAI RIM FORMATION, W.V. Boynton, Lunar and Planetary Laboratory, University of Arizona, Tucson.

The origin of the thin (50 μm) rims on Ca,Al-rich inclusions (CAI) has not been well understood until recently. It now seems clear that the rims are a refractory residue formed by a flash heating of the CAI surface. This work will review the evidence for rim formation by flash heating and discuss the astrophysical constraints the process puts on conditions in the solar nebula.

Evidence that CAI rims formed as a residue. Boynton and Wark (1) found that REE patterns in rims were identical to those in the underlying CAI except that 1) the concentrations of the REE were higher in the rim by factors of three to five, and 2) the most volatile REE, Eu and sometimes Yb, were depleted. These observations were found regardless of whether the original REE pattern was unfractionated, fractionated as a smooth function of size due to mineral preference effects, or fractionated in an irregular way (Group II pattern) due to REE volatility. Formation from the underlying material is the only way to account for the similarity of these patterns. They suggested that the flash heating formed a thin melt zone. After the melt quenched, the multiple, mono-mineralic layers were generated by a solid-state metasomatism with the addition of Mg and Si from the environment.

Two criticisms of this model have been suggested, but neither is valid. Fahey et al. (2) noted that the rim is isotopically lighter in Mg than the interior, contrary to expectations of a refractory residue. What is relevant, however, is that the rim is normal in isotopic composition, and the interior is isotopically heavy. This result is expected since the Mg in the rim is the result of the metasomatism, not the flash heating. Laughlin et al. (3) noted that the REE content of the rim perovskites were similar to those of the interior and suggested that the enrichment of REE in the rim is merely due to an over abundance of perovskite in the rim. Since Ti is a highly refractory element, and perovskite is the major carrier of Ti, it follows that the flash heating would be expected to maintain a nearly constant REE/perovskite ratio.

Astrophysical Constraints. If the surface of a spherical, 1 cm. diameter CAI, initially at 100K, is instantaneously heated to 1825K, the center of the CAI will begin to melt in about six seconds. A shorter time of about one second can be derived from the requirement that melilite not melt at a distance of 200 μm from the rim. From the factor of three enrichment in refractory elements and the 50 μm thickness of the rim, the amount of material lost during the vaporization can be estimated at about 100 μm. This amounts to about 32 mg/cm^2 and requires over 300 Joules to vaporize. Assuming the timescale is on the order of one second, 300 watts/cm^2 are required.

Formation Environments. Finding the proper environment to turn this heat source on and off in such a short time is difficult. Heating with photons requires that the CAI be placed in a 4π radiation field at 2800K. Electromagnetic discharge (4) has problems with the timescales and requires a tenuous atmosphere. Atmospheric entry could work, but only if the CAI enters a steep pressure gradient at high velocities; falling to the nebular plane is not sufficient. Entry into a planetary atmosphere only works if the nebular gas is dissipated (in order to accelerate the CAI), which seems unlikely, and a means is found to get the CAI out of the planet after it formed.

Summary. The constraints on CAI rim formation seem relatively well understood. The rims are ubiquitous; virtually all CAI have them. It remains a challenge to find an astrophysical process that satisfies the constraints.

References. (1) LPS XVIII, 117, 1987; (2) GCA 51, 3215, 1987; (3) Meteoritics 22, 439, 1987; (4) Levy & Araki, Icarus, in press, 1988.

Al-Mg ISOTOPIC SYSTEMATICS AND METAMORPHISM IN FIVE COARSE-GRAINED ALLENDE CAIs

Glenn J. MacPherson, *National Department of Mineral Sciences, National Museum of Natural History, Smithsonian Institution, Washington, DC 20560*

Albert J. Fahey, Laura L. Lundberg and Ernst Zinner, *McDonnell Center for the Space Sciences, Washington University, St. Louis, MO 63130.*

The record for the presence of ^{26}Al in refractory inclusions from primitive meteorites is complicated by metamorphic processes that affected the Mg isotopic systematics in these objects. Hutcheon [1] found that ^{26}Mg excesses in type B1 CAIs from Allende fell on an Al-Mg isochron with $(^{26}Al/^{27}Al) \approx 5 \times 10^{-5}$ while other CAIs (type A, B2) show evidence for disturbed Mg. Huneke *et al.* [2] and Armstrong and Wasserburg [3], however, detected disturbed Al-Mg isotopic systematics in WA, a type B1 inclusion. In an attempt to understand the metamorphic processes experienced by coarse-grained CAIs we have studied the petrology and Al-Mg systematics of five Allende inclusions.

Two of the inclusions are Type A (3529-30; 3658), the rest are Type B. 3529-Z is a normal Type B inclusion in which all of the textures and mineral zonations are consistent with a simple one-stage melt solidification model. The remaining four inclusions all show features indicative of complex histories that include local recrystallization, melilite compositional zoning in the immediate vicinity of spinel and pyroxene inclusions (3529-21; 3529-30; 3658), local conversion of coarser-grained tabular melilites into finer-grained polygonal-granular mosaics (3529-21; 3529-41; 3658) and intense kink-banding (3529-30; 3529-41). Ion probe measurements of Mg isotopes and Al/Mg ratios were made in different minerals. The results are shown in Fig. 1. All inclusions except 3529-Z show evidence for disturbed Al-Mg systematics. Most interesting are the observations in inclusions 3658 and 3529-41. In 3658 anorthite crystal #2 shows the same $^{26}Mg/^{24}Mg$ ratio for $Al/^{24}Mg$ ratios varying by a factor of two. Four anorthite crystals from 3529-41 fall close to a line with a slope of 4.1×10^{-5} but several melilite data points are distinctly above this line (together with three pyroxenes and one spinel, they define a line with almost twice the slope). One melilite point does not have any ^{26}Mg excess. The most likely explanation for these observations is isotopic equilibration of localized regions after decay of some or all ^{26}Al, leading to higher $^{26}Mg/^{24}Mg$ ratios in relatively Al-poor melilite, rather than a higher initial $^{26}Al/^{27}Al$. A similar behavior of the Al-Mg system was seen in a fine-grained Allende inclusion [4].

References: [1] Hutcheon (1982) Am. Chem. Soc. Symp. Ser. No. 176, 95-128. [2] Huneke *et al.* (1983) Geochim. Cosmochim. Acta 47, 1635-1650. [3] Armstrong and Wasserburg (1983) LPS XIV, 11-12. [4] Brigham *et al.* (1986) LPS XVII, 85-86.

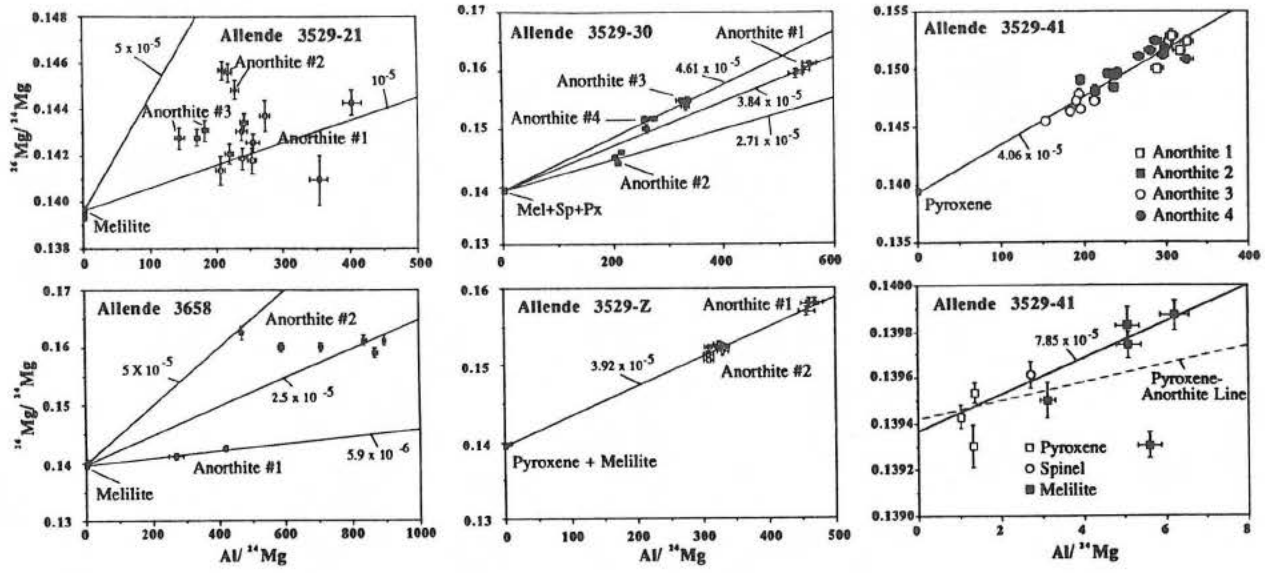

ESTIMATION OF POSSIBLE THERMAL HISTORY OF A VIGARANO CAI.

C.CAILLET[1], J.I. GOLDSTEIN[2], D.VELDE[1], A. El GORESY[3]; [1]Laboratoire de Pétrologie Minéralogique, Université Pierre et Marie Curie, Paris VI, 4 Place Jussieu, 75252 CEDEX 05, FRANCE; [2]Lehigh University, Whitaker Laboratory #5, Bethlehem, PA 18015, USA; [3]MPI Kernphysik P.O. Box 103980, 6900 Heidelberg, FRG.

A polished thin section of a type B1 CAI in Vigarano 477B was examined with an SEM and analyzed with an electron microprobe. The CAI measured 4 x 2.3 mm and is surrounded by typical rimming layers. Melilites, few fassaite crystals poikilitically enclose spinels. Three types of metal-rich grains occur in this inclusion <1>: (1) Large and numerous grains located in the spinel-rich core of the CAI consist of kamacite (4.9 Wt % Ni) and taenite (31-48 Wt % Ni). They contain sometimes Os, Ir, Ru and Re but without Pt. (2) Small Pt-bearing nuggets and (3) Pt-bearing veins. Types (2) and (3) are located near the rim.

The largest metal-rich grain (65-25 μm) shows two distinct FeNi metals, scheelite, molybdenite, OsRu needles and Fe- V- Cr-oxide in its fluffy mantle.

The aim of this study is an attempt to estimate the thermal history of the CAI using Ni-concentration profiles across kamacite and taenite.

Electron microprobe profile across taenite-kamacite boundary in this grain shows interesting features. There is a sharp increase of Ni content from kamacite (4.9 %) to taenite (33 %). The highest concentrations of Os, Ir, Ru, Re are in the Ni-rich metal with an increase of Os, Ir at the two metal interface.

Existing models of calculation <2,3> to estimate the cooling rates are not valid for Vigarano. New results suggest that kamacite and taenite were in equilibrium near 500°C. The taenite of 33 % Ni is in equilibrium with kamacite at 500°C. This grain does not show "M-profile". This could indicate either (1) fast cooling to 500°C and then a period of growth or (2) fast cooling to low temperatures followed by reheating to 500°C. In the first case, it would take about 10^6 years to grow 6 μm of kamacite if the Ni-diffusion coefficient in taenite controlled the process. In the second case, it would take about 10^4 years upon reheating to 500°C assuming that the Ni diffusion coefficient in kamacite controlled the process. The kamacite (4.9 % Ni) in equilibrium with taenite indicates a lower equilibrium temperature <400°C which would require 44 % Ni in taenite. Therefore, measurements of phase equilibria in Fe, Ni, P, Ir, Ru, Re, Os alloys at 400-800°C will be performed because their presence <4,5> may complicate the system.

OsRu exsolutions were probably formed in-situ during this long stage at 500°C. In contrast, scheelite and molybdenite with the high Re-contents (4.76 % and 1.36 % respectively) could have preceded the incorporation in the CAI. The transformation times between 10^4 and 10^6 years are a reasonable first approximation.

REFERENCES:

<1> Caillet C., Mac Pherson G.J., El Goresy A. (1988) Abstract for the 19th Lunar and planet. sci. conf., p. 156-157.
<2> Goldstein J.I. and Short J.M. (1967) GCA, 31, p. 1733-1770.
<3> Wasson J.T. (1971) Meteoritics, 6, p. 139-147.
<4> Romig A.D., Jr and Goldstein J.I. (1980) Met. Trans., 11, p. 1151-1159.
<5> Dean D.C. and Goldstein J.I. (1986) Met. Trans., 17, p. 1131-1138.

RELATIONSHIPS BETWEEN COMPACT TYPE A AND SPINEL-RICH INCLUSIONS INFERRED FROM A COMPOSITE CAI; S.M. Kuehner and L. Grossman[1], Dept. of the Geophysical Sciences, The University of Chicago, Chicago, IL 60637. [1]Also Enrico Fermi Institute, The University of Chicago.

The Allende inclusion TS60F1 (10mm X 5mm) is a loosely packed aggregate of irregularly-shaped, rounded, spinel-, perovskite- rich nodules (SPR, ~90% of inclusion) upon which is attached a hemispherical melilite-rich region (1.7mm dia.) resembling a compact type A inclusion (CTA). Spinel-rich inclusions have been proposed (1,2) to be the residual material produced after extensive partial melting/volatilization of interstellar material, with less extensively processed material forming types A and B CAIs. A study of TS60F1 was initiated to evaluate the genetic relationship between the SPR nodules and the associated CTA. As the physical relationship between the CTA and SPR nodules is somewhat ambiguous due to the fragmented nature of the contact, conclusions are based mainly on chemical and textural criteria.

The CTA and the individual SPR nodules (180μm to 1.8mm) are extensively altered, with melilite and spinel+perovskite replaced by fine sprays of anorthite whose intersertal voids are partly filled with sodalite. Individual nodules and the CTA margin adjacent to the Allende matrix are also enclosed by concentric hedenbergite, Al-diopside, sodalite+anorthite and, in some cases, phyllosilicate rim layers. Unaltered SPR nodule interiors are composed of ~30% subhedral perovskite (~5μm dia.) set in a massive spinel matrix. Rarely, perovskite grains reach ~50μm, but these have a highly irregular outline. EPMA of perovskite from any individual nodule reveals two distinct populations: a group high in ZrO_2 (0.3-0.6 wt%) with a restricted range of Ce_2O_3 (0.05-0.15 wt%), and a low ZrO_2 group (<0.05-0.20 wt%) having a wider range of Ce_2O_3 (<0.05-0.30 wt%). These populations correspond, respectively, to the SRE-rich and SRE-poor groupings of (2), but these chemical groupings do not coincide with any obvious division based on perovskite morphology. Spinel grains in the unaltered SPR nodules are FeO-poor (<2 wt%) with minor V_2O_3 (0.14-0.20 wt%), Cr_2O_3 (0.08-0.17 wt%) and undetectable ZnO. Relict spinel in the altered SPR regions is enriched in FeO (to 14 wt%) with coupled increases in ZnO (to 0.5 wt%) and V_2O_3 (to 0.3 wt%). One unaltered SPR region contains an irregularly-shaped crystal of melilite (270μm X 80μm) that grades texturally from an inclusion-free center (Ak_{34}) into a region of melilite (Ak_{2-7}) + rounded spinel and minor perovskite at the grain edge. Adjacent to this crystal, the nodule is dominated by spinel+perovskite with minor melilite (Ak_{4-10}).

Excluding alteration minerals, the CTA is composed of >95% melilite, minor rounded spinel grains and lesser perovskite. The melilite is homogeneous, Ak_{15-17}, but becomes slightly more gehlenitic towards the margins (Ak_{8-11}). Spinel grains are FeO-poor (<1.2wt%) but differ from unaltered spinel in the SPR nodules in being enriched in V_2O_3 (0.[illegible]-0.56wt%) and Cr_2O_3 (0.18-0.25wt%). Perovskite compositions fall in the low ZrO_2 group of the SPR nodules. The outer margin of the CTA, internal to the rim layers described above, is composed of an ~75μm wide spinel layer that has inward-projecting, jagged, patchy extensions and contains numerous perovskite (<10μm) and irregularly-shaped melilite inclusions. Spinel in the CTA margin is identical in composition and style of alteration to spinel in the SPR nodules. The perovskite compositions fall in the Zr-rich group as defined in the SPR nodules, and thus differ from those of perovskite in the CTA interior.

This study of TS60F1 shows that the range of spinel and perovskite compositions in the margin of the CTA is similar to that found in the unaltered regions of the SPR nodules, implying a similar process was involved in their formation. The origin of spinel+perovskite margins on melilite-rich CAIs may be the result of incomplete volatilization during a period of flash-heating (3,4). Such a process is consistent with the CTA melilite becoming slightly less Ak-rich near the spinel margin. Rare, incompletely digested melilite grains in the SPR nodules may indicate that the nodules formed through more extensive volatilization of CTA material, which would also result in mixing of the two perovskite populations. The extreme abundance of perovskite in the nodules suggests this process was accompanied by the introduction of Ti. One possible difficulty in ascribing the origin of SPR nodules to distillation of CTA-like material is the absence of porosity within the nodules. It is not clear whether volatilization would produce a massive spinel-perovskite residue, or one composed of friable, porous aggregates.

REFERENCES: (1) Cohen, R.E. *et al.* (1983) GCA 41, 1739. (2) Kornacki, A.S. and Wood, J.A. (1985) GCA 49, 1219. (3) Boynton,W.V. and Wark, D.A. (1985) Meteoritics 20, 613. (4) Laughlin, J.R. *et al.* (1986) Meteoritics 21, 430.

RELICT REFRACTORY ELEMENT RICH PHASES IN TYPE B CAI; M.L. Johnson, D.S. Burnett, Geol. Planet. Sci., Caltech, Pasadena, CA 91125; D.S. Woolum, Physics Dept. Calif. State Univ., Fullerton, CA 92634.

Of the possible processes involved in Type B CAI history, igneous processes are the most tractable for study. Temperature and time scales inferred [1,2] are commensurate with feasible laboratory simulations. We have previously reported melilite (mel) crystal liquid partition coefficients, Di [3], for Sm, Yb, Sr (Eu++ analog), and Y (Ho analog). Our data for akermanite (Ak) 30 mel compositions is in good agreement with literature data where direct/extrapolated comparisons are possible [4,5,6,7]. Even allowing for significant variations in Di with progressive crystallization, comparisons of predictions for the initial (0-30%) fractional crystallization of mel with our Sr, Y contents obtained for mel cores in Allende Type B CAI, with comparable Ak contents, indicate that the natural data substantially exceed (factors of 1.5-2.5x) those predicted. Similar results are obtained for Y, Zr in fassaite (fass) based on estimates of the Di from literature data. In this case, excesses of these trace elements are up to factors of about X5. Thus, while the trace elements observed in natural CAI (Sr in mel and Y,Zr in fass) are in qualitative agreement with igneous partitioning, the trace element abundances are higher than quantitative predictions.

Actinide data are also available for individual mel grains from Type B CAI [8,9,10]. For mel, U-Di values near 1 are needed to explain the U abundances of early-crystallizing mel. This seems unreasonable for such a highly incompatible element like U, and we have demonstrated this for Th. Mel Th-Di values for the synthetic samples previously described were obtained using Th-alpha-track radiography. $Di(Th) = 8.4 \times 10^{-3}$. Comparisons of predictions for Th with Th in natural samples [8] indicate enhancement factors (natural/predicted) of about 100!

Excesses of lithophile trace elements thus suggest that relict unmelted phases were incorporated in CAI. There is general agreement that some spinel is relict. But spinel can't account for the refractory lithophile enrichments observed. [8] suggested perovskite (pv) as a likely candidate. We have searched for surviving relict grains in 3, mm-sized Allende mel. All inclusions were characterized, but most were metals. There were two submicron pv grains. Pv are rare, but they must be relict, since pv is soluble in Type B CAI melts. We have searched for evidence of resorbed pv by looking for Ti hot spots in Allende mel. As shown in the figure, there is a general decrease in Ti with Ak, which is contrary to predictions based on our Ti D_i value (0.020). There are also three distinct Ti hot spots evident. Subsequent high resolution SEM observations of the spots analyzed revealed a submicron pv inclusion for one of the hot spots, but there was no visible inclusion at the other two, in the SEM or with high magnification transmitted light optical observation. Detailed profiles show hot spot sizes of 10-20 microns. These might be sites of resorbed pv. However, actinide data indicate that relict pv is unlikely to account for the observed trace element data. TS23 mel data show[8] a CI normalized U/Ti ratio of about 10, but the corresponding pv ratio is approximately 1. This requires another trace element carrier(s). High resolution SEM and optical observations also were made of anorthite that had yielded U stars in the [8] study. These too showed no evidence for visible inclusions to which the actinide-rich sources could be attributed.

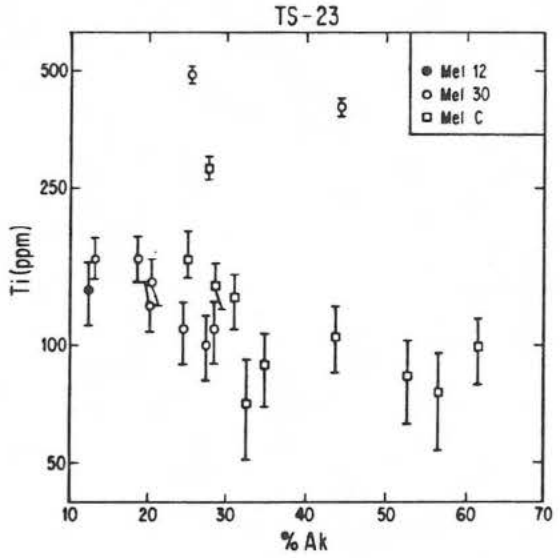

References[1] Stolper E. (1982) GCA 46, 2159. [2] Stolper E. & Paque J.M. (1986) GCA 50, 1785. [3] Woolum D.S., et.al. (1988) LPS 19, 1295. [4] Beckett J., et.al. (1988) LPS 19, 49. [5] Ringwood (1975) The Moon 12, 12. [6] Nagasawa, et.al. (1980) EPSL 46, 431. [7] Kuehner S.M., et.al. (1988) LPS 19, 653. [8] Murrell M. & Burnett D. (1987) GCA 51, 985. [9] Schirck J. (1975) Thesis. Washington University, St. Louis. [10]Wark D. (1984) Thesis. University of Melbourne.

PETROGENESIS OF A HIBONITE-PYROXENE SPHERULE FROM MURCHISON;
Trevor R. Ireland, Albert J. Fahey, and Ernst K. Zinner, Physics Department and McDonnell Center for the Space Sciences, Washington University, St. Louis, MO 63130, U.S.A.

Murchison grain 7-228 is a pyroxene spherule approximately 120 μm in diameter with several euhedral to subhedral hibonite laths in the core (≤50×10 μm). Small amounts of fayalitic olivine are present partially filling voids in the pyroxene and between the hibonite laths. Fayalitic olivine is a common rim phase around hibonite-bearing inclusions. The hibonite is stoichiometric with ~3% TiO_2. The pyroxene has a composition near $(Ca_{1.1}Mg_{0.3}Al_{0.5}Ti_{0.1})(Si_{1.5}Al_{0.5})O_6$.

The REE pattern of 7-228 hibonite is typical of PLAC-type hibonites (Ireland, 1988; Ireland *et al.*, 1988), and is similar to the Allende Group III pattern (Fig. 1). It has a Eu depletion (Eu*/Eu=0.13), but no Yb anomaly. The relatively volatile trace-elements Sr, Ba, Nb, and V are also depleted. The hibonite REE pattern is fractionated with a decrease in the normalised abundances from 45×C1 at La, to 8×C1 at Lu. The REE pattern of the pyroxene is complementary to the hibonite in that it is fractionated from 8×C1 at La to 36×C1 at Lu; Eu does not show any large deviation from the fractionation trend (Fig. 2). The pyroxene is enriched in Nb and V relative to the hibonite, but is depleted in Ba. The bulk REE pattern for 7-228 would be flat at ~20×C1 with a Eu depletion if the inclusion consisted of equal proportions of hibonite and pyroxene. However the exposed section of 7-228 has only around 10% hibonite.

Mg isotopic analysis of hibonite from 7-228 shows only a small excess in ^{26}Mg ($\delta^{26}Mg$ = +1.5 ± 1.1 ‰ (2σ) despite high Al/Mg; a characteristic feature of the PLACs. The pyroxene has low Al/Mg and $\delta^{26}Mg$ of –2.9±1.4 ‰. The slope of the Al-Mg isochron is $(^{26}Al/^{27}Al)_0$=1.7 (±0.7) × 10^{-5} with $(\delta^{26}Mg)_0$ = –3.1±1.5 ‰ (Fig. 3). The Mg isotopic systematics are consistent with the *in situ* decay of ^{26}Al in 7-228 from an initial composition that was depleted in ^{26}Mg. Ca and Ti isotopic compositions for the hibonite and pyroxene show large excesses in the n-rich isotopes (Table 1). The compositions of the two phases are the same within errors with $\delta^{48}Ca$ ~+39 ‰ and $\delta^{50}Ti$ ~+21 ‰; $\delta^{49}Ti$ is ~+5 ‰, while $\delta^{42}Ca$, $\delta^{43}Ca$, and $\delta^{47}Ti$ are within error of normal.

The similarity in the Ca and Ti isotopic compositions of hibonite and pyroxene indicates that the hibonite and pyroxene are cogenetic. The complementary nature of the fractionations of the REE patterns, the morphology of the hibonite crystals, and the coexistence of hibonite and pyroxene indicate that this inclusion crystallised from a melt rather than directly from gas-solid condensation. References: Ireland (1988) GCA, submitted; Ireland et al., (1988) GCA, submitted.

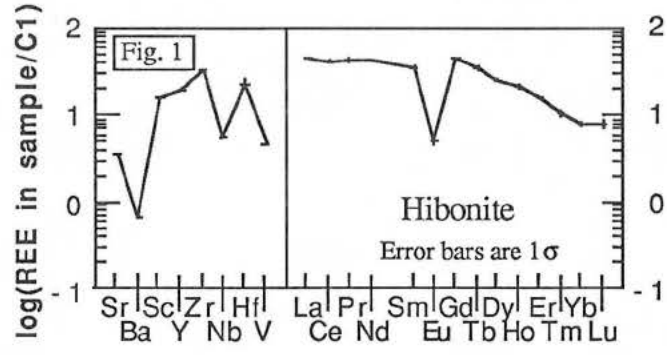

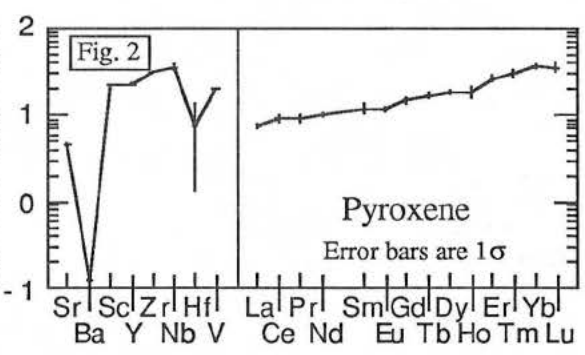

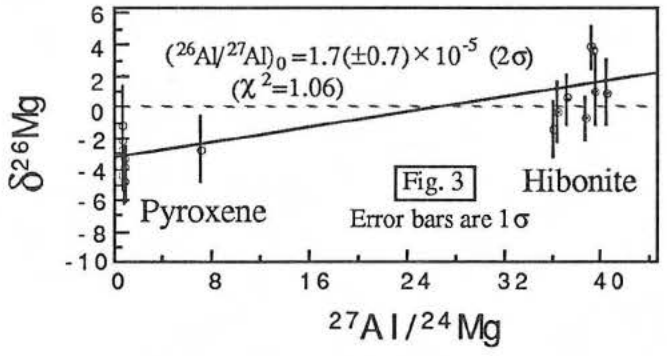

Table 1

Sample	$\delta^{48}Ca$	$\delta^{50}Ti$
Pyroxene	35.5±4.3	21.4±7.0
Hibonite	41.9±3.5	21.1±4.9
	Errors are 2σ	

CORRELATED ISOTOPE FRACTIONATION AND FORMATION OF PURPLE FUN INCLUSIONS
C. A. Brigham, I. D. Hutcheon, D. A. Papanastassiou and G. J. Wasserburg. The Lunatic Asylum, Div. Geol. & Planet. Sci., Caltech, Pasadena CA 91125.

Allende coarse-grained inclusions characterized by a distinct purple color and high spinel contents (≤50 vol%) exhibit a higher frequency of FUN isotopic anomalies (≈20%) than the general CAI population (≤6%). We used the ion microprobe to measure Mg, Si, Cr and Fe isotopic compositions of three Purple Spinel-rich Inclusions (PSI=ψ) which are petrographically similar to Type B CAI to investigate: 1) variations in isotopic fractionation within inclusions, including secondary phases; 2) correlated isotopic fractionation; and 3) excess ^{26}Mg.

Isotope fractionation factors F_{Mg}, F_{Si}, F_{Cr} and F_{Fe} were obtained by measuring deviations in the isotopic ratios relative to the values in standards. B7F6 exhibited uniform F_{Mg} (17°/oo) for interior spinels and fassaite, but a gradient toward lower F_{Mg} for spinel near the edge. Fassaite exhibits variable F_{Si} (10-14°/oo), while hedenbergite exhibits F_{Si}=0. Anorthite analyses yield a limit: $^{26}Al/^{27}Al=5\times10^{-6}$. B7H10 spinel and fassaite show uniform F_{Mg}=36°/oo. Fassaite shows uniform F_{Si}=16°/oo. Olivine mantling spinel grains exhibits F_{Mg}≈11°/oo and F_{Si}=0. DH8 spinels exhibit a range in F_{Mg} of 9°/oo (30-39°/oo), which is not correlated with FeO content. DH8 fassaite shows uniform F_{Mg}=30°/oo, but variable F_{Si} (11-15°/oo). DH8 anorthite exhibits uniform F_{Si}= 15.0°/oo and an upper limit: $^{26}Al/^{27}Al\leq1\times10^{-7}$. DH8 spinels exhibit variable F_{Cr} (7-15°/oo), but only small F_{Fe}<3°/oo.

The data indicate large positive fractionation for Mg, Si and Cr, but no fractionation for Ca, Ti and Fe. The magnitudes of fractionation for Mg and Si for B7H10 and DH8 are the largest observed for any Allende CAI. Two inclusions (DH8 and B7F6) exhibit substantial variations in isotopic fractionation for Mg, Si and Cr. Since petrographic observations suggest crystallization from a melt, isotopic variability may be attributed to addition of normal material. Isotopically normal Si in hedenbergite and olivine requires gas-solid reaction with normal Si during alteration. In B7H10, olivine with F_{Si}=0 and F_{Mg}=11°/oo mantles spinel with F_{Mg}=34°/oo, suggesting an alteration reaction: Sp→Ol+Fp; requiring addition of all Si and 2/3 Mg in olivine from an isotopically normal gas phase.

An excellent correlation is observed between the magnitudes of fractionation for elements of similar volatility (Mg, Si, Cr), emphasizing the importance of kinetic processes involving distillation for the production of isotopically heavy Mg, Si and Cr. Assuming that Mg and Si are the only major elements lost by evaporation, a Rayleigh model can be used to estimate a precursor ψ composition. Substantial mass loss (72% for B7H10) is required to produce the measured F_{Mg} and F_{Si}. Calculated initial compositions are consistent with formation by evaporation of a precursor with a composition similar to that of ordinary chondrules. Variable fractionation for Mg, Si and Cr and the lack of Fe fractionation result from alteration involving addition of normal material. This model explains the chemical composition and extreme isotope fractionation in ψ starting with a simple precursor and well-understood processes; however, it does not explain the absence of FUN effects in many ψ, the association of UN effects with extreme fractionation or the relation of ψ to normal CAI. ψ differ from Type B CAI in their high spinel contents and absence of melilite. A second model postulates formation of ψ from a precursor similar to Type B CAI, containing melilite which has been completely altered to secondary phases. (#624)

FURTHER ISOTOPIC AND CHEMICAL INVESTIGATIONS OF AN ISOTOPICALLY HETEROGENEOUS VIGARANO INCLUSION;

Andrew M. Davis[1] and Glenn J. MacPherson[2], [1]James Franck Inst., Univ. of Chicago, Chicago, IL 60637; [2]Dept. of Mineral Sciences, Natl. Museum of Natural History, Smithsonian Inst., Washington, DC 20560.

We previously reported isotopic [1,2] and petrologic [2] data for USNM 1623-5, a forsterite-bearing FUN inclusion from Vigarano and the first known inclusion in which correlated mineralogic and isotopic evidence clearly fingerprint the operation of a secondary volatilization event. We have continued our study of this inclusion and present here further isotopic, petrologic and trace element data.

Trace elements. Trace element analyses of melilite and fassaite by ion microprobe show that these phases have complementary REE patterns consistent with igneous partitioning. Interior melilite ($Åk_{85}$) has a HREE-depleted pattern with a positive Eu anomaly (15 x C1)—LREE have enrichments of 0.3-2 x C1, HREE are near the detection limits of 0.1-1 x C1, and Y, which partitions like HREE, has an enrichment of 0.1 x C1. Fassaite is LREE depleted (La—13 x C1) with relatively uniform enrichments of HREE (Gd to Lu—35 x C1). It has a negative Eu anomaly (10 x C1) and no anomalies at Ce or Yb. The extremely low concentrations of REE in åkermanitic melilite are in accord with recent measurements of REE partitioning in melilite [3,4]. The absence of an Yb anomaly suggests that the bulk inclusion has a group I pattern like that of the forsterite-rich Allende FUN inclusion CG-14 [5].

Petrology and isotopic composition. In the Al-rich mantle immediately overlying fassaite, fassaite has been replaced by an intergrowth of Mg-poor melilite and perovskite. Detailed electron microprobe analyses show that less than 20% of the Ti in the fassaite in contact with this mantle is trivalent. In contrast, 20-50% of the Ti in interior fassaite is trivalent. This suggests that fassaite near the rim was oxidized during the thermal event that led to breakdown of fassaite and mass loss. The oxidizing conditions may have been caused by the oxygen-rich vapor generated by volatilization of the inclusion.

The Al-rich assemblage (spinel, gehlenite, hibonite) of the outer mantle is incompatible with the interior forsterite-rich one. This observation coupled with the mantle's enrichment in isotopically heavy Mg and Si compared to interior forsterite led us to propose that the mantle formed by volatilization of the outer layers of the inclusion [2]. One particularly interesting feature of the mantle is a porous, fine grained aggregate of spinel, perovskite and gehlenite-rich melilite overlying contiguous portions of the inclusion. This material could be interpreted as: 1) part of the volatilization residue that is no longer coherent, 2) as a recondensate from volatilization or 3) as an unrelated assemblage that just happens to be attached to the inclusion. Mg isotopic measurements of this fine grained material show it to be strongly mass fractionated ($\Delta^{25}Mg \sim 30$ ‰/amu), like the rest of the inclusion. The porous material must therefore be part of the volatilization residue, because recondensed material should be isotopically lighter than the interior. Also, material unrelated to the rest of the inclusion is extremely unlikely to have isotopically heavy Mg. Meteorite matrix adjacent to the porous refractory material is of normal magnesium isotopic composition within analytical uncertainty.

Implications. Our additional data for 1623-5 strengthen the interpretation of the outer Al-rich mantle as a volatilization product and shed light on the nature of the process that produced it. The heating event must have been very rapid in order that only the outermost 200 μm of the inclusion was melted. If the volatilization took place in the solar nebula, the process must have been rapid enough to maintain locally oxidizing conditions. The degree of volatilization of the mantle relative to the core was at least 60-80%, yet the isotopic mass fractionation so produced was <5 ‰/amu for Mg. It is hard to see how a similar sort of volatilization process could have produced the ~30 ‰/amu fractionation of Mg in the bulk inclusion, since the bulk inclusion is a less refractory assemblage than many relatively unfractionated CAIs.

References: (1) Clayton R. N. *et al.* (1987) *LPS XVIII*, 185. (2) MacPherson G. J. *et al.* (1987) *Meteoritics* **22**, 451. (3) Beckett J. R. *et al.* (1988) *LPS XIX*, 49. (4) Kuehner S. M. *et al.* (1988) LPS XIX, 653. (5) Clayton R. N. *et al.* (1984) *GCA* **48**, 535.

THE DISTRIBUTION OF TRACE ELEMENTS IN AN ALLENDE TYPE B1 INCLUSION

A.K. Kennedy, J.R. Beckett and I.D. Hutcheon, Division of Geological and Planetary Sciences 170-25, Caltech, Pasadena, CA 91125

Zoning patterns of trace elements (TE) in minerals from Ca-, Al-rich inclusions (CAIs) may reflect how they formed [1] and/or yield information on secondary processes. We have measured abundances of the REE, Ba, Be, Sc and Ti in a single melilite (Mel) crystal (X1) from the mantle of the Allende type B1 inclusion Egg-6 [2] and in the rim of a coexisting clinopyroxene (CPX) at the core/mantle interface. TE zoning profiles in Mel from Egg-6 are compared with those predicted by [1] for fractional crystallization of Mel in type B CAIs.

TE were analyzed with the Panurge ion microprobe (SIMS) using high mass resolving power (RP>3300) for Sc and Ti and energy filtering (RP~500) for all other elements. Doped Mel and CPX glasses were used as SIMS standards with sensitivity factors from [3] or based on analyses of CPX and whitlockite from Angra dos Reis. Some REE intensities were also corrected for oxide interferences [4]. Major element concentrations were determined by EDS.

The analyzed Mel X1 is normally zoned from Ak33 near the outer edge of the mantle to Ak62 near the core/mantle interface. Both Ce and La concentrations rise from an initial 5X chondritic with increasing X_{Ak}, decrease at intermediate X_{Ak}, then drop precipitously to ~1X chondritic above Ak60. Ba concentrations rise with X_{Ak} from 32 (Ak33) to 80 (Ak58) ppm then drop to 46ppm (Ak62). Be (~chondritic) increases from 0.2 to 0.6 ppm over the range Ak33-Ak62 while Sc (<1ppm) is very low for all Mel. In contrast, Ti (33-83ppm) concentrations are highly variable and negatively correlated. Near the Mel/CPX contact, Mel is LREE enriched with a large positive Eu anomaly while CPX is LREE depleted with a negative Eu anomaly (Fig. 1). These REE patterns are similar to those for CPX and Mel separates from an Allende type B CAI [5]. If the Mel and CPX rims equilibrated with the same melt (L), then the X1/L distribution coefficient for CPX is 5 times lower than that of Mel for Eu, 3-15 times higher for LREE and ~80 times higher for HREE. The marked decrease in Ba and REE concentrations in Mel for X_{Ak}>0.6 may coincide with the appearance of CPX in the crystallization sequence. The initial rise in REE concentrations with X_{Ak} was not observed by [1] in air experiments and may be due to substitution of TE on defect sites or partial re-equilibration of meteoritic Mel. Erratic Ti zoning may reflect exsolution in Mel.

[1] Beckett, J.R. et al. (1988) Lunar Planet. Sci. XIX, 49. [2] Meeker, G.P. et al. (1983) Geochim. Cosmochim. Acta **47**, 707. [3] Spivack, A.J. et al. (1988) In preparation. [4] Zinner E. and Crozaz G. (1986) Int. J. Mass Spect. Ion Proc. **69**, 17. [5] Mason B. and Martin (1974) Earth Planet. Sci. Lett. **22**, 141.

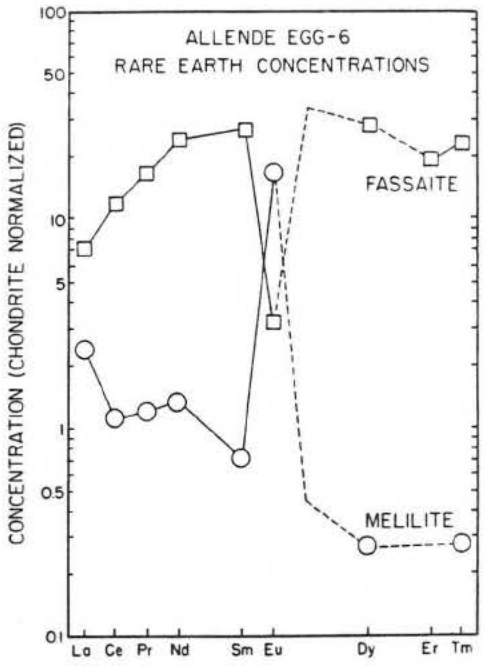

Fig. 1. REE patterns of coexisting CPX and Ak62 Mel from Egg-6.

CLINOPYROXENE IN TYPE B1 CAI; Hiroko Nagahara[1] and Hiroshi Nagasawa[2]; [1]Geol. Inst., Univ. Tokyo, Hongo, Tokyo 113, Japan; [2]Dept. Chemistry, Gakushuin Univ., Mejiro, Tokyo 171, Japan

HN3-1 is a typical type B1 CAI from Allende, which comprizes nearly equal amounts of melilite (Mel), Ti-rich clinopyroxene (Tpx) and anorthite (An) with numerous spinel (Sp). Combined petrological [1], chemical [2], and isotopic [3-5] studies have revealed that HN3-1 shows various disequilibrium features; REE patterns of mineral separates appear to be formed through crystallization from liquid but with positive Yb anomalies in Mel and An, oxygen isotopic compositions of mineral separates are widely distributed along Allende "mixing" line with minor difference between Mel and An, and Ca isotopic composition is different among Mel, Tpx, and An. It is thus suggested that all of the four major minerals in HN3-1 should contain either visible or invisible relicts.

In order to search the carriers of chemical and isotopic anomalies, color mapped photos were taken with ultra-high speed wide-area multi-analyzer (CMA) of entire area of two thin sections and many discrete areas of HN3-1. Tpx shows an interesting compositional zoning which has not been noticed in the conventional back-scattered electron images. Most Tpx show concentric zoning with Al, Ti, and V-rich core and Si and Mg-rich rim. However, elemental distribution pattern in some of them is not symmetrical; in Tpx 3, Al, Ti and V decrease and Mg and Si increase from one side of the grain to the opposite side. The adjacent mineral to Al, Ti, and V-enriched side of the Tpx is usually Mel, however, not all Tpx adjacent to Mel show asymmetrical zoning. Rarely, Tpx adjacent to An shows asymmetrical elemental distribution. Some Tpx show quite unique elemental distribution; Tpx 9 has concentrically zoned Ti distribution but the grain can be divided into two portions as to Al, Mg, and Si contents both of which portions show weak compositional zoning. This shows that compositionally different two Tpx grains had coalesced before melting and Ti was redistributed during melting and/or subsequent cooling.

CMA photographs show that some Tpx grains contain compositionally distinguishable rectangular or triangle areas, 100 to 200 um in size. They have different compositions from surrounding areas on oxide-oxide diagrams. They should be visible relicts.

Mel should also contain relicts which carry Yb anomaly, however, there are not any evidence of relicts on CMA photographs. Cations in Mel might have redistributed at high temperatures because of large diffusion rate. EPMA analyses revealed that Sps have small but systematic compositional difference for the occurrence; those in a single grain of Tpx, those in a single An grain, those forming a framboid, and those forming a pallisade have slightly different composition. This suggests that Sp has kept the primary composition including oxygen isotopes. Although An should contain relicts carrying Yb anomaly as well as Mel, there is no evidence of relicts

Present results show that not only the visible relicts but also most Tpx could be relicts though they partly exchanged cations with Mel at high temperature. This shows that Tpx did not crystallize from a liquid, rather previously existed grains recrystallized to form larger grains as they now are. Oxygen isotopic composition demonstrates that the precursor of Mel and An originated in the solar system and Sp and Tpx were from another star or supernova. Large oxygen isotopic anomaly in Tpx may have been inheritated from earlier generation which slightly changed during melting. Though the liquidus temperature of Mel is much higher than that of Tpx, considerable amounts of Mel melted probably because of finer grain size to form the Mel mantle.

References: [1] Nagahara,H. et al.(1987) LPSC, XVIII, 694 [2] Nakamura,N. et al.(1987) ibid., 698 [3] Mayeda,T.K. et al. (1986) LPSC, XVII, 526 [4] Birck,J.L. and Lugmair,G.W. (1987) Meteoritics, 22, 326 [5] Prombo,C.A. and Lugmair,G.W. (1987) ibid.,483, (1988) LPSC, XIX, 951

"ADSORBED" OXYGEN IN THE SANTA CATHARINA ATAXITE, Jun Saito and H. Takeda, Mineralogical Institute, Faculty of Science, University of Tokyo, Hongo Tokyo 113 Japan

Santa Catharina is known for its high nickel (1) and oxygen contents (2,3). Because oxygen was detected in the specimen proved to be no oxides by the Mössbauer method (2), we have studied this meteorite by an electron probe microanalyser (EPMA), analytical electron microscope (AEM) and ion probe microanalyser. The oxygen content was quantitatively analysed by applying the ZAF correction. The specimen of Santa Catharina supplied by M. Prinz, Amer. Museum Natl. History is devoid of oxide minerals.

The polished sections show no sign of oxidation and reveal two different areas. Darker colored patches of tetrataenite about 20 to 100 microns in diameter, are distributed in shiny matrix of taenite with about 33 wt. % nickel. No kamacite spindles are present in the taenite portion. The AEM images of the oxygen-rich areas show aggregates of small grains (4), but electron diffraction did not show oxide reflections except for minor thin akaganeite surrounding the hole produced by ion-milling, which was produced after sample preparation. X-ray diffraction of the tetrataenite portions with minor matrix taenites also did not show reflections of known iron oxide minerals.

About 3 to 10 wt. % of oxygen is detected in the tetrataenite portions, while Fe/Ni weight ratios stay always about one. The oxygen content is not correlated to the distance from cracks, and the BEI of the oxygen-rich portions by EPMA show distinct boundary between the darker and the lighter portions. This is clearly shown by Chemical Map Analysis (CMA) of oxygen. This evidence suggests that the terrestrial corrosion through cracks is not the main source for oxygen. The depth profiles from the surface of the tetrataenite portion of oxygen by the ion-probe show no decreasing of oxygen abundances except for one case, where gradual decrease was observed.

Because the above evidence suggest that the oxygen may be adsorbed in the tetrataenite structure, we carried out heating experiments of small chips, for which the presence of oxygen has been confirmed, up to 195°C in vacuum. The oxygen contents of the lighter areas of BEI decreased drastically down to 1 to 2 wt.%, whereas those of the darker area stays nearly constant at the level of 4 to 5 wt.%. After exposing the same specimen to the atmosphere for about two days, the oxygen contents increased again to nearly the original level.

The above observation and adsorption behavior during the heating experiment strongly suggest that the oxygen is adsorbed in the tetrataenite structure. The origin of the adsorbed oxygen may be due to terrestrial environment, but the adsorbing property may have been aquired by some preterrestrial events.

References: (1) Buchwald V. F. (1975) Handbook of iron meteorites. Univ. of California Press. (2) Lovering A. F. and Andersen C. A. (1965) Science, 147, 734-736. (3) Danon J. et al. (1979) Nature, 277, 283-284. (4) Jago R.A. (1979) Nature 279, 413-415.

THE CAPE YORK METEORITE AS A METAL SOURCE FOR PREHISTORIC CANADIAN ESKIMOS

Allen P. McCartney (Univ. of Arkansas) and Jerome Kimberlin

Twenty-eight iron and 10 native copper artifacts were found during the 1976 excavation of two Thule Eskimo archaeological sites (c. A.D. 1200-1300) at southeastern Somerset Island (Fig. 1; 1). The iron pieces represent the largest collection known from a Thule period site in the Canadian Arctic, although at least 125 iron pieces have been excavated at contemporaneous sites in northwestern Greenland. Because iron used by Thule Eskimos could have derived from meteoritic or terrestrial sources, Kimberlin analyzed 13 of the 28 specimens by neutron activation at Brookhaven National Laboratory and determined that 10 were of Cape York meteorite pieces (2), one piece was of a meteorite other than that of Cape York, and two were of non-meteoritic iron, probably of 11th-13th century Norse origin.

Ni content of the 10 Cape York specimens ranges between 6.71-7.92%, matching that of artifacts and unaltered pieces of the Cape York meteorite in Greenland (type IIIA, medium octahedrite; 2, 3, 4). The eleventh piece differed from the Cape York pieces in Ni content (4.98%) and in internal ratios of Co/Ir, Ir/Fe, and Co/Fe calculated between three gamma-ray peaks. This piece may represent a heretofore unreported meteorite. Buchwald and Mosdal (3) demonstrate that Greenlandic irons used prehistorically and during the Norse period are of three uniform and distinctive types: Cape York meteorite (northwestern Greenland), telluric iron (Disko Bay area), and Norse wrought iron (southern Greenland).

Somerset Island is located midway between Cape York and the Thule site of Silumiut, on northwestern Hudson Bay, where we have previously identified artifacts of Cape York meteorite pieces and wrought iron (5). Small numbers of iron fragments are widely known at Thule sites throughout the Canadian Arctic. These irons have, by and large, not been analyzed, but they are expected to be primarily Cape York meteorite and Norse wrought iron. An "epi-metallurgy" arose among precontact Canadian Eskimos that connected isolated communities through "down-the-line" trade networks. This metallurgy was technologically based on cold-hammering (and thereby hardening) of irons into traditional knife, graver, projectile point, and other shapes. Late Dorset Eskimos, who preceded Thule peoples in the eastern Canadian Arctic, were using Cape York irons at least as early as A.D. 800, suggesting a minimal age for that large shower to be 1200 years ago.

(1) McCartney, A.P. n.d. Late Prehistoric Metal Use in the New World Arctic. In: Late Prehistoric Development of Alaska's Native People, R. Shaw et al., eds, Aurora: Alaska Anthro. Assoc. Mon. Series (in press).

(2) Buchwald, V.F. 1975 Handbook of Iron Meteorites. Univ. of Calf. Press.

(3) Buchwald, V.F. & G. Mosdal 1985 Meteoritic Iron, Telluric Iron, and Wrought Iron in Greenland. Med. om Grøn. (Man & Soc.) 9.

(4) Wasson, J.T. 1974 Meteorites. Springer-Verlag.

(5) McCartney, A.P. & D.J. Mack 1973 Iron Utilization by Thule Eskimos of Central Canada. Amer. Antiquity 38(3)328-339.

Fig. 1

AEM INVESTIGATION OF THE PLESSITE STRUCTURE OF A IIIB IRON METEORITE --- GRANT

J. Zhang, D.B. Williams and J.I. Goldstein, Department of Materials Science and Engineering, Lehigh University, Bethlehem, PA 18015

The decomposed structure of the black and duplex plessite regions in the iron meteorite Grant has been studied using analytical electron microscopy. The scale of the structural and chemical analysis was less than 100 nm. The results, combined with those of the electron microprobe and the scanning electron microscope, lead to a better understanding of the low temperature phase transformations that the metallic phase of meteorites experienced.

We found that the duplex plessite which has a Ni content approximately that of the bulk meteorite is decomposed into a coarse equilibrium mixture of teanite and kamacite with the Ni composition of 50 wt% and 4 wt% respectively. The micron sized teanite pricipitates are fcc and are sometimes twinned. There was no indication of FeNi ordering.

We found that the black plessite region which has a Ni content up to 20 wt% is also decomposed. The size of the teanite precipitates are smaller in higher Ni regions, typically 20 nm for 17 wt% areas and 100 nm for 12 wt% areas. The teanites of the black plessite region have 50 wt% Ni, the same composition as that of the teanites in the duplex region, see Figure 1. The structure of the teanite is fcc but no twinning or ordering was observed. The kamacite composition of this region is higher than the equilibrium value of about 4 wt% as found in the duplex region.

The results are consistent with the current Fe-Ni phase diagram, as shown in figure 2, except for the absence of FeNi ordering. The martensite in the plessite decomposed at different temperatures according to the local Ni composition. The absence of ordered FeNi is most likely due to shock effects in the Grant meteorite.

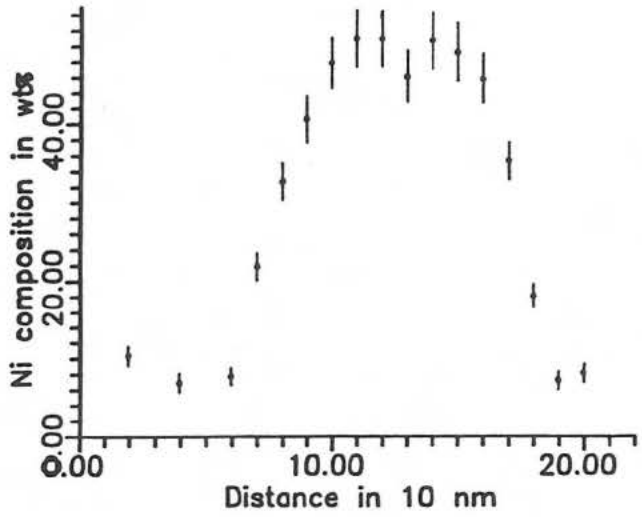

Fig.1 Ni composition profile of a teanite precipitate in 14 wt% Ni area by X-ray energy dispersive spectrometer of the AEM.

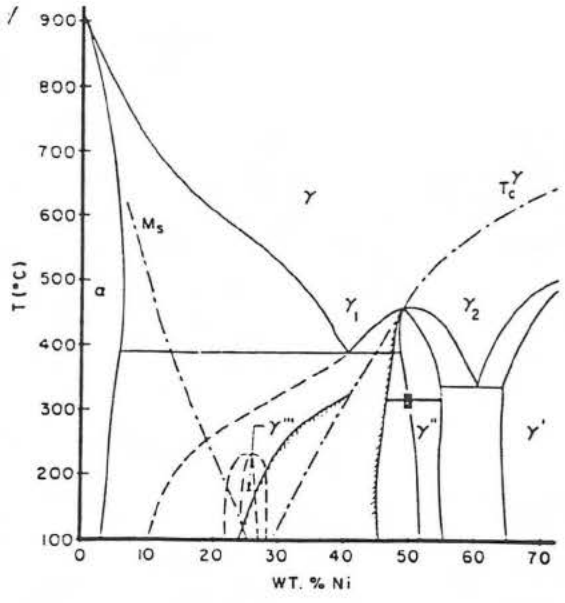

Fig.2 Fe-Ni equilibrium phase diagram, Reuter et al. (1987)

Reference

K.B. Reuter,D.B. Williams and J.I. Goldstein, Metallurgical Transactions in press.

ANGRA DOS REIS: COMPLEX SILICATE FRACTIONATIONS

A.H. Treiman[1], J.H. Jones[2], M.-J. Janssens[3], R. Wolf[3] & M. Ebihara[3]
[1]Geology Department, Boston Univ., Boston MA 02215 [2]SN-4, NASA/JSC, Houston TX 77058
[3]Enrico Fermi Inst., Univ. Chicago, Chicago IL 60637

Angra dos Reis (AdoR) is a unique fassaite-rich achondrite, interpreted as a metamorphosed porphyritic lava [1,2]. Abundances of refractory lithophile elements (RLE) suggest that the AdoR magma formed from a complexly fractionated source. Fractionation was as complex as terrestrial or lunar basalts, and suggests that AdoR formed on a planetary body.

Elemental abundances in AdoR (relative to CI) show depletions attributable to volatility, metal/silicate fractionation [3], and silicate/silicate (or oxide) fractionation (new and literature data [4]). The last, indicative of silicate igneous processes, is best seen in the abundances of RLE, which are not affected by volatility or metal fractionation.

Among trivalent cations, the most abundant are the MREE (35-40xCI). Larger cations (the LREE) are depleted by up to 40% (La=24xCI). Smaller cations are also depleted: HREE by up to 30% (Lu=28xCI); Sc by 80% (8xCI); V by 90% (3.3xCI); and Al by 85% (6.0xCI). Cation abundance is a smooth function of ionic radius. Titanium was not trivalent during the depletion of smaller trivalent cations, because it is much more abundant than trivalent ions of comparable size (Sc, V).

Abundances of tetravalent cations range from 34xCI for Ti (the smallest radius) to 20xCI for Th (the largest). Abundance is a linear function of cation radius.

The only truly refractory divalent lithophile element in AdoR is calcium; abundances of Sr, Ba, and Mg are probably affected by volatility. Calcium's abundance is less than 20xCI, suggesting depletion in AdoR's source.

Based on RLE abundances, the source of AdoR experienced at least two fractionations: removal of a phase enriched in large-radius (highly incompatible) cations; and removal of a phase rich in small trivalent cations. The former removal suggests that AdoR's source was depleted by loss of a silicate melt fraction prior to AdoR's formation. Ador's depletions of Al, Sc, and V, but not Ti, may have been caused by fractionation of aluminous minerals at an oxygen fugacity near IW or QFM. Fractionation of melilite would deplete AdoR's source in Al and Ca, but not in Sc or V. Fractionation of hibonite could have caused depletions in Al, Sc, and V, but probably not the HREE. Fractionation of pyroxene could cause depletions in Sc, V, and the HREE; to have caused depletion of Al, the pyroxene must have been more aluminous than AdoR's own pyroxene, and fractionation must have been extensive. Complex fractionation processes are necessary in any case, because neither melilite nor hibonite are on AdoR's solidus.

Supported by NASA NAG9-168 (Treiman) and NAG9-52 (E. Anders).

[1] Treiman A.H., 1988, Lunar Planet. Sci. XIX, 1203. [2] Prinz M. et al., 1977, Earth Planet. Sci. Lett. 35, 317. [3] Jones J.H. et al., 1988, this volume. [4] Ma M.-S. et al., 1977, Earth Planet. Sci. Lett. 35, 331.

EXPERIMENTAL TRACE ELEMENT PARTITIONING FOR SYNTHETIC LEW 86010 ANALOGS: PETROGENESIS OF A UNIQUE ACHONDRITE. G. McKay (SN4, NASA-JSC, Houston, TX 77058), L. Le, J. Wagstaff, and D. Lindstrom (Lockheed EMSCO, 2400 NASA Rd. 1, Houston, TX 77058)

Petrographic examination of antarctic meteorite LEW 86010 [1,2,3,4,5] indicated that this sample is a unique achondrite which shows marked chemical fractionations from primitive chondritic material, and has strong affinities to the pyroxene-rich achondrite Angra Dos Reis. It is clear from textural characteristics and phase compositions that LEW 86010 crystallized from a melt.

Phase equilibrium studies [6] indicate that the bulk composition of LEW 86010 [2,3] is very close to multiple saturation with olivine, fassiatic pyroxene, and anorthite at its liquidus temperature (~1190°C). Thus it is highly probable that this sample represents a crystallized melt which was produced by either fractional crystallization or partial melting of a gabbroic source region on the meteorite's parent body. It is therefore likely that at least some of the highly fractionated chemical characteristics of this sample were produced by igneous differentiation.

It would be desirable to constrain the effects of igneous differentiation by petrogenetic modeling. However, such modeling requires knowledge of crystal/liquid partition coefficients. The compositions of the phases involved in the differentiation of LEW 86010 are unusual, with very Ca- and Al-rich melts and fassiatic pyroxene containing ~4-12 wt% Al_2O_3. Although the Ca content of pyroxene is known to have a a strong effect on REE partition coefficients [7], little is known about the effect of Al content. Therefore, in order to obtain accurate partition coefficients to constrain the petrogenesis of LEW 86010, we are undertaking an experimental study of trace element partitioning behavior in synthetic LEW 86010 analogs using our standard techniques [e.g., 7]. Preliminary results for pyroxene and plagioclase are presented in the figure below. Each point represents the average of distribution coefficients obtained on several different crystals from each of several different runs. The error bars represent ± 2 standard deviations of the mean.

We note the following major features of the distribution coefficient patterns: (1) The pyroxene/liquid pattern is very similar in shape and absolute value to that measured by Grutzeck *et al.* [8] for low-Na compositions in the DI-AN-AB system. Thus, either the high Al content of LEW 86010 pyroxene does not have a major effect on partitioning behavior, or its effect is compensated by other factors. (2) The pyroxene pattern shows a slight negative Eu anomaly at the oxygen fugacities of the experiments (IWx10). (3) The plagioclase pattern shows a steep decrease towards the HREE, as reported for synthetic lunar melts by McKay [9]. (4) The plagioclase pattern shows a large positive Eu anomaly, which no doubt depends strongly on fO_2.

The partition coefficients presented here represent a foundation upon which petrogenetic models of LEW 86010 may be constructed as bulk REE data become available for this sample. In addition to the above overall characteristics, pyroxene REE partition coefficients appear to be positively correlated with pyroxene Al content, but the details of this correlation remain to be worked out.

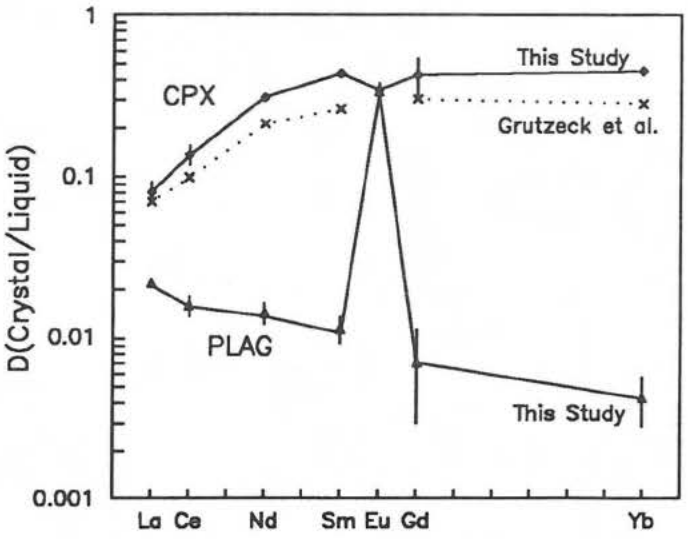

REFERENCES:

[1] Mason (1987) *Antarctic Meteorite Newsletter* 10, no. 2. [2] McKay *et al.* (1988) *Lunar and Planetary Science XIX*, 762. [3] Prinz *et al.* (1988) *Lunar and Planetary Science XIX*, 949. [4] Goodrich (1988) *Lunar and Planetary Science XIX*, 399. [5] Delaney and Sutton (1988) *Lunar and Planetary Science XIX*, 265. [6] McKay *et al.* (1988) *Lunar and Planetary Science XIX*, 760. [7] McKay and Wagstaff (1986) *Geochimica et Cosmochimica Acta* 50, 927. [8] Grutzeck *et al.* (1974) *Geophys. Research Letters* 1, 273. [9] McKay (1982) *Lunar and Planetary Science XIII*, 493.

ION PROBE ANALYSIS OF MELT VEINS IN META78008 UREILITE;
J. L. Berkley, SUNY College at Fredonia, NY 14063

Siliceous melt veins occur in a number of ureilites (eg. 1, 2) interstitial to major silicate grains (olivine/pyroxene), and less commonly penetrating fractures in silicate grains. They consist of a siliceous glass (commonly also enriched in Al and alkalis) enclosing skeletal quench crystals of pyroxene, or rarely olivine. Unusually thick melt veins occur in META78008 (a rare, augite-bearing ureilite) approaching 200 microns in diameter in some areas (10-20 microns is the norm). Veins consist of glass with up to 70 wt.% SiO_2, 18% Al_2O_3, 7% CaO, 3% Na_2O, and 0.8% K_2O. Quench crystals include skeletal, magnesian pigeonite (mg=98;Wo≅6) and minor silica grains. Minute, low-Ni, Fe-Ni metal blebs are ubiquitous. Similar veins have been previously interpreted as originating externally to the ureilite host, introduced therein by injection during a late-stage shock-reduction event (1,2). To better gauge the origin of melt veins in META78008, ion microprobe analyses (A. Shimizu lab, MIT; D. Higmont, analyst) were performed on melt veins and major silicates for REE and other trace/minor elements (Sr, Sc, V, Cr, Ti).

REE analyses of glass plus quench crystals (no beam overlap with carbon or major silicates) show a relatively flat C1-normalized pattern, with 3X avg. enrichment relative to C1. Neither batch nor fractional fusion of typical ureilite ultramafic assemblage can account for this pattern. Nevertheless, various lines of evidence suggest that most of the META78008 melt was derived by internal melting and concommitant reduction of - augite. Specifically, (a) vein thickness significantly increases along augite grain boundaries, but thins or is absent at ol-ol and ol-pig boundaries, (b)augite grains display irregular (reaction?) grain boundaries with melt veins, and contain isolated pockets of melt internally ("islands" of unconsumed augite occur in melt veins in some areas), (c) transition element and Sr trends in the melt show parallel trends compared to augite, (d) mass balance modeling shows that appropriate mixtures of melt plus reduced augite margins (enriched in Ca/Al, Mg/Fe relative to core) can reproduce augite core compositions reasonably well. Better results are achieved by considering loss of Cr and Fe to reduced metal blebs, and addition of Si to the melt by ol reduction. Thus, in this particular ureilite, melt veins were wholly or mostly internally derived by non-equilibrium partial melting and reduction of augite and, to a much lesser extent, olivine. This process was probably triggered by sudden decompression coupled with rapid, temporal heating during an impact event.

REFERENCES

1. Goodrich C. A., Keil K., Berkley J. L., Laul J. C., Smith M. R., Wacker J. F., Clayton R. N., Mayeda T. K. (1988) Meteoritics 22, 191-218
2. Goodrich C. A. and Berkley J. L. (1985) Lunar and Planetary Sci. XVI, 280-281.

Nd AND Sr ISOTOPIC ANALYSES OF UREILITES: EVIDENCE FOR CHEMICAL ACTIVITY AT 3.74 Ga OR YOUNGER . *C.A. Goodrich, **P.J. Patchett, and *M.J. Drake, *Lunar and Planetary Laboratory, ** Dept. of Geosciences, University of Arizona, Tucson, AZ 85721.

Ureilites have chemical characteristics indicative of planetary igneous processes [1,2], but primitive oxygen isotopic characteristics suggestive of nebular processes [3]. Age data are fundamental to resolving this conflict. We report Nd and Sr isotopic data which indicate that ureilites experienced some chemical event at 3.74 Ga or younger.

Analytical: We analyzed whole-rock samples (1-1.4g) of Novo Urei, Kenna (3 samples), and ALHA77257. Sample preparation, dissolution, chemical separation, and measurement followed procedures described previously [4]. Blank corrections were negligible. Allende (Smithsonian powder, split # 2) was analyzed as a check on accuracy. Our measured Rb and Sr concentrations and Sr isotopic composition are comparable to those of [5] (Smithsonian powder split # 3), and yield a model age of 4.48 Ga relative to BABI. Our Sm-Nd data fall on a 4.55 Ga isochron through the reference chondritic composition of [6], and within the range of bulk chondritic compositions of [6] .

Results: The Kenna samples (K1, K2 and K3) showed surprising heterogeneity, considering their large sizes. K1 and K3 appear to be dominated by the volumetrically-minor, LREE-enriched component [7,8], while K2 is dominated by the LREE-depleted ultramafic assemblage. The five whole-rock samples plot on a line with a slope corresponding to an age of 3.74 Ga, on an Sm-Nd isochron plot (Fig. 1). The samples do not plot on a line on a Rb-Sr isochron plot, but form a general trend with an extremely shallow slope. There is no correlation between $^{87}Sr/^{86}Sr$ and $^{143}Nd/^{144}Nd$, nor between Rb/Sr and Sm/Nd.

Discussion: One possible interpretation of the Sm-Nd line is that it is an isochron, giving the crystallization age of ureilites. In this case, ureilites are surprisingly young, consistent with the interpretation of [2]. However, the observation that K2 plots at one end of the line while K1 and K3 plot at the other end, suggests that it is a mixing line with an ultramafic endmember and a LREE-enriched endmember. Under this assumption, if the ultramafic assemblage is 4.55 Ga old, then its composition would be given by the intersection of the ureilite line and the 4.55 Ga isochron in Fig. 1. If it is younger, it would plot to the right of this point on the ureilite line. If the ultramafic assemblages of all ureilites are the same age, they should plot on an isochron. This implies that if their age is anything other than 3.74 Ga, then the Kenna, Novo Urei, and ALHA77257 ultramafic assemblages must have nearly identical Sm/Nd. If the ultramafic assemblages are 4.55 Ga, and the LREE-enriched component formed as an extreme differentiate of similar material (same ε_{Nd}), then the age of the LREE-enriched component is 3.74 Ga (Fig. 2). If it was derived from less-depleted material (lower ε_{Nd}), then it must be younger. The Rb/Sr data do not distinguish between these possibilities, but do indicate a young chemical event. The lack of correlation between Rb/Sr and Sm/Nd suggests that the LREE-enriched component is not a normal igneous differentiate.

Analyses of separated samples of the ultramafic assemblages and LREE-enriched components should help determine whether these components are of different ages (or 3.74 Ga is the crystallization age of ureilites), and if so what those ages are. In any case, Sm-Nd and Rb-Sr data show that ureilites have experienced some chemical event at 3.74 Ga or younger. The nature of that event, and its effect on the oxygen isotopes of ureilites is not yet known.

[1] W.V. Boynton *et al.* (1976) GCA **40**, 1439. [2] C.A. Goodrich *et al.* (1987) GCA **51**, 2255. [3] R.N. Clayton and T.K. Mayeda, (1988) LPS **19**, 197. [4] C.A. Goodrich *et al.* (1988) LPS **19**, 405. [5] M. Tatsumoto *et al.* (1976) GCA **40**, 617. [6] S.B. Jacobsen and G.J. Wasserburg (1980) EPSL **50**, 139. [7] A.H. Spitz and W.V. Boynton (1986) Meteoritics **21**, 515. [8] A.H. Spitz *et al.* (1988) LPS **19**, 1111.

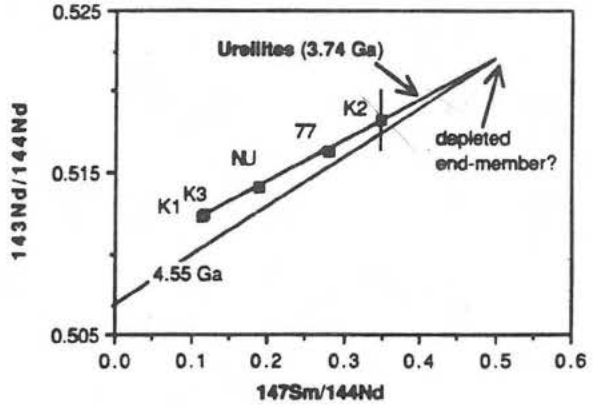

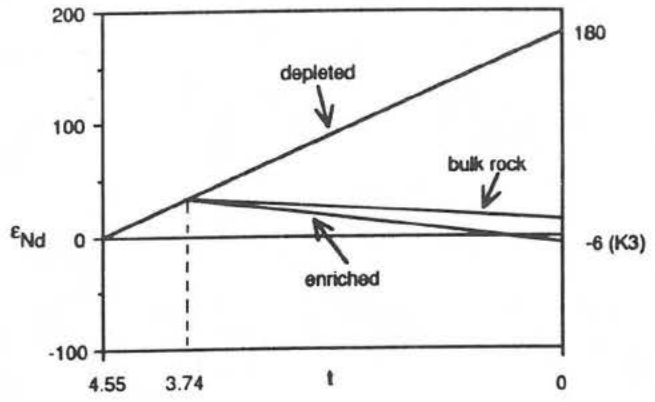

TRACE ELEMENT ANALYSIS OF UREILITE METEORITES: EXTENDING THE RANGE OF CHARACTERIZED SAMPLES; A.H. Spitz and William V. Boynton; Lunar and Planetary Laboratory; University of Arizona; Tucson, AZ 85721

We have used instrumental and radiochemical neutron activation analysis to determine Sc, Cr, Mn, Fe, Co, Ni, As, REE, W, Re, Os, Ir and Au for bulk samples of ALHA77257, ALHA81101, ALHA82130, PCA82506, Kenna and Novo Urei and for acid-treated samples of the first five of these in order to characterize more completely the ureilite class.

RESULTS: The ureilites analyzed range from Fa_{0-5} to Fa_{21} (Berkley groups 1-3 (1)) and include representatives from the three oxygen isotope groupings Clayton (2). Siderophile element correlations follow those seen in Haverö, Kenna, Goalpara and Novo Urei (3,4,5,6) but with lower correlation coefficients [Figure 1]. As with the mechanically-separated vein material of Haverö and Kenna (3,6), the leachates in our experiment plot to the high Ir end relative to their bulk Ir indicating that the acid leaching removes the carbon-rich vein material.

The bulk rare-earth element (REE) patterns [Figure 2] of the three newly analyzed Antarctic ureilites (ALHA77257, ALHA81101 and ALHA82130) do not display the pronounced v-shape patterns seen in earlier analyses of Kenna, Goalpara and Roosevelt County 027 but do show at least the LREE and HREE enrichments seen in Novo Urei and Haverö (3,4,7). Although residues of acid treatment for Kenna, PCA82506 and ALHA81101 show the loss of LREE-bearing material, the ALHA77257 and ALHA82130 residues do not as clearly.

DISCUSSION: The new trace element data are similar to literature data in both behavior and abundance. These data extend the range of analyzed ureilites. The results confirm that the ureilites are a highly variable group in elemental abundances; the clear groupings evident in the Fe/Fe+Mg values (1) and oxygen isotope values (2) among other major characteristics cannot be applied directly to the trace elements.

REFERENCES:

(1) Clayton R.N. and Mayeda T.K. (1988), submitted to GCA. (2) Berkley J.L., Taylor G.J., Keil K., Harlow G.E. and Prinz M. (1980) GCA 44, p.1579-1597. (3) Wänke H., Baddenhausen H., Spettel B., Teschka F., Quijano-Rico M., Dreibus G. and Palme H. (1972) Meteoritics 7, p 579-590. (4) Boynton W.V., Starzyk P.M. and Schmitt R.A. (1976) GCA 40, 1439-1447.(5) Higuchi H., Morgan J.W., Ganapathy R. and Anders E. (1976) GCA 40, p.1563-1571. (6) Janssens M.-J., Hertogen J., Wolf R., Ebihara M. and Anders E. (1987) GCA 51, p.2275-2283. (7) Goodrich C.A., Keil K., Berkley J.L., Laul J.C., Smith M.R., Wacker J.F., Clayton R.N. and Mayeda T.K. (1988) Meteoritics 22, p.191-218.

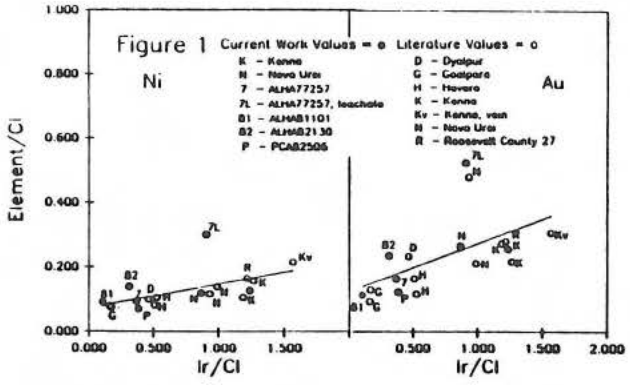

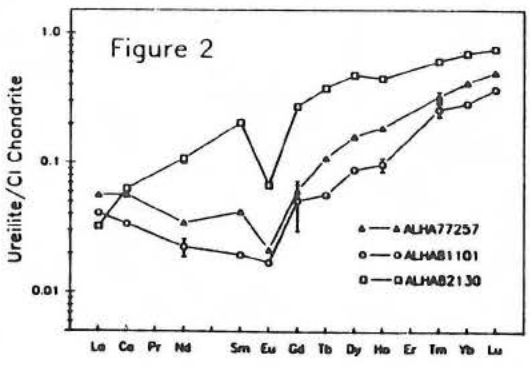

WHAT WE THINK WE KNOW FROM NOBLE GASES IN SHERGOTTITE EETA 79001

R. C. Wiens*, A-020, Scripps Oceanographic Inst., UCSD, La Jolla, CA 92093 *also Dept. of Chemistry

The gases in shergottite EETA 79001 have raised many unanswered questions. Noble gas and nitrogen data appear to support a martian origin for this meteorite, while colinearity along a mass fractionation line for oxygen isotopes, as well as certain petrographic considerations link the eight SNC meteorites together. Yet the SNC's are diverse in chemical compositions and textures, as well as in their cosmic ray exposure ages.

Gases in EETA 79001 glass apparently consist of more than one trapped gas component[1]. The component similar to the martian atmosphere (termed SPB[2]) is released at ~1100°C from the glass, while the second component (earlier called indigenous[1]; here we use EETV) is released from vesicles by crushing. The latter is more terrestrial-like in its isotopic ratios[3], with $^{129}Xe/^{132}Xe < 1.27$ and $^{40}Ar/^{36}Ar < 690$, but it is different from air or any possible simple fractionation thereof--the air Ar/Xe ratio would have to be lowered, while the Kr/Xe ratio needs to be increased significantly to satisfy both isotopic and elemental constraints. Assumption of a Chassigny-like $^{129}Xe/^{132}Xe$ ratio (=1.03)[4] for EETV gas yields $^{36}Ar/^{132}Xe$ and $^{84}Kr/^{132}Xe$ ratios of 916 and 33.6, respectively, much higher than in Chassigny and Shergotty[4,5], though it is interesting to note that a fractionation proportional to the square root of the masses is not far off.

The EETV component bears a trace of resemblance isotopically to SPB gas in its spallation-free $^{36}Ar/^{38}Ar$ value of 4.9 ± 0.2, intermediate between the chondritic/terrestrial value, at 5.35, and the SPB ratio, at 4.1 ± 0.2[1]. If the EETV component is from the martian interior (which one may say is the least unlikely source) it implies that the anomalously low SPB $^{36}Ar/^{38}Ar$ ratio, which is thought to be representative of the martian atmosphere, is not a planet-wide phenomenon. That this ratio in the EETV gas is still low compared to most other solar system argon reservoirs raises the question of whether subduction of atmospheric gases could have lowered it from an initial ratio similar to terrestrial. Arguing against this is the fact that tectonic processes appear almost nonexistent on Mars compared to the Earth. It has also been demonstrated[1] that the present-day cosmic ray flux is insufficient to account for the suggested excess ^{38}Ar in the martian atmosphere on a reasonable timescale. Alternately, a source of low $^{36}Ar/^{38}Ar$ could have accreted relatively late on Mars, most of which degassed into the atmosphere. A late veneer is one way to explain the apparently higher $^{129}Xe/^{132}Xe$ ratio in the martian atmosphere than in the mantle[5]. However, such a source of low $^{36}Ar/^{38}Ar$ is totally unknown in the solar system.

References: [1]Wiens R.C., Becker R.H., and Pepin R.O. (1986) Earth Planet. Sci. Lett. 77, 149-158. [2]Swindle T.D., Caffee M.W., and Hohenberg C.M. (1986) Geochim. Cosmochim. Acta 50, 1001-1015. [3]Wiens R.C. and Pepin R.O. (1987) Meteoritics 22, 527-528. [4]Ott U. (1987) preprint, subm. to Geochim. Cosmochim. Acta. [5]Ott U. and Begemann F. (1985) Nature 317, 509-512.

NEW NOBLE GAS DATA FOR SNC METEORITES: ZAGAMI, LAFAYETTE, AND ETCHED NAKHLA;

U. Ott, H.P. Löhr, and F. Begemann,
Max-Planck Institut f. Chemie, Saarstraße 23, D-6500 Mainz, F.R.G.

Trapped noble gases in Shergotty have been suggested [1,2] to be a mixture of a Chassigny type component, characterized by an extremely fractionated elemental abundance pattern but Xe of solar isotopic composition [1,2], and a component prevalent in the glass of shergottite EETA 79001 (SPB-gases; [3,4]) which may be unfractionated shock-implanted gases from the Martian atmosphere [5,6]. New data for the shergottite Zagami (see also [7]) point to more complexity in that the elemental pattern is similar to that in EETA 79001 glass (Fig. 1) but the $^{129}Xe/^{132}Xe$ ratio is much lower (Fig. 2). The ratio of ^{40}Ar to trapped ^{36}Ar in the 800°C release (about 7% of the total ^{40}Ar) agrees with the ratio in SPB-Ar (~2300) and Shergotty, but is only ~1060 in the main high-temperature release. - New data for the nakhlite Lafayette show its noble gases to be very similar to those in Nakhla; trapped ^{36}Ar is too low to be discernible from the spallogenic component and in a $^{129}Xe/^{132}Xe$ vs. $^{84}Kr/^{132}Xe$ plot the data points fall above the Chassigny-EETA 79001 mixing line. If nakhlites are to contain the same two components as shergottites, the SPB-component must be strongly fractionated, with the $^{84}Kr/^{132}Xe$ ratio about five times lowered (Fig.2). The carrier(s) of this fractionated component appear(s) to be easily soluble. Treatment of an aliquant of Nakhla H1 with 6N HCl dissolved 15% by weight (essentially olivine) and removed ~60% of trapped high-temperature ^{132}Xe but ~90% of radiogenic $^{129}Xe^*$ moving, in Fig. 2, the data point down towards Chassigny. Also lost are more than 95% of the $^{79}Br(n,\gamma)$-produced $^{80}Kr^*$ which is unambiguous proof that the HCl-soluble portion of Br was present in the meteorite during its exposure to the cosmic radiation. Possibly, the H_2O-leachable halogens in Nakhla are not due to terrestrial contamination [8] but, together with other weathering products [9] are of Martian origin and contain a sample of fractionated Martian atmosphere.

	^{36}Ar	$^{36}Ar_t$	^{40}Ar	^{132}Xe	129/132	$(36/132)_t$	$(84/132)_t$	$(129/132)_t$
Zagami Z1	96.4	74.9	79300	0.096	1.49	801	18.75	1.51
Lafayette L11	126	--	58600	0.187	1.25	-	1.63	1.26
Lafayette L3	124	--	70800	0.088	1.31	-	1.65	1.29
Nakhla R12	153	--	30900	0.028	1.28	-	1.90	1.18
Nakhla H1 [1,2]	136	--	23421	0.057	1.79	-	3.32	1.90
Chassigny PB4 [1,2]	23.6	8.1	29507	0.432	1.03	19	1.23	1.03
SPB-gas [10,11]	--	--	--	--	--	579	20.3	2.40

Gas abundances in 10^{-10} cm^3 STP/g. For Zagami and the nakhlites only the gas released after preheating to 800°C is given.

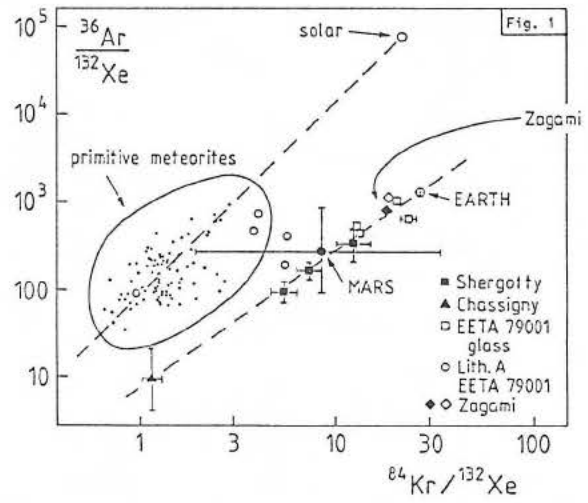

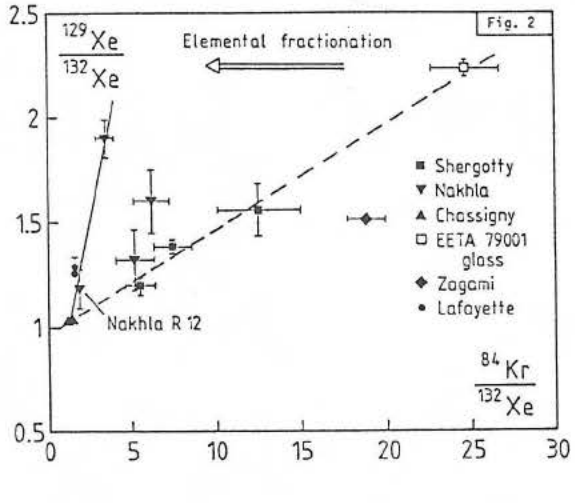

References: [1] Ott U. and Begemann F. (1985) Nature 317, 509. [2] Ott U. (1988) GCA, in press. [3] Bogard D.D. and Johnson P. (1983) Science 221, 651. [4] Becker R.H. and Pepin R.O. (1984) EPSL 69, 225. [5] Bogard D.D. et al. (1986) PLPSC 17, JGR 91, E99. [6] Wiens R.C. and Pepin R.O. (1988) GCA 52, 295. [7] Bogard, D.D. et al. (1984) GCA 48, 1723. [8] Dreibus G. and Wänke H. (1987) Icarus 71, 225. [9] Carr R.H. et al. (1985) Nature 314, 248. [10] Hunten D.M. et al. (1987) Icarus 69, 532. [11] Swindle T.D. et al. (1986), GCA 50, 1001.

CALCIUM CARBONATE IN NAKHLA: FURTHER EVIDENCE FOR PRE-TERRESTRIAL SECONDARY MINERALS IN SNC METEORITES.

S. J. Wentworth[1] and J. L. Gooding[2], [1]Lockheed/EMSCO, 2400 NASA Rd. 1, Houston, TX 77058; [2]SN21/Planetary Science Branch, NASA/Johnson Space Center, Houston, TX 77058.

Introduction. Identification and characterization of pre-terrestrial secondary minerals in SNC meteorites would be of great importance in understanding the low temperature, aqueous geochemistry on the SNC parent body, which is suspected to be Mars. Previous work [1,2] showed that calcite, calcium sulfate, and secondary aluminosilicates in shergottite EETA79001 may be of pre-terrestrial origin. Evolved-gas analyses of Nakhla revealed intriguing evidence for indigenous carbonates [3], making Nakhla an important target for further investigation of secondary minerals. As a supplement to our previous work on Nakhla [4], we confirm the occurrence of discrete grains of calcium carbonate.

Samples and Methods. Untreated bulk samples of Nakhla were examined by scanning electron microscopy (SEM) and energy-dispersive X-ray spectrometry (EDS) by methods used for the EETA79001 shergottite [2]. Samples were subdivided from 500-mg chips supplied by the British Museum (BM1911,369 and BM1913,26), from two different specimens. Both exterior (fusion-crusted) and interior (> 2 cm depth) materials were studied. Parallel SEM/EDS studies were made on whole-rock powder supplied by the Open University (OU), comprising the same material that gave carbon-isotopic evidence for pre-terrestrial carbonates [3].

Results and Discussion. Two interior samples of Nakhla, the OU powder and BM1913,26B, definitely contain calcium carbonate. In the OU powder, one small (~2 μm) grain of Ca-carbonate occurred as an anhedral, rounded grain attached to the wall of a shallow fracture in a larger (~50 μm) fresh pyroxene grain. Ca-carbonate in BM1913,26B was found in one area (~100 μm across) consisting of very fine-grained material as thin, irregular patches on a fracture surface as well as small fracture fillings. The carbonate-bearing substrate consisted of pyroxene and chlorapatite. Alteration of adjacent silicates (possibly the "residual mesostasis" component) was indicated by traces of K and Cl in pyroxene-like phases.

Secondary salts are common in Nakhla [4]. Chlorides are ubiquitous at trace levels in all exterior and interior samples. Ca-sulfate is present in exterior and interior portions of one specimen (BM1911,369) and Mg-sulfate is present in one exterior sample (BM1913,26A). None of those phases, however, show clear paragenetic associations with the Ca-carbonate.

Ca-carbonate in Nakhla may be of preterrestrial origin because it has not been found in exterior samples. Both morphologies of Ca-carbonate in Nakhla are similar to varieties found in shergottite EETA79001 [2]. The unusual rounded shape of the Ca-carbonate in the OU powder may be the result of thermal decrepitation, as was previously inferred for at least one variety of carbonate in EETA79001.

References. [1] Gooding J. L. and Muenow D. W. (1986) *Geochim. Cosmochim. Acta, 50,* p. 1049-1059. [2] Gooding J. L. et al. (1988) *Geochim. Cosmochim. Acta, 52,* p. 909-915. [3] Carr R. H. et al. (1985) *Nature, 314,* p. 248-250. [4] Wentworth S. J. and Gooding J. L. (1988) *Lunar Planet. Sci. XIX,* p. 1261-1262.

Author Index